Carbon dynamics and trophic relationships in a human impacted and mangrove dominated tropical estuary (Can Gio, Vietnam)

Frank David

MUSEUM NATIONAL D'HISTOIRE NATURELLE

Ecole Doctorale Sciences de la Nature et de l'Homme – ED 227

Année 2017

N° attribué par la bibliothèque
|_|_|_|_|_|_|_|_|_|_|_|_|_|

THESE

Pour obtenir le grade de

DOCTEUR DU MUSEUM NATIONAL D'HISTOIRE NATURELLE

Spécialité : Ecologie aquatique et biogéochimie

Présentée et soutenue publiquement par

Frank DAVID

Le 28 septembre 2017

Dynamique du carbone et relations trophiques dans un estuaire à mangrove sous pression anthropique (Can Gio, Vietnam)

Sous la direction de **:**

M. Meziane, Tarik, Professeur, MNHN

M. Marchand, Cyril, Chargé de recherche, IRD

JURY :

M. Meziane, Tarik	**Professeur MNHN, Paris**	**Directeur de Thèse**
M. Marchand, Cyril	**Chargé de recherche IRD, Vietnam**	**Directeur de Thèse**
M. Bouillon, Steven	**Professeur associé Université de Leuven, Belgique**	**Rapporteur**
M. Bec, Alexandre	**Maître de conférences Université Blaise Pascal, Clermont-Ferrand**	**Rapporteur**
M. Olivier, Frédéric	**Professeur MNHN, Concarneau**	**Président du jury**
Mme Michaud, Emma	**Chargée de recherche CNRS Université de Bretagne Occidentale, Brest**	**Examinatrice**
Mme Lamy, Dominique	**Maître de conférences Université Pierre et Marie Curie, Paris**	**Examinatrice invitée**

The sharp salt air of the living sea mingles with the odour of decay;
all around is life and death, and every fresh tide brings change

Private lives – An exposé of Singapore's Mangroves

(cf. chapitre 5)

REMERCIEMENTS

Un travail de thèse est avant tout quelque chose de personnel, mais il est nécessairement nourri et rendu possible par de nombreuses personnes qui en enrichissent le contenu par leurs interrogations, leurs critiques et leurs réflexions. En ce sens, je tiens en premier lieu à remercier mes deux directeurs de thèse, Tarik Meziane et Cyril Marchand, qui ont rendu possible, amélioré, et clarifié le travail présenté ci-après, ainsi que les membres du jury qui ont accepté de l'évaluer.

Tarik, merci de m'avoir accueilli dans ton laboratoire au sein du Muséum National d'Histoire Naturelle, de m'avoir fait confiance pour la réalisation de ce projet et d'avoir su poser les bonnes questions pour le faire avancer.

Cyril, merci de m'avoir accueilli chez toi, au Vietnam, pour les missions de terrain, d'avoir permis mon accès à la mangrove et aux équipements d'échantillonnage puis d'avoir toujours été très constructif et réactif suite à mes sollicitations.

Je tiens aussi à remercier l'ensemble de l'équipe RESAQUA pour tous ces bons moments passés en votre compagnie, notamment Najet, toujours la patate et le poing levé, Guillaume, Silvia, Pierrick, Domy, Cédric, Thibaud, Jean-Michel, Blandine, Xavier, Elisabeth, Fred, Marc, Isabelle, Simone et enfin Hervé, parti bien trop tôt. Merci aux stagiaires qui ont contribué à analyser les échantillons récoltés, avec dans l'ordre de leur passage Guillaume, Julie, Alice, Aurélie et enfin Baptiste, qui a mené le projet de décomposition des effluents de crevetticulture depuis la phase expérimentale jusqu'à une première version de la rédaction.

Merci à Marine pour toute cette iconographie d'espèces de la mangrove et à Audrey, pour ton dessin de *Rhizophora* repris d'une manière ou d'une autre dans chacun des chapitres de ce mémoire.

Toute ma gratitude aussi à l'équipe avec qui j'ai pu travailler au Vietnam, en premier lieu Nho, Vinh et Pierre, vous êtes les meilleurs partenaires de terrain que l'on puisse avoir, aussi bien sur le plan humain que scientifique. Merci aussi aux chercheurs du Centre Asiatique de Recherche sur l'Eau et de l'université des sciences d'Ho Chi Minh Ville pour votre accueil et votre partage de savoirs.

Enfin, merci à tous ceux que j'ai oublié, dont probablement certains qui ont beaucoup contribué à ce travail, ainsi qu'à mes colocs, mes amis, ma famille et par dessus tout à Marie, juste parce que tu es merveilleuse.

AVANT-PROPOS

Ce mémoire de thèse résume 3 années de recherche sur la dynamique du carbone et les relations trophiques dans la mangrove de Can Gio, au sud du Vietnam. Ce travail a pu être effectué grâce à l'obtention d'une bourse du Ministère de l'Enseignement Supérieur et de la Recherche auprès de l'école doctorale 227 « Science de la Nature et de l'Homme : écologie et évolution », du Muséum National d'Histoire Naturelle (MNHN). Les missions d'échantillonnage ainsi que les équipements utilisés sur le terrain ont principalement été financés par la Fondation Air Liquide, en soutien à l'Institut de Recherche pour le Développement (IRD) pour un projet visant à mesurer la capacité de la mangrove au Vietnam à fixer le CO_2. Ceci, dans le cadre de l'observatoire des mangroves sous l'influence des changements climatiques développé dans la zone Indo-Pacifique.

Ce travail a pour objectif d'étudier le cycle du carbone dans l'estuaire traversant la mangrove de Can Gio, au sud du Vietnam, ainsi que les relations trophiques le long de l'estuaire traversant la mangrove et dans un chenal de vidange. Les résultats présentés sont issus de 3 campagnes d'échantillonnage. La première en saison sèche, uniquement le long de l'estuaire traversant la mangrove. La deuxième en saison humide, le long de l'estuaire et dans un chenal de vidange, et la dernière afin de simuler en laboratoire le devenir d'effluents crevetticoles une fois rejetés dans l'estuaire.

Ce mémoire est composé d'une introduction (en français) dont le rôle est de présenter le contexte du projet de recherche ainsi qu'une partie de la bibliographie ayant servi de support aux travaux réalisés. Le corps du texte est divisé en 7 chapitres (en anglais) qui constituent chacun un article scientifique soumis pour publication dans une revue internationale, ou en cours de préparation avant leur soumission. Le format proposé intègre des images (sauf précision, de source personnelle) de manière à rendre la lecture plus agréable mais celles-ci ne seront pas systématiquement proposées pour publication. Enfin, la conclusion (en français) replace les résultats énoncés dans les chapitres précédents au sein d'un contexte plus large et en réponse aux objectifs fixés en introduction.

TABLE DES MATIERES

PARTIE 2 : Structure et fonctionnement du réseau trophique

LISTE DES ABBREVIATIONS

ANCOVA = ANalysis of COVAriance
ARA = ARachidonic Acid
BrFA = Branched Fatty Acid(s)
C/N = mass ratio of Carbon/Nitrogen
C/N_m = molar ratio of Carbon/Nitrogen
EEA = Extracellular Enzymatic Activities
EF = shrimp pond EFfluents
EPA = leucine-aminopeptidase Exo-Proteolytic Activity
EPA = EicosaPentanoic Acid
FAME = Fatty Acid Methyl Ester(s)
DIC = Dissolved Inorganic Carbon
DO = Dissolved Oxygen
DOC = Dissolved Organic Carbon
FA = Fatty Acid(s)
FCO_2 = CO_2 Flux at the water/air interface
HCMC = Ho Chi Minh City
HUFA = Highly Unsaturated Fatty Acid(s)
IRGA = InfraRed Gas Analyser
Leu-MCA = L-leucine-MethylCoumarinylAmide
MI = MIxture of 10% shrimp pond effluents and 90% river water
MUFA = MonoUnsaturated Fatty Acid(s)
N-MDS = Non-Metric Multidimensional Scaling
NMI = Non Methylene Interrupted fatty acids
OM = Organic Matter
PCA = Principal Component Analysis
pCO_2 = CO_2 partial pressure in the water column
POC = Particulate Organic Carbon
PIC = Particulate Inorganic Carbon
PUFA = PolyUnsaturated Fatty Acid(s)
SAFA = SAturated Fatty Acid(s)
RV = RiVer water
SML = Surface Micro Layer
SPM = Suspended Particulate Matter
SPOM = Suspended Particulate Organic Matter
SS = Sum of Squares
TAlk = Total Alkalinity
TOC = Total Organic Carbon (DOC + POC)

LISTE DES FIGURES

INTRODUCTION GENERALE

PARTIE 1 : Dynamique du carbone au cours de son transit dans l'estuaire

PARTIE 2 : Structure et fonctionnement du réseau trophique

LISTE DES TABLEAUX

PARTIE 1 : Dynamique du carbone au cours de son transit dans l'estuaire

PARTIE 2 : Structure et fonctionnement du réseau trophique

LISTE DES PHOTOS

INTRODUCTION GENERALE

PARTIE 1 : Dynamique du carbone au cours de son transit dans l'estuaire

PARTIE 2 : Structure et fonctionnement du réseau trophique

Introduction générale

1. Biologie des mangroves

1.1. Généralités

Les mangroves sont des écosystèmes se développant à l'interface entre la terre et l'océan dans les zones tropicales et subtropicales. Ces forêts sont structurées par les palétuviers, qui sont des plantes ligneuses capables de tolérer des conditions extrêmes de salinité, courant et température, ainsi qu'un sol vaseux et souvent anoxique. Les racines aériennes des palétuviers stabilisent le sédiment et fournissent un substrat sur lequel peuvent s'installer de nombreuses espèces de plantes halophytes et d'animaux. Au-dessus du niveau de l'eau, les arbres et leur canopée accueillent des insectes, mammifères, reptiles, amphibiens et oiseaux, tandis que sous la surface se développent des communautés d'algues, éponges, gastéropodes, bivalves, crustacés, poissons, etc. Beaucoup de ces espèces animales ou végétales peuvent être amenées à passer d'un milieu à l'autre au gré des marées et en fonction de ses adaptations, pour se nourrir, pour échapper aux prédateurs ou pour un meilleur accès à la lumière. Dans certains groupes, comme chez les gastéropodes, on retrouve plusieurs niveaux de dépendance au milieu terrestre ou aquatique, et l'alternance des marées rythme l'activité biologique de certaines espèces (Houlihan 1979, Norton et al. 1990). D'autres groupes, comme les singes, aiment généralement assez peu l'eau et ne se risquent pas à descendre sur un sol inondé à marée haute, tandis que la plupart des poissons évitent de rester bloqués dans des flaques d'eau à marée descendante au risque de mourir asphyxiés (Ng et al. 2007). Les Périophtalmes constituent une exception dans le groupe des poissons puisqu'ils ont des adaptations leur permettant de vivre aussi bien dans un milieu aérien humide que dans l'eau. Ce sont des espèces très répandues dans les mangroves, de même que les crabes violonistes, dont les mâles portent une pince démesurément grande et qu'ils agitent lors des parades sexuelles sur le sédiment découvert à marée basse (Image 0-1).

Image 0-1 : Individus mâles de crabe violoniste (Ocypodidae; à gauche) et de Périophtalme (*Boleophthalmus boddarti* ; à droite) dans la mangrove de Can Gio

La productivité primaire nette de l'ensemble des mangroves à l'échelle mondiale est estimée à 218 ± 72 Tg C/an (Bouillon et al. 2008a). Ramenée à la superficie totale utilisée pour le calcul (160 000 km^2), cette productivité nette représente 1 362,5 ± 450 g C/m^2/an, faisant des mangroves les écosystèmes parmi les plus productifs au monde (Luyssaert et al. 2007). La structuration particulière des sols et leur saturation en eau quasi permanente font aussi des mangroves les écosystèmes tropicaux qui stockent la plus grande quantité de carbone par unité de surface (Alongi 2014). Ce stockage est d'environ 100 000 g C/m^2, dont 60 à 90% dans le sol, soit environ 10 fois plus qu'une forêt tempérée ou qu'une forêt tropicale non-inondée (Donato et al. 2011). Les processus de dégradation nécessitant de l'oxygène ne sont possibles que dans les premiers millimètres de profondeur du sédiment, qui devient rapidement anoxique dans ce milieu saturé en eau et alimenté en matière organique par les détritus de surface et la rhizosphère (Alongi 2009). La dégradation bactérienne de la matière organique conduit à une stratification du sédiment due de l'utilisation successive de l'oxygène, des nitrates, des oxydes de manganèse et de fer, et des sulfates comme accepteurs d'électrons (Froelich et al. 1979) (Figure 0-1). En absence d'oxygène, l'oxydation des sulfates est généralement le processus dominant de décomposition de la matière organique (Kristensen et al. 2008). Ce phénomène est à l'origine de l'odeur d'œufs pourris (sulfure d'hydrogène - H_2S) qui émane des sols de mangrove et constitue une des caractéristiques de ces milieux.

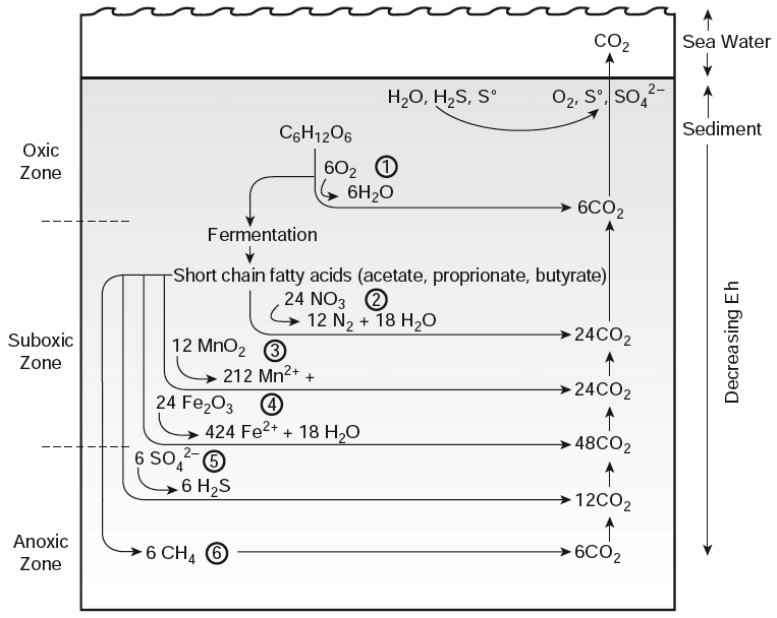

Figure 0-1 : Stratification des processus de dégradation microbienne dans les sédiments de mangrove. Extrait d'Alongi (2009)

1.1. Distribution spatiale

La répartition des forêts de mangroves correspond approximativement à la zone dans laquelle la température de l'océan ne descend pas en dessous de 20°C en hiver (Duke et al. 1998). Les mangroves se rencontrent principalement dans la zone tropicale et subtropicale de toutes les régions du monde, avec une distribution qui s'éloigne plus ou moins de l'équateur en fonction des courants océaniques. Ainsi, dans l'hémisphère sud les mangroves s'étendent plus vers le sud sur la côte Est des continents que sur la côte Ouest, ce qui reflète la distribution respective des courants océaniques chauds et froids (Figure 0-2). L'adaptation à la vie dans des milieux salés et saturés en eau s'accompagne de coûts énergétiques liés à l'acquisition de nutriments, à la tolérance au sel ou à la reproduction. Avec l'augmentation de la latitude (nord ou sud), la productivité primaire nette des mangroves diminue, réduisant ainsi leur vitesse de croissance, succès de reproduction et d'autres paramètres leur permettant de se maintenir dans leur environnement. Certains phénomènes, comme le gel du xylème, ont des conséquences plus importantes sur les arbres que sur des plantes plus petites comme celles peuplant les marais salés et ainsi les écosystèmes de mangroves ne sont pas suffisamment compétitifs pour se développer dans les zones tempérées, et sont généralement remplacés par d'autres milieux comme les marais salés (Hogarth 2015).

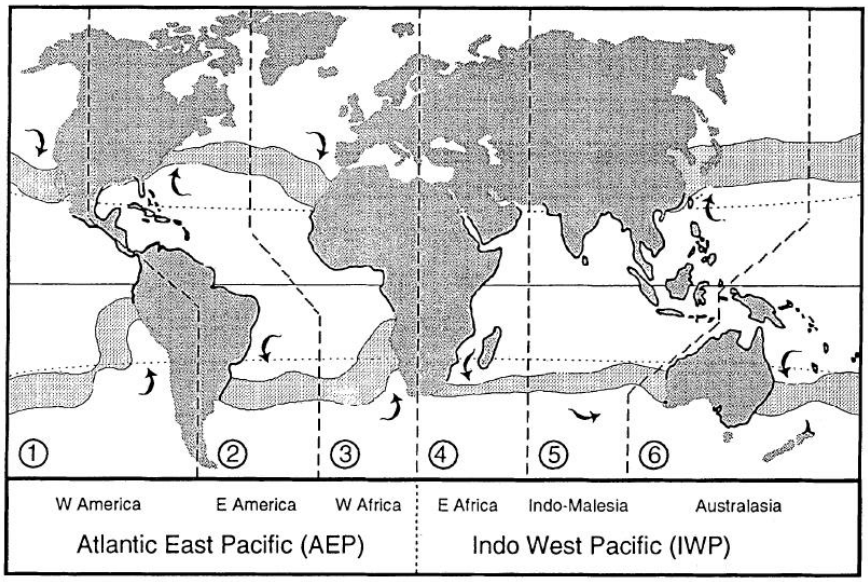

Figure 0-2 : Distribution mondiale des mangroves en relation avec l'isotherme 20°C de l'océan en été et en hiver (bande grise). Les pointillés verticaux séparent les grandes régions biogéographiques. Extrait de Duke et al. (1998)

Il existe 9 ordres, 20 familles, 28 genres et environ 70 espèces de palétuviers à travers le monde (Hogarth 2015). L'Indopacifique est la région qui présente la plus grande diversité d'espèces de palétuviers, avec 57 espèces dont la majeure partie appartient aux familles Avicenniaceae, Rhizophoraceae et Sonneratiaceae. L'Indonésie regroupe à elle seule 19% des mangroves de la planète, l'Australie 10% et le Brésil et le Nigéria 7% chacun, tandis qu'une des dernières estimations fiables réalisée en 2000 indiquait une superficie totale des mangroves de 157 000 km^2 (FAO 2007). Le Vietnam accueillait alors 1 570 km^2 de mangroves sur son territoire (1% de la superficie mondiale), dont 20% dans la mangrove de Can Gio (FAO 2007, Tuan et Kuenzer 2012).

Au-delà d'une distribution mondiale régulée par les conditions climatiques et les zones biogéographiques, on retrouve aussi une zonation nette des espèces de palétuviers au sein même d'un écosystème (Duke et al. 1998). Cette zonation est induite par des facteurs externes comme la salinité, la nature du sédiment et sa composition physico-chimique, son élévation et l'amplitude des marées, qui sont les principales contraintes évolutives qui ont conduit à la diversification et à la spécialisation des palétuviers. Ces conditions suivent généralement des gradients au sein d'une mangrove, selon la proximité de l'océan, les zones d'érosion et d'accrétion et la maturité du couvert végétal. Le degré d'adaptation à ces conditions induit une zonation horizontale des espèces, en relation avec le gradient de salinité depuis l'amont vers l'aval de la mangrove, et une zonation verticale, déterminée par l'élévation du sol qui définit la fréquence des inondations et la stabilité du sédiment. On retrouve par ailleurs différentes organisations spatiales au sein des mangroves, selon la prédominance des apports d'eau douce depuis les rivières, l'influence de la marée et l'exposition à la houle (Woodroffe 1992). Ainsi la mangrove peut se structurer sur une zone sédimentaire plane bordée de cours d'eau (« overwash type »), sur une frange littorale (« fringe type »), selon l'éloignement à la bordure d'un estuaire (« riverine type ») ou sur une zone plane éloignée des cours d'eau (« basin type ») (Figure 0-3).

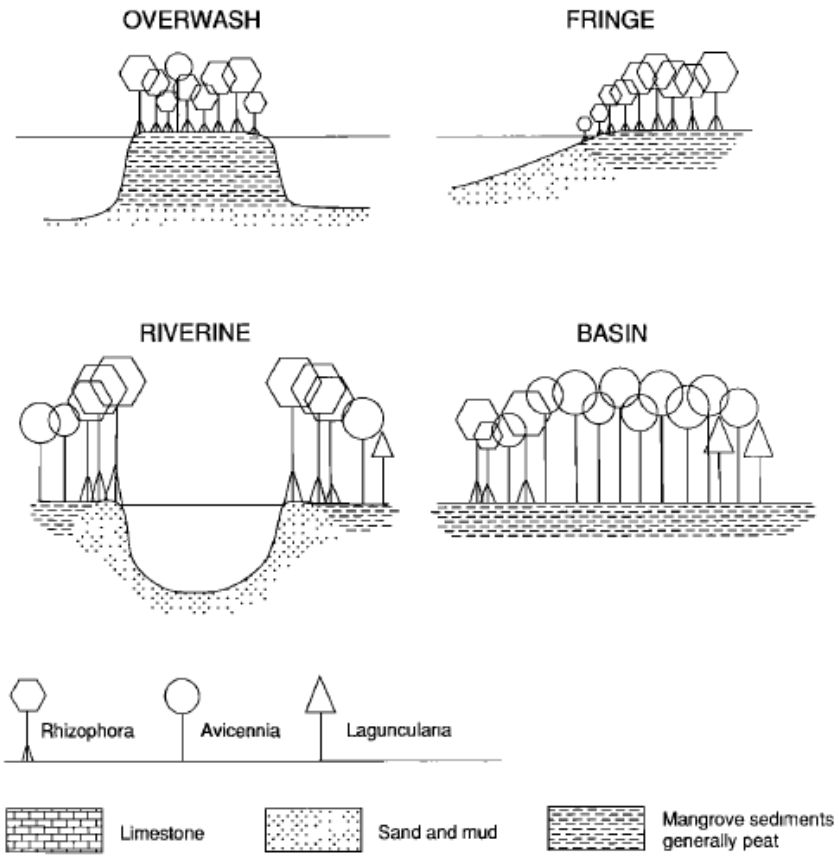

Figure 0-3 : Différentes organisations spatiales de mangroves selon la géomorphologie de la zone de développement. Extrait de Woodroffe (1992)

1.2. Adaptations des palétuviers

Afin de tolérer les conditions extrêmes dans lesquelles ils se développent, les palétuviers ont généré des adaptations morphologiques, physiologiques et écologiques particulières qui varient selon les taxons et les propriétés physico-chimiques de leur habitat. Ces adaptations peuvent se regrouper essentiellement autour de 3 axes : la résistance au sel, la capacité à capter de l'oxygène et à s'ancrer au sol et les stratégies de reproduction.

1.2.1. Résistance au sel

Le principal problème de la vie dans un environnement salé est lié au fort potentiel osmotique, donc au risque de dessiccation des cellules et à la difficulté à absorber l'eau. De plus, une concentration élevée en sel dans les cellules inhibe l'activité de la plupart des enzymes (Hogarth 2015). Les palétuviers sont des plantes halophytes physiologiquement

adaptés à des niveaux variables de salinité et possèdent des mécanismes pour lutter contre le fort potentiel osmotique de leur milieu environnant. Les stratégies de résistance comprennent l'exclusion du sel, sa sécrétion par des glandes dédiées (on parle alors d'excrétion), son stockage et son compartimentage dans certains tissus, et une osmorégulation particulière (Reef et Lovelock 2015). Ainsi, diverses espèces d'*Avicennia*, *Rhizophora* et *Sonneratia* empêchent le sel de pénétrer dans leur xylème au niveau des racines afin que celui-ci n'interfère pas avec leur métabolisme (mécanisme d'excrétion). Des espèces de *Xylocarpus* et *Excoecaria* stockent le sel dans leurs feuilles avant de les perdre au moment de la préparation d'une nouvelle saison de croissance et de fructification. D'autres enfin, notamment les *Avicennia*, possèdent des glandes au niveau des feuilles leur permettant d'exsuder de sel (mécanisme de sécrétion). Cependant, si la majorité du sel est exclu, il n'est pas possible d'obtenir un potentiel osmotique suffisamment élevé pour absorber de l'eau. La production de molécules organiques colloïdales incluant des sucres et des acides aminés permet alors à la plante de compenser la perte de potentiel osmotique due à l'exclusion du sel, sans pour autant nuire à son métabolisme puisque ces molécules sont des constituants usuels de la sève des plantes (Popp et al. 1985).

1.2.2. Système racinaire

Les sols de mangroves sont très pauvres en oxygène et deviennent rapidement anoxiques en profondeur (Alongi 2009). Parmi les adaptations les plus emblématiques des palétuviers, on retrouve diverses formes racinaires adaptées à la fois à l'ancrage sur un sédiment parfois très instable et à la respiration. Ce système racinaire, inféodé aux conditions spécifiques des mangroves, ne pénètre pas profondément dans le substrat anoxique mais se développe latéralement selon des morphologies variées (Hogarth 2015). Les racines en échasse sont typiques des *Rhizophora* et sont recouvertes de lenticelles qui forment des pores permettant le passage de l'oxygène. Les *Avicennia* et les *Sonneratia* ont des racines horizontales qui s'étendent sur plusieurs mètres et d'où sortent des structures verticales nommées pneumatophores qui sont à la fois photosynthétiques et recouvertes de lenticelles et enfin, les *Bruguiera* et les *Xylocarpus* ont des racines formant régulièrement un coude qui perce la surface du sol (Figure 0-4).

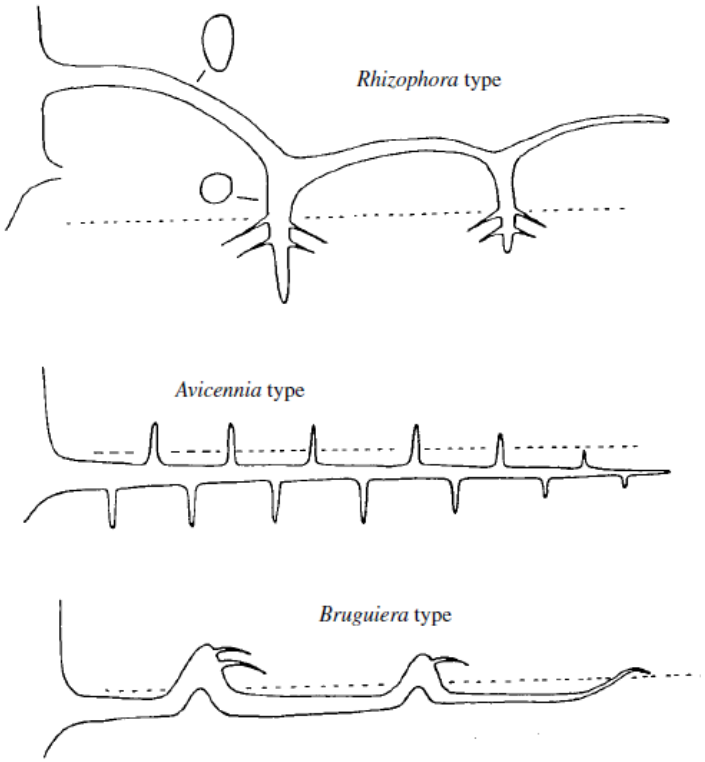

Figure 0-4 : Différentes formes de systèmes racinaires des palétuviers. Extrait de Hogarth (2015)

1.2.3. Reproduction

Pour coloniser et se maintenir à l'interface entre la terre et l'océan, qui est une zone d'échange importante soumise à la houle et aux courants marins, certains palétuviers ont développé des mécanismes de reproduction particuliers. L'un des plus répandus est la viviparité, dont la forme la plus avancée s'observe dans le genre *Rhizophora* et qui consiste en la germination et le développement de propagules sur la plante mère (Hogarth 2015). Ces embryons ne se déshydratent pas et n'entrent pas dans une phase de dormance, comme les graines classiques, mais germent, se développent et commencent leur activité photosynthétique alors qu'ils sont encore attachés à leur plante mère, profitant ainsi des apports nutritifs de leur hôte en restant protégés d'une agression prématurée par l'eau salée. Les *Avicennia* et *Aegiceras* présentent une forme de reproduction très similaire avec des propagules plus petites et nommée cryptoviviparité, tandis que d'autres genres se reproduisent de manière plus conventionnelle et forment des fruits et graines allant d'une très petite taille pour les espèces de *Sonneratia* jusqu'à un fruit de 3 kg pour les *Xylocarpus*. Lorsque la marée est haute les propagules qui se détachent de leur hôte se plantent directement dans le sédiment découvert et se développent au pied de leur plante mère,

tandis qu'à marée haute elles flottent et sont transportées par le courant. La faculté de dispersion des propagules dépend de leur temps de flottaison, allant de quelques jours pour *Avicennia marina* et sans limitation de durée pour *A. germinans*, et du temps pendant lequel elles peuvent rester viables, oscillant de quelques semaines pour *Laguncularia racemosa* à plusieurs mois pour les *Rhizophora*.

1.3. Services écosystémiques

Les mangroves sont des écosystèmes qui fournissent d'importants services d'ordre économique, social et environnemental et que l'on regroupe sous le nom de services écosystémiques. Ces bénéfices peuvent être classés selon plusieurs catégories incluant la contribution à de bonnes relations sociales entre les populations, comprenant les usages spirituels, religieux et récréatifs, la sécurité, sur le plan de l'accès aux ressources naturelles et de la protection face aux évènements climatiques, la santé, à la fois des hommes et des écosystèmes, et enfin, la fourniture de ressources naturelles (Figure 0-5).

Une grande partie des services fournis par la mangrove a une portée essentiellement locale et bénéficie aux populations vivant à proximité. Parmi les plus importants on retrouve l'utilisation des palétuviers et d'autres plantes associées ; à la fois pour la construction d'habitations, le chauffage, la production de charbon, la fabrication de meubles et de nasses à poissons, et la récole de miel, fruits, produits pharmaceutiques, vin et palmes pour la confection des toits d'habitation (Duke et al. 2014). La diversité des espèces et l'héritage culturel associé à ces milieux ont permis d'en établir une très grande diversité d'usages, incluant aussi la pêche et la récolte de bivalves, gastéropodes, crustacés et poissons. L'exploitation de ces milieux génère peu de revenus car l'effort de capture est important comparé à la valeur marchande de la plupart des espèces récoltées. Cependant, les mangroves fournissent à des petites communautés des moyens de subsistance qu'il est possible d'obtenir avec peu de moyens. La quantité de poissons et de fruits de mer récoltés dans les mangroves est en moyenne de 90 kg/ha/an, et peut aller jusqu'à 225 kg/ha/an (FAO 2007). Dans les pays ayant des populations pauvres et vulnérables, notamment en Afrique, Asie et Amérique du Sud, elles fournissent aux familles un complément de revenus en conditions normales et peuvent assurer la survie des populations en cas de crise alimentaire, comme l'on en connait aujourd'hui encore au Nigeria, en Somalie ou au Yémen (FAO 2007).

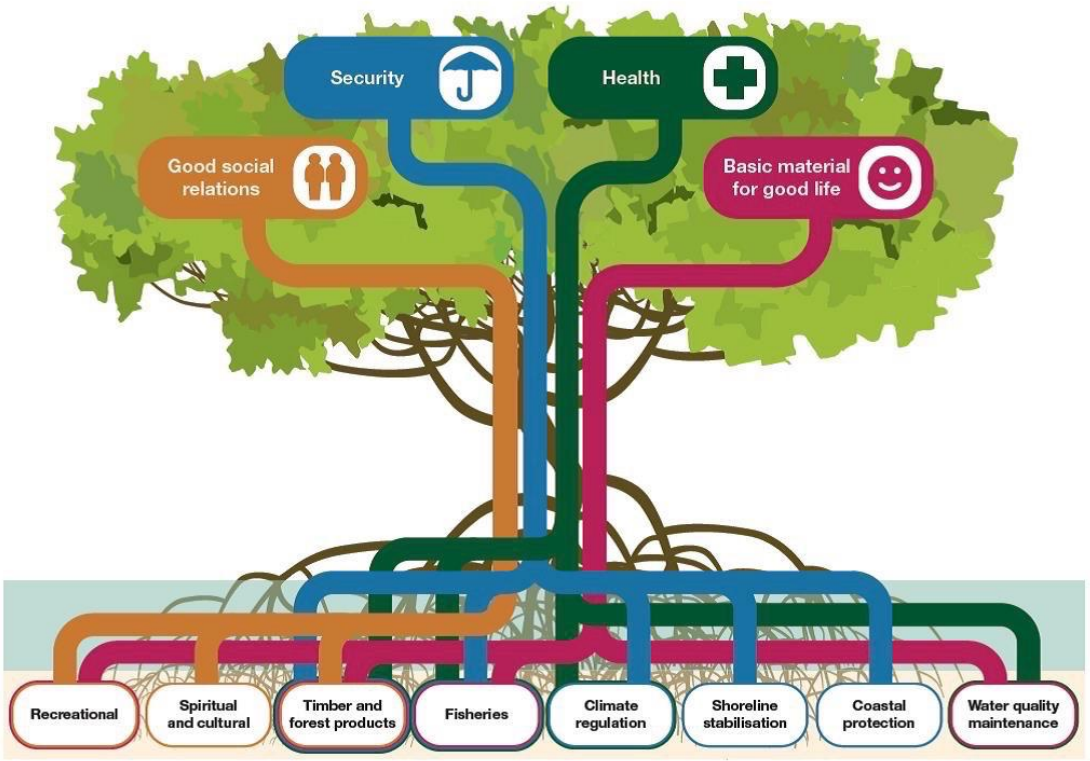

Figure 0-5 : Principaux bénéfices de la mangrove et liens avec des grandes catégories de services écosystémiques. Extrait de Duke et al. (2014)

En plus de la fourniture de ressources naturelles que l'on peut qualifier de services réguliers, les mangroves constituent une barrière physique à des phénomènes climatiques imprévisibles ou chroniques comme le sont les tsunamis et les cyclones. Lorsque les vagues traversent la mangrove, l'énergie est dissipée par la présence des racines, des troncs et du feuillage, conduisant à une diminution de 20 à 90% de l'énergie des vagues pour 100 m de mangrove traversés (Mazda et al. 1997, Alongi 2008). En Floride, des observations de terrain couplées à la modélisation numérique ont montré une diminution de 40 à 50 cm de la hauteur des inondations par kilomètre de mangrove traversé lors d'un cyclone à progression rapide (Zhang et al. 2012). Sur des terrains relativement plats comme certaines zones sur lesquelles se développent les mangroves, cette diminution peut grandement réduire les surfaces endommagées par les tsunamis et les cyclones. C'est pourquoi, à la suite du typhon Haiyan, qui a fait plus de 6000 morts en novembre 2013 aux Philippines, le gouvernement a décidé d'investir 20 millions de dollars dans la plantation de mangroves, dont 50% des surfaces naturelles avaient été rasées depuis 1918, d'abord pour en exploiter le bois, puis plus récemment afin de créer des bassins d'élevage de crevettes (Duke et al. 2014).

D'autres services écosystémiques ont une portée plus large et contribuent aux équilibres mondiaux du climat et à la reproduction des espèces marines. Les mangroves séquestrent d'importantes quantités de carbone en raison de leur productivité primaire et de l'accumulation de sédiments provenant de l'amont des bassins versants. La faible respiration des sols due au manque d'oxygène permet un stockage à long terme de ce carbone, offrant des perspectives de piégeage de carbone d'origine anthropique et de lutte contre le changement climatique (Howard et al. 2017). Ce piégeage est estimé à 226 ± 39 g C/m^2/an, soit environ 36 ± 6 Tg C/an pour la totalité des mangroves de la planète (Mcleod et al. 2011). Le puits de carbone constitué par les mangroves correspond à 0.9% de l'accumulation annuelle de carbone atmosphérique induite par les activités humaines (4 Pg C/an ; Ciais et al. 2014). Cette valeur reste faible mais loin d'être insignifiante en considérant que les mangroves occupent seulement 0.03% de la superficie totale de la planète. Par ailleurs, les mangroves fournissent de la nourriture en abondance et de nature variée pour les espèces animales, incluant les feuilles d'arbres, mais aussi le phytoplancton, les micro-algues benthiques, lichens, biofilms, etc. (Robertson et Blaber 1992, Lee et al. 2001, Bouillon et al. 2004). Leur structure physique complexe induite par les racines aériennes, les faibles profondeurs et la turbidité importante réduit la pression de prédation comparée aux écosystèmes adjacents. Ainsi, les mangroves servent de refuge et de zone de reproduction pour une grande quantité d'espèces marines, soutenant ainsi le recrutement et la productivité secondaire des écosystèmes côtiers (Beck et al. 2001, Nagelkerken et al. 2008). Lorsque les mangroves sont détruites, une réduction du volume des pêches sur les côtes à proximité est généralement constatée. Cette réduction pourrait représenter 480 kg de poisson par an et par hectare de mangrove déboisé (FAO 2007).

2. Dynamique du carbone dans les estuaires tropicaux

2.1. Origine et sources

Le carbone est le principal atome constituant les molécules du vivant. Il représente environ 50% de la biomasse sèche de la matière organique aquatique (Cabaniss et al. 2005) et ainsi, sa disponibilité est indispensable au soutien des réseaux trophiques. L'étude du cycle biogéochimique du carbone est par ailleurs nécessaire à la compréhension des mécanismes qui induisent les changements climatiques actuels, notamment causés par deux gaz à effet de serre : le dioxyde de carbone (CO_2) et le méthane (CH_4) (Borges et Abril 2011, Bianchi et Bauer 2011).

Au sein des réseaux hydrographiques, le carbone est transporté à la fois sous forme organique et inorganique, la seconde étant en quantités légèrement supérieure à la première (Huang et al. 2012). Les estuaires sont localisés à l'interface entre le milieu terrestre et océanique et reçoivent de ce fait des apports depuis le bassin versant environnant et depuis la zone côtière. La matière organique provenant de l'amont est constituée de fragments de végétaux, animaux ou excréments d'animaux terrestres récoltés par les rivières à la suite du ruissellement des eaux de surface, tandis que la matière provenant de l'océan est synthétisée principalement par les algues unicellulaires qui se développent dans la zone photique de la colonne d'eau (Bianchi et Bauer 2011). Le carbone inorganique, quant à lui provient essentiellement de la dissolution des roches carbonatées ($CaCO_3$; Huang et al. 2012) et de la minéralisation de la matière organique. La productivité primaire au sein même des estuaires varie en fonction de la disponibilité des nutriments, de la turbidité qui limite la pénétration de la lumière et de facteurs physiques comme la température ou la dynamique des échanges avec l'océan (Cloern et al. 2014). La valeur moyenne de la productivité primaire du phytoplancton y est de 252 g C/m^2/an, avec une majorité de valeurs de production nette en estuaires tropicaux allant de 100 à 500 g C/m^2/an (Cloern et al. 2014), soit des valeurs bien inférieures à la productivité nette des mangroves qui se développent à leur proximité immédiate (1 362,5 ± 450 g C/m2/an ; Bouillon et al. 2008a). En raison de l'importance des apports depuis l'amont, la respiration excède généralement la production primaire et ainsi la plupart des estuaires sont net hétérotrophes, c'est à dire qu'ils libèrent plus de carbone minéral qu'ils n'en fixent. Le CO_2 étant ainsi sursaturé dans l'eau par rapport à l'atmosphère,

contrairement aux océans, les estuaires libèrent du CO_2 qui est émis à l'interface eau/air (Chen et al. 2013).

Les formes organiques et inorganiques du carbone sont divisées en fractions dissoute et particulaire sont la séparation dépend principalement de raisons méthodologiques (Harvey 2006). Ces fractions séparent les molécules libres de celles contenues dans les cellules ou fixées à des agrégats de matière (Figure 0-6). La taille limite qui sépare les deux fractions est généralement de 0,20, 0,45 ou 0,70 µm, ce qui correspond à la porosité des filtres en acétate de cellulose ou en fibre de verre (GF/F) les plus couramment utilisés pour l'échantillonnage.

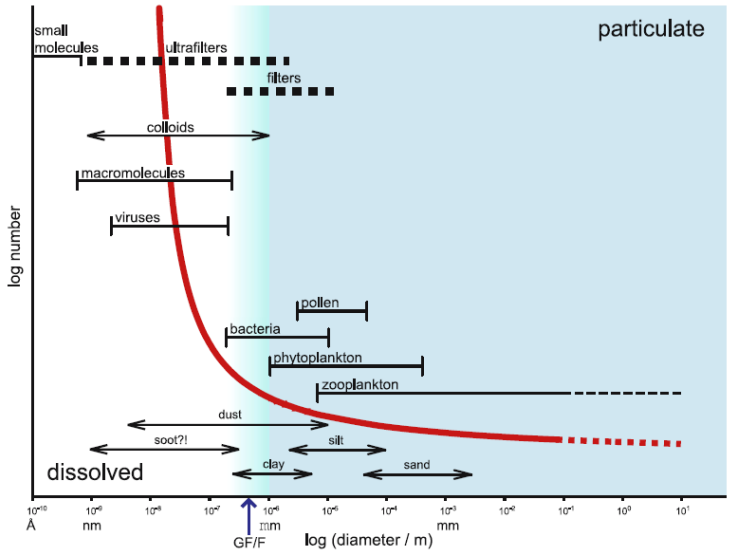

Figure 0-6 : Principales particules rencontrées dans les milieux aquatiques et leur diamètre en fonction de leur abondance (données log). La zone de transition entre les couleurs indique la taille limite qui sépare généralement la fraction dissoute de la fraction particulaire à l'aide de filtres GF/F.
Extrait de Harvey (2006)

Hors de l'eau, au niveau des zones non immergées des mangroves, le carbone est fixé en grande majorité par les palétuviers mais aussi par des plantes associées et des micro- et macro-algues benthiques ou fixées aux racines et sur les troncs des arbres (Hogarth 2015). Les recherches se sont à l'origine focalisées sur les feuilles mortes comme base de la chaine alimentaire dans les réseaux trophiques de mangrove (Odum et Heald 1975). Cependant, des études plus récentes mettent en évidence le rôle des feuilles vivantes, fleurs, pollens et propagules dans le soutien des réseaux trophiques, ainsi que des sources ne provenant pas des palétuviers comme les micro- et macro-algues benthiques ou épiphytes et le phytoplancton (Wafar et al. 1997, Sousa et Dangremond 2011). En effet, les feuilles d'arbre ont un ratio carbone/azote (C/N) bien trop élevé pour pouvoir être considérées comme de

bonne qualité nutritionnelle pour les organismes vivants et la manière dont les organismes qui se nourrissent de feuilles obtiennent l'azote nécessaire à leur métabolisme reste un mystère (Harada et Lee 2016). Les micro- et macro-algues, les plantes vasculaires marines et les bactéries ont quant à elles un ratio C/N bien plus bas (Bianchi et Bauer 2011) et compatible avec une fourniture d'azote en quantité suffisante pour les consommateurs.

2.2. Spéciation

Sous sa forme inorganique, le carbone dissous (DIC ; « dissolved inorganic carbon ») se divise en quatre espèces chimiques : CO_2, H_2CO_3, HCO_3^- et CO_3^{2-} (Park 1969). Les deux premières sont souvent regroupées sous la forme $CO_{2\,(aq)}$. Elles sont liées par une constante de solubilité (K_0) qui diminue à la fois avec la température et avec la salinité (Weiss 1974). Les espèces $CO_{2(aq)}$, HCO_3^-, et CO_3^{2-} sont liées à des constantes de dissociation (K_1 et K_2), qui varient elles aussi en fonction de la température et de la salinité (Millero et al. 2006, Millero 2010). Les pK_1 et pK_2 de l'acide carbonique varient respectivement de 8,8 à 9,6 et de 5,8 à 6,2, avec les valeurs les plus faibles observées à forte salinité et haute température. Ainsi, aussi bien dans les grandes rivières dont le pH varie de 5 à 9 (Abril et al. 2015), que dans les eaux océaniques qui ont un pH de 7,9 à 8,2 (Takahashi et al. 2014), le carbone dissous est principalement sous sa forme HCO_3^-.

Le carbone inorganique particulaire (PIC ; « particulate inorganic carbon ») se retrouve quant à lui dans les grandes rivières principalement sous la forme de débris de roches carbonatées ($CaCO_3$; Meybeck 1982). Il est souvent peu considéré dans les études portant sur la dynamique du carbone. D'une part, car sa concentration est liée à celle du carbone dissous et lui est environ 2 à 80 fois inférieure (Huang et al. 2012). D'autre part, car son étude nécessite une méthodologie particulière avec deux analyses pour un même échantillon, l'une du carbone particulaire total et l'autre du carbone particulaire organique, le PIC étant la différence des deux. Dans la zone pélagique des océans, par opposition aux grandes rivières, le PIC se trouve dans le squelette des coccolithophores. Lorsqu'elles meurent, ces algues unicellulaires sédimentent dans l'océan profond et forment les roches carbonatées qui seront de nouveau érodées par les rivières plusieurs millions d'années plus tard.

Sous sa forme organique, le carbone dissous (DOC ; « dissolved organic carbon ») est contenu en partie dans les protéines, les polysaccharides et les lipides mais une grande partie

des formes chimiques sous lesquelles se trouve ce carbone est encore indéterminée (Mannino et Harvey 2000, Harvey 2006). Après 100 jours de dégradation, une matière organique dissoute d'origine algale perd plus de 94% de sa biomasse et presque la totalité de la biomasse restante est de nature indéterminée (Harvey 2006). La matière organique dissoute est souvent caractérisée par son poids moléculaire plutôt que par sa composition chimique, et la majeure partie du DOC des océans est de faible poids moléculaire (< 1000 Da) et résistant à la dégradation biologique (Harvey 2006). Le DOC joue cependant un rôle central dans le recyclage du carbone (Figure 0-7) car c'est sous cette forme que les bactéries sont capables de l'assimiler et de rendre les nutriments de nouveau disponibles pour les producteurs primaires selon un cycle nommé « boucle microbienne » (Azam 1998).

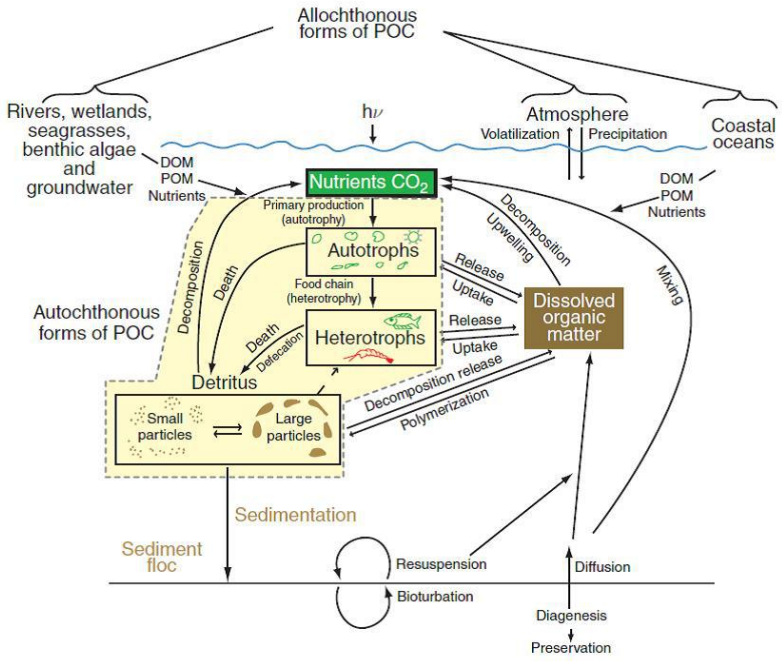

Figure 0-7 : Cycle biogéochimique du carbone en zone estuarienne mettant en avant la position centrale du DOC dans le recyclage de la matière organique. Extrait de Bianchi et Bauer (2011)

Le carbone organique particulaire (POC ; « particulate organic carbon ») est principalement contenu dans des acides aminés et des polysaccharides (Mannino et Harvey 2000). La matière organique qui en est composée est constituée d'organismes unicellulaires et de fragments végétaux ou animaux agrégés entre eux par des processus de coagulation (Verney et al. 2009, Bianchi et Bauer 2011). Les particules exopolymériques transparentes (TEP ; « transparent exopolymeric particles »), qui peuvent être formées par des processus biotiques et abiotiques (Passow 2002), jouent un rôle important dans l'agrégation du POC et

le cycle du carbone (Mari et al. 2017). En effet, en fixant des composés organiques dissous ou de petite taille dans une matrice collante, les TEP court-circuitent la boucle microbienne et rendent accessible une partie de la matière organique aux échelons trophiques supérieurs (Passow 2002). Dans les zones estuariennes, l'agrégation des particules est particulièrement importante en raison de l'énergie transmise par le courant et du cycle de remise en suspension de la matière, floculation, chute, déposition et érosion (Verney et al. 2009).

2.1. Outils de suivi

L'étude de la dynamique du carbone et la compréhension des mécanismes qui lui sont liés fait appel à des outils de mesure à la fois quantitatifs et qualitatifs. Ces outils permettent de mesurer la masse de carbone dans chacun des compartiments à un instant donné, de quantifier des processus qui permettent sa transformation et le passage d'un compartiment à l'autre, et enfin de déterminer l'origine et la nature des sources qui ont contribué à enrichir ces compartiments.

2.1.1. Analyse des quantités

Quelle que soit la spéciation initiale du carbone considéré, sa quantification se fait le plus souvent sous ses formes gazeuses (CO_2, CO, CH_4) et par l'intermédiaire d'un analyseur à infra-rouge (IRGA ; « infrared gas analyser »). L'air à analyser est injecté dans un tube à une extrémité duquel est émis un rayon infra-rouge qui est ensuite réceptionné à l'autre extrémité. La différence d'intensité du rayon entre l'émission et la réception est proportionnelle à la pression partielle du gaz analysé. Ces analyses peuvent être effectuées directement sur le terrain à l'aide d'appareils portatifs (Image 0-2a), permettant ainsi de mesurer la composition chimique de l'air atmosphérique ou de l'air contenu dans un volume confiné donné. Dans le cas de la mesure de la pression partielle des gaz dans la colonne d'eau, il est nécessaire d'utiliser un équilibreur qui permet d'accélérer les échanges gazeux entre la colonne d'eau et l'air extérieur (Frankignoulle et al. 2001). Il en existe plusieurs types, avec chacun ses avantages et ses inconvénients (Santos et al. 2012, Webb et al. 2016). Dans les estuaires, les plus utilisés sont constitués d'un cylindre vertical rempli de billes de verre (« marble equilibrator » ; Frankignoulle et al. 2001 ; Image 0-2b) ou à l'intérieur duquel l'eau est injectée par un asperseur (« shower head equilibrator » ; Santos et al. 2012). L'équilibreur

permet d'obtenir un volume d'air dont la pression partielle de chacun des gaz est égale à celle de l'eau analysée, et qui est connecté à un IRGA par un circuit fermé.

Pour les autres formes du carbone le principe général est le même, mais l'analyse nécessite des équipements plus précis et doit se faire en laboratoire. L'équilibreur est remplacé par une chambre d'oxydation catalytique qui permet d'oxyder toutes les molécules contenant du carbone en dioxyde de carbone (CO_2), puis l'analyse consiste à mesurer la quantité de CO_2 ainsi produite avec un IRGA. L'échantillon, qui peut être de l'eau filtrée pour l'analyse du carbone dissous ou le filtre ayant servi à la filtration pour le carbone particulaire, est placé dans une chambre close et oxydé à haute température (680°C pour les appareils Shimadzu® TOC-L). Avant l'oxydation, l'échantillon est traité à l'acide puis le gaz est purgé et ainsi l'appareil analyse uniquement les formes organiques du carbone.

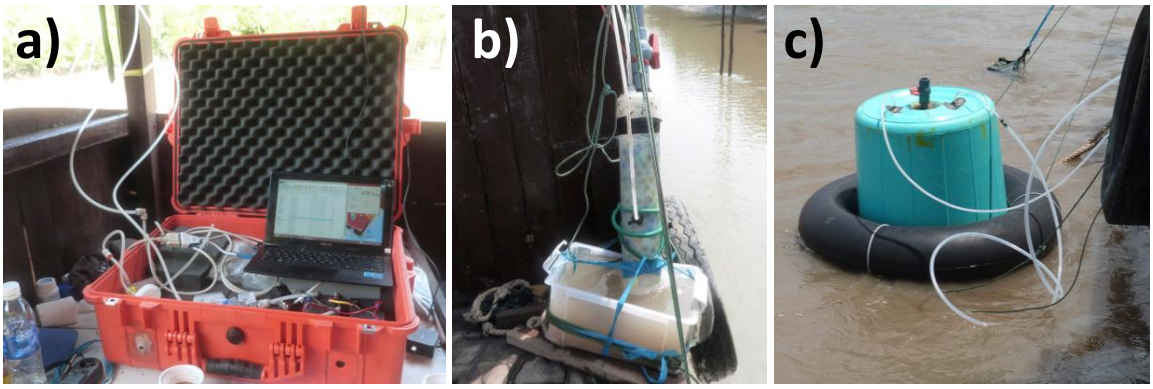

Image 0-2 : Equipements utilisés pour l'analyse du CO_2 lors des campagnes d'échantillonnage. a) analyseur infra-rouge (IRGA) ; b) équilibreur à billes ; c) chambre d'incubation flottante

Le DIC se quantifie généralement de manière indirecte à partir de l'alcalinité due aux carbonates et du pH de l'échantillon (Park 1969). Dans les eaux de surface, l'alcalinité due aux carbonates est généralement assimilée à l'alcalinité totale (Talk ; « Total Alkalinity »), qui correspond à la capacité de l'eau à neutraliser un acide, soit à la quantité d'acide nécessaire pour amener le pH de l'échantillon à 7. L'analyse se fait par incréments successifs d'acide chlorhydrique (HCl) en et surveillant les variations du pH. Les constantes de dissociation de l'acide carbonique (Millero et al. 2006, Millero 2010) sont ensuite utilisées pour calculer les concentrations de chacune des formes du carbone composant le DIC.

2.1.2. Analyse de processus

L'analyse des quantités permet d'obtenir un bilan à un instant donné de la répartition du carbone dans un environnement, tandis que l'étude des processus de transformation de ce carbone ou de la cinétique de passage d'un compartiment à un autre permet d'ajouter une notion de dynamique aux études, et de prédire la cinétique de variation des stocks de chacun des compartiments. Les processus les plus étudiés dans les estuaires sont la respiration aérobie et la production primaire (Cloern et al. 2014). Le premier consomme de l'oxygène pour transformer les formes organiques du carbone en CO_2 et en retirer de l'énergie, tandis que le second utilise du CO_2 pour synthétiser de la matière organique et rejeter de l'oxygène. La quantification de ces deux processus se fait de manière similaire, à l'aide d'une mesure initiale d'oxygène dans un échantillon d'eau, ensuite placé dans un contenant ne permettant pas d'échanges avec l'air environnant. Une seconde mesure faite après un temps d'incubation induisant une variation significative de la quantité d'oxygène permet d'estimer la respiration ou la production.

Un autre processus important lorsque l'on s'intéresse au rôle des estuaires tropicaux dans la régulation du climat est l'émission des gaz à effet de serre, le principal étant le CO_2. Les estuaires sont généralement net hétérotrophes et libèrent du CO_2 qui est émis à l'interface eau/air (Chen et al. 2013). Ces flux peuvent être estimés par des équations tenant compte de lois physiques et intégrant des variables comme la vitesse du vent et du courant, la turbidité ou la profondeur de la masse d'eau (Wanninkhof et al. 1992, Raymond and Cole 2001, Borges et al. 2004, Abril et al. 2009, Ho et al. 2016). La fiabilité de ces équations est cependant beaucoup critiquée, notamment dans les estuaires très dynamiques des zones tropicales où la turbulence et la température de l'eau élevée peuvent induire des émissions particulièrement importantes (Müller et al. 2016). D'autres méthodes utilisant le rejet puis le traçage de gaz rares (Ho et al. 2016), l'utilisation d'un dispositif d'Eddy Covariance (Huotari et al. 2013) ou le déploiement de chambres d'incubation flottantes ont aussi été employées (Guerin et al. 2007, Lorke et al. 2015, Leopold et al. 2017). Ces dernières sont positionnées à l'interface eau/air et enferment un volume d'air qui se charge progressivement des gaz émis par la colonne d'eau qu'elles surplombent (Image 0-2c). Une boucle en circuit fermé permet à l'air de la chambre de passer dans un IRGA et la pente de la droite de régression entre le

temps et la pression partielle en CO_2, ramenée au volume de la chambre et à la surface de contact eau/air, permet de quantifier les échanges (Figure 0-8).

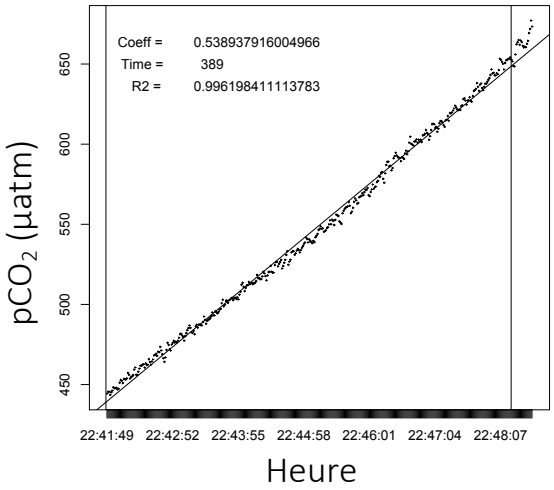

Figure 0-8 : Exemple de variation temporelle de la pression partielle en CO_2 dans une chambre d'incubation positionnée à l'interface eau/air. Coeff = pente de la droite de régression en µatm/seconde ; Time = temps au cours duquel la droite de régression est calculée (les deux lignes verticales symbolisent le début et la fin de l'intégration) ; R2 = coefficient de détermination du modèle linéaire. Fréquence d'acquisition de l'IRGA = 1 valeur par seconde (1 Hz)

Enfin, certains outils permettent d'estimer la cinétique de dégradation de molécules spécifiques par les organismes vivants et le recyclage du carbone. L'analyse de l'activité de dégradation de l'enzyme α-aminopeptidase est l'une des méthodes les plus couramment utilisées comme indicateur de la dégradation des protéines par les organismes procaryotes (Hoppe et al. 1993, Lamy et al. 2009). Le principe est d'ajouter dans un échantillon un substrat protéique (leucine) dont le carbone α est lié à une molécule qui devient fluorescente lorsqu'elle est séparée de son substrat, la 7-Amino-4-methylcoumarine (Hoppe et al. 1993). La quantité de fluorochrome libérée au bout d'un temps d'incubation donné représente l'activité potentielle de dégradation, tenant compte du fait que dans les conditions de l'expérience le substrat est largement en excès, contrairement au milieu naturel. Cet indicateur ne permet pas de relier directement une activité potentielle à une quantité de carbone libérée par unité de temps dans le milieu naturel, mais elle permet de comparer des sites entre eux et de mettre en évidence des zones particulièrement favorables à la dégradation (Cunha et al. 2000, Patel et al. 2000, Cunha et Almeida 2006). L'activité potentielle de dégradation de l'enzyme α-aminopeptidase est influencée par la quantité de matière organique présente dans le milieu naturel (Lamy et al. 2009), mais aussi par son origine et sa composition qualitative (Baltar et al. 2017).

2.1.3. Marqueurs qualitatifs

Afin de déterminer l'origine et la nature des sources qui ont contribué à enrichir les différents compartiments du carbone, on utilise des marqueurs moléculaires. La matière organique dissoute et particulaire des estuaires constitue un réservoir composite de matière vivante et détritique d'origine aquatique et terrestre et fortement remaniée lors du transit estuarien (Bianchi et Bauer 2011). Afin de tracer l'origine de ce carbone sous ses différentes formes, l'un des marqueurs les plus communs est la signature isotopique ($\delta^{13}C$). Dans le milieu naturel, le carbone est présent sous la forme de deux isotopes stables, le carbone 12 (^{12}C) et le carbone 13 (^{13}C). Lors de la photosynthèse, les plantes fixent préférentiellement le carbone le plus léger (^{12}C), induisant un appauvrissement du rapport $^{12}C/^{13}C$ ($\delta^{13}C$ en ‰) dans la matière organique produite par rapport au CO_2 (ou HCO_3^-) environnant. Selon des spécificités du métabolisme de chaque grand groupe d'espèces végétales, le fractionnement isotopique, c'est à dire la différence entre le rapport $^{12}C/^{13}C$ de la source de carbone et celui de la matière produite, est différent (Figure 0-9). Ce ratio est assez peu remanié lors de la décomposition microbienne (Bouillon et al. 2011) et ainsi la signature isotopique du mélange de matière vivante et détritique des estuaires reflète les différentes sources la constituant. Par convention, le $\delta^{13}C$ est exprimé relativement à un standard mondial constitué de rostres de bélemnites provenant d'un gisement de Caroline du Sud (« Pee Dee Belemnite »). Il est mesuré par combustion de l'échantillon à analyser et injection du CO_2 ainsi produit dans un spectromètre de masse. Les appareils utilisés mesurent aussi la quantité de carbone organique présente dans l'échantillon.

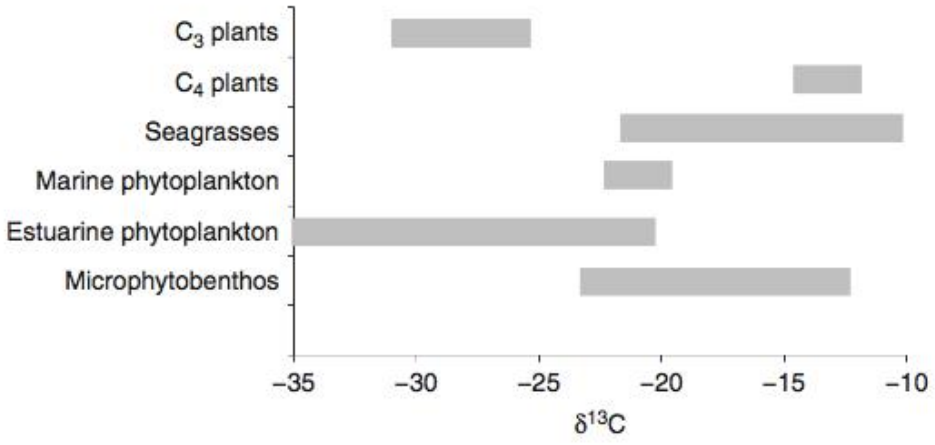

Figure 0-9 : Gamme de signatures isotopiques $\delta^{13}C$ rencontrées dans différents grands groupes de producteurs primaires des écosystèmes estuariens. Extrait de Bouillon et al. (2011)

Un autre marqueur qualitatif du carbone dont la fiabilité a été largement démontrée est l'analyse des acides gras, qui sont les principaux constituants des lipides. Bien que leur contribution au carbone organique total soit faible (0,1 à 5% ; Currie et Jones 1988, Canuel 2001), ils sont des composants essentiels du vivant (Bergé et Barnathan 2005). Certains sont exclusivement synthétisés par des groupes définis d'organismes ou en proportion spécifique (Kaneda 1991, Dalsgaard et al. 2003). Ainsi, leurs proportions relatives dans la matière organique reflète elles aussi les différentes sources la constituant (Meziane et al. 1997, Bodineau et al. 1998, Mortillaro et al. 2012, Boëchat et al. 2014). Cependant, ils sont rapidement dégradés suite à la mort cellulaire, notamment ceux possédant plusieurs insaturations (Wakeham 1995, Marty et al. 1996, Pan et al. 2014). Ainsi, dans les milieux aquatiques les acides gras sont principalement utilisés comme indicateurs de la biomasse vivante, capables de mettre en évidence des efflorescences algales, des développements bactériens ou des apports relativement récents de matière détritique (Napolitano et al. 1997, Meziane et Tsuchiya 2002, Xu et Jaffé 2007, Moynihan et al. 2016). Etant donné les faibles quantités de lipides dans la matière organique, l'analyse des acides gras se fait uniquement sur la matière particulaire qui peut être concentrée et récoltée en quantité suffisante par filtration. Les acides gras sont d'abord extraits d'un échantillon par ajout d'une mixture d'eau/méthanol/chloroforme (1/2/1), puis saponifiés pour briser les liaisons esters (1h30 ; 90°C) et enfin méthylés et injectés en chromatographie en phase gazeuse pour être séparés puis identifiés. Une vidéo détaillant le protocole d'analyse utilisé au laboratoire et adapté de Bligh and Dyer (1959) et Meziane et al. (2007), filmée et montée par un groupe d'étudiants de licence, est disponible ici: https://www.youtube.com/watch?v=WsHqAMDsLX0.

Ces mêmes marqueurs isotopes et acides gras sont utilisés pour qualifier les relations trophiques entre les différentes espèces végétales et animales d'un écosystème et le transfert de la matière organique dans les réseaux trophiques (Fry 2006, Budge et al. 2006, Kelly et Schiebling 2012). En plus de la signature isotopique du carbone, d'autres éléments sont utilisés tels que l'azote, le souffre, l'oxygène et l'hydrogène (Fry 2006), ce qui rajoute des variables dans les modèles de mélange bayésiens utilisés pour préciser le régime alimentaire des espèces étudiées (Parnel et al. 2010). L'utilisation de ces marqueurs est basée sur le principe d'assimilation des substances nutritives avec le moins de remaniement possible, induisant une composition moléculaire d'un consommateur proche de celle de ses proies (« you are what you eat »). Ces principes sont tout de même à considérer avec certaines

précautions. Ainsi, les consommateurs fixent préférentiellement l'isotope le plus lourd et utilisent l'isotope le plus léger pour leur métabolisme, ce qui induit une augmentation des ratios isotopiques dans les consommateurs par rapport à leurs proies selon un facteur de fractionnement. Ce dernier est d'environ +0,5‰ pour le carbone et +2,3‰ pour l'azote (McCutchan et al. 2003), qui sont les deux éléments les plus étudiés, mais varie selon l'espèce considérée et la source de nourriture ingérée (Vanderklift et Ponsard 2003, Bui et Lee 2014). La composition en acides gras des organismes, quant a elle, dépend de la quantité de lipides stockés dans les tissus adipeux sans modification, du remaniement métabolique des acides gras voués à remplir des fonctions spécifiques comme assurer la fluidité membranaire, et de la biosynthèse de nouvelle molécules (Budge et al. 2006). Ces facteurs varient eux aussi en fonction de l'espèce considérée, mais aussi de leur état physiologique et des conditions du milieu (Hall et al. 2006, Meziane et al. 2007, Pan et al. 2014).

3. Pressions anthropiques subies

3.1. Déforestation

De par leur localisation à l'interface entre la terre et l'océan, les mangroves sont des écosystèmes hautement soumis à la pression anthropique. Les activités humaines sont la principale cause de la répartition inégale de la population mondiale, avec une plus forte densité sur les côtes océaniques en raison de l'accès à l'eau et des possibilités de transport et d'échanges commerciaux. Entre 1980 et 2005, la superficie totale des mangroves mondiale est passée de 188 000 à 152 000 km^2, avec une diminution de 1% par an entre 1980 et 1990 et de 0.66% par an entre 2000 et 2005 (FAO 2007). Les plus fortes diminutions se retrouvent en Asie, qui concentre environ 40% des mangroves de la planète et où le taux de déboisement était de 1.4% par an entre 1980 et 1990 et de 1% par an entre 2000 et 2005 (FAO 2007). Ce taux est cependant en diminution grâce à la prise de conscience des services écosystémiques fournis par les mangroves et la mise en place de zones protégées. En Asie du Sud-est, le taux annuel de déboisement des mangroves était de 0.18% entre 2000 et 2012. La plus forte diminution de superficie a eu lieu en Indonésie, avec 480 km^2 de mangroves détruites sur la période, et la plus forte proportion de la superficie totale a été déboisée au Myanmar, avec 5.5% perdus entre 2000 et 2012, soit 278 km^2 (Richards et Friess 2016). L'aquaculture est la principale cause de la déforestation des mangroves en Asie du Sud-est, et 30% des mangroves déboisées ont été converties en bassins aquacoles entre 2000 et 2012, avec une dominance particulièrement marquée en Indonésie (Figure 0-10).

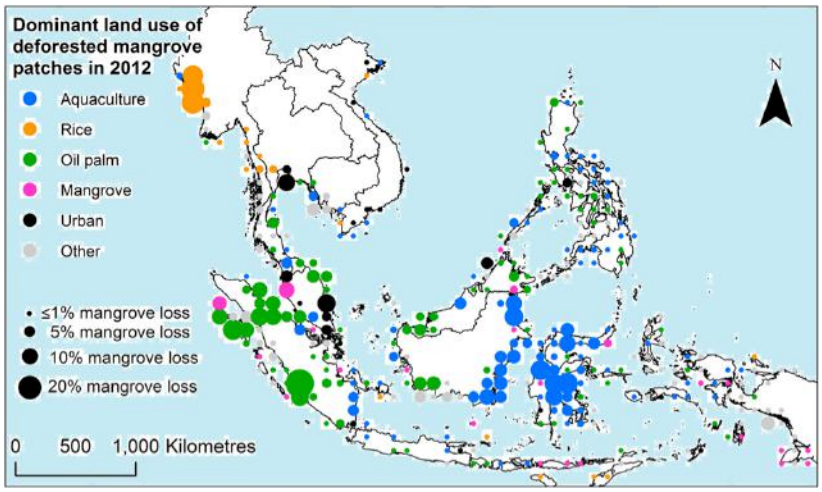

Figure 0-10 : Pourcentages de mangroves perdues (« loss ») entre 2000 et 2012 en Asie du Sud-est et type d'utilisation des sols ayant suivi la déforestation. Modifié de Richards et Friess (2016)

L'élevage des crevettes tropicales nécessite des renouvellements d'eau réguliers dans les bassins et une salinité comprise entre 10 et 30‰, faisant des mangroves un lieu idéal pour l'établissement des zones de production (Anh et al. 2010). La crevetticulture a connu un développement exponentiel depuis une trentaine d'années avec une croissance moyenne de 11% par an entre 1984 et 2015 (FAO 2017). En 2015, l'Asie concentrait 85% de la production mondiale de crevettes pénéides, avec 4 pays dominant la production mondiale qui sont la Chine (1 900 000 t), l'Indonésie (600 000 t), le Vietnam (550 000 t) et l'Inde (500 000 t) (Figure 0-11). Les autres causes majeures de la déforestation des mangroves sont la riziculture, responsable de 87.6% de la destruction des mangroves au Myanmar, et la plantation de palmiers à huile, responsable de 38.2% des pertes en Malaisie (Figure 0-10).

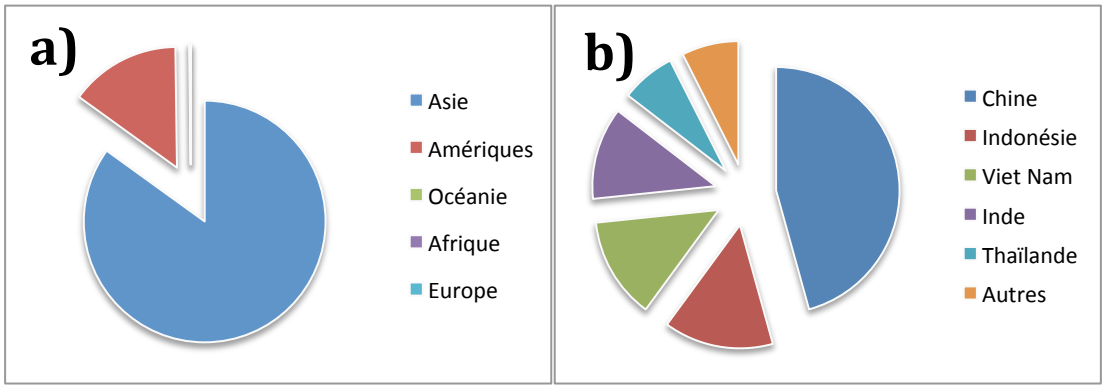

Figure 0-11 : Répartition a) de la production mondiale de crevettes pénéides par continent et b) de la production asiatique par pays. Données issues de FAO (2017)

Au Vietnam, les mangroves ont subi successivement les effets de pratiques sylvicoles inadaptées, favorisant la monoculture de *Rhizophora apiculata*, la destruction de la végétation et des sols par l'épandage massif de défoliants pendant la guerre (1963-1975) et enfin l'intense développement de la crevetticulture. L'ex-Indochine (Vietnam, Cambodge) comptait 4 500 km^2 de mangroves dans les années 1940, incluant 3 300 km^2 dans le bassin du Mékong dont 2 000 km^2 dans la seule péninsule de Ca Mau, à l'extrémité sud du pays (Fromard et Kiet 2002). En 1964, juste avant les bombardements de la guerre et l'épandage massif de défoliants, la mangrove du Vietnam du sud couvrait 2 100 km^2, dont 1 500 km^2 dans la région de Ca Mau. En 1980, le chiffre de 2 700 km^2 pour l'ensemble du pays est donné, puis 2 100 km^2 en 1990 et enfin 1 600 km^2 en 2000 (FAO 2007). Cette déforestation semble depuis enrayée, avec une perte estimée à seulement 0.25% entre 2000 et 2012 et principalement induite par l'urbanisation (Richards et Friess 2016).

3.2. Apport d'effluents contaminés

3.2.1. Eléments traces métalliques

Les mangroves sont nécessairement localisées au niveau des zones les plus en aval des bassins versants. Elles sont favorisées par l'existence de deltas qui créent d'importantes zones humides mais qui les soumettent aux apports des eaux provenant de l'ensemble du bassin versant environnant. Avec le développement de l'urbanisation et de l'agriculture industrielle, ces apports se sont progressivement chargés de substances naturellement présentes dans l'environnement (nutriments, éléments traces métalliques) ou non (pesticides, hydrocarbures, antibiotiques) et en quantités et proportions pouvant être différentes des zones non soumises aux rejets anthropiques (Fry et Cormier 2011, Lewis et al. 2011). Des concentrations élevées en éléments traces métalliques ont ainsi été mesurées dans les sédiments, les feuilles d'arbres et différents constituants des réseaux trophiques de mangrove incluant les crabes, bivalves, gastropodes, poissons, etc. Des tests de toxicité ont mis en évidence des effets néfastes de certains métaux tels que le zinc, plomb, cuivre et cadmium et de pesticides tels que l'atrazine ou le naphtalène, sur la survie, la reproduction ou les facultés motrices des plantes ou des animaux (Lewis et al. 2011).

3.2.2. Hydrocarbures

Les mangroves sont aussi vulnérables à des polluants flottants venant des océans comme les sont les hydrocarbures, en raison de fuites depuis les zones de stockage et les raffineries ou de vidanges sauvages et de naufrages d'embarcations de transport provoquant des marées noires. Le balancement des marées rejette les hydrocarbures sur les zones intertidales, couvrant les surfaces lipophiles des plantes et des animaux et bloquant ainsi leur respiration (Duke 2016). Lors de pollutions majeures, la plupart des organismes atteints meurt au bout de quelques jours ou de quelques mois tandis que les pollutions chroniques provoquent des malformations, une diminution des facultés de reproduction et de la productivité ou des mutations génétiques (Lewis et al. 2011, Duke 2016).

3.2.3. Antibiotiques

La contamination par les antibiotiques est aussi un problème majeur dans les écosystèmes de mangrove, notamment suite au développement de l'élevage industriel de crevettes qui nécessite un emploi considérable de substances chimiques destinées à lutter contre les épidémies (Gräslund et al. 2003). De nombreux cas d'antibiorésistance ont été mis en évidence dans les sols de mangrove, notamment à des substances communément utilisées en crevetticulture telles que l'acide oxolinique, le triméthoprime ou le sulfaméthoxazole (Le et al. 2005, Ghaderpour et al. 2015, Kathleen et al. 2016). La menace principalement induite est que cette antibiorésistance soit ensuite transmise à des bactéries pathogènes humaines. Par ailleurs, des fonctions microbiennes telles que la dénitrification peuvent être réduites par la présence d'antibiotiques dans des eaux usées. A une concentration de 1 µmol/L, le sulfaméthoxazole diminue de 54% le taux de disparition journalier des nitrates sur un substrat expérimental en anaérobie (Underwood et al. 2011). Cette même concentration correspond à la dose létale nécessaire pour tuer 50% des colonies d'une culture cellulaire de *Pseudomonas putida*, une bactérie connue pour ses facultés à dégrader des composés organiques tels que les hydrocarbures (Al-Ahmad et al. 1999). Des concentrations 2 à 6 fois supérieures à cette valeur seuil ont été mesurées dans la colonne d'eau de canaux adjacents aux bassins d'élevage de crevettes dans le nord du Vietnam (Le et Munekage 2004). Dans les sédiments, cette concentration était 1 000 fois supérieure à la valeur mesurée dans la colonne d'eau, laissant présager d'importants effets néfastes sur leur fonctionnement biologique.

3.2.4. Nutriments

L'apport de nutriments conduit à une productivité primaire benthique accrue dans les mangroves, notamment à la surface des sédiments soumis au rejet d'eaux résiduelles d'élevage crevetticole (Molnar et al. 2014). Au cours d'un cycle de production, seulement 29% de l'azote et 16% du phosphore apporté aux crevettes par l'aliment et les fertilisants est assimilé (Avnimelech et Ritvo 2003). L'eau des bassins d'élevage est renouvelée régulièrement afin de maintenir des paramètres optimaux pour les crevettes (Anh et al. 2010). Les eaux résiduelles sont rejetées dans les écosystèmes adjacents, notamment les mangroves, qui agissent comme des filtres biologiques et réduisent naturellement la charge en nutriments susceptibles de provoquer l'eutrophisation des eaux côtières. Pour capter les

nutriments générés par 1 ha d'élevage intensif de crevettes, 2 à 22 ha de mangroves sont nécessaires (Robertson et Phillips 1995). L'utilisation de cette capacité de phytoremédiation s'accompagne toutefois de changements dans la structure des communautés benthiques. Une plus forte concentration de diatomées et de bactéries se rencontre à la surface des sédiments recevant des eaux chargées en nutriments, que celles-ci proviennent d'élevages crevetticoles (Aschenbroich et al. 2015), de terres agricoles (Meziane et Tsuchiya 2002) ou d'effluents domestiques prétraités (Bouchez et al. 2013). Une plus grande biomasse de crabes est soutenue par les mangroves soumises aux rejets d'eaux résiduelles urbaines du Kenya et du Mozambique, comparées aux zones préservées, alors que l'abondance des gastéropodes est diminuée (Cannicci et al. 2009). Par ailleurs, les apports de nutriments conduisent à un meilleur état apparent des palétuviers, avec des concentrations en pigments chlorophylliens et une productivité primaire accrue (Fry et Cormier 2011, Herteman et al. 2011), mais une sensibilité plus importante aux stress environnementaux tels que la sécheresse et l'augmentation de la salinité des eaux (Lovelock et al. 2009). Le rapport entre certains nutriments est modifié par rapport aux zones non soumises aux rejets, avec une dominance des nutriments majoritaires C, N et P, par rapport à d'autres tels que K, Ca, Mg, Cu et B, mais sans pour autant qu'il soit possible de mesurer les conséquences de ces déséquilibres (Fry et Cormier 2011).

Enfin, l'apport de nutriments modifie les propriétés physico-chimiques des sédiments de mangrove et leur capacité à fixer certains éléments. Le potentiel d'oxydo-réduction diminue dans les sols soumis au rejet d'effluents crevetticoles, réduisant la mobilité des métaux (Marchand et al. 2011) et pouvant ainsi amplifier l'effet de bioaccumulation induit par le rejet d'effluents chargés en éléments traces métalliques. Une diminution des stocks de carbone organique est observée dans les sols soumis aux rejets d'effluents crevetticoles, causée par un accroissement de l'activité bactérienne de minéralisation et une réduction de la capacité de stockage des sols (Suárez-Abelenda et al. 2014).

4. La mangrove de Can Gio

4.1. Caractéristiques

Le district de Can Gio est situé à 50 km au Sud de Hô Chi Minh ville et couvre une superficie totale d'environ 720 km^2 (Figure 0-12). Il s'étend de 10° 22' à 10° 40' Nord en latitude et de 106° 46' à 107° 01' Est en longitude, soit environ 35 km du Nord au Sud et 30 km d'Est en Ouest (Tuan et Kuenzer 2012). La zone couverte par la forêt de palétuviers est de 320 km^2, soit environ 20% de la superficie totale des mangroves du Vietnam. La surface couverte par les cours d'eau est de 220 km^2 et une superficie de 180 km^2 est dédiée à des activités économiques telles que la crevetticulture ou la production de sel (Nam et al. 2014).

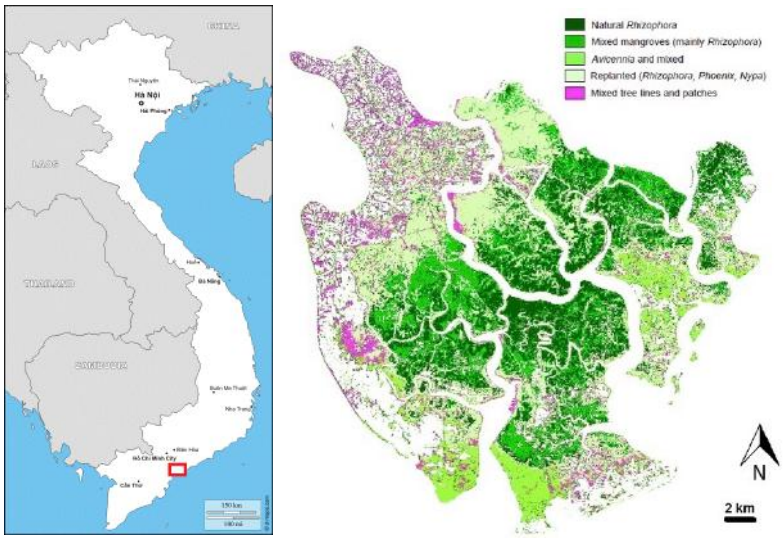

Figure 0-12 : Localisation et différentes zones de la mangrove de Can Gio établies à partir d'une image du satellite SPOT de 10 m de résolution spatiale prise en 2011. Extrait de Tuan et Kuenzer (2012)

La mangrove de Can Gio se développe sur le delta formé à l'embouchure du bassin versant de la rivière Saigon-Dong Nai qui draine une superficie de 40 600 km^2, soit environ 12% de la superficie totale du Vietnam, et décharge annuellement 37,4 Gm^3 d'eau dans le sud de la mer de Chine (Ringler et al. 2002). Le bassin versant de la rivière Dong Nai couvre des zones hydro-géographiques distinctes incluant les hauts plateaux du centre du Vietnam et le nord du bassin du Mékong et permettant une connectivité entre les deux bassins durant la saison des pluies. Le complexe hydrographique est situé dans la zone tropicale rythmée par une alternance de saison sèche (novembre à avril) et de saison des pluies (mai à octobre), avec 87% du débit annuel concentré entre avril/mai et juillet/aout (Ringler et al. 2002).

La topographie de Can Gio est relativement plane avec une élévation majoritairement comprise entre 0 et 1,5 m et allant jusqu'à 10 m dans une zone du nord-est de la mangrove (Nam et al. 2014). La zone est soumise au balancement des marées, avec une inondation biquotidienne d'une amplitude comprise entre 2 et 4 m selon la période et la proximité de l'océan. La température moyenne annuelle à Can Gio est de 25,8°C avec des moyennes mensuelles allant de 25,5 à 29°C et une amplitude journalière de 5 à 7°C. L'humidité relative est de 80% et descend jusqu'à 60% durant la saison sèche, tandis que l'ensoleillement est de 5 à 9 heures par jour (Nam et al. 2014).

La mangrove de Can Gio est une importante réserve de biodiversité et accueille 36 espèces de palétuviers divisées en 19 genres et 15 familles, ainsi que de nombreuses espèces associées aux écosystèmes de mangroves (Tuan et al. 2002). Le faciès de végétation dominant est constitué de plantations de *Rhizophora apiculata*, dont environ 200 km^2 ont été plantés dans le district de Can Gio depuis les années 1980 (Fromard et Kiet 2002). Les autres espèces majoritaires sont *Avicennia alba* et *Phoenix paludosa*. La première est une espèce pionnière tolérante à des salinités élevées et capable de coloniser des substrats meubles nouvellement formés, tandis que la seconde se retrouve essentiellement sur des zones plus élevées formant des communautés mixtes avec des espèces comme *Acrostichum aureum* ou *Nypa fruticans* (Figure 0-13).

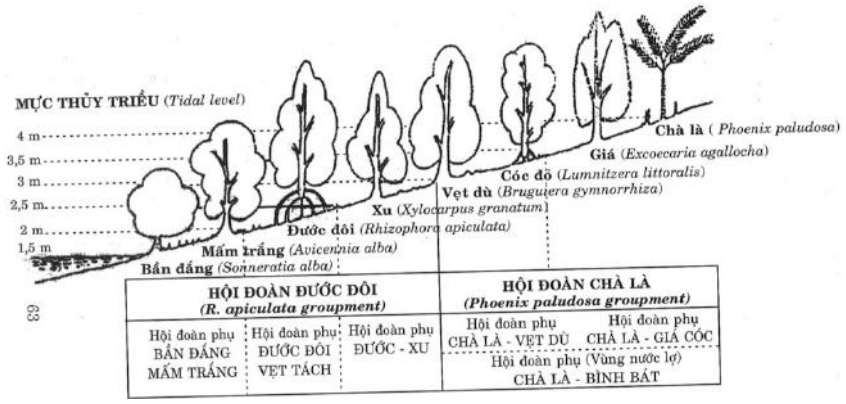

Figure 0-13 : Zonation verticale des groupements d'espèces végétales dans la mangrove de Can Gio. Extrait de Tuan et al. (2002)

La mangrove de Can Gio accueille aussi une grande diversité d'espèces animales, incluant des crustacés, mollusques et poissons d'intérêt commercial. Parmi ceux-ci, les crevettes *Metapenaeus ensis*, *Penaeus merguiensis* et *Penaeus monodon*, les crabes *Scylla serrata*, les gastéropodes *Cerithidea obtusa* et *Cerithidea quoyii*, les bivalves *Tegillarca*

granosa, et *Meretrix lyrata* ou encore les poissons *Coilia macronagthus* et *Lates calcarifer* (Image 0-3). Par ailleurs, on retrouve dans la mangrove de Can Gio diverses espèces d'oiseaux dont certaines classées « en danger d'extinction » ou « vulnérable » sur la liste rouge de l'Union Internationale de Conservation de la Nature, comme par exemple le Chevalier tacheté *Tringa guttifer* ou le marabout chevelu *Leptoptilos javanicus*. Enfin, la mangrove accueille des sangliers, singes, loutres, félins, varans et serpents (Tuan et al. 2002).

Image 0-3 : Espèces communes de mollusques et crustacés rencontrées dans la mangrove de Can Gio et vendues pour la consommation humaine. A gauche les crevettes géantes tigrées (*Penaeus monodon*), au second plan les coques de sang (*Tegillarca granosa*), au troisième plan les palourdes asiatiques (*Meretrix lyrata*) et au fond les escargots potamides (*Cerithidea obtusa* et *Cerithidea quoyii*).

4.2. Historique

La mangrove de Can Gio a subi d'importants dommages durant la guerre ayant opposé les forces américaines au front national de libération du Vietnam du sud. Afin de supprimer la couverture des combattants vietnamiens, près de 72 millions de litres de défoliants ont été déversés par voie aérienne sur les forêts du Sud-Vietnam de 1962 à 1972, avec une intensité particulière en 1967 (Fromard et Kiet 2002). Ces produits étaient principalement constitués d'agent orange (mélange 2:1 de deux molécules herbicides, l'acide 2,4-dichlorophénoxyacétique (2,4-D) et l'acide 2,4,5-trichlorophénoxyacétique) et d'agent blanc (mélange 4:1 de 2,4-D et d'acide 4-Amino-3,5,6-trichloropicolinique ou Piclorame), particulièrement efficace sur les plantes dicotylédones, auxquelles appartiennent la plupart des mangroves dont les genres *Rhizophora* et *Avicennia*. A la suite de ces déversements, la mangrove de Can Gio était pratiquement totalement détruite (Tuan et al. 2002). Des inventaires réalisés par photographies aériennes en 1973 montraient que plus de 1 000 km^2 de mangroves avaient été atteints dans le Sud-Vietnam, ainsi que 230 km^2 de forêts

marécageuses à *Melaleuca*. Les espèces *Rhizophora apiculata* et *Rhizophora mucronata* avaient alors pratiquement disparues de la mangrove de Can Gio, et ne restait que des groupes de *Ceriops tagal*, *Excoecaria agallocha* et *Phoenix paludosa*, qui ont mieux résisté. Certaines espèces comme *Avicennia alba* ont ensuite recolonisé les milieux vierges par rejets à partir des troncs défoliés (Fromard et Kiet 2002).

Lorsque la mangrove de Can Gio est entrée sous la juridiction de Ho Chi Minh ville, en 1978, il ne restait qu'une végétation en très mauvaise condition avec dans certaines zones des arbres jeunes ne dépassant pas 2 m et dans d'autres une végétation principalement arbustive (Tuan et al. 2002). Dans le cadre d'un vaste programme de restauration du pays et afin de créer une ceinture verte autour d'Ho Chi Minh ville, la décision a été prise de restaurer la mangrove de Can Gio. Entre 1978 et 2000, 300 km^2 de forets ont été nouvellement plantées ou restaurées. Une tentative de privatisation des parcelles forestières a été tentée en 1987 mais une mauvaise gestion a rapidement conduit à une dégradation du couvert végétal. En 1990, le gouvernement a décidé de céder des petites parcelles (en moyenne 1 km^2) à des familles pauvres en échange d'un engagement à préserver de la mangrove. Les familles reçoivent depuis une rente fixe leur permettant de subvenir à leurs besoins et s'engagent à protéger la mangrove des coupes de bois illégales. Ils complètent cette rente par une exploitation durable de l'écosystème, selon des critères établis par une entité publique, et incluant la pêche et l'agriculture vivrière.

Suite aux efforts qui ont été fait pour réhabiliter l'écosystème et permettre le maintien d'une biodiversité importante, la mangrove de Can Gio a été désignée en 2000 comme la première réserve de biosphère du Vietnam par le programme sur l'Homme et la biosphère de l'organisation des nations unies pour l'éducation, la science et la culture (UNESCO). La mangrove de Can Gio est aujourd'hui une fôret mature dont la diversité génétique des palétuviers est comparable à celle d'autres mangroves d'Asie du Sud-Est (Arnaud-Haond et al. 2009). Elle est représentative des mangroves hautement productives de cette région, avec un stockage de carbone dans la strate mature de 910.7 ± 32.2 Mg C ha^{-1}, dont 667.4 ± 11.8 MgC ha^{-1} (73%) dans le sediment (Donato et al. 2011, Dung et al. 2016).

4.3. Menaces actuelles

La mangrove de Can Gio dispose d'un cadre juridique et de limites spatiales bien établies qui permettent de la considérer comme relativement bien préservée de la déforestation. En revanche, celle-ci est soumise aux rejets d'eaux contaminées provenant de l'amont. Environ 8 km au nord de la limite juridique de la mangrove, la rivière Saigon rejoint le fleuve principal du bassin versant de la rivière Dong Nai et emporte avec elle les eaux résiduelles d'Ho Chi Minh ville (environ 13 millions d'habitants), qui est l'une des mégalopoles les plus dynamiques et densément peuplées d'Asie du Sud-est. En conséquence d'un système d'assainissement des eaux domestiques et industrielles inefficient et de la riziculture intensive en amont, la qualité biologique de la rivière Saigon est fortement dégradée. Des niveaux élevés de pesticides, nutriments, éléments traces métalliques et une charge organique importante ont été mesurés dans ses eaux et sédiments (Anh et al. 2003, Strady et al. 2017). Le débit de la rivière Saigon est 10 fois inférieur à celui du fleuve Dong Nai (Ringler et al. 2002). Ainsi, ces polluants sont dilués avant d'entrer dans la mangrove et donc difficile à tracer, mais leur bioaccumulation dans le réseau trophique est susceptible d'avoir des conséquences à long terme et difficilement quantifiables sur les organismes vivants dans la mangrove de Can Gio.

Après avoir récolté les eaux résiduelles d'Ho Chi Minh ville, le fleuve Dong Nai draine les bassins d'élevage crevetticoles localisés dans la zone tampon, majoritairement déboisée, de l'Est de la mangrove de Can Gio (Figure 0-12). Bien que les gouvernements de nombreux pays d'Asie du Sud-est encouragent la conversion des mangroves en zones aquacoles depuis les années 1960, cette activité s'est tardivement développée au Vietnam, avec une explosion des volumes de production depuis les années 2000 (Figure 0-14).

Les mangroves du Vietnam ont été relativement peu touchées par la déforestation entre 2000 et 2012 (Richards et Friess 2016). L'augmentation des volumes de production de crevettes résulte surtout de l'intensification des méthodes d'élevage. La superficie cultivée sur l'ensemble du Vietnam a été multipliée par 2 entre 2000 et 2007 tandis que les volumes produits ont été multipliés par 4 (Ha et Bush 2010). Cette intensification s'est accompagnée d'une utilisation plus importante d'aliments, pesticides, antibiotiques et fertilisants avec une toxicité sur le milieu naturel qui reste incertaine (Anh et al. 2010). Les eaux renouvelées des bassins sont rejetées dans les canaux adjacents puis rejoignent le fleuve Dong Nai qui se

divise en plusieurs bras pour former le delta sur lequel se développe la mangrove. Ces effluents présentent une charge organique importante ainsi que des concentrations élevées en nutriments et antibiotiques (Le et Munekage 2004, Anh et al. 2010).

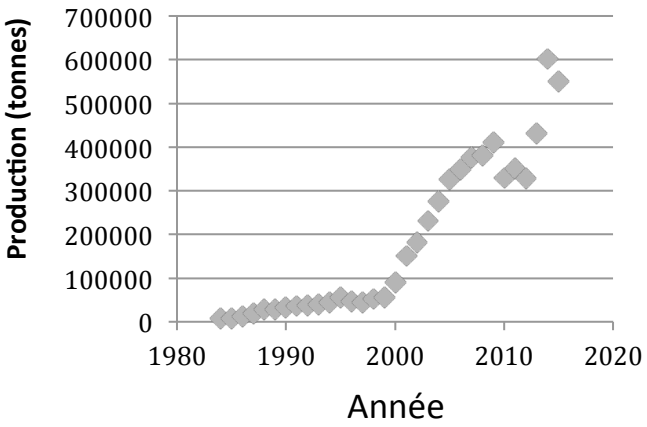

Figure 0-14 : Evolution temporelle de la production de crevettes pénéides au Vietnam. Données issues de FAO (2017)

Une autre menace importante pour la mangrove de Can Gio est l'érosion des sols qui altère les berges et diminue progressivement la zone couverte par la forêt au profit des surfaces occupées par les cours d'eau (Tuan et Kuenzer 2012). Ce phénomène est particulièrement marqué le long de du chenal principal de l'estuaire, qui traverse la mangrove en son centre et constitue la principale voie de navigation pour les porte-conteneurs qui assurent les échanges commerciaux entre le Vietnam et les pays environnants. Elle permet à des embarcations de grande capacité de charge d'entrer dans le port d'Ho Chi Minh Ville, qui provoquent lors de leur passage des vagues frappant les berges et induisant progressivement le déracinement des arbres qui empêchaient jusqu'alors l'érosion des sols (Image 0-4).

Image 0-4 : Berge à marée basse du chenal principal de l'estuaire traversant la mangrove de Can Gio mettant en évidence le phénomène d'érosion favorisé par le passage des porte-conteneurs

5. Objectifs de l'étude

Dans un contexte de changement climatique, le rôle des écosystèmes dans la régulation du climat est de plus en plus discuté et certaines zones comme les mangroves, même si leur superficie est faible à l'échelle du globe, peuvent fixer une part non négligeable des émissions anthropiques de gaz à effet de serre (Howard et al. 2017). Les mangroves sont des zones de forte productivité capables de stocker de grandes quantités de carbone (Donato et al. 2011, Alongi 2014, Marchand 2017). Cependant, Bouillon et al. (2008a) révèlent une différence de plus de 50% entre la quantité de carbone fixée par les mangroves et la somme des flux permettant d'estimer son devenir (minéralisation, export de carbone organique, enfouissement). Cette différence pourrait en partie s'expliquer par une sous-estimation de la minéralisation, conduisant à d'importants exports de carbone dissous (DIC) et au relargage de CO_2 depuis les masses d'eau et les sols (Bouillon et al. 2008a, Maher et al. 2013).

Les estuaires à mangrove sont des lieux de transfert entre la partie terrestre de la mangrove, dans laquelle les palétuviers fixent le CO_2 atmosphérique, et le milieu océanique, dans lequel la fixation du CO_2 provient essentiellement du phytoplancton. C'est une zone susceptible à la fois d'exporter du carbone vers l'océan et d'en importer, rendant ainsi les bilans de transfert difficiles à interpréter. De plus, les mangroves sont à la fois des zones de nurserie pour de nombreuses espèces côtières et des zones d'alimentation dans lesquelles les animaux mobiles (poissons et crustacés essentiellement) pénètrent lors du flot et exportent la matière qu'ils y ont ingéré lors du jusant (Nagelkerken et al. 2008). Ainsi, alors que les écosystèmes terrestres échangent principalement du carbone avec l'atmosphère, les mangroves sont à la fois connectées au compartiment océanique, par les chenaux puis les estuaires, et au compartiment atmosphérique. Ce travail de thèse a pour objectif d'étudier le cycle du carbone dans l'estuaire traversant la mangrove de Can Gio ainsi que les organismes macroscopiques susceptibles de transporter une fraction de ce carbone sous une forme difficilement quantifiable ; ceci, afin de mieux comprendre les bilans de carbone à l'échelle de l'ensemble de l'écosystème.

En complément de cette étude, trois autres sujets de thèse s'intéressent au fonctionnement biogéochimique de la mangrove de Can Gio. L'un par l'étude des stocks de carbone dans la zone terrestre de la mangrove, et des échanges avec le compartiment atmosphérique (Vinh Truong Vanh, université de Nong Lam, Ho Chi Minh Ville), un autre par

la spéciation des éléments traces métalliques dans les sédiments et la colonne d'eau de l'estuaire principal et d'un chenal prenant sa source dans la mangrove (Nho Nguyen Thanh, université des Sciences, Ho Chi Minh Ville), et enfin, un dernier par l'étude des cycles biogéochimiques du carbone, azote et oxygène dans ce même chenal et la zone intertidale qui lui est adjacente (Pierre Taillardat, université Nationale, Singapour).

La différence de plus de 50% entre la quantité de carbone fixée par les mangroves et la somme des flux permettant d'estimer son devenir révèle un manque de données quantitatives permettant de contraindre les budgets de carbone (Bouillon et al. 2008a), mais suggère aussi que les processus contrôlant la dynamique de ce carbone sont mal compris, et donc difficiles à quantifier. Ainsi, bien qu'il soit indéniable que les estuaires émettent de grandes quantités de CO_2 vers l'atmosphère, l'origine du carbone organique qui y est minéralisé est encore incertaine (Cai 2011). De plus, la colonne d'eau de l'estuaire n'est pas nécessairement homogène, et certaines masses d'eau, comme la microcouche de surface, pourraient jouer un rôle important dans la minéralisation de la matière organique de l'océan (Cunliffe et al. 2013), et aussi potentiellement des estuaires (Santos et al. 2011). En effet, cette zone est un réceptacle pour les rejets anthropiques pouvant favoriser l'activité du compartiment procaryotique et donc la boucle microbienne (Mari et al. 2017). Afin de d'apporter des éléments de réponse à ces différentes questions, les objectifs suivants ont été définis :

Objectif 1 : quantifier les différentes formes du carbone, ainsi que les flux de CO_2 à l'interface eau/air dans le chenal principal traversant la mangrove.

Objectif 2 : identifier l'origine du carbone organique et son devenir au cours du transit estuarien dans le chenal principal traversant la mangrove.

Objectif 3 : quantifier l'activité de dégradation des procaryotes dans différentes masses d'eau au cours du transit estuarien dans le chenal principal traversant la mangrove.

En plus des nombreux facteurs naturels affectant le cycle du carbone dans les mangroves, ces écosystèmes sont soumis à une pression anthropique importante de par leur localisation le long des côtes tropicales. Les mangroves reçoivent des effluents contaminés qui contribuent à enrichir les stocks de carbone de ces écosystèmes, mais aussi susceptibles d'affecter les processus de transformation de ce carbone (Trott et al. 2004, Aschenbroich et

al. 2015). Au Vietnam, le développement de la crevetticulture exerce une pression sur la mangrove de Can Gio en rejetant dans le milieu des effluents chargés en carbone organique et en nutriments (Anh et al. 2010). Cependant, en milieu naturel le devenir de ces effluents est souvent difficile à tracer et masqué par une grande variabilité naturelle des indicateurs d'impact les plus classiques, comme les concentrations en nutriments et la productivité primaire du phytoplancton (Trott et Alongi 2000).

Objectif 4 : caractériser en conditions expérimentales l'impact potentiel des rejets d'effluents crevetticoles sur la dynamique du carbone dans un écosystème de mangrove.

Bien que les mangroves soient vues comme des zones de nurserie pour de nombreuses espèces côtières ainsi que des zones d'alimentation pour les animaux mobiles (Nagelkerken et al. 2008), les relations trophiques dans ces écosystèmes sont encore assez mal comprises (Sousa et Dangremond 2011), avant même que l'on y rajoute l'influence d'éventuelles perturbations anthropiques. La ressource primaire de base, les feuilles de palétuviers, semble difficilement pouvoir subvenir seule aux besoins physiologiques des consommateurs, même pour les espèces les plus spécialisées dans leur assimilation comme les crabes de la famille des Sesarmidae (Harada et Lee 2016). Ainsi, il est probable que les imports de matière organique depuis l'océan ou certains processus de transformation du carbone provenant des feuilles de palétuviers soient indispensables au soutien des réseaux trophiques.

Objectif 5 : mesurer les variations de la qualité nutritionnelle de la matière organique particulaire au cours d'un cycle tidal dans un chenal de vidange relativement préservé de l'influence des activités humaines.

Objectif 6 : caractériser le régime alimentaire des espèces les plus communes dans cette même zone préservée et l'importance relative des différentes ressources de base.

Enfin, les espèces animales présentent généralement une certaine tolérance à la fois à des conditions environnementales variables et à la pression anthropique. Ainsi, les mangroves subissent de fortes variations journalières de pH, salinité, etc., pouvant affecter le métabolisme des organismes qui s'y développent, mais aussi des variations spatiales et

saisonnières de la qualité de la matière organique susceptible de servir de ressource alimentaire pour les consommateurs. Les rejets anthropiques sont un facteur supplémentaire pouvant affecter la chaine trophique, ce qui peut avoir des répercussions sur les espèces ayant une valeur commerciale et ainsi affecter l'un des services écosystémiques fournis par la mangrove qui est de produire des ressources alimentaires pour les populations humaines.

Objectif 7 : qualifier l'influence de la variabilité naturelle de certains facteurs et de la pression anthropique sur le métabolisme d'espèces cibles présentes dans la mangrove.

Ce mémoire est organisé en 7 chapitres qui répondent chacun à un des objectifs ci-dessus et dans l'ordre énoncé. Il est divisé en deux parties englobant, pour l'une, les chapitres se focalisant sur la dynamique du carbone au cours du transit estuarien, et pour l'autre, les chapitres traitant de la structure et du fonctionnement du réseau trophique. Ces deux parties constituent deux axes d'études contribuant à mieux aborder le cycle du carbone dans les estuaires à mangrove. Chaque partie est précédée d'un résumé en français reprenant les avancées scientifiques apportées par les différents chapitres la constituant.

PARTIE 1 :

Dynamique du carbone au cours de son transit dans l'estuaire

Résumé

Les estuaires sont des environnements clés pour l'établissement de bilans de carbone à l'échelle de la planète. Bien que couvrant une superficie très restreinte des masses d'eau libres (0,3%), comparés aux plateaux continentaux (7,2%) et aux océans (92,5%), les estuaires sont des lieux d'intense remaniement du carbone, et qui émettent de grandes quantités de CO_2 vers l'atmosphère. Cependant, les quantités exactes de carbone qui sont émises par la colonne d'eau lors du transit estuarien, l'origine du carbone minéralisé et les processus qui induisent sa minéralisation ne sont pas pleinement maitrisés du fait des variabilités spatio-temporelles qui les affectent. Ainsi, les 4 chapitres qui constituent cette première partie visent à mieux comprendre la dynamique du carbone dans l'estuaire traversant la mangrove de Can Gio.

Les chapitres 1 et 2 s'intéressent essentiellement à la quantité des différentes formes de carbone transportées dans l'estuaire, aux émissions de CO_2 et à la qualité nutritionnelle de la fraction organique particulaire de ce carbone. Les résultats présentés ont été acquis au cours des 2 missions d'échantillonnage en milieu naturel visant à comparer le fonctionnement biogéochimique de l'estuaire en saison sèche et en saison humide. Au cours de ces campagnes, 4 sites répartis entre l'extrémité aval de la ville de Ho Chi Minh et la côte de la mer de Chine ont chacun été suivis durant un cycle tidal complet (24 h). Cette approche nous a permis d'obtenir des séries de données continues (paramètres physico-chimiques de la masse d'eau, pression partielle en CO_2, données météorologiques) et discrètes selon un pas de temps de 2 h (émissions de CO_2, alcalinité, fractions dissoutes et particulaires du carbone organique, acides gras et isotopes stables de la matière particulaire).

L'approche quantitative présentée dans le chapitre 1 met en évidence l'intense pression anthropique sur l'écosystème avec, au niveau du site le plus proche d'Ho Chi Minh Ville, un pourcentage de saturation en oxygène descendant jusqu'à 17% en saison humide (0,9 mg L^{-1}), une pression partielle en CO_2 allant jusqu'à 5 000 µatm et jusqu'à 5,1% de poids sec de carbone organique dans la matière particulaire en suspension. Par ailleurs, l'une de nos hypothèses était que les apports de carbone inorganique depuis les sols de mangrove augmentaient de manière significative la quantité de carbone inorganique transportée par l'estuaire. Les résultats obtenus ne confirment pas cette hypothèse mais suggèrent que les apports depuis les sols de mangrove entretiennent les émissions élevées de CO_2 qui sont

mesurées sur l'ensemble de l'estuaire, avec toutefois des valeurs plus importantes là encore au niveau du site le plus proche d'Ho Chi Minh Ville, suggérant que les rejets anthropiques contribuent aux fortes émissions de CO_2 mesurées à l'interface eau/air. Ces émissions varient de 74 à 876 mmolCO_2 m^{-2} j^{-1}, soit des valeurs environ 10 fois supérieures aux moyennes calculées dans les synthèses bibliographiques disponibles pour les estuaires tropicaux, présageant que le rôle des estuaires tropicaux dans la régulation du climat pourrait être encore plus important que précédemment établi dans la littérature.

L'approche qualitative présentée dans le chapitre 2 met en évidence les variations spatiales et temporelles à court et long terme de la composition de la matière organique particulaire, permettant ainsi d'appréhender les transformations subies par le carbone au cours du transit estuarien. Nous avons émis l'hypothèse que 4 facteurs variant à différentes échelles spatiales et temporelles (saison, salinité, concentration en particules en suspension et lumière du jour) pouvaient expliquer la majeure partie des différences de la composition en acides gras, isotopes stables du carbone et de l'azote et ratio massique C/N entre échantillons prélevés au cours des deux campagnes et sur l'ensemble des sites. Les résultats obtenus valident cette hypothèse et confirment que la saison et la salinité, cette dernière étant considérée comme un traceur du mélange entre eau douce et eau salée, sont deux variables importantes contrôlant la composition de la matière particulaire en suspension. Ainsi, la matière organique est d'origine plus autotrophe et proportionnellement moins détritique en saison humide, probablement en raison d'une plus forte activité de minéralisation augmentant la disponibilité des nutriments au cours de cette saison. Par ailleurs, d'autres variables moins communément étudiées ont aussi une forte influence sur la matière particulaire en suspension. Ainsi, le compartiment bactérien est en premier lieu affecté par la quantité de matière en suspension dans la colonne d'eau, tandis que le compartiment phytoplanctonique subit des variations journalières de sa composition en acides gras presque aussi élevées que la variation saisonnière, laissant supposer d'intenses transformations du carbone au cours du transit estuarien.

Le chapitre 3 s'intéresse à l'activité de dégradation des procaryotes dans différentes masses d'eau au cours du transit estuarien. Les résultats présentés ont aussi été acquis au cours des 2 missions d'échantillonnage en milieu naturel, mais la fréquence d'échantillonnage à été réduite à deux prélèvements par cycle tidal en saison sèche (marée haute et marée basse) et à un seul prélèvement en saison humide (marée haute). Au cours de la saison sèche,

3 différentes masses d'eau ont été échantillonnées : la micro-couche de surface, correspondant aux 50-100 premiers µm de la colonne d'eau, la sub-surface et la lame de fond. Cette approche contraste avec celle des deux chapitres précédents ou seule la couche de sub-surface a été prise en compte. Par ailleurs, en saison humide un cinquième site localisé dans un chenal de mangrove a été rajouté à l'étude, tandis que seule la couche de sub-surface a été échantillonnée. Nous avons émis l'hypothèse que la micro-couche de surface et la lame de fond étaient deux zones particulièrement actives de la colonne d'eau, dans lesquelles on pouvait s'attendre à une plus forte abondance de procaryotes et à une activité de dégradation des protéines (exo-enzyme leucine-aminopeptidase) plus importante. Les résultats obtenus valident cette hypothèse pour l'activité de dégradation dans la lame de fond mais l'infirment en ce qui concerne les abondances et l'activité de dégradation dans la micro-couche de surface. Nous avons aussi émis l'hypothèse que l'activité de dégradation des procaryotes était plus importante au cours de la saison humide, comme nous le suggère le chapitre 2. Toutefois, les résultats obtenus indiquent une activité de dégradation 10 fois supérieure en saison sèche comparée à la saison humide, sans différence d'abondance des cellules procaryotiques. L'activité mesurée est celle de l'exo-enzyme leucine-aminopeptidase, dont le rôle est d'hydrolyser les macromolécules en substances monomériques et ainsi permettre leur transport à travers la membrane cytoplasmique. Un plus fort degré de polymérisation, ou une matière organique moins labile, est de ce fait susceptible d'induire un relargage plus important d'enzymes de la part des procaryotes. Ainsi, notre étude suggère que des variations spatiales et temporelles de la qualité de la matière organique influencent la libération d'enzymes par les procaryotes.

Enfin, le chapitre 4 s'intéresse à l'impact potentiel des rejets d'effluents crevetticoles sur la qualité de la matière organique de l'estuaire. Les résultats présentés sont issus d'une expérimentation en conditions contrôlées menée au Centre Asiatique de Recherches sur l'Eau d'Ho Chi Minh Ville. Des échantillons d'eau ont été prélevés dans des bassins d'élevage de crevettes ainsi que dans un chenal estuarien à proximité de la zone aquacole, puis conservés au laboratoire avec agitation (eaux pures + mélange 90% eau de chenal/10% eau de bassin) pendant 16 jours afin de suivre l'évolution temporelle de la composition en acides gras, isotopes stables ($\delta^{13}C$ et $\delta^{15}N$) et ratio C/N de la matière organique particulaire. Les résultats obtenus indiquent une dégradation rapide des lipides dans les effluents d'élevage, avec une perte de 50% des acides gras au cours de la première journée et de 75% au bout de 4 jours

d'incubation. De plus, ils suggèrent que le phytoplancton, très abondant dans les effluents d'élevage, entame sa décomposition immédiatement dans le mélange des eaux tandis que dans les eaux pures, il se maintient au cours des premières 24 h en consommant ses réserves lipidiques. Nous avons émis l'hypothèse que le mélange des eaux favorisait des voies biologiques de dégradation différentes de celles empruntées par la matière organique dans chacune des masses d'eau prise isolément, notamment en raison d'assemblages bactériens différents. Les résultats obtenus confirment cette hypothèse et révèlent une proportion particulièrement élevée de l'acide gras 18:1ω7 dans le mélange des eaux (23.6% du total des acides gras après 4 jours d'incubation). Bien qu'ubiquiste, cet acide gras n'a été observé en si grande proportion que dans les phospholipides des protéobactéries du groupe alpha, comme par exemple *Paracoccus denitrificans*. Celles-ci sont capables de dénitrification aérobie, produisant du N_2O qui est un gaz à effet de serre important. Ainsi, bien que ces résultats soient relativement éloignés de nos objectifs de départ, ils laissent entrevoir des enjeux importants concernant les effets du rejet d'effluents crevetticoles sur les émissions de gaz à effet de serre en zone estuarienne.

Chapter 1: Carbon biogeochemistry and CO_2 emissions in a human impacted and mangrove dominated tropical estuary (Can Gio, Vietnam)

DAVID Frank, MEZIANE Tarik, TRAN-THI Nhu-Trang, TRUONG VAN Vinh, NGUYỄN THÀNH Nho, TAILLARDAT Pierre and MARCHAND Cyril

Under revisions for publication in Biogeochemistry

1. Abstract

The quantitative contribution of tropical estuaries to the atmospheric CO_2 budget has large uncertainties, both spatially and seasonally. We were interested in the seasonal and spatial variations of carbon biogeochemistry along the salinity gradient of the Can Gio mangrove estuary (Southern Vietnam), whose watershed is highly urbanised. We sampled four sites distributed from the downstream end of Ho Chi Minh City (upstream the mangrove) to the South China Sea coast at two seasons (dry season in January-February 2015 and wet season in September-October 2015) during 24 h time series. High organic load, dissolved oxygen saturation down to 17%, and CO_2 partial pressure (pCO_2) up to 5,000 µatm at the freshwater endmember of the estuary reflected the intense human pressure on this ecosystem. In addition, our study evidences that releases from mangrove soils affect the water column pCO_2 at the scale of this large tropical estuary (~600 m wide and 10-20 m deep). It is, to our best knowledge, the first study to report direct measurements of both water pCO_2 and CO_2 emissions in a Southeast Asian tropical estuary located in a highly urbanised watershed. It shows that the contribution of such estuaries may have been previously underestimated in global CO_2 budgets, with CO_2 emissions up to 876 mmol m^{-2} d^{-1} at the freshwater endmember of the estuary and corresponding gas transfer velocity k_{600} ranging from 1.7 to 11 m d^{-1}, about 2 to 4 times higher than k_{600} estimated using published literature equations.

2. Introduction

Although estuaries represent a very restricted surface area (0.3%) compared to continental shelves (7.2%) and open oceans (92.5%), they play a determinant role in global biogeochemical cycles (Borges 2005, Chen et al. 2013). Estuaries receive large amounts of terrestrial carbon under dissolved and particulate forms from the surrounding watershed (Huang et al. 2012, Chen et al. 2013). This terrestrial carbon is heavily processed before entering the marine environment, but the exact extent of speciation changes between the organic and inorganic or dissolved and particulate forms, and how much of each of these forms of carbon actually enters the oceans remains uncertain (Chen et al. 2013).

Being generally net heterotrophic, estuaries act as sources of CO_2 to the atmosphere, while continental shelves are highly productive autotrophic ecosystems and act as sinks of CO_2 (Cai 2011, Hofmann et al. 2011). In a context of climate change, identifying natural sinks and sources of CO_2 to the atmosphere and understanding how they are influenced by anthropogenic pressure is a major concern (Regnier et al. 2013). Despite high loads of carbon in estuaries originate from inland watersheds, Cai (2011) argued that the large amount of CO_2 degassing observed in coastal waters must be supported by lateral transport of carbon from the surrounding coastal wetlands, such as mangroves, which are highly productive ecosystems (Alongi 2014). Moreover, high loads of dissolved inorganic carbon (DIC) are released from surrounding soils, especially when they are covered with mangrove forests, and this carbon can be a major input in coastal budgets (Bouillon et al. 2008a, Atkins et al. 2013).

Recently published global estimates of estuarine CO_2 fluxes (FCO_2) vary nevertheless substantially, both spatially and seasonally, and the quantitative contribution of estuaries to the atmospheric CO_2 budget has large uncertainties (Chen et al. 2013). Such uncertainties are partially due to the method employed to estimate gas exchanges, which was historically based on CO_2 partial pressure (pCO_2) measurement, itself often calculated from the carbonate system equilibrium constants (Chen et al. 2013), and compiled using a function of wind speed (Wannikhof 1992). Uncertainties could be of high importance especially in Southeast Asia, considered as a hotspot of aquatic CO_2 emissions to the atmosphere (Regnier et al. 2013) due to high organic carbon concentrations in rivers (Müller et al. 2016) and the presence of megacities with poorly effective wastewater treatment systems (Strady et al. 2017). The use of floating chambers has recently gained interest for constraining estuarine

CO_2 emissions since it provides a direct measurement of the flux, while gas exchange rates based on field measurement relationships are often site-specific (Rosentreter et al. 2017) and difficult to generalise.

Our study aims to understand seasonal and spatial changes in carbon biogeochemistry and to quantify CO_2 degassing fluxes in a human impacted and mangrove dominated Southeast Asian tropical estuary (Can Gio, Southern Vietnam). We hypothesised that (1) organic carbon concentrations and pCO_2 would be higher during the wet season due to the leaching of inland watersheds (2) both DIC and CO_2 releases from surrounding mangrove soils could be traced at the scale of a large estuary such as the Saigon-Dong Nai Rivers system (3) emissions of CO_2 would be particularly high due to both anthropogenic pressure and the surrounding presence of the mangrove ecosystem. Our dataset is based on two sampling campaigns (dry season in January-February 2015 and wet season in September-October 2015), which include 24 h time series on four sites distributed from the downstream end of Ho Chi Minh City (upstream the mangrove) to the South China Sea coast. To our best knowledge, this study provides the first set of direct measurements for both water pCO_2 and FCO_2 in a Southeast Asian tropical estuary located in a highly urbanised watershed.

3. Materials and methods

3.1. Study Area

The Saigon-Dong Nai Rivers basin has a total catchment area of 40.6×10^3 km^2, approximately 12% of the total terrestrial area of Vietnam, and a main stream length of 628 km (Nippon Koei 1996). Total basin runoff is estimated at 37.4×10^6 m^3 yr^{-1} and precipitations average 2000 mm yr^{-1} (Ringler et al. 2001). The study area is located in a tropical monsoonal environment with a wet season from June to October and a dry season from November to May (Nam et al. 2014). During the wet season, the area receives 90% of its annual precipitations and the river discharge may be up to 30 times higher than lower values measured during the dry season. At the downstream end of Ho Chi Minh City (Southern Vietnam; ~13 million inhabitants), the Saigon-Dong Nai River splits and forms a delta which drains the 719.6 km^2 of the Can Gio district, designated in 2000 by the UNESCO as the first mangrove biosphere reserve in Vietnam (Tuan and Kuenzer 2012). The north-east border of

the biosphere reserve is dedicated to socio-economic development, mostly intensive shrimp farming (24.5% of the total area). Tidal amplitude is variable over time and ranges between 2 to 4 m depending on the season and proximity to the coast line (Tuan and Kuenzer 2012).

We selected the study sites to be at the interface between land uses (Figure 1-1): A) at the downstream end of Ho Chi Minh City (10°39'55"N 106°47'30"E); B) between shrimp farms and the mangrove forested area (10°34'19"N 106°50'11"E); C) in the centre of the mangrove protected core (10°31'04"N 106°53'13"E); and D) between the mangrove forested area and the South China Sea coast (10°29'32"N 106°56'55"E). All sites were located on the main estuarine channel, which has steep eroded banks, a width of about 600 m and 10-20 m depth.

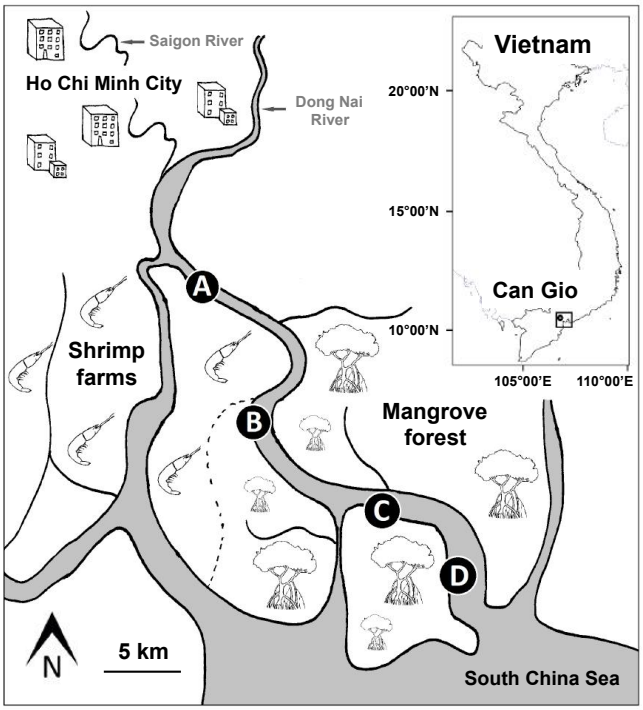

Figure 1-1: Map of the sampling area in the Can Gio mangrove (Southern Vietnam). A, B, C and D indicate the sampling sites along the estuary

3.2. Data collection

We monitored water surface carbon biogeochemistry over 24 h time series during the dry (January-February) and monsoon (September-October) periods in 2015. Salinity, pH and water temperature were measured continuously using a Yellow Spring Instrument® meter (YSI 6920) immersed 30 cm below water surface and calibrated before each survey. Dissolved oxygen (DO) was monitored similarly with a Hobo® data logger (HOBO U26-001) also

calibrated before each survey. Salinity and pH were not recorded at site C during the dry season due to YSI probe dysfunction. Salinity was estimated using a linear relationship established on the three other sites between salinity and alkalinity (salinity = 16.1 × alkalinity (mmolC L^{-1}) - 7.1; R^2 = 0.99; n = 39). The maximum difference at sites A, B and D during the dry season between calculated and probe measured salinity was 1.8, which was low compared to the amplitude of the salinity gradient (7 to 25). We used these calculated values for establishing relationships between salinity and DOC, POC, %POC, FCO_2 and associated graphical representations. Current velocity and water depth were measured every hour with a Global Water® FP 101 flow meter handled 30 cm below water surface and a Plastimo® Echotest II depth sounder directed towards the bottom. Air temperature, relative humidity, wind velocity and precipitations were measured using a Hobo® weather station located on the top of the sampling boat (4.5 m above water level; Image 1-1).

Image 1-1: Sampling boat, weather station and floating chamber used during the wet season sampling

We measured pCO_2 continuously using a marble-type equilibrator made of a 1.8 L Plexiglas® cylinder (inner diameter 8 cm; height 40 cm) filled with glass marbles to increase gas exchange between the flowing water and the headspace air (Frankignoulle et al. 2001, Yoon et al. 2016). Water was pumped 30 cm below water surface at a constant rate of 1 L min^{-1} and injected at the top of the equilibrator, while a similar volume of air connected to a closed air loop was flowing from bottom to the top. The closed air loop was connected a Li-Cor Biosciences® infrared gas analyser (IRGA) after passing through a silica gel container and a particle filter. We measured pCO_2 using an IRGA model LI-8100A at all sites during the dry

season and at site A during the wet season, and we used an IRGA model LI 840 at site B, C and D during the wet season. Infrared gas analysers were calibrated before each survey with pure nitrogen (0 µatm CO_2) and two CO_2 standards (545 ± 11 and 2867 ± 58 µatmCO_2) manufactured by Air Liquide®.

We measured FCO_2 using a floating chamber anchored to the sampling boat (Image 1-1). Every two hours, five measurements of FCO_2 were performed with an incubation period of 5-6 min. The chamber was made of a plastic waste bin (top radius 40 cm; bottom radius 45 cm; height 55 cm) surrounded by an inner tube and weighted with a 5 kg metal chain to increase stability (inner air volume 48.2 L; air-water contact surface 0.152 m^2). A closed air loop was connected from the chamber to a Li-Cor Biosciences® IRGA (model LI 820) after passing through a silica gel container and a particle filter. Due to important cargo traffic on the estuary and night work it was too dangerous to drift with the chamber. Consequently, we kept only chamber measurements performed when current velocity was under 0.2 m s^{-1} for the analysis (about 20% of the time). This value of current velocity was considered as critical by Lorke et al. (2015) and our results confirmed such observations (data not provided).

Three replicates of surface water were sampled every two hours (13 samplings per 24 h time series) using a 10 L plastic bucket. Depending on turbidity, 250 mL to 1.2 L of water was immediately vacuum-filtered through pre-combusted (5 h at 450°C) and pre-weighted glass fibre filters (Whatman® GF/F 0.7 µm), collecting 10 to 80 mg of suspended particulate matter (SPM). Filtered water was stored in 40 mL Falcon® tubes for further titration of total alkalinity (TAlk), and in 15 mL Falcon® tubes after acidification to stop microbial activity for further determination of dissolved organic carbon (DOC). During the wet season, one sample of unfiltered water was positively filtered through 0.2 µm Sartorius® cellulose acetate syringe filters (to reduce water-air gas exchanges) and stored leaving no air space or bubbles in 23 mL glass vials for further determination of $\delta^{13}C_{DIC}$. Filters were preserved at -25°C until analysis of particulate organic carbon (POC) and water samples were stored at 4°C until determination of TAlk, DOC and $\delta^{13}C_{DIC}$. Results of replicated measurements were averaged before statistical analyses.

3.3. Analytical methods and calculations

We calculated the relative dissolved oxygen saturation (% DO) in the water using the ratio of measured oxygen concentration and oxygen solubility at the same salinity and temperature, according to the relations provided by Benson and Krause (1984).

We determined TAlk by Gran electrotitration with 50 µL increments of HCl 0.01 N (accuracy estimated at ± 0.01 mmol L^{-1}). We calculated DIC concentration using pH and TAlk, according to the relations provided by Park (1969) and assuming that TAlk ≈ carbonate alkalinity. Considering the estimated accuracy of TAlk, an uncertainty of 0.05 pH and negligible effects of uncertainties in salinity and temperature, the accuracy of DIC calculations was > 0.05 mmol L^{-1}. Dissociation constants of carbonic acid were obtained using the equations provided by Millero et al. (2006) and updated by Millero (2010) for estuarine waters, taking into account salinity and temperature. The carbonate system equilibrium constants (Park 1969) were employed to calculate theoretical pCO_2 during the wet season, using pH and TAlk.

We analysed $\delta^{13}C_{DIC}$ during the wet season only in the stable isotopes laboratory of the Geotop research centre at the Université du Québec in Montréal (Canada). A few mL of sample water was transferred into a 3 mL glass vial using a syringe through a septum. Glass vials were previously filled with 12 drops of 100% H_3PO_4, and purged with Helium. Headspace CO_2 originating from acidification was analysed using a Micromass MicroGasTM system coupled to an Isoprime 100TM Isotope Ratio Mass Spectrometer (IRMS) in continuous flow mode. Replicate $\delta^{13}C_{DIC}$ measurements from similar samples yielded an overall analytical uncertainty < 0.1‰. We constructed a theoretical mixing line between fresh and marine waters as described in Bouillon et al. (2011). DIC isotopic compositions and concentrations at the riverine and marine endmembers were taken at site A at salinity ~0 and at site D at salinity ~26.

Organic carbon (DOC and POC) was analysed at the Institut de Recherche pour le Développement in Nouméa (New Caledonia) with a Shimadzu® TOC-L series analyser using a 680°C combustion catalytic oxidation method. The analyser was combined with a solid sample module (SSM-5000A) for measurements of POC, and a 40% glucose standard was used for calibrations. Repeated measurements of the standard at different concentrations indicated a measurement deviation < 2% for both POC and DOC.

We calculated FCO_2 from the slope of gas partial pressure versus time and taking into account air temperature, using the following equation:

$$FCO_2 = \frac{\delta pCO_2}{\delta t} \times \frac{V}{R \times T \times S}$$

where FCO_2 is the water-air CO_2 flux (µmol m^{-2} s^{-1}), δpCO_2 / δt is the variation of pCO_2 versus time (µatm s^{-1}), V is the total volume of the chamber (m^3), R is the ideal gas constant (atm m^3 K^{-1} mol^{-1}), T is the absolute air temperature (K), and S is the incubation chamber contact surface (m^2).

We determined the gas transfer velocity k using measurements of ΔpCO_2 and FCO_2 and calculation of α (Weiss 1974). The theoretical equation established to express CO_2 fluxes as a function of salinity, temperature and pCO_2 is on the form: $FCO_2 = \alpha \times k \times \Delta pCO_2$, where FCO_2 is the water-air CO_2 flux (mol m^{-2} d^{-1}), α is the CO_2 solubility coefficient (mol m^{-3} atm^{-1}) (Weiss 1974), k is the gas transfer velocity (m d^{-1}) and ΔpCO_2 is the difference in partial pressure of CO_2 between water and the overlying atmosphere (atm). We then normalised k to a Schmidt number of 600 (Sc = 600 for CO_2 at 20 °C in freshwater) for further comparisons with published values:

$$k_{600} = k \times \frac{600}{Sc^{-0.5}}$$

where Sc is the Schmidt number of CO_2 at a given temperature and salinity and raised to the power -0.5 in turbulent systems (Wanninkhof 1992). Constants for the Schmidt number calculation were provided for salinity 0 and 35 by Wanninkhof (1992) and inferred to our dataset salinities assuming a conservative mixing ratio between fresh and marine waters (Borges et al. 2004). Theoretical gas exchange rates were calculated according to Wanninkhof (1992), using wind velocity at 10 m high (compiled using the Amorocho and Devries (1980) relationship) and water temperature (W92), and Rosentreter et al. (2017), using wind velocity at 10 m high, water depth and current velocity (R17).

We considered that the site A during the wet season was the freshwater endmember of the estuary, with salinity close to zero showing no mixing with marine waters. On the opposite, site D during both seasons represented the marine endmember. A simple two source mixing of freshwater and seawater could then be used to identify possible lateral inputs of DIC to the estuary. We used analysis of covariance (ANCOVA) to test wheter a given monitored parameter was affected by the estuarine transit or the season, considering salinity as a quantitative variable and season as a qualitative variable. Residuals distribution was

tested for normality and data were log-transformed when necessary. The Fisher statistic (F-test) was reported and subscript numbers indicate variables and residuals degrees of freedom. One factor linear regressions were used to calculate intercept and slope coefficient of the relationship between a given monitored parameter and salinity or SPM. For statistical tests, the criterion for rejecting the null hypothesis (alpha value) was set to 5%. Continuous probe measurements (salinity, pH, DO, pCO_2 and weather parameters) were discretised using smooth.spline function with R (R Core Team 2017) and setting a time lapse corresponding to that of the water sampling or the chamber flux measurements. For statistical analysis and graphical representations involving only continuously measured parameters, a step of two hours was set (13 values per 24 h), except for pCO_2 where a step of 20 minutes was set to increase precision of individual site representations. Statistical analyses and graphical representations were performed using R (R Core Team 2017).

4. Results

4.1. Physico-chemical parameters

During the 24 h time series, daytime air temperature reached 28-29°C in January-February (dry season) and 31-32°C in September-October (wet season). During both seasons, photosynthetically active radiation (PAR) was up to 2,000 µmol m^{-2} s^{-1} and wind speed ranged from 0 to 10 m s^{-1}, with 90% of values under 4.3 m s^{-1} during the dry season and under 3.6 m s^{-1} during the wet season. At night, air temperature dropped to 20-22°C during the dry season, and to 24-25°C during the wet season. The main difference between seasons was heavy rainfall events generally occurring in the afternoon or early night (wet season) and reaching 50 mm hr^{-1} during short periods of time (1-2 hours).

Salinity, temperature, pH and DO saturation in water varied significantly over the 24 h time series and were synchronised with tidal cycles. Salinity along the 40 km of the Can Gio mangrove estuary ranged from 7 to 26 during the dry season, and from 0 to 25 during the wet season (Figure 1-2). Water temperature ranged from 26 to 29°C during the dry season, and from 29 to 31°C during the wet season. Both pH and DO saturation increased linearly with salinity and this relationship was significantly affected by season (ANCOVA; $F_{2,88}$ = 738.9 and 444.9; $p_{salinity} < 0.001$ for both, $p_{season} < 0.001$ for both; $R^2 > 0.9$ for both). Lower DO

saturation and higher pH were observed during the wet season for a given salinity, with a mean difference of -10.4% in DO saturation and +0.1 in pH.

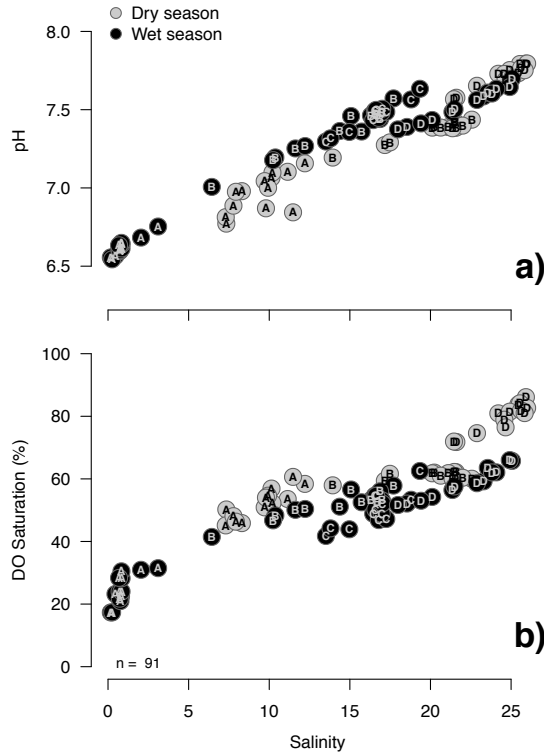

Figure 1-2: Distribution of a) pH and b) dissolved oxygen saturation (%) along the salinity gradient of the Can Gio mangrove estuary. Continuous data were discretised using a 2 h step (13 values per 24 h tidal cycle)

4.1. Carbon pools

Means and ranges of carbon pools are provided in Table 1-1. DIC was the dominant carbon pool in the Can Gio mangrove estuary, with concentration 1.3 to 7.9 times higher than that of total organic carbon (TOC). DIC increased linearly with salinity and this relationship was significantly affected by season (ANCOVA; $F_{2,88} = 1620$; $p_{salinity} < 0.001$ and $p_{season} < 0.01$; $R^2 = 0.97$; Figure 1-3a). Higher DIC concentrations were observed during the wet season for a given salinity, with a mean difference of +0.05 mmol L^{-1}. $\delta^{13}C_{DIC}$ ranged from -15.4 to -4.7‰ during the wet season, with lowest values observed at lowest salinity (Figure 1-3b). The theoretical mixing line of $\delta^{13}C_{DIC}$ was graphically following measurements over the entire salinity gradient (Figure 1-3b).

Table 1-1: Mean values of measured parameters at the different sampling sites

	Dry season				Wet season			
Site	A	B	C	D	A	B	C	D
Sampling date	14/15 Jan.	21/22 Jan.	27/28 Jan.	2/3 Feb.	22/23 Sep.	27/28 Sep.	6/7 Oct.	15/16 Oct.
Tidal coefficient	46	107	51	80	50	115	48	78
TAlk (mmol L^{-1})	1.04 [0.87-1.17]	1.70 [1.31-1.83]	1.84 [1.71-1.99]	1.96 [1.78-2.12]	0.56 [0.48-0.73]	1.41 [0.93-1.61]	1.53 [1.34-1.67]	1.83 [1.66-1.93]
DIC (mmol L^{-1})	1.14 [0.96-1.31]	1.72 [1.37-1.85]	n.a.	1.90 [1.76-2.05]	0.78 [0.72-0.89]	1.44 [1.02-1.60]	1.54 [1.34-1.68]	1.81 [1.68-1.89]
DOC (mmol L^{-1})	0.27 [0.21-0.32]	0.28 [0.19-0.39]	0.24 [0.19-0.33]	0.34 [0.27-0.40]	0.21 [0.10-0.35]	0.18 [0.14-0.30]	0.17 [0.15-0.20]	0.21 [0.14-0.29]
POC (mmol L^{-1})	0.07 [0.05-0.12]	0.20 [0.07-0.33]	0.09 [0.05-0.22]	0.10 [0.05-0.27]	0.17 [0.09-0.33]	0.26 [0.11-0.50]	0.08 [0.06-0.11]	0.10 [0.07-0.20]
TSM (mg L^{-1})	29 [16-60]	157 [55-361]	72 [40-167]	61 [29-122]	49 [23-137]	147 [51-283]	35 [23-51]	63 [40-121]
DIC/TOC	3.5 [2.7-4.0]	4.4 [2.5-6.9]	n.a.	4.4 [3.1-5.5]	2.2 [1.3-3.5]	3.5 [2.0-5.4]	6.1 [5.1-7.0]	6.1 [3.8-7.9]
DOC/POC	4.2 [2.5-6.8]	1.7 [0.7-3.0]	3.0 [0.9-5.2]	4.2 [1.2-7.3]	1.3 [0.7-2.2]	0.9 [0.4-2.0]	2.2 [1.6-3.1]	2.1 [1.3-3.4]

n.a. = not available

Dissolved organic carbon was not significantly affected by salinity but a seasonal difference was evidenced (ANCOVA; $F_{2,101}$ = 33.0; $p_{salinity}$ = 0.80 and $p_{season} < 0.001$). Lower DOC concentrations were observed during the wet season for a given salinity, with a mean difference of -0.09 mmol L^{-1}. Particulate organic carbon was also not significantly affected by salinity but it was affected by season (ANCOVA; $F_{2,94}$ = 4.27; $p_{salinity}$ = 0.46 and p_{season} = 0.02; Figure 1-4a). Higher POC concentrations were observed during the wet season for a given salinity, with a mean difference of +0.04 mmol L^{-1}. The explanatory power of both regressions was yet very low (R^2 = 0.40 and 0.08, respectively for DOC and POC).

Suspended particulate matter was not significantly affected either by salinity or season (ANCOVA; $F_{2,101}$ = 1.72; $p_{salinity}$ = 0.08 and p_{season} = 0.81) but percentage of POC in SPM decreased significantly with salinity without significant effect of season on this relationship (ANCOVA with log transformed %POC values; $F_{2,94}$ = 131.3; $p_{salinity} < 0.001$ and p_{season} = 0.16; R^2 = 0.74; Figure 1-4b). Particulate organic carbon thus increased significantly with SPM concentration and an effect of season on this relationship was evidenced (ANCOVA; $F_{2,94}$ = 336.9; $p_{salinity} < 0.001$ and $p_{season} < 0.001$; Figure 1-5). Higher POC concentrations were observed during the wet season for a given SPM concentration, with a mean difference of +0.04 mmol L^{-1}.

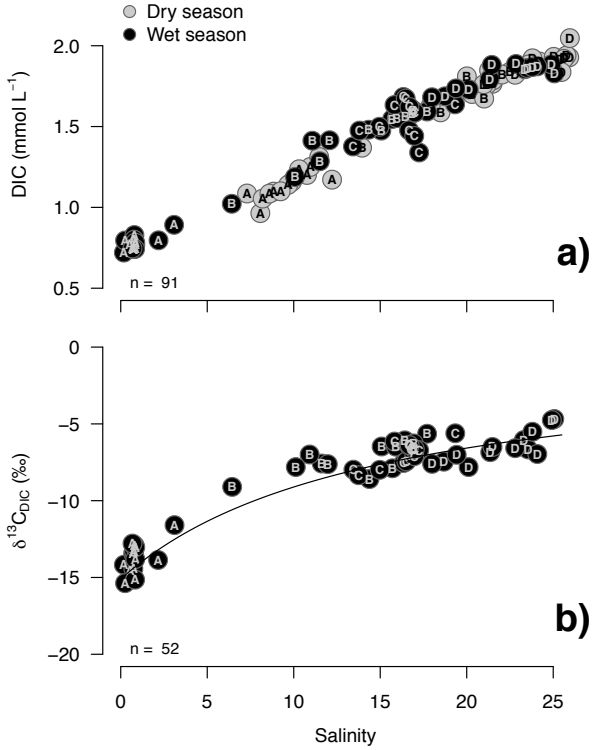

Figure 1-3: Distribution of a) dissolved inorganic carbon (mmol L^{-1}) and b) $\delta^{13}C_{DIC}$ (‰) along the salinity gradient of the Can Gio mangrove estuary

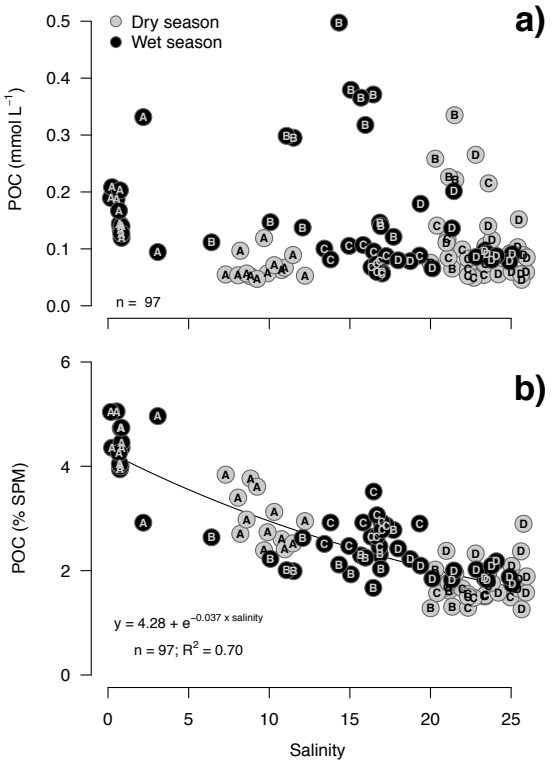

Figure 1-4: Distribution of a) particulate organic carbon (mmol L^{-1}) and b) particulate organic carbon (% suspended particulate matter) along the salinity gradient of the Can Gio mangrove estuary

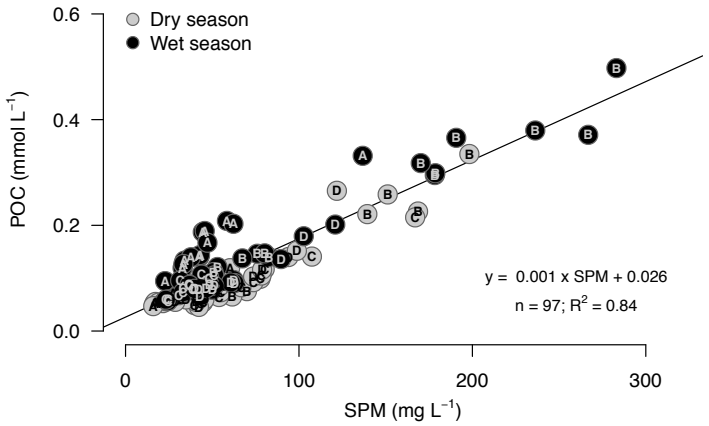

Figure 1-5: Distribution of particulate organic carbon (mmol L^{-1}) as a function of suspended particulate matter concentration in the Can Gio mangrove estuary

Partial pressure of CO_2 ranged from 660 to 3,000 µatm during the dry season, and from 740 to 5,000 µatm during the wet season (Figure 1-6 and Figure 1-7). It decreased linearly with salinity and a significant effect of season on this relationship was evidenced (ANCOVA; $F_{2,74}$ = 71.5; $p_{salinity}$ < 0.001 and p_{season} < 0.001). However, we could not measure pCO_2 at site B and C during the dry season due to technical problems and the explanatory power of the linear regression based on wet season values only was very low (R^2 = 0.47). Difference in pCO_2 between low and high tide during the wet season seemed to depend on the tidal stage rather than on salinity and to be affected by tidal amplitude. It was close to 2000 µatm when tidal coefficient was under 80 (sites A, C and D) and reached 3000 µatm during strong spring tide (site B; Table 1-1 and Figure 1-7). During the wet season, linear regressions performed between salinity and pCO_2 for each site individually revealed higher slope coefficients than the regression considering the four sites (-530.4 to -201.3 vs. -78.6; Figure 1-6 and Figure 1-7). Theoretical pCO_2 notably differed from measured values, especially at site A where theoretical values were far above measured pCO_2, but trends related to the tidal stage remained similar (Figure 1-8).

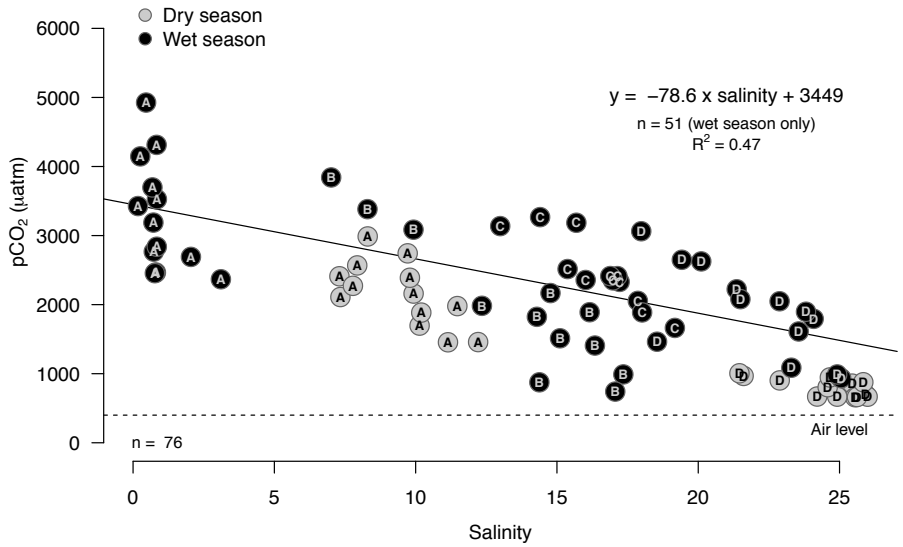

Figure 1-6: Distribution of CO_2 partial pressure (µatm) along the salinity gradient of the Can Gio mangrove estuary. Continuous data were discretised using a 2 h step (13 values per 24 h tidal cycle)

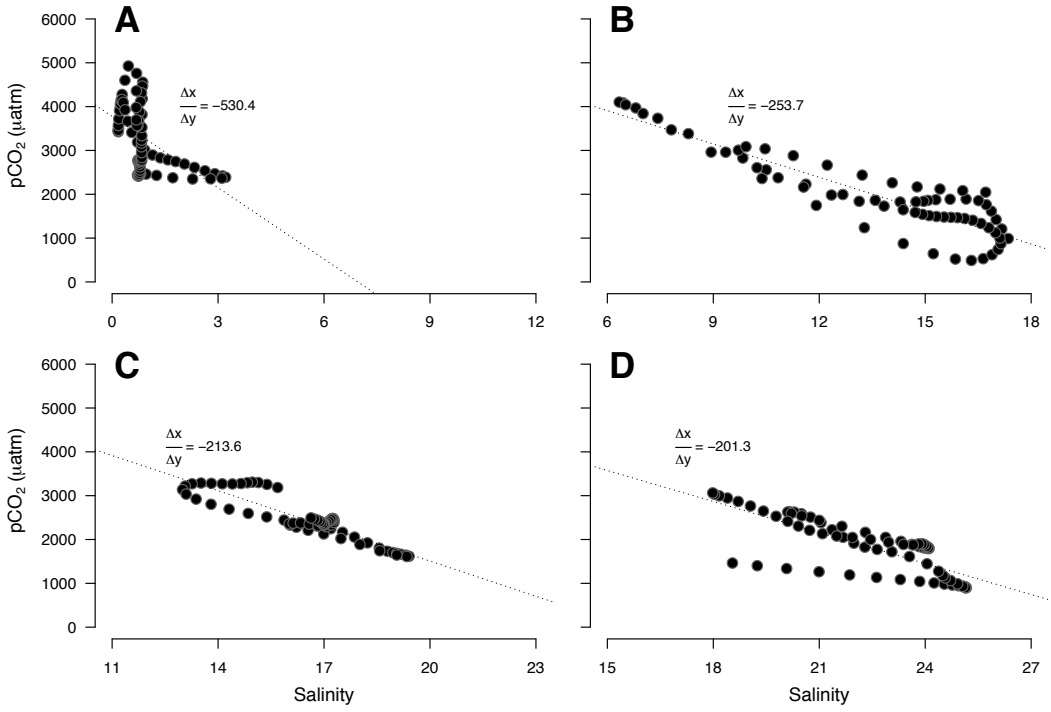

Figure 1-7: Distribution of CO_2 partial pressure (µatm) as a function of salinity during the wet season 24 h tidal cycles in the Can Gio mangrove estuary. Continuous data were discretised using a 20 min step (73 values per 24 h tidal cycle). Letters at the upleft corner indicate the sampling site

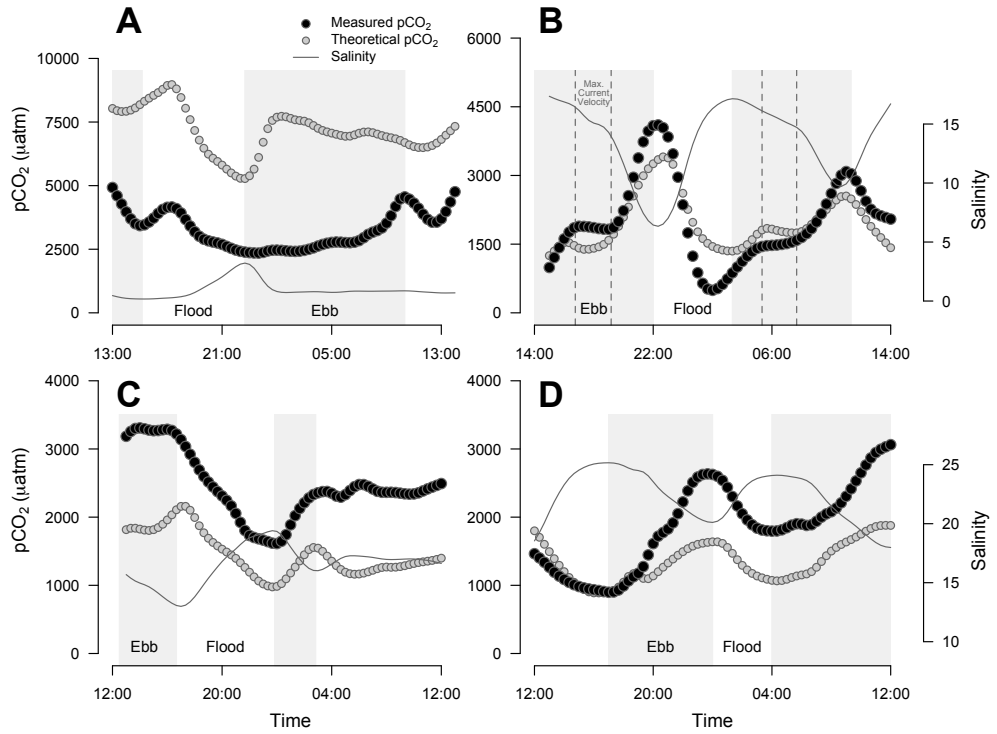

Figure 1-8: Distribution of CO_2 partial pressure (µatm) and salinity during the wet season 24 h tidal cycles in the Can Gio mangrove estuary. Continuous data were discretised using a 20 min step (73 values per 24 h tidal cycles). Theoretical pCO_2 (µatm) was calculated using pH and Talk, according to the carbonate system equilibrium constants (Park 1969). Letters at the upleft corner indicate the sampling site

4.2. Water-air CO_2 fluxes

Emissions of CO_2 at low current velocity ranged from 74 to 792 mmol m^{-2} d^{-1} during the dry season, and from 128 to 876 mmol m^{-2} d^{-1} during the wet season (Figure 1-9a). A linear relationship was observed between FCO_2 and salinity, without significant effect of season on this relationship (ANCOVA; $F_{2,20}$ = 27.7; $p_{salinity}$ <0.001 and p_{season} = 0.19; Figure 1-9a). Corresponding k_{600} ranged from 6.4 to 11.0 m d^{-1} during the dry season and from 1.7 to 10.9 m d^{-1} during the wet season (Figure 1-9b), with significantly higher values obtained during the dry season (Student test; t_{20} = 2.46; p = 0.02). Both theoretical gas exchange velocities (W92 and R17) differed considerably from our experimental values, yielding lower k_{600} values, always remaining under 7 m d^{-1} for W92 (on average 3.9 ± 2.4 times higher than measured k_{600}; n = 17) and under 4 m d^{-1} for R17 (on average 2.2 ± 1.0 times higher than measured k_{600}; n = 17).

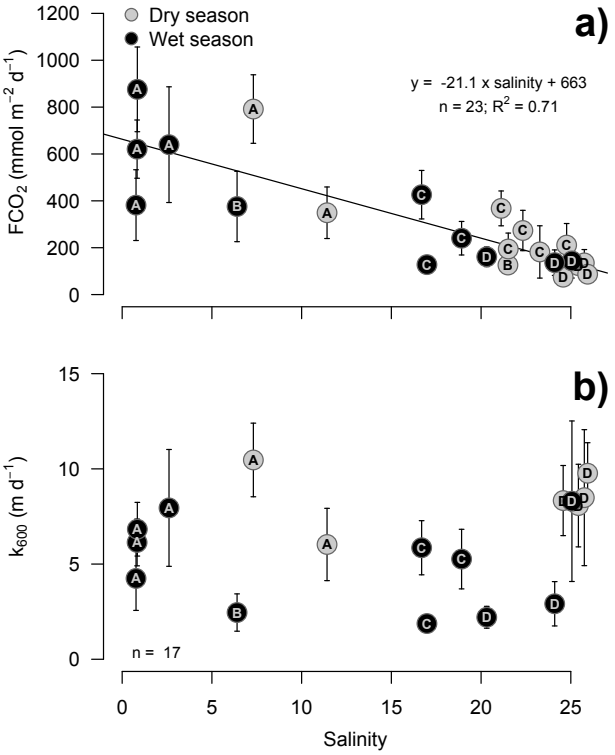

Figure 1-9: Distribution of a) CO_2 emissions (mmol m^2 d^{-1}) and b) CO_2 gas transfer velocity (m d^{-1}) along the salinity gradient of the Can Gio mangrove estuary. Note that error bars correspond to standard deviation of 4-5 replicated measurements

5. Discussion

5.1. Physico-chemical functioning of the estuary

Salinity at the marine endmember of our study (D) did not exceed 26, remaining far from the usual value of 35 for marine waters and suggesting a strong dilution of coastal waters by riverine inputs, due to the proximity of the Mekong delta. During the wet season, DO concentration dropped to 0.9 mg L^{-1} (17% DO saturation) at the freshwater endmember of the Can Gio mangrove estuary (site A at salinity ~0; Figure 1-2b), which may lead to highly detrimental effects on living organisms and biogeochemical cycling (Cloern 2001, Yin et al. 2004). Such depleted levels of oxygen have been only observed in highly urbanised estuaries, such as the Scheldt estuary in the Netherlands or the Recife estuarine system in Brazil, whose watershed are highly polluted by wastewaters of anthropogenic origin (Borges and Abril 2011, Noriega et al. 2013). In other Vietnamese aquasystems, such as the Mekong River, reported DO saturation levels were always >60% through the year (Borges and Abril 2011). Low levels of oxygen in the Can Gio mangrove estuary are probably due to elevated inputs of

labile organic matter, which enhance oxygen consuming decomposition processes. Also, seasonal difference in DO saturation indicates that oxygen consumption is higher during the wet season. However, in contrast with our measurements, higher organic matter decomposition should have led to lower pH during the wet season. Other factors, such as a seasonal difference in the nature of inputs, might counterbalance pH lowering due to organic matter decomposition.

We thus suggest that the Can Gio mangrove estuary is highly impacted by an intense anthropogenic pressure in the higher watershed of the Saigon – Dong Nai River, as observed by Strady et al. (2017). We expect the high oxygen demand to contribute to elevated levels of pCO_2 in the water column and to cause high CO_2 emissions at the water-air interface in the estuary.

5.2. Carbon distribution and speciation

Particulate organic carbon concentrations in the estuary (0.05-0.50 mmol L^{-1}; Table 1-1) were within the range reported for large Asian rivers by Le et al. (2017), with values usually ranging from 0.01 to 0.75 mmol L^{-1}. POC inputs increased during the monsoon season probably as a result of increased runoff. However, %POC in SPM were higher whatever the season (1.26-5.05%; Figure 1-4b) than the average %POC of tropical Asian rivers (1.23%; Huang et al. 2012). Since Can Gio district is located downstream the densely populated Ho Chi Minh City, elevated %POC values at the freshwater endmember of the estuary are probably due to anthropogenic inputs of organic matter (Strady et al. 2017). In benthic sediments of the Saigon-Dong Nai River, Minh et al. (2007) measured highest %POC in Ho Chi Minh City urban canals and values decreased towards the South China Sea, reinforcing the idea that elevated %POC originates from anthropogenic inputs. The non-linear decrease of %POC along the salinity gradient of the Can Gio mangrove estuary suggests that organic matter is decomposed during water transit rather than just diluted with marine waters, thus consuming oxygen and releasing CO_2 within the water column.

The relationship between POC and SPM (Figure 1-5) is a general feature in estuaries and the equation linking both parameters in the present study is similar to that obtained by Le et al. (2017) in northern Vietnam. As a result, POC concentrations were closely related to SPM concentrations, which were themselves driven by a well-known cycle of suspension,

flocculation, settling, deposition, erosion, and resuspension (Verney et al. 2009). In our study, we observed highest SPM values just after the maximum current velocity was reached (unpublished data), most probably as a result of resuspension.

Dissolved organic carbon concentrations in the Can Gio mangrove estuary (0.10-0.40 mmol L^{-1}; Table 1-1) were also within the range reported for large Asian rivers by Le et al. (2017), with values usually ranging from 0.01 to 0.71 mmol L^{-1}, and slightly under the average concentration reported by Huang et al. (2012) for tropical Asian rivers (0.43 mmol L^{-1}). DOC variability could not be linked to any physical or chemical parameters measured during the 24 h time series. Mangrove ecosystems may act as sources of DOC in estuaries (Dittmar et al. 2006, Leopold et al. 2017), while DOC is sensitive to photodegradation (Scully et al. 2003, Dittmar et al. 2006) and biological factors such as microbial activity (Adame et al. 2012, Baltar et al. 2017). A high turnover of the DOC pool is thus to be expected, leading to the absence of correlation with the salinity gradient. In addition, the lower DOC concentrations during the wet season suggest that inputs were lower during this season or/and that DOC was more efficiently mineralised.

Dissolved inorganic carbon concentration at the freshwater endmember of the estuary (0.7-0.8 mmol L^{-1}; Figure 1-3a) was low compared to other tropical Asian estuaries, usually exhibiting DIC concentrations above 1 mmol L^{-1} (Huang et al. 2012, Li et al. 2013). Despite this, DIC was the dominant form of carbon brought by the watershed to the estuary (1.3 to 4 times higher than TOC; Table 1-1). DIC concentrations in rivers vary widely depending on the catchment geology and weathering rates (Guo et al. 2008, Bouillon et al. 2011). The Saigon-Dong Nai River basin is dominated by igneous rocks likely to have a low carbonate content (Vietnam geological map available here: http://urlz.fr/4hM7). Biogeochemical processes such as biological uptake (photosynthesis) and CO_2 degassing to the atmosphere (Guo et al. 2008) can also lower DIC concentration. This latter process may be substantial in the Can Gio mangrove estuary since we measured elevated CO_2 emissions especially in the upstream part of the estuary (Figure 1-9a).

$\delta^{13}C_{DIC}$ was down to -15.4‰ at the freshwater endmember of the Can Gio mangrove estuary (site A at salinity ~0; Figure 1-3b). $\delta^{13}C_{DIC}$ in estuaries depend on a combination of weathering rate of mineral carbonates with $\delta^{13}C$~0, organic carbon respiration producing DIC with similar $\delta^{13}C$ to that of the organic carbon source, and removal of CO_2 with $\delta^{13}C$ values 7 to 10‰ lower than that of HCO_3^-, among other factors that we considered less significant in

our study (Finlay 2003, Miyajima et al. 2009). In a simplified form, inputs of highly $\delta^{13}C$-depleted CO_2 from heterotrophic respiration (-30 to -25‰ in river waters and sediments; Miyajima et al. 2009) would decrease $\delta^{13}C_{DIC}$, and CO_2 emissions would increase $\delta^{13}C_{DIC}$ because of preferential release of $\delta^{13}C$ depleted CO_2. In our study, DIC entering the estuary had $\delta^{13}C$ values closer to those obtained by heterotrophic respiration than to those due to mineral carbonates weathering. We thus suggest that organic carbon respiration substantially contributes to the DIC concentration in the water column.

Measures of DIC and $\delta^{13}C_{DIC}$ showed nearly conservative patterns along the salinity gradient of the Can Gio mangrove estuary (Figure 1-3). Lateral inputs from mangrove soils are generally richer in DIC with more depleted $\delta^{13}C$ values than nearby estuarine waters (Miyajima et al. 2009, Abril et al. 2013, Maher et al. 2013). We expected such inputs to have maintained the $\delta^{13}C_{DIC}$ below the theoretical mixing line during the water transit, as observed by Miyajima et al. (2009) in the Khura mangrove dominated estuary in Thailand. In our study, mangrove soils inputs were probably too low to be traced at the scale of a large estuary such as that of the Saigon-Dong Nai River. We thus reject our hypothesis that DIC releases from surrounding mangrove soils contribute to the inorganic carbon enrichment of the water column.

Partial pressure of CO_2 substantially varied during tidal cycles along the salinity gradient of the Can Gio mangrove estuary (Figure 1-6). In acidic, organic-rich freshwaters (site A), theoretic calculation using pH and TAlk probably overestimated pCO_2 (Abril et al. 2015). Higher slope coefficients of individual regressions on direct pCO_2 measurements (Figure 1-7) compared to the overall regression (Figure 1-6) suggest that CO_2 was added to the water column during ebb, probably from lateral and groundwater inputs, whether from aquaculturally altered floodplain or mangrove soils (Borges and Abril 2011, Atkins et al. 2013, Leopold et al. 2017). Then, CO_2 may be lost because of emissions towards the atmosphere (Atkins et al. 2013, Müller et al., 2016, Leopold et al. 2017) or utilisation by autotrophic organisms (Borges and Abril 2011; Li et al. 2013). Autotrophic production would however increase DO saturation during day, what we do not observe in our estuary, suggesting that CO_2 losses are mostly due to water-air emissions. As a consequence, during ebb, measured pCO_2 tend to rise above the theoretical values of pCO_2, obtained from the carbonate system equilibrium, and during flood it tends to drop below, especially at site B and D that were monitored during strong spring tides (Figure 1-8 and Table 1-1). Actually, we chose to monitor

the four sites under different tidal intensity, which could have affected the functioning of the tidal pumping and the intensity of releases from the mangrove ecosystem (Call et al. 2015). Our choice however increases the variability of background conditions within each season and strengthens the comparison among seasons. At the middle of ebb tide, the measured pCO_2 rises more slowly, indicating that inputs are lower or losses are higher during this stage. This phenomenon was particularly pronounced at site B, monitored during a strong spring tide (tidal coefficient 115; Table 1-1) and where maximum current velocity reached 1.3 m s^{-1} (data not showed). We did not expect inputs to be lower at the middle of the ebb tide compared to the beginning and the end of this period. However, current velocity was maximum at this moment and water turbulence created by current velocity may increase CO_2 emissions in estuaries (Borges et al. 2004, Ho et al. 2016). Thus, pCO_2 dynamics in the water column of the Can Gio mangrove estuary is suggested to be notably controlled by both lateral inputs from adjacent wetlands and emissions towards the atmosphere, and this dynamics is probably affected by current velocity.

Nevertheless, dissolved CO_2 constituted only a small fraction of DIC, ranging from 19 to 133 µmol L^{-1} after conversion using Henry's law ($[CO_{2\ (aq)}] = K_0 \times pCO_2$; Weiss 1974). It represented on average 10 to 1% of DIC, respectively at the riverine and marine endmembers of the estuary and thus even though tidal variations of pCO_2 were evidenced, their effect on DIC is low.

5.3. CO_2 emissions at the water-air interface

Distribution of FCO_2 along the salinity gradient revealed, at low current velocity, higher values at the freshwater endmember of the estuary compared to its marine counterpart. These emissions reflect the pCO_2 decrease during water transit. High CO_2 inputs are brought at the freshwater endmember of the estuary as well as organic matter, which is decomposed during water transit, as described earlier. The system tends towards equilibrium with atmospheric air when reaching the mouth of the estuary.

Emissions of CO_2 in the Can Gio mangrove estuary were about 10 times higher than average values reported for northern hemisphere low latitude estuaries (388.4 at salinity = 13 vs. 38.9 mmol m^{-2} d^{-1} in the review of Chen et al. 2013; Figure 1-9a). Similar FCO_2 than measured in our study were observed in two macrotidal estuaries in western Sarawak

(Malaysia), where CO_2 fluxes were determined with a floating chamber, and estimated to range from 38.4 to 734.2 mmol m^{-2} d^{-1} (Müller et al. 2016). The use of floating chambers has been a matter of debate since it may create artificial turbulence at the water-air interface, increasing FCO_2 (Matthews et al. 2003, Lorke et al. 2015). Floating chambers are, however, more susceptible to disruption in low turbulence environment compared to high turbulence environment (Vachon et al. 2010). We intended to reduce artificial turbulences by using a large volume floating chamber with wall extension into the water and weighted to increase stability, and we only displayed FCO_2 measured at low current velocity, reducing the disruptions induced by chamber anchorage (Lorke et al. 2015). We thus feel confident about the validity of our measurements.

Most of CO_2 flux measurements available in the literature were determined using pCO_2 and the gas transfer velocity k (Chen et al. 2013). Published values of k_{600} are, however, based on a theoretical calculation, using equations established for temperate systems (Raymond and Cole 2001, Borges et al. 2004) or for the ocean-air interface (Wanninkhof et al. 1992). The estimation of k has been of major interest over the last decades and various authors have sought for variables to constrain the predictions of FCO_2. The gas transfer velocity is affected by velocity of wind and current, water depth and turbidity (Wanninkhof 1992, Abril et al. 2009, Rosentreter et al. 2017). In our study, values of k_{600} derived from floating chamber measurements (Figure 1-9b) may have been affected by such parameters, but no correct prediction of k could be established, suggesting that other factors may also affect the gas transfer velocity, such as organic carbon load, tidal stage, day/night alternance or cargo traffic. Wind velocity, which is usually considered as crucial parameter influencing water-air exchanges, especially in low turbulence environments (Wanninkhof 1992), was not especially high in the Can Gio mangrove estuary and may not strongly affect gas exchange rates compared to other parameters affecting turbulence. In addition, monitoring the four sites under different tidal intensity could also have affected CO_2 emissions and a larger dataset would be necessary to partition the effect of each factor. Nevertheless, our values of k_{600} remained higher than theoretical gas exchange velocities (W92 and R17), suggesting that CO_2 emissions would have been underestimated using available relationships. In tropical estuaries, high temperatures, which decrease CO_2 solubility in the water and increase the gas exchange velocity, can partially explain high FCO_2 (Müller et al. 2016). Moreover, the watershed of Can Gio mangrove estuary is strongly impacted by anthropogenic pressure and

the mineralisation of labile organic carbon may have increased CO_2 exchange rates. We thus suggest that the use of floating chambers could help to refine the carbon budget of tropical coastal ecosystems with high organic matter load.

6. Conclusions

High inputs of labile organic matter from the Saigon – Dong Nai River watershed induce low DO saturation and high pCO_2 in the Can Gio mangrove estuary and reflects the intense human pressure at the freshwater endmember of the ecosystem. Lower DO saturation, higher pCO_2 and higher %POC in SPM during the wet season indicate higher inputs of labile organic matter during this rainy season, probably because of soil leaching.

Contrary to our hypothesis, DIC releases from adjacent wetlands are probably too low to be traced at the scale of a large estuary such as the Saigon-Dong Nai River. However, our study highlights that during ebb tide CO_2 inputs from adjacent wetlands substantially contributed to the water column pCO_2 enrichment and moved the carbonate system towards disequilibrium relatively to theoretical pCO_2 obtained from TAlk and pH. It is, to our best knowledge, the first to evidence that releases from mangrove soils affect the water column pCO_2 at the scale of a large tropical estuary (~600 m wide and 10-20 m deep), as previously observed in smaller mangrove creeks (Abril et al. 2013, Atkins et al. 2013, Call et al. 2015). In addition, our study shows that pCO_2 has to be studied using direct measurements in such highly dynamic environments.

The Can Gio mangrove estuary act as a strong source of CO_2 to the atmosphere, with highest emissions at the anthropogenically impacted freshwater endmember of the estuary. These high CO_2 emissions might be due to both the high water temperature of our estuary (26 to 31°C) and the high organic load (up to 5% of POC in SPM). Although the factors controlling CO_2 emissions could not have been clearly evidenced in our study, nor whether they were affected by the presence of the mangrove, we showed that emissions under low current velocity (< 0.2 m s^{-1}) would have been strongly underestimated (2 to 4 times) using available published equations to estimate the gas transfer velocity k_{600}. We thus suggest that strongly impacted large tropical estuaries have to be more extensively studied to refine their carbon budget, which may have been underestimated at the global scale since much Southeast Asian watersheds are subject to strong anthropogenic pressure. Taking into

account sharp cautions, the use of floating chambers could help to refine such budgets, allowing direct measurements of water-air CO_2 emissions.

7. Acknowledgments

The authors would like to thank the Air Liquide Foundation for providing financial support for gas analysers and samplings field trips. The support of the PEPS CNRS-IRD "Mangrove" is also gratefully acknowledged. Vietnamese students and the Can Gio mangrove management board are gratefully thanked for their help during the field trips.

Chapter 2: Fatty acid and stable isotope ($\delta^{13}C$ and $\delta^{15}N$) composition of suspended particulate matter in a human impacted and mangrove dominated tropical estuary (Can Gio, Vietnam)

DAVID Frank, MARCHAND Cyril , THINEY Najet, TRAN-THI Nhu-Trang and MEZIANE Tarik

Submitted for publication in Marine Environmental Research

1. Abstract

Suspended particulate matter (SPM) is a key component of coastal food webs and its nutritional quality is determinant to sustain trophic webs. The present study aims to investigate seasonal and short-term variations in SPM composition of the Can Gio mangrove estuary and to examine the biological processes occurring during SPM transit. We postulated that i) SPM composition was affected by season, salinity, SPM concentration and daylight, ii) each of these factors influenced different compartments of the SPM pool (i.e. bacteria, phytoplankton, detrital organic matter).

Fatty acids (FA), stable isotopes ($\delta^{13}C$ and $\delta^{15}N$) and C/N ratios of SPM were determined during 24 h time series at two contrasting seasons and at four sites scattered from the upper mangrove zone to the South China Sea coast. Estuarine water SPM was dominated by saturated and monounsaturated FA, indicating that organic matter mainly originated from decaying material. The fatty acid composition of SPM exhibited higher dissimilarity during tidal cycles than that measured between the different sampling sites. A higher contribution of polyunsaturated and branched FA during the wet season revealed a higher biological activity, most probably due to higher mineralisation rates and higher nutrient availability during this season. Short-term variations in the SPM composition during tidal cycles showed an increasing contribution of BrFA correlated to SPM concentrations and a higher contribution of polyunsaturated FA during daytime. Our study highlights that the quality of SPM changes at both short and long temporal scales, which in turn may have implications on the feeding ecology of estuarine organisms and in the estimation of tropical estuaries carbon budget.

2. Introduction

Estuaries are land-ocean boundaries where nutrients and organic matter (OM) are intensely processed before entering the marine environment (Wollast 2003). In tropical ecosystems, OM is exported in higher proportion under dissolved forms (Huang et al. 2012) but it becomes available for higher trophic levels only after being assimilated through the microbial loop (Azam 1998). Suspended particulate matter (SPM), comprising living cells and decaying particles along with mineral compounds, plays an essential role in marine food webs (Volkman and Tanoue 2002). A wide variety of zooplancton species, such as crustacean larvae, feed on estuarine SPM while they migrate though estuaries to complete their life cycle (Riera et al. 2000). Assessing the origin and fate of SPM in estuaries, and especially in mangrove dominated ones, allows to understand the functioning of these systems, both to design the food web architecture in coastal habitats (Meziane and Tsuchiya 2002, Alfaro et al. 2006, Kelly and Scheibling 2012) and to better estimate carbon budgets (Kristensen et al. 2008, Cai 2011, Hofmann et al. 2011). It may also reveal the contribution of anthropogenic inputs, such as agriculture, aquaculture or urban sewages to the bulk OM (Boëchat et al. 2014).

Lipids and especially fatty acids (FA) were used as environmental tracers to discriminate sources of OM in water and sediments of aquatic ecosystems (Bodineau et al. 1998, Mortillaro et al. 2011, Antonio and Richoux 2015). These organic compounds are synthesised with various degrees of specificity by living organisms, allowing, for instance, to measure the contribution of several taxa to the bulk OM (Dalsgaard et al. 2003, Bergé and Barnathan 2005). In aquatic ecosystems, FA were notably used to trace bacteria (iso- and anteiso-branched chain FA - BrFA; Mortillaro et al. 2011, Boëchat et al. 2014), phytoplankton (polyunsaturated FA - PUFA and 16:1ω7/16:0 ratio; Napolitano et al. 1997, Canuel 2001) and sewage effluents (SewFA: 15:0 + 16:0 + sum of 16:1 + 18:0 + sum of 18:1; Boëchat et al. 2014). However, very few FA are exclusive to any kind of OM. Thus, such biomarkers should preferentially be coupled with other tracers, such as isotopic and elemental compositions of SPM, that are also able to discriminate OM sources and identify biogeochemical processes in estuaries (Middelburg and Herman 2007, Mortillaro et al. 2011, 2016, Bergamino et al. 2014). Indeed, $\delta^{13}C$ and C/N ratio are usually employed to partition terrestrial vs. marine OM in

estuaries, while $\delta^{15}N$ allows to understand its diagenesis (Middelburg and Herman 2007) and can been used as an integrated N-load measurement (McClelland and Valelia 1998).

The SPM composition in estuaries, and therefore its nutritional quality, is impacted by seasonal changes, with generally a higher contribution of terrestrial OM during the wet season (Mortillaro et al. 2011, Boëchat et al. 2014). However, the opposite trend has also been observed, with reduced autochthonous primary production during the dry season (Xu and Jaffé 2007). The SPM composition also varies as a function of salinity (Bodineau et al. 1998, Shilla et al. 2011, Antonio and Richoux 2015), showing the dilution of terrestrial OM with marine OM (Middelburg and Herman 2007, Wu et al. 2012). At shorter temporal scale, the concentration of SPM is strongly affected by tidal currents (Eisma 1986, Wang et al. 2013). SPM transport is driven by a well-known cycle of suspension, flocculation, settling, deposition, erosion, and resuspension, where flocculation process plays a major role as it controls the size, structure, and density of suspended particles, and thus their ability to settle or to remain suspended in the water column (Verney et al. 2009). Flocs are aggregated by mucopolysaccharides and made up of an active biological component (primarily bacteria, although at times other organisms can be incorporated), a detrital biological component (organic fragments), inorganic particles such as clay minerals, carbonates and fine sand, and water held within or flowing through pores (Eisma 1986, Droppo 2001, Verney et al. 2009). Finally, natural populations of estuarine phytoplankton exhibit high diurnal physiological state variability as a response to light or nutrient limitation, notably with regard to lipids concentration (Madariaga 2002, Halsey and Jones 2015). In turbid estuaries, light is often the limiting factor for autotrophic production. Phytoplankton spends most of the time in darkness and photosynthesis only occurs in short intermittent periods when phytoplankton is transported in the euphotic zone (Lancelot and Muylaert 2011).

The present study aims to investigate seasonal and short-term variations in the SPM composition of the Can Gio mangrove estuary and to examine the biological processes occurring during SPM transit. We measured fatty acids, stable isotopes ($\delta^{13}C$ and $\delta^{15}N$) and C/N ratios of SPM in sub-surface water along the salinity gradient of the Can Gio mangrove estuary during two sampling campaigns (dry season in January-February 2015 and wet season in September-October 2015), which included 24 h survey on four sites distributed from the downstream end of Ho Chi Minh City (HCMC; ~13 million inhabitants) to the South China Sea coast. We also sampled potential sources of SPM from upstream rivers, anthropogenic

releases and a mangrove tidal creek. We postulated that the SPM composition variability induced by season and salinity could be lower than that of other factors such as tide induced SPM resuspension or daylight. We hypothesised that: (1) HCMC urban canal releases strongly contributed to the SPM pool in the Can Gio mangrove estuary, (2) the relative contribution of terrestrial OM to the SPM pool would be higher during the wet season due to enhanced soils erosion, (3) high SPM concentrations would be linked to high proportions of bacterial biomarkers and more degraded OM and, (4) sub-surface water would be enriched in phytoplanktonic biomarkers during the day.

3. Materials and methods

3.1. Study area

The Saigon River flows through Ho Chi Minh City (Southern Vietnam; ~13 million inhabitants) and drains urban canals before joining the Dong Nai River, exhibiting annual discharge roughly 10 times higher than that of the Saigon River (Nippon Koie 1996). After a few kilometres, the Saigon-Dong Nai River splits again and forms a delta, which drains the Can Gio mangrove forest, covering an area of 719.6 km^2 and accounting for 20% of Vietnam's mangrove forests (Tuan and Kuenzer 2012). In 2000, the UNESCO designated Can Gio as the first mangrove biosphere reserve in Vietnam and a clear land use regulation was established. Forested areas account for 44.5% of the total surface coverage and waterways for 31%, while 24.5% of the land area is dedicated to socio-economic development, mostly shrimp farming (Nam et al. 2014). The climate of Can Gio is monsoonal with a wet season from June to October and a dry season from November to May (Nam et al. 2014). The mangrove experiences a semidiurnal tidal regime with its amplitude ranging between 2 to 4 m, depending on season and proximity to the sea (Tuan and Kuenzer 2012).

We selected the study sites to be at the interface between land uses (Figure 2-1): A) at the downstream end of Ho Chi Minh City (10°39'55"N 106°47'30"E); B) between shrimp farms and the mangrove forested area (10°34'19"N 106°50'11"E); C) in the centre of the mangrove protected core (10°31'04"N 106°53'13"E); and D) between the mangrove forested area and the South China Sea coast (10°29'32"N 106°56'55"E). All sites were located on the main estuarine channel, which has steep eroded banks, a width of about 600 m and a depth

averaging 12 m. These characteristics make the estuary not favourable towards benthic productivity.

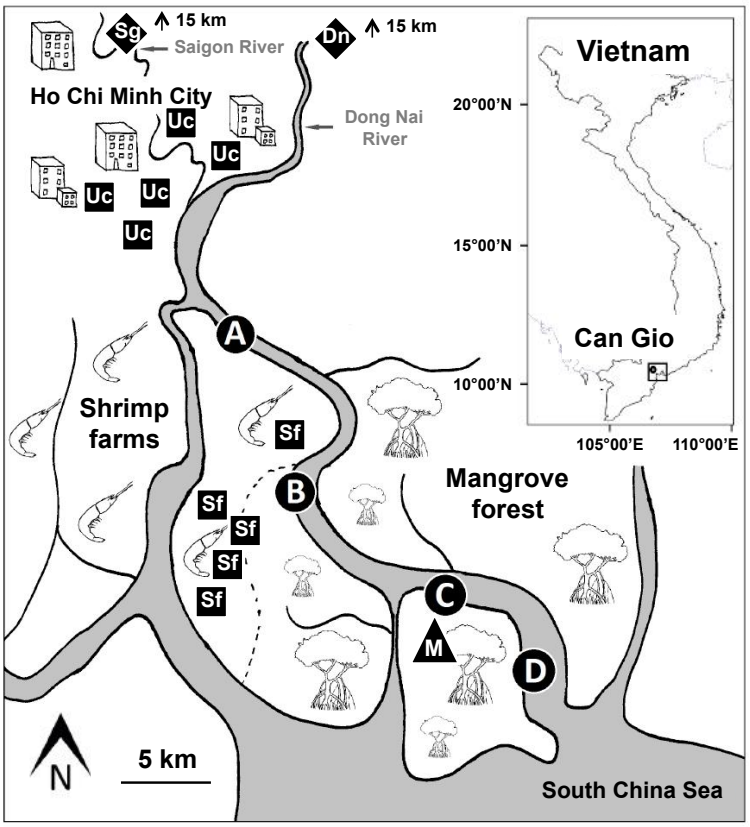

Figure 2-1: Localisation map of the Can Gio mangrove estuary (Southern Vietnam). A, B, C and D indicate the sampling stations along the estuary and other symbols indicate sampling of SPM sources (Sf = Shrimp farms; Uc = Urban canals; Sg = Saigon River, Dn = Dong-Nai River; M = Mangrove creek)

3.2. Sampling strategy

We monitored surface SPM during 24 h time series during the dry (January-February) and monsoon (September-October) periods in 2015. Salinity was measured using a Yellow Spring Instrument® meter (YSI 6920) immersed 30 cm below water surface and calibrated before each survey. Values were not recorded at site C during the dry season due to probe dysfunction and were estimated using a linear relationship established on the three other sites between alkalinity measured on the same filtered water samples and salinity (salinity = 16.1 × alkalinity (mmolC L^{-1}) – 7.1; R^2 = 0.99; n = 39, unpublished data). The maximum difference between calculated and probe measured salinity was 1.8, which was relatively low given the amplitude of the monitored salinity gradient (0 to 26).

Five samples of surface water were taken every two hours (13 samplings per 24 h time series) using a 10 L bucket. Samples were immediately vacuum-filtered through pre-combusted (5 h at 450°C) and pre-weighted glass fibre filters (Whatman® GF/F 0.7 µm) until complete clogging of the filters. It required 250 mL to 1.2 L of estuarine water and allowed the collection of 10 to 80 mg of SPM, depending on turbidity. In addition, we collected potential sources of SPM at low tide during the wet season upstream from Ho Chi Minh City (Saigon River 10°58'51"N 106°38'36"E and Dong Nai River 10°56'45"N 106°48'20"E; Image 2-1a), within five urban canals (Image 2-1b), from five active shrimp ponds, and twice at two hours interval during ebb tide in a mangrove channel (10°30'24"N 106°52'57"E; Figure 2-1). The Saigon River mostly collects urban wastewaters from urban canals located in HCMC, while shrimp ponds water is periodically renewed and pumped out (Anh et al. 2010) to adjacent canals connected to the estuary near site B (Figure 2-1). Finally, mangrove soils release high loads of SPM during ebb tide due to erosion of surface sediments (Bouillon et al. 2007). All filters were immediately stored at -25°C until analyses.

Image 2-1: a) Sampling site on the Dong Nai River upstream HCMC and
b) urban canal located within HCMC and releasing wastewaters in the estuary

3.3. Sample processing

Filters were first freeze-dried and weighted for SPM determination. Then, four filters of SPM per sampling event were used as replicates for the analysis of fatty acids and the remaining filter was used for dual ($\delta^{13}C$ and $\delta^{15}N$) stable isotopes analysis and C/N ratio determination. We measured stable isotopes and C/N ratio on the four sites during both seasons, while FA were measured on the four sites during the dry season but only on site B and D during the monsoon season. Replicated analyses of FA were averaged before statistical analyses.

We extracted lipids following a slightly modified protocol of Bligh and Dyer (1959), as described in Meziane et al. (2007). Tricosanoic acid (23:0) was used as an internal standard and 5 µg of methyl tricosanoate provided by Sigma-Aldrich® was added to every sample prior to extraction. Lipids were extracted with 4mL of a water:methanol:chloroform mixture (1:2:1, v:v) enhanced by two 20 min steps of sonication. The lipid fraction, contained in the chloroform, was retrieved after phases were separated by centrifugation (3000 rpm, 1400 rcf, 5 min), and evaporated under nitrogen (N_2) flux. Dried lipid extracts were saponified using a methanol:sodium hydroxide (2N) mixture (2:1, v:v) during 1 h 30 min at 90°C. Fatty acid esters were then methylated into fatty acid methyl esters (FAME) using boron trifluoride-methanol (BF_3-CH_3OH) and stored at -25°C. FAME were quantified by gas chromatography analysis (Varian 3800-GC), using a flame ionisation detector. The oven temperature was set at 60°C and held for 1 min, raised at 40°C min^{-1} to 150°C and held for 3 min, and then increased to 240°C at 3°C min^{-1} and held for 25 min. We identified fatty acids using coupled gas chromatography mass spectrometry (Varian 450-GC; Varian 220-MS) and comparison of GC retention times with commercial standards (Supelco® 37 component FAME mix). We reported the values as % of total FA or absolute concentrations (µg L^{-1} or µg $mgSPM^{-1}$).

We analysed stable isotope ratios at the University of California Davis Stable Isotope Facility (Department of Plant Sciences, UC Davis, Davis, California) using a Vario EL Cube elemental analyser (Elementar Analysensysteme GmbH, Hanau, Germany) interfaced to a PDZ Europa 20–20 isotope ratio mass spectrometer (Sercon Ltd., Cheshire, U.K.). We prepared the samples in tin capsules by scraping the SPM clogging the filters and after 4 h of HCl 37% fumigation and then Davis University performed the analysis. Carbon and nitrogen stable isotope ratios were reported in parts per thousand (‰), using standard delta notation ($\delta^{13}C$ and $\delta^{15}N$), and are relative to V-PDB (Vienna PeeDee Belemnite) and atmospheric air, respectively. We calculated the C/N ratio using the mass abundance of carbon and nitrogen in a given sample.

3.4. Data analyses

We compared FA proportions in anthropogenic sources (urban canals and shrimp pond effluents) vs. estuarine sites using non-parametric Kruskal-Wallis rank sum test multiple comparisons due to the low amount of data (5 per anthropogenic sources and 13 per

estuarine site). We identified groups of samples differing from one another using Wilcoxon pairwise comparisons (α= 5%). Non-metric multidimensional scaling (N-MDS) of the FA profiles (% total FA) was used to examine the proximity between SPM samples taken in the main waterways (upstream rivers, estuarine sites and mangrove tidal creek). We challenged the effect of season, salinity (taken as a proxy of fresh vs. marine waters mixing ratio), SPM concentration and daylight on the composition of FA (%BrFA as indicator of bacteria, %SewFA as indicator of decomposition state of OM, and %PUFA and 16:1ω7/16:0 ratio as indicators of phytoplankton), stable isotopes and C/N ratios using sequential analysis of covariance (Type I ANCOVA). Salinity and SPM dry mass were considered as quantitative variables, and season and presence of daylight were set as qualitative variables. Sequential ANCOVA were used to test whether our set of biomarkers in the SPM were correlated with independent and highly variable factors. We chose the order in which the terms were introduced in the model according to the expected effect of each factor, allowing to test the effect of each subsequent variable relative to the preceding model. In the model using FA, we introduced SPM first because data were not equally distributed among seasons (Table 1), while we started with salinity in the model using stable isotope ratios for the same reason. We tested all other factors in pairs and they showed no correlation with one another. SPM data were natural log transformed before analyses to alleviate heteroscedasticity and improve normality. We reported models sum of squares (SS), Fisher test value (F value) and probability of obtaining the same value considering the null hypothesis true (p). Statistical analyses and graphical representations were performed using R (R Core Team 2017).

4. Results

Salinity ranged from 7 to 26 during the dry season and from 0 to 25 during the wet season. SPM concentration ranged from 14 to 293 mg L^{-1} and exhibited important tide induced variability, with highest SPM values measured just after the maximum current velocity was reached (unpublished data). $\delta^{13}C$ ranged from -27.6‰ to -24.5‰ with lowest values observed at site A during the dry season (Figure 2-2a). $\delta^{15}N$ ranged from 2.7‰ to 9.1‰ with higher values observed at site A during the wet season (Figure 2-2b). Finally, C/N ratios ranged from 5.3 to 12.3 (Figure 2-3b).

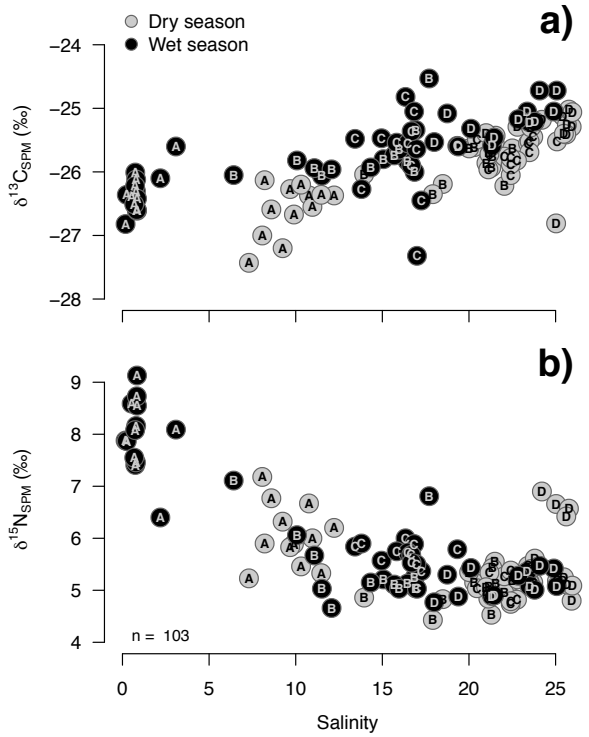

Figure 2-2: a) $\delta^{13}C$ and b) $\delta^{15}N$ of SPM expressed as a function of salinity in the Can Gio mangrove estuary. Letters in bubbles correspond to the sites where samples were taken

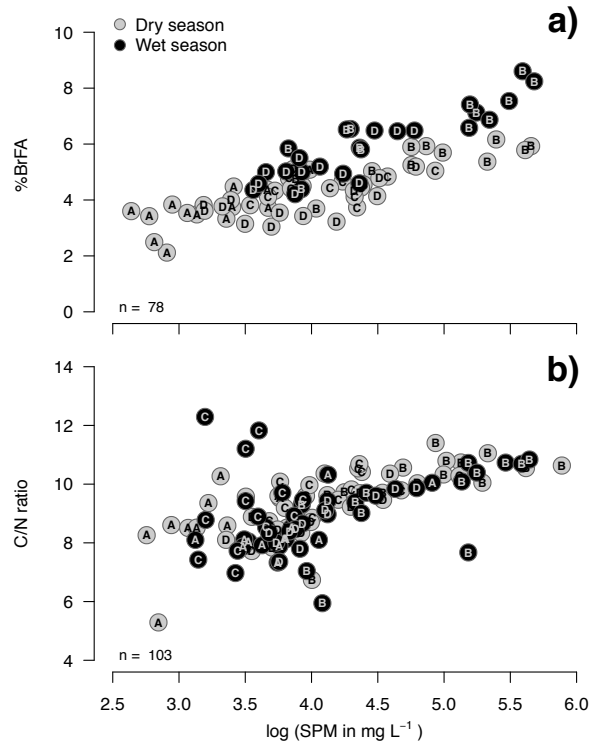

Figure 2-3: a) BrFA (%) and b) C/N ratio of SPM expressed as a function of SPM concentrations in the Can Gio mangrove estuary. Letters in bubbles correspond to the sites where samples were taken

We identified up to 42 FA in the SPM samples of the Can Gio mangrove estuary and contributing sources (Table 2-1 and Table 2-2). Predominant FA were saturated fatty acids (SFA) 16:0, 18:0 and 14:0 and monounsaturated fatty acids (MUFA) 18:1ω9, 16:1ω7, 18:1ω7 and 22:1ω9. As postulated, the SPM fatty acid composition of estuarine sites exhibited variability during tidal cycles that encompassed site induced differences (Figure 2-4). During both seasons, a general trend ordering the sites according to the salinity gradient was, however, highlighted. SPM originating from the upstream Dong Nai River was located at the beginning of this gradient during the wet season, while SPM originating from the Saigon River was placed farther from the estuarine sites point dispersal. Samples taken in the mangrove channel also stepped out the estuarine points, between the Saigon River and estuarine SPM (Figure 2-4). The Dong Nai River SPM exhibited lower %PUFA, %MUFA and 16:1ω7/16:0 ratio than the Saigon River, and higher %SFA, while the mangrove channel showed intermediate %PUFA, %SFA and 16:1ω7/16:0 ratio values, and a %MUFA similar to that of the Saigon River (Table 2-2).

Table 2-1: Mean (±SD) fatty acid composition of SPM during the 24 h tidal cycles in the Can Gio mangrove estuary

Fatty acids (%)	Dry Season				Wet Season	
	Site A (n = 13)	Site B (n = 13)	Site C (n = 13)	Site D (n = 13)	Site B (n = 13)	Site D (n = 13)
Saturated						
12:0	2.0 ± 1.8	2.0 ± 1.5	2.0 ± 1.7	1.7 ± 1.4	2.6 ± 1.5	2.5 ± 1.4
13:0	0.2 ± 0.2	0.3 ± 0.2	0.3 ± 0.2	0.2 ± 0.1	0.7 ± 0.3	0.6 ± 0.3
14:0	6.0 ± 1.6	5.6 ± 1.5	6.4 ± 1.8	7.1 ± 2.0	8.7 ± 1.5	9.0 ± 1.0
15:0	2.0 ± 0.7	2.2 ± 0.7	2.2 ± 0.9	2.7 ± 0.9	2.8 ± 0.4	2.4 ± 0.4
16:0	32.6 ± 5.3	28.9 ± 4.3	33.3 ± 4.7	34.8 ± 4.2	28.4 ± 2.2	30.0 ± 2.1
17:0	1.0 ± 0.2	1.3 ± 0.3	1.2 ± 0.2	1.2 ± 0.3	1.4 ± 0.2	1.3 ± 0.3
18:0	16.3 ± 4.8	16.5 ± 4.3	16.8 ± 5.5	13.2 ± 4.0	7.8 ± 1.3	7.8 ± 1.7
19:0	0.3 ± 0.3	0.5 ± 0.3	0.4 ± 0.3	0.3 ± 0.2	0.6 ± 0.2	0.5 ± 0.2
20:0	0.7 ± 0.2	0.9 ± 0.2	0.7 ± 0.2	0.7 ± 0.2	0.5 ± 0.1	0.7 ± 0.4
21:0	0.2 ± 0.1	0.3 ± 0.2	0.2 ± 0.1	0.2 ± 0.1	0.1 ± 0.1	0.0 ± 0.0
22:0	0.7 ± 0.2	0.8 ± 0.3	0.6 ± 0.2	0.6 ± 0.2	0.5 ± 0.1	0.3 ± 0.1
24:0	0.9 ± 0.5	1.1 ± 0.6	0.7 ± 0.5	0.8 ± 0.6	0.2 ± 0.2	0.1 ± 0.1
26:0	0.3 ± 0.2	0.5 ± 0.3	0.4 ± 0.2	0.4 ± 0.2	n.d.	n.d.
∑SFA	**62.9 ± 9.3**	**60.3 ± 8.3**	**64.7 ± 8.4**	**63.4 ± 7.5**	**54.3 ± 2.9**	**55.3 ± 3.7**
Monounsaturated						
14:1ω5	0.2 ± 0.2	0.2 ± 0.2	0.2 ± 0.3	0.3 ± 0.2	0.4 ± 0.1	0.3 ± 0.1
16:1ω9	2.1 ± 1.9	2.2 ± 2.0	2.1 ± 2.1	3.0 ± 1.8	2.2 ± 0.9	1.5 ± 0.5
16:1ω7	4.3 ± 1.7	5.2 ± 1.5	5.2 ± 1.9	5.0 ± 1.7	8.5 ± 1.0	10.3 ± 1.5
17:1ω9	0.4 ± 0.4	0.7 ± 0.4	0.4 ± 0.4	0.6 ± 0.4	0.3 ± 0.2	0.2 ± 0.1
17:1ω7	0.4 ± 0.2	0.6 ± 0.1	0.6 ± 0.2	0.4 ± 0.2	0.7 ± 0.1	0.9 ± 0.2
18:1ω9	10.3 ± 3.5	12.5 ± 4.2	11.7 ± 3.9	11.5 ± 3.9	12.7 ± 2.3	10.7 ± 1.6
18:1ω7	2.5 ± 0.8	3.9 ± 1.1	3.3 ± 1.0	2.6 ± 0.7	5.7 ± 1.0	6.4 ± 1.0
20:1ω11	0.3 ± 0.1	0.3 ± 0.1	0.4 ± 0.2	0.3 ± 0.1	0.2 ± 0.1	0.1 ± 0.1
20:1ω9	0.1 ± 0.1	0.1 ± 0.1	0.1 ± 0.1	0.1 ± 0.1	0.1 ± 0.1	0.1 ± 0.1
22:1ω9	7.9 ± 4.8	3.5 ± 3.1	1.1 ± 0.9	1.0 ± 1.4	0.9 ± 0.6	0.2 ± 0.3
∑MUFA	**28.4 ± 8.4**	**29.2 ± 7.7**	**25.0 ± 6.9**	**24.9 ± 6.2**	**31.6 ± 3.0**	**30.7 ± 2.8**
Polyunsaturated						
16:2ω6	n.d.	n.d.	n.d.	n.d.	0.3 ± 0.1	0.2 ± 0.1
16:2ω4	0.2 ± 0.1	0.3 ± 0.2	0.4 ± 0.2	0.5 ± 0.2	0.6 ± 0.2	0.8 ± 0.4
16:3ω4	0.2 ± 0.1	0.4 ± 0.2	0.5 ± 0.2	0.6 ± 0.3	0.8 ± 0.4	1.1 ± 0.5
16:4ω3	0.2 ± 0.1	0.2 ± 0.2	0.2 ± 0.2	0.3 ± 0.1	0.4 ± 0.1	0.3 ± 0.1
18:2ω6	1.3 ± 0.5	1.3 ± 0.5	1.3 ± 0.5	1.4 ± 0.6	1.3 ± 0.4	1.3 ± 0.3
18:3ω3	0.8 ± 0.7	0.4 ± 0.5	0.5 ± 0.4	0.8 ± 0.4	0.5 ± 0.5	0.7 ± 0.3
18:4ω3	0.6 ± 0.6	0.4 ± 0.5	0.6 ± 0.5	1.1 ± 0.6	0.4 ± 0.4	0.6 ± 0.3
20:4ω6	0.2 ± 0.1	0.3 ± 0.1	0.3 ± 0.3	0.3 ± 0.1	0.6 ± 0.2	0.7 ± 0.3
20:5ω3	1.0 ± 0.4	1.2 ± 0.5	1.5 ± 0.6	1.9 ± 0.8	1.9 ± 0.6	2.5 ± 0.7
22:6ω3	0.6 ± 0.3	0.7 ± 0.4	0.7 ± 0.3	1.1 ± 1.0	0.5 ± 0.3	0.7 ± 0.3
∑PUFA	**5.1 ± 2.2**	**5.2 ± 2.2**	**5.9 ± 2.1**	**7.9 ± 2.8**	**7.3 ± 2.2**	**8.9 ± 2.4**
Branched						
14:0iso	0.3 ± 0.1	0.4 ± 0.1	0.3 ± 0.1	0.3 ± 0.1	0.9 ± 0.1	0.6 ± 0.1
15:0iso	1.0 ± 0.3	1.5 ± 0.4	1.2 ± 0.3	1.0 ± 0.3	2.0 ± 0.5	1.5 ± 0.3
15:0anteiso	0.8 ± 0.2	1.1 ± 0.2	0.9 ± 0.2	0.8 ± 0.2	1.2 ± 0.3	0.9 ± 0.2
16:0iso	0.5 ± 0.1	0.8 ± 0.2	0.6 ± 0.2	0.5 ± 0.1	0.7 ± 0.2	0.5 ± 0.1
17:0iso	0.6 ± 0.1	0.8 ± 0.2	0.8 ± 0.2	0.7 ± 0.2	0.9 ± 0.2	0.9 ± 0.1
17:0anteiso	0.5 ± 0.2	0.7 ± 0.2	0.6 ± 0.3	0.4 ± 0.1	0.9 ± 0.3	0.7 ± 0.2
∑BrFA	**3.6 ± 0.9**	**5.3 ± 1.0**	**4.4 ± 0.9**	**3.8 ± 0.8**	**6.7 ± 1.2**	**5.2 ± 0.9**
∑FA (µg mgSPM^{-1})	1.0 ± 0.5	0.3 ± 0.2	0.5 ± 0.2	0.8 ± 0.4	0.6 ± 0.3	0.7 ± 0.2
SPM (mg L^{-1})	27.2 ± 11.6	141.5 ± 83.2	65.8 ± 28.3	55.1 ± 30.0	150.9 ± 86.9	62.6 ± 27.2
% SewFA	69.8 ± 5.0	71.1 ± 3.6	74.4 ± 3.6	72.7 ± 2.9	68.1 ± 2.8	69.1 ± 2.7
16:1ω7/16:0	0.14 ± 0.06	0.19 ± 0.07	0.16 ± 0.07	0.15 ± 0.06	0.30 ± 0.04	0.35 ± 0.06
Salinity	9.7 ± 1.5	20.2 ± 2.3	22.6 ± 1.3	24.6 ± 1.5	13.9 ± 3.4	22.1 ± 2.4
n Day/Night	6/7	6/7	7/6	6/7	5/8	6/7

Σ SewFA 15:0 + 16:0 + 16:1 + 18:0 + 18:1
n.d. = not detected

Table 2-2: Mean (±SD) fatty acid composition of SPM sources in the Can Gio mangrove estuary

Fatty acids (%)	Wet Season				
	Shrimp farms (n = 5)	Urban canals (n = 5)	Mangrove chennal (n = 2)	Saigon River (n = 1)	Dong Nai River (n = 1)
Saturated					
12:0	0.3 ± 0.1	1.3 ± 0.6	1.8 ± 0.0	1.1	2.2
13:0	0.1 ± 0.0	0.2 ± 0.2	0.4 ± 0.1	0.5	0.7
14:0	13.2 ± 3.8	4.1 ± 0.7	7.8 ± 1.2	4.5	5.3
15:0	0.9 ± 0.1	2.0 ± 0.8	2.8 ± 0.3	2.2	2.7
16:0	27.2 ± 2.1	30.7 ± 4.8	27.9 ± 0.7	23.5	29.2
17:0	0.4 ± 0.1	0.6 ± 0.1	1.2 ± 0.1	1.0	1.2
18:0	2.1 ± 0.8	7.6 ± 2.2	5.7 ± 0.8	6.5	9.6
19:0	n.d.	0.1 ± 0.0	0.4 ± 0.1	0.3	0.4
20:0	0.1 ± 0.1	0.3 ± 0.2	0.3 ± 0.0	0.5	0.8
21:0	n.d.	n.d.	n.d.	0.1	0.1
22:0	0.1 ± 0.0	0.2 ± 0.1	0.4 ± 0.0	0.4	0.7
24:0	n.d.	n.d.	n.d.	n.d.	0.1
∑SFA	**44.3 ± 4.9**	**47.1 ± 5.6**	**48.8 ± 1.2**	**40.5**	**53.0**
Monounsaturated					
14:1ω3	0.4 ± 0.3	n.d.	n.d.	0.1	n.d.
14:1ω5	0.2 ± 0.1	0.3 ± 0.1	0.4 ± 0.0	0.4	0.5
16:1ω9	2.4 ± 0.8	2.0 ± 0.9	1.9 ± 0.5	4.1	3.8
16:1ω7	19.8 ± 4.2	14.5 ± 4.6	13.3 ± 0.8	15.4	8.8
17:1ω9	0.0 ± 0.0	0.1 ± 0.0	0.2 ± 0.0	0.2	0.4
17:1ω7	0.2 ± 0.1	0.2 ± 0.1	0.4 ± 0.0	0.3	0.3
18:1ω11	0.4 ± 0.2	0.6 ± 0.6	n.d.	n.d.	n.d.
18:1ω9	5.6 ± 1.6	15.2 ± 3.9	10.6 ± 0.7	13.5	13.6
18:1ω7	4.5 ± 1.9	6.2 ± 0.9	7.2 ± 0.2	7.0	4.5
20:1ω11	n.d.	n.d.	n.d.	0.1	0.1
20:1ω9	0.1 ± 0.1	0.1 ± 0.1	0.1 ± 0.0	0.1	0.1
22:1ω9	0.1 ± 0.1	0.2 ± 0.2	0.2 ± 0.0	0.9	2.3
∑MUFA	**33.8 ± 2.3**	**39.2 ± 3.0**	**34.2 ± 1.8**	**42.1**	**34.4**
Polyunsaturated					
16:2ω6	1.2 ± 1.3	0.3 ± 0.2	0.3 ± 0.1	0.5	0.1
16:2ω4	1.3 ± 1.1	0.3 ± 0.3	1.0 ± 0.2	0.5	0.2
16:3ω4	1.1 ± 1.2	0.4 ± 0.4	1.8 ± 0.4	0.3	0.1
16:3ω3	0.6 ± 0.3	0.6 ± 0.4	n.d.	n.d.	n.d.
16:4ω3	0.9 ± 0.4	0.2 ± 0.2	0.3 ± 0.1	0.6	0.3
18:2ω6	3.0 ± 1.3	5.4 ± 2.9	1.3 ± 0.1	3.1	2.4
18:3ω3	3.8 ± 1.3	0.7 ± 0.4	0.6 ± 0.4	2.5	1.2
18:4ω3	1.2 ± 0.9	0.2 ± 0.1	0.4 ± 0.2	0.6	0.4
20:4ω6	0.5 ± 0.2	0.2 ± 0.1	0.8 ± 0.0	1.2	0.4
20:5ω3	2.3 ± 1.8	0.5 ± 0.5	3.3 ± 0.8	1.4	0.6
22:6ω3	0.6 ± 0.3	0.3 ± 0.0	0.4 ± 0.2	0.6	0.7
∑PUFA	**16.4 ± 5.1**	**9.1 ± 3.2**	**10.2 ± 3.5**	**11.2**	**6.4**
Branched					
14:0iso	1.3 ± 0.6	0.4 ± 0.1	0.9 ± 0.0	1.0	0.9
15:0iso	2.1 ± 0.5	2.1 ± 0.7	2.1 ± 0.1	2.2	2.3
15:0anteiso	0.8 ± 0.1	1.2 ± 0.3	1.3 ± 0.1	1.0	1.1
16:0iso	0.4 ± 0.1	0.4 ± 0.0	0.7 ± 0.1	0.7	0.7
17:0iso	0.8 ± 0.5	0.4 ± 0.2	1.0 ± 0.1	0.8	0.6
17:0anteiso	0.2 ± 0.1	0.3 ± 0.0	0.9 ± 0.1	0.6	0.7
∑BrFA	**5.5 ± 1.1**	**4.7 ± 1.0**	**6.8 ± 0.5**	**6.2**	**6.2**
∑FA (µg mgSPM^{-1})	20.7 ± 4.9	20.1 ± 16.0	0.6 ± 0.0	3.6	1.5
SPM (mg L^{-1})	106.0 ± 53.8	115.3 ± 74.6	228.2 ± 27.6	20.0	40.2
% SewFA	62.4 ± 2.9	78.0 ± 3.1	69.5 ± 4.4	72.2	72.2
16:1ω7/16:0	0.74 ± 0.18	0.49 ± 0.21	0.48 ± 0.02	0.66	0.29

Σ SewFA 15:0 + 16:0 + 16:1 + 18:0 + 18:1

n.d. = not detected

The concentration of FA per mg of SPM was about 20 times higher in shrimp farm effluents and urban canals compared to the estuarine sites (Table 2-1 and Table 2-2). The %PUFA was higher in shrimp farm effluents compared to any of the estuarine sites (Kruskal-Wallis test plus Wilcoxon pairwise comparisons; $X_{7,\ PUFA} = 41.6$, $p < 0.001$), while %SFA was lower ($X_{7,\ SFA} = 58.7$, $p < 0.001$). The %SewFA was lower in shrimp farm effluents compared to any of the estuarine sites, but higher in urban canals (Kruskal-Wallis test plus Wilcoxon pairwise comparisons; $X_{7,\ SewFA} = 53.6$, $p < 0.05$).

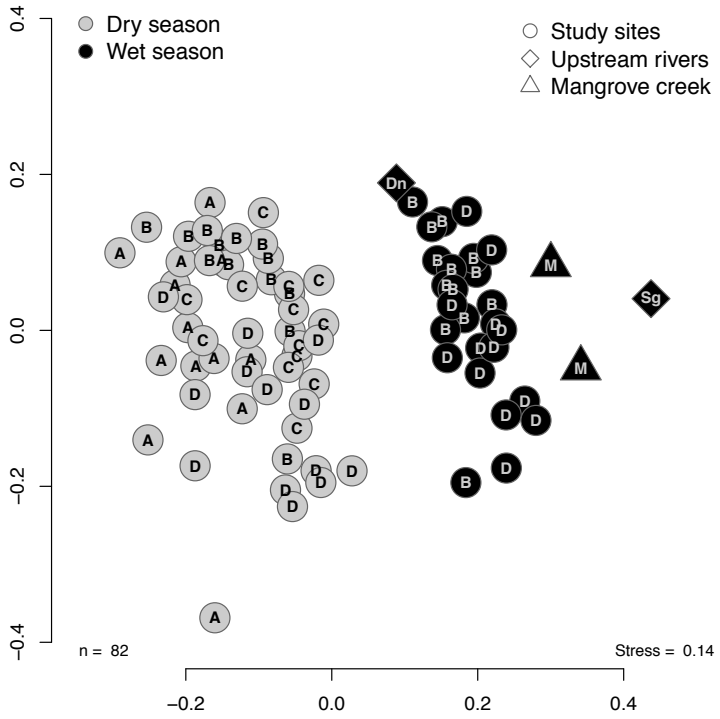

Figure 2-4: Two-dimensional representation of the N-MDS using fatty acid proportions (%) in SPM (Sg = Saigon River; Dn = Dong-Nai River; M = Mangrove creek). Other letters in bubbles correspond to the sites where samples were taken during 24 h tidal cycles

The ANCOVA revealed that season was the most significant variable affecting %SewFA, %PUFA and the 16:1ω7/16:0 ratio (Table 2-3 and Table 2-4). Values of %SewFA were higher during the dry season, whiles values of %PUFA and 16:1ω7/16:0 ratio were higher during the wet season (Table 2-1 and Figure 2-5). The %BrFA and $\delta^{13}C$ were also affected by season as second most explanatory variable (Table 2-3 and Table 2-4), with lower values observed during the dry season (Figure 2-2a and Figure 2-3a). Salinity was the most significant variable affecting $\delta^{13}C$ and $\delta^{15}N$, both decreasing with salinity (Table 2-4 and Figure 2-2). It also influenced %SewFA and C/N ratio as second most explanatory variable and to a lesser extent

%PUFA, with %SewFA and %PUFA increasing with salinity and C/N ratio decreasing with salinity (Figure 2-5). The amount of SPM had the most explanatory power for the %BrFA and C/N ratio, with values increasing with SPM concentration (Figure 2-3). The daylight presence was the second most explanatory variable affecting %PUFA, with higher values observed during day (Figure 2-6) and an explained variability proportion (SS/Total SS) close to that of season (Table 2-3).

Table 2-3: Summary of ANCOVA between fatty acids (%) and environmental variables

Category		Decomposition and wastes						Primary production					
Indicator		%BrFA			%SewFA			%PUFA			16:1ω7/16:0		
	df	SS	Fvalue	p	SS	Fvalue	p	SS	Fvalue	p	SS	Fvalue	p
ln(SPM)	1	82.5	385.2	<0.001	8.7	1.4	0.25	0.0	0.0	0.90	0.08	41.2	<0.001
Salinity	1	7.1	33.1	<0.001	90.0	14.1	<0.001	39.0	15.4	<0.001	0.00	2.6	0.1
Season	1	16.6	77.7	<0.001	147.1	23.0	<0.001	83.1	32.7	<0.001	0.42	227.1	<0.001
Day/Night	1	4.8	22.3	<0.001	3.6	0.6	0.45	76.8	30.2	<0.001	0.01	4.1	<0.05
Ln(SPM) × Salinity	1	0.9	4.0	<0.05	11.3	1.8	0.19	0.1	0.0	0.85	0.00	2.0	0.2
Ln(SPM) × Season	1	0.5	2.4	0.13	12.0	1.9	0.18	2.5	1.0	0.33	0.00	0.4	0.5
Ln(SPM) × D/N	1	0.2	1.1	0.31	2.1	0.3	0.57	5.7	2.3	0.14	0.00	0.1	0.7
Salinity × Season	1	0.4	1.7	0.19	36.2	5.6	<0.05	3.9	1.5	0.22	0.01	3.9	0.1
Salinity × D/N	1	0.1	0.4	0.56	11.5	1.8	0.18	1.8	0.7	0.41	0.00	0.9	0.4
Season × D/N	1	0.1	0.3	0.59	11.3	1.8	0.19	0.8	0.3	0.58	0.01	2.8	0.1
Residuals	67	14.3			429.1			170.2			0.00		
Total	77	127.4			762.9			383.8			0.65		

Σ BrFA 14:0-i + 15:0-i + 15:0-ai + 16:0-i + 17:0-i + 17:0-ai
Σ SewFA 15:0 + 16:0 + 16:1 + 18:0 + 18:1
Σ PUFA 16:2ω4 + 16:3ω4 + 18:2ω6 + 18:3ω3 + 18:4ω3 + 20:5ω3 + 20:4ω6 + 22:5ω3 + 22:6ω3

Table 2-4: Summary of ANCOVA between stable isotopes and C/N ratio and environmental variables

Indicator		δ^{13}C-SPM			δ^{15}N-SPM			C/N ratio		
	df	SS	F value	p	SS	F value	p	SS	F value	p
Salinity	1	13.4	95.1	<0.001	63.0	300.7	<0.001	10.4	9.9	<0.01
ln(SPM)	1	0.3	1.8	0.18	5.9	28.3	<0.001	39.6	37.7	<0.001
Season	1	4.9	35.1	<0.001	0.0	0.0	0.8	2.9	2.7	0.10
Day/Night	1	0.1	0.5	0.50	1.4	6.6	<0.05	2.3	2.2	0.14
Salinity × Ln(SPM)	1	0.0	0.0	0.84	1.0	5.0	<0.05	0.1	0.1	0.71
Salinity × Season	1	0.7	4.7	<0.05	16.2	77.2	<0.001	1.4	1.4	0.25
Salinity × D/N	1	0.4	3.0	0.09	1.1	5.2	<0.05	1.3	1.2	0.27
Ln(SPM) × Season	1	0.2	1.5	0.23	0.2	1.1	0.3	2.2	2.1	0.15
Ln(SPM) × D/N	1	0.0	0.0	0.85	2.3	11.1	<0.01	0.2	0.2	0.63
Season × D/N	1	0.3	2.3	0.14	0.5	2.5	0.1	0.4	0.4	0.55
Residuals	92	13.0			19.3			96.6		
Total	102	33.3			110.9			157.4		

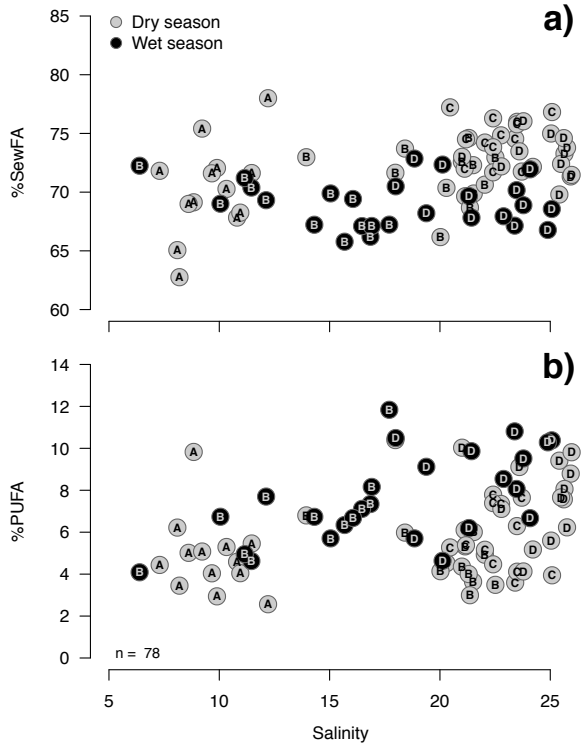

Figure 2-5: a) SewFA (%) and b) PUFA (%) of SPM expressed as a function of salinity in the Can Gio mangrove estuary. Letters in bubbles correspond to the sites where samples were taken

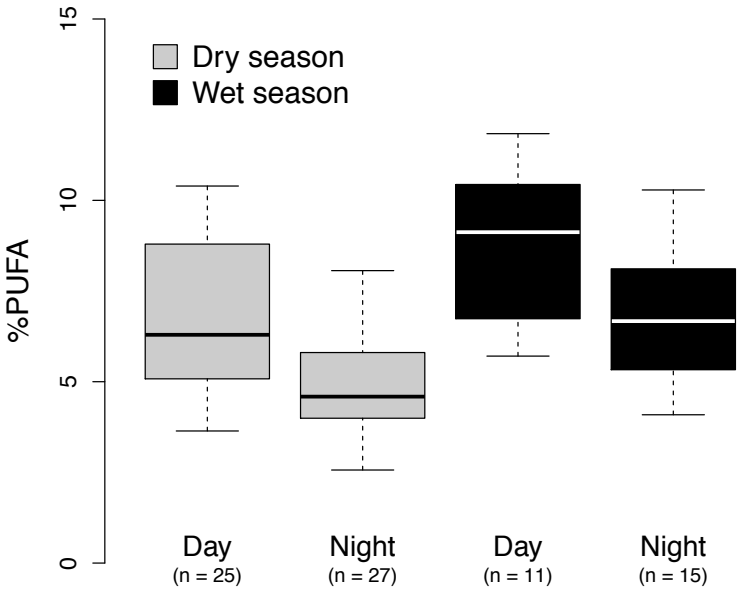

Figure 2-6: Boxplot of PUFA (%) in SPM separated according to season and presence of daylight in the Can Gio mangrove estuary

5. Discussion

5.1. Sources contribution to the overall SPM

SPM in the Can Gio mangrove estuary had a similar proportion of SewFA than other anthropogenically impacted sub-tropical and temperate mangrove estuaries of Japan and New Zealand and tropical systems of Brazil (Table 2-5), where OM was mostly of detrital origin (Alfaro et al. 2006, Sakdullah and Tsuchiya 2008, Mortillaro et al. 2011, Boëchat et al. 2014). Actually, FA 15:0, 16:0, 16:1, 18:0 and 18:1 are main constituents of highly degraded OM (Wakeham 1995). Thus, instead of specifically tracing human released OM, the SewFA biomarker more generally indicates an advanced decomposition state of SPM, which is a common feature in tropical estuaries. The PUFA proportion in the Can Gio mangrove estuary was low (2.6 to 11.8%) but still in the range observed in other large tropical rivers such as the Brasilian Rio das Mortes, where Boëchat et al. (2014) concluded to a small contribution of algae and other autochthonous autotrophic organisms to the overall SPM pool. Considering the high water turbulence and turbidity of the estuary, with current velocity up to 1.7 m/s and estimated light penetration of less than 1 m (unpublished data), such results were expected.

Table 2-5: Overview of 20 literature data on SPM fatty acid composition (%) in aquatic ecosystems

Location	Ecosystem	% BrFA	% SewFA	% PUFA	16:1ω7/16:0	n	Reference
Dong Nai River estuary, Vietnam	Mangrove estuary	2.1 - 8.6	62.9 - 78.0	2.6 - 11.8	0.06 - 0.43	6	This study
Manko River estuary, Japan	Mangrove estuary		64.4 - 74.0	6.9 - 15.8	0.26 - 0.49	4	Sakdullah and Tsuchiya 2009
Manko River estuary, Japan	Mangrove estuary	0.5 - 4.9	47.9 - 87.7	14.1 - 47.7	0.09 - 0.94	12	Shilla et al. 2011
Matapouri Estuary, New Zealand	Mangrove estuary		56.4 - 84.3	5.4 - 10.4	0.05 - 0.11	3	Alfaro et al. 2006
Amazon River, Brasil	Tropical river	3.7 - 5.4	60.3 - 67.4	11.5 - 19.1	0.22 - 0.71	6	Mortillaro et al. 2011
Rio das Mortes, Brasil	Tropical river	4.0 - 6.7	56.8 - 65.0	4.3 - 6.6	0.07 - 0.08	4	Boëchat et al. 2014
Camaleão Lake, Brasil	Tropical lake	10.4	61.1	8.6	0.02	1	Mortillaro et al. 2016
Florida Bay, Florida (USA)	Subtropical shelf	0.6 - 3.9		0.2 - 35.0	0.10 - 0.80	18	Xu and Jaffé 2007
Chesapeake Bay, Virginia (USA)	Temperate estuary	0.0 - 13.1	34.3 - 80.1	4.1 - 57.1	0.17 - 3.74	42	Canuel 2001
Kowie River estuary, South Africa	Temperate estuary	3.0 - 9.6	52.3 - 70.7	6.0 - 20.3	0.00 - 0.75	12	Antonio and Richoux 2016
Krka River, Italy	Temperate estuary	1.6 - 8.2	60.2 - 70.6	5.6 - 31.8	0.14 - 0.80	13	Scribe et al. 1991
Morlaix River estuary, France	Temperate estuary	3.6 - 6.6	55.6 - 73.6	7.1 - 25.2	0.26 - 0.56	13	Quéméneur and Marty 1994
San Franciso Bay, California (USA)	Temperate estuary	0.7 - 7.6	21.5 - 59.9	9.6 - 55.4	0.07 - 1.68	30	Canuel 2001
York River estuary, Virginia (USA)	Temperate estuary		48.7 - 62.1	18.6 - 32.4	0.78 - 1.62	6	McCallister et al. 2006
Biscay Bay, France	Temperate shelf	1.3 - 5.2	45.3 - 75.6	5.2 - 37.4	0.01 - 0.41	8	Chouvelon et al. 2015
Chausey Archipelago, France	Temperate shelf	2.8 - 3.8	64.6 - 76.9	7.5 - 19.3	0.01 - 0.20	6	Moynihan et al. 2016
Elkhorn Slough, California (USA)	Temperate shelf	3.0 - 6.1	28.5 - 40.7	15.7 - 23.6	0.22 - 0.27	3	Fischer et al. 2014
Yangtze River estuary, China	Temperate shelf		36.9 - 66.0	9.3 - 53.9	0.08 - 0.17	2	Wang et al. 2015
Pilley's Tickle Bay, Canada	Subarctic shelf	2.4 - 5.2		32.0 - 54.0	0.2 - 2.23	4	Budge et al. 2001
Trinity Bay, Canada	Subarctic shelf	0.5 - 0.9	28.4 - 35.7	29.4 - 54.8	0.5 - 1.94	4	Budge and Parrish 1998
Beaufort Sea, Alaska (USA)	Arctic shelf	0.9 - 3.6	34.9 - 81.9	8.5 - 42.3	0.07 - 1.54	12	Connelly et al. 2015

Σ BrFA 14:0-i + 15:0-i + 15:0-ai + 16:0-i + 17:0-i + 17:0-ai
Σ SewFA 15:0 + 16:0 + 16:1 + 18:0 + 18:1
Σ PUFA 16:2ω4 + 16:3ω4 + 18:2ω6 + 18:3ω3 + 18:4ω3 + 20:5ω3 + 20:4ω6 + 22:5ω3 + 22:6ω3

The similarity between SPM fatty acid composition of the Dong Nai River upstream Ho Chi Minh City and of the estuary indicates that inputs from the Saigon River were highly diluted after the junction of the two rivers (Figure 2-4). Even though SPM originating from

urban canals was far more concentrated in FA than estuarine SPM (Table 2-1 and Table 2-2), and even though the SPM fatty acid composition of the Saigon River was substantially different from that of the Dong Nai River (Table 2-2 and Figure 2-4), the FA signatures we measured at the estuarine sites were close to that of the Dong Nai River upstream HCMC. These results are consistent with a discharge of the Dong Nai River about 10 times higher than that of the Saigon River (Nippon Koie 1996). Strady et al. (2016) measured high levels of nutrients and trace metals in the Saigon-Dong Nai River in HCMC and drew the same conclusion, observing a strong dilution of both contaminants after the two rivers junction. Sewage effluents are rapidly decomposed after being released in marine waters, as shown by Marty et al. (1996) who observed a 70% loss of total FA after incubating during three days an effluent-seawater mixture. Therefore, sewage effluents signature was not observed in the estuarine sites because of both dilution and rapid decomposition, thus adding available nutrients to the ecosystem.

High PUFA proportion in shrimp ponds indicates important autotrophic production, as revealed by the detection of PUFA originating from algae biosynthetic pathways, such as 16:2ω4, 16:3ω4 or 16:4ω3 (Table 2-2; Kelly and Scheibling 2012). The relative PUFA contribution could have been an interesting shrimp pond effluents tracer since it was much higher in the effluents compared to the estuarine waters (Table 2-1 and Table 2-2). However, PUFA proportion at site B water, which is supposed to be the most influenced by shrimp farming, was not especially higher than in the other sites (Table 2-1). PUFA are known to rapidly decompose in decaying material (Jaffé et al. 1995, Wakeham 1995) and might be promptly mineralised once entering the estuary. Shrimp pond effluents are not directly discharged into the mangrove but rather in adjacent canals connected to the estuary. Water in shrimp ponds is renewed by 15% every 10 days and there is no synchronisation of production cycles between farmers or according to a seasonal cycle (Anh et al. 2010). It is therefore most likely that shrimp pond effluents are rapidly assimilated by the ecosystem and serve as a fuel for the microbial loop, similarly to urban sewage.

Clear differences of FA profiles between the mangrove channel and the estuarine SPM reveal that the presence of the mangrove forest influences the SPM quality (Figure 2-4). However, the dissimilarity between the two sets of samples taken in the mangrove channel at the interval of two hours, which illustrates the strong short-term SPM variability in this

tropical mangrove (Figure 2-4), do not allow to identify a specific FA biomarker tracing the influence of mangrove modified SPM in the estuary.

Among the five SPM sources we identified in the Can Gio mangrove estuary (upstream Dong Nai and Saigon Rivers, urban wastewaters, shrimp pond effluents and mangrove creek), only the dominant contribution of the Dong Nai River SPM could be clearly evidenced. Thus, we suggest that tracing the different sources contribution to the estuarine SPM is necessary, but to better understand changes in its quality we also need to know the factors that underlie *in situ* transformation of SPM during its transit from HCMC to the ocean.

5.2. Effect of season and water-mixing ratio on the SPM composition

The higher %PUFA measured during the wet season indicates that OM exhibited higher freshness during this season (Figure 2-5b and Figure 2-6). PUFA are actually more rapidly degraded than other FA and the PUFA proportion in SPM is an indicator of the decomposition state of OM (Jaffé et al. 1995, Wakeham 1995). This higher freshness was also highlighted by the lower SewFA contribution to the overall FA, the higher BrFA contribution, the higher 16:1ω7/16:0 ratio and the higher $\delta^{13}C$ values during the wet season (Table 2-3). The lattest indicator also show that the contribution of OM of terrestrial origin was poorer during the wet season for a given salinity compared to OM of estuarine or marine origin wich is much more enriched in ^{13}C (Middelburg and Herman 2007). Such results were unexpected since wet season in tropical ecosystems is generally associated with higher soil leaching and higher inputs of terrigenous OM to estuaries (Mortillaro et al. 2011, Boëchat et al. 2014), which are assumed to be in a more advanced state of decomposition than autochthonously produced OM. Higher inputs may nevertheless increase bacterial activity and bacterial loads in the estuary during the wet season, as observed in the Okinawan Manko estuary (Shilla et al. 2011). We suggest that during the wet season, it is the higher bacterial load that increases the mineralisation rate, and thus the availability of nutrients, resulting in higher autotrophic production in the Can Gio mangrove estuary.

We used salinity as a conservative tracer to identify water-mixing ratio in the estuary. As expected, the $\delta^{13}C$ increase along the salinity gradient traduces a shift from OM of terrestrial origin to OM of marine origin (Figure 2-2). This observation is strengthened by the %PUFA increase correlated to the salinity gradient (Figure 2-5b), which suggests that the

contribution of freshly produced vs. decomposing OM is higher in marine waters compared to the upper watershed. Dominating PUFA affected by the salinity gradient were 20:5ω3, 16:2ω4 and 16:3ω4 (Table 2-1) that are diatom indicators in marine ecosystems (Dalsgaard et al. 2003). Assuming an increase of diatom presence along the salinity gradient, the absence of salinity effect on the 16:1ω7/16:0 ratio, also considered a liable diatom biomarker (Napolitano et al. 1997), was unexpected. However, the FA 16:1ω7 is an ubiquitous FA found in mostly any living organism (Dalsgaard et al. 2003, Bergé and Barnathan 2005) and we suggest that in ecosystems were algal contribution is always low, the 16:1ω7/16:0 ratio cannot reliably trace diatom biomass changes in SPM.

The $\delta^{15}N$ values of suspended particles in estuaries result from the balance between external inputs of ammonium vs. nitrate and heterotrophic processing of OM (Middelburg and Herman 2007). The isotopic value of $\delta^{15}N$ in estuarine particles and organisms can provide an integrated N-loading measurement (McClelland and Valelia 1998, Middelburg and Herman 2007). In the present study, the $\delta^{15}N$ decrease along the salinity gradient reflects the dilution of nitrogen-rich waters originating from the watershed and indicating a strong anthropogenic pressure on the ecosystem, with nitrogen-poor marine waters.

In the above discussion, we evidenced higher SPM freshness during the wet season and dilution of freshwater SPM with marine SPM along the salinity gradient, but we could not explain why the SPM fatty acid composition of estuarine sites exhibited variability during tidal cycles that encompassed site induced differences (Figure 2-4). The variability that could be explained by the mixing ratio of fresh vs. marine waters, approximated by salinity, and season, actually remained low compared to the total variability exhibited by the dataset (SS salinity + SS season / Total; Table 2-3 and Table 2-4). We thus suggest that other factors, such as tide induced resuspension or daylight, may contribute to short-term (few hours) changes in the SPM composition.

5.3. Short-time changes in the SPM composition

In the present study we assume that during the 24 h time series upstream inputs of SPM were roughly stable and that short-term increases in SPM concentration were mostly due to particle resuspension, as generally observed in turbid estuaries (Wang et al. 2013). Increasing SPM concentrations were correlated with increasing %BrFA in SPM, indicating that

bacterial contribution to the overall pool of OM was higher in resuspended particles (with short settling-time) compared to longer settling-time particles (Figure 2-3a). We suggest that these resuspended particles are the sites of an intense heterotrophic activity and that their resuspension and aggregation with others, due to flocculation (Eisma 1986, Verney et al. 2009), enhance the processing of OM in the estuary. The C/N ratio increase with increasing SPM concentration suggests that the contribution of higher plant organic fragments increased with particle resuspension (Figure 2-3b). Indeed, plant derived OM has a C/N ratio much higher than bacterial cells (>20 vs. 4-5; Middelburg and Herman 2007). However, FA are known to decompose rapidly in OM compared to other compounds (Marty et al. 1996), which may indicate that this lipidic compound reflects the living fraction of SPM. Bacteria thus constitutes the biologically active fraction of short settling-time particles, while the overall active + detrital OM pool of these tide-resuspended particles is enriched in higher plant derived OM compared to longer settling-time particles, as indicating by their C/N ratio. Resuspended particles are thus dominated by detrital OM but they might bare an intense mineralisation activity due to their high bacterial load.

The day/night (D/N) factor had the second most explanatory power for the %PUFA variable, just after the season (Table 2-3), with higher values measured during daytime evidencing autotrophic production in surface waters during the day (Figure 2-6). Considering the high water turbulence and turbidity of the estuary, such results were surprising. Indeed, in turbid estuaries photosynthesis only occurs in short intermittent periods when phytoplankton is transported in the euphotic zone (Lancelot and Muylaert, 2011). In experimental conditions under diel light cycle, lipid content of the species *Dunaliella bioculata* was twice higher in the presence of light compared to dark (Halsey and Jones, 2015). We thus suggest that despite most probable low primary production, because of high turbidity and as reveald by the small contribution of PUFA in the Can Gio mangrove estuary, phytoplankton diel lipid storage notably modified the quality of SPM in sub-surface water during the day.

6. Conclusions

Fatty acids, stable isotopes ($\delta^{13}C$ and $\delta^{15}N$) and C/N ratios revealed a dominant contribution of decaying organic material to the overall SPM pool in the Can Gio mangrove estuary. In addition, a higher contribution of polyunsaturated and branched fatty acids to the SPM pool was measured during the wet season, revealing a higher biological activity during this season.

We hypothesised that HCMC sewage effluents strongly contributed to the Can Gio mangrove estuary SPM, but analyses revealed that waters originating from urban canals were rapidly diluted and decomposed once entering the estuary. Similarly, contribution of wastewaters from shrimp ponds could not be traced along the estuarine gradient, probably because OM was rapidly mineralised in transitional canals before entering the estuary. Our study shows that FA can hardly be used as quantitative tracers to constrain the contribution of different OM sources in estuaries. However, they provide an integrative measurement of the SPM composition at the time of sampling, qualitatively comparing on the same scale the relative contribution of detrital OM, bacterial OM and microalgae OM.

Substantial short-term variations in the SPM composition during tidal cycles were evidenced. First, an increasing contribution of BrFA correlated to SPM concentration revealed the presence of flocculated particles that are suggested to be the sites of an intense heterotrophic activity. Secondly, a higher contribution of PUFA during daytime suggested that phytoplankton, even though most probably poorly abundant in this turbid estuary, has the ability to modify SPM quality at short temporal scales through lipid storage. Fatty acid profiling represents a high workload and one could ask whether the same conclusions could have been reached using stable isotopes supplemented with chlorophyll a data. Our study shows that FA are more sensitive to daily changes in SPM composition than stable isotopes, and since we suggest that increasing PUFA relative abundance in sub-surface water during the day originates from lipid storage rather than cell division, chlorophyll a data would probably not highlight such phenomenon. We thus believe that FA represent an effective tool to evaluate factors affecting SPM quality in estuaries at short time scale, which in turn may have implications on the feeding ecology of estuarine organisms and in the estimation of tropical estuaries carbon budget.

Chapter 3: Prokaryotic abundance, cell size and extracellular enzymatic activity in a human impacted and mangrove dominated tropical estuary (Can Gio, Vietnam)

DAVID Frank, MEZIANE Tarik, MARCHAND Cyril, ROLLAND Guillaume, PHAM Aurélie, NGUYỄN THÀNH Nho and LAMY Dominique

1. Abstract

Organic matter (OM) in aquatic environments is mostly constituted by compounds of high molecular weight that cannot be directly transported through the cytoplasmic membrane of microbial cells. Exoenzymes are thus essential as they hydrolyse macromolecules into monomeric substances, allowing them to fuel the microbial loop. This study aimed to collect data on the variability of prokaryotic abundance and leucine-aminopeptidase exo-proteolytic activity (EPA) at vertical, spatial and seasonal scales in the water column of a tropical mangrove ecosystem (Can Gio, Vietnam). Prokaryotic abundance ranged from 1.2 to 5.7 x 10^9 cells L^{-1} and EPA ranged from 24 to 505 nmol L^{-1} h^{-1}. Season was the variable most influencing EPA, most likely because the nature of OM entering the estuary differed, but without affecting prokaryotic abundance. During the dry season, the macromolecules composing the dissolved organic matter (DOC) were probably more resistant to degradation, thus requiring higher amounts of extracellular enzymes to be hydrolysed into monomeric substances. Spatial differences in EPA also suggested that the nature of OM to be decomposed varied, with particularly high activities close to the shrimp farming area and within a tidal mangrove creek. Our study thus highlights the ability of prokaryotes to regulate their release of extracellular enzymes as a response to OM quality.

2. Introduction

Tropical estuaries are land-ocean boundaries receiving high loads of organic matter (OM) from upstream rivers and adjacent floodplains, especially when nearby areas are covered with mangrove forests (Cai 2011, Alongi et al. 2014). Prokaryotes, including bacteria and archaea, are the major consumers of this OM, releasing nutrients and carbon dioxide (CO_2) in the surrounding environment for the benefit of primary producers. Transfer between the OM pool and the nutrient compartment is a determinant mechanism of organic matter cycling in the water column, known as the microbial loop (Azam 1998). In addition, OM conversion by prokaryotes into edible biomass for protozoa and higher trophic levels plays a substantial role in sustaining the grazing food chain (Sherr and Sherr 1988). Therefore, prokaryotes and their ability to mineralise OM are essential for controlling the fluxes of carbon and nutrients in tropical coastal ecosystems. Yet, when, where, and how OM is decomposed into nutrients and CO_2 is not fully understood.

The majority (>95%) of OM in aquatic environments is constituted by compounds of high molecular weight that cannot be directly transported through the cytoplasmic membrane of microbial cells (Chróst 1991). These polymeric compounds have to be hydrolysed through the action of extracellular enzymes and converted into monomeric substances before being consumed by prokaryotes. Extracellular enzymes can be dissolved in the water, adsorbed to dead or living phytoplanktonic or bacterial cells, or bound to particle aggregates (Chróst 1991, Smith et al. 1992). Extracellular enzymatic activities (EEA) often constitutes the limiting step of the whole process of OM cycling (Arnosti 2011) and thus, the turnover rates of various compounds have been used to evaluate the efficiency of the microbial community to mineralise OM in coastal waters (Patel et al. 2000, Cunha and Almeida 2006, Lamy et al. 2009, Bhaskar and Bhosle 2008). The leucine-aminopeptidase activity (exo-proteolytic activity, EPA) is one of the most commonly used indicator of OM hydrolysis. It represents the general ability of prokaryotes to hydrolyse proteins (Hoppe 1993) and thus it informs on the efficiency of the ecosystem to recycle nitrogen, which is the principal limiting nutrient in marine production (Fernandes 2011).

In the water column of tropical mangrove ecosystems, the activity of prokaryotes greatly varies among seasons, and highest prokaryotic activity has generally been measured during the monsoon period (Bano et al. 1997, Bhaskar and Bhosle 2008, Gonsalves et al.

2009). However, while salinity and water stratification are major factors controlling EPA rates in temperate estuaries (Cunha et al. 2000, Patel et al. 2000, Cunha and Almeida 2006), little attention has been given to the vertical and spatial variability of EPA in mangrove ecosystems. In addition, the origin of OM impact EEA, and mangrove-derived OM particularly enhance EPA in laboratory experiments (Baltar et al., 2017). In previous studies, we measured carbon pools and CO_2 emissions at the water-air interface in the Can Gio mangrove estuary and we showed that the distribution of carbon and OM quality varied along the salinity gradient of the estuary and according to the tidal stage and the season (see Chapter 1 and Chapter 2). Indeed, OM was more autochthonous during the wet season, with higher proportion of polyunsaturated fatty acids, indicative of phytoplankton, and branched fatty acids, indicative of bacteria (see Chapter 2). We may thus expect that prokaryotic abundances and activities would also vary at short spatial and temporal scales in this estuary. Moreover, the sea surface micro-layer (SML), operationally defined as the top 50-100 µm of the ocean surface, is a particularly active compartment of the water column that could play a substantial role in OM degradation (Cunliffe et al. 2013, Mari et al. 2017). It may serve as a receptacle for anthropogenic pollutants and thus its study is particularly relevant in an estuary located down a megacity such as Ho Chi Minh City (Strady et al. 2017). Finally, bottom waters are enriched in suspended particles due to resuspension (see Chapter 2), and might be preferential sites for prokaryote colonisation (Becquevort et al. 1998, De Souza et al. 2003).

In the present study we explored vertical, spatial and seasonal variations in the prokaryotic activity of the Can Gio mangrove water column. Prokaryotic abundances, cell sizes and leucine-aminopeptidase activities were measured at three layers of the water column: (1) surface micro-layer, (2) sub-surface layer and (3) bottom layer. Our measurements were distributed at five sites located from the downstream end of Ho Chi Minh City (HCMC) to the South China Sea coast and during two seasons (dry season in January-February 2015 and wet season in September-October 2015). We hypothesised that (1) prokaryotes would be more abundant and more active in the surface micro-layer and in the bottom water layer of the estuary, (2) EPA would vary at short spatial and temporal scales in the estuary, due to short-term and spatial variations in OM composition, especially during the dry season when the lower river discharge increased the delineation of the water layers and (3) the ability of prokaryotes to mineralise organic matter might be higher during the wet season, when inputs of OM are suspected to be higher. Determining the ability of prokaryotes to mineralise

organic matter, and therefore making nutrients available for primary producers will contribute to understand OM cycling in tropical estuaries.

3. Materials and methods

3.1. Study area

The Can Gio mangrove is located at the downstream end of Ho Chi Minh City (Southern Vietnam; ~13 million inhabitants) and flooded by the Saigon-Dong Nai River, discharging annually 37.4×10^6 m^3 of freshwater to the South China Sea and whose basin covers a total catchment area of 40.6×10^3 km^2 (12% of the total terrestrial area of Vietnam; Ringler et al. 2002). The climate in Can Gio is monsoonal with a wet season from June to October and a dry season from November to May. Tidal amplitude is variable over time and ranges between 2 to 4 m depending on the season and distance from the sea (Nam et al. 2014). In 2000, the UNESCO designated the 719.6 km^2 of the Can Gio district as the first mangrove biosphere reserve in Vietnam and a clear land use regulation was established. The east border of the mangrove is fringed by shrimp farms and salt producing lands, covering roughly 20% of the total biosphere reserve surface area, while the rest of the district is preserved from deforestation and mostly covered with mature trees of the species *Rhizophora apiculata*.

We selected the study sites on the main estuarine channel to be at the interface between land uses (Figure 3-1): A) at the downstream end of Ho Chi Minh City (10°39'55"N 106°47'30"E); B) between shrimp farms and the mangrove forested area (10°34'19"N 106°50'11"E); C) in the centre of the mangrove protected core (10°31'04"N 106°53'13"E); D), and between the mangrove forested area and the South China Sea coast (10°29'32"N 106°56'55"E). At all these sites the estuary has steep eroded banks, a depth of about 10-15 m and a width of about 600 m. Site E exhibited very different physical characteristics. It was located in a 1-3 m deep and 30 m large mangrove tidal creek of the mangrove protected core, which do not receive freshwater upstream inputs (10°30'24"N 106°52'57E; Figure 3-1).

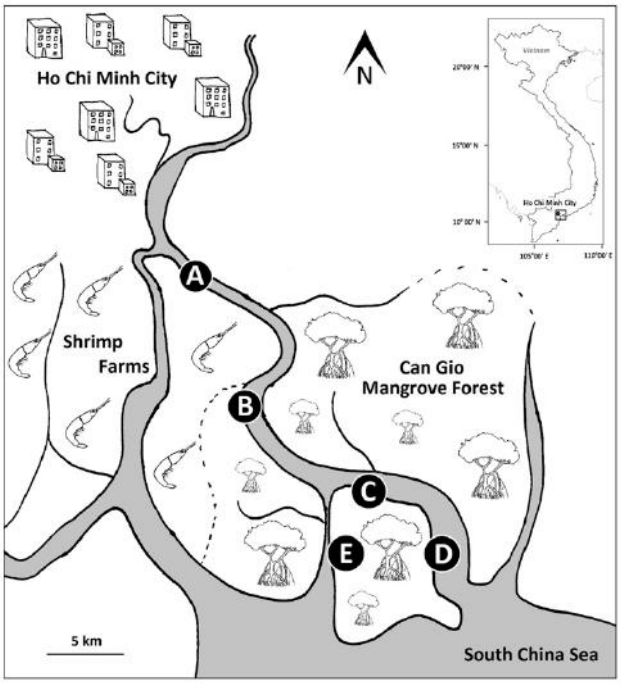

Figure 3-1: Map of the sampling area in the Can Gio mangrove (Southern Vietnam). A, B, C, D and E indicate the sampling stations along the estuary and within the tidal creek

3.2. Sampling strategy

We collected sub-surface water from the bow of a sampling boat using a 10 L plastic bucket immersed 10 cm below water level. We sampled bottom water using a 2 L weighted bottle (Image 3-1b) opened roughly 1 m above the bottom of the estuary. Samples from the SML were taken using a glass plate sampler (Image 3-1b). The glass plate was immersed vertically and withdrawn at an approximate rate of 20 cm s^{-1}, following the recommendations of Harvey and Burzell (1972). It was then wiped between two plastic squeegees fixed face to face to remove the adhering SML, which was falling by gravity into a polyethylene bottle. We repeated the procedure of dipping, withdrawing and wiping the plate to obtain a sufficient volume of samples for the analyses.

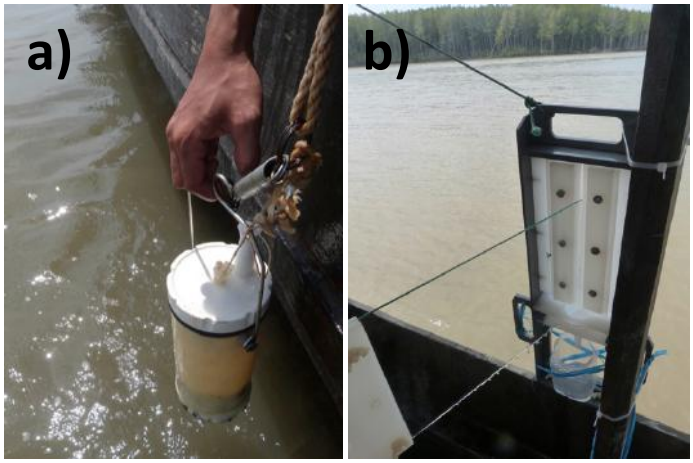

Image 3-1: a) Weighted bottle and b) glass plate sampler used for water layers sampling in the Can Gio mangrove estuary

Sub-samples of water were immediately vacuum-filtered through pre-combusted (5 h at 450°C) and pre-weighted glass fibre filters (Whatman® GF/F 0.7 µm) to measure suspended particulate matter concentration (SPM). Filters obtained from sub-surface water filtration were used for particulate organic carbon (POC) determination and filtered water was acidified and stored at 4°C in 15 mL Falcon® tubes for determination of dissolved organic carbon (DOC).

We expected the vertical and spatial variations of the prokaryotic activity to be higher during the dry season, due to the lower river discharge increasing the water retention time in the estuary and probably increasing the delineation of the water layers (SML, sub-surface, bottom) and associated biological compartments. Thus, samples were taken from the three water layers during the dry season while only the sub-surface water layer was sampled during the wet season. In addition, samples were taken twice during a tidal cycle during the dry season, at high tide and low tide, and only at high tide during the wet season. The site E, which was not surveyed during the dry season, was included in our sampling plan during the wet season to explore the prokaryotic compartment in an area distant from the main estuarine channel. Three replicates were used for bacterial counting and cell size measurements. Four and five replicates were analysed for EPA during the dry season and the wet season, respectively.

3.3. Sample processing

Sub-samples for bacterial counting were immediately preserved in 4.5 mL sterile Abdos Cryo Vials® and buffered with 0.2 µm pre-filtered formalin (4 % final concentration). Bacteria were stained using the 4'-6-diamino-2-phenylindole (DAPI) fluorescent stain that binds strongly to A-T rich regions in DNA, following the method described by Porter and Feig (1980). Ten to twelve randomly selected fields (to count at least 500 cells) were photographed using a Leica epifluorescence microscope coupled with a digital camera measuring light emission at 450 nm after excitation at 350 nm. Prokaryotes numeration and cell size measurements were performed with the open source image-processing program ImageJ v1.5. We binarised monochromatic pictures to automatically count nearly circular aggregates of fluorescent pixels, which we assumed to be prokaryote cells. We measured cell size using a Feret box enclosing the cell and considering that the cell diameter roughly equals the average distance between maximal and minimal Feret diameters (Loferer-Kröbbacher et al. 1998, Merkus et al. 2009).

The leucine-aminopeptidase exo-proteolytic activity (EPA) was measured in the unfiltered fraction using the fluorigenic substrate analogue L-leucine-methylcoumarinylamide (Leu-MCA; Hoppe 1993). The substrate was added to 1.8 mL of water sub-samples and incubated during 1 h at *in situ* temperature and low natural light intensity. At the end of the incubation period, the enzymatic cleavage activity was stopped using Sodium Dodecyl Sulfate (1 % final concentration). Controls in duplicates were run similarly, except that the stopper solution was added before the substrate. The cleavage of Leu-MCA resulted from the exoproteolytic activity and was linearly related to the MCA fluorescence. Saturation curves were carried out to determine the saturating substrates concentration and 800 µM final concentrations were used for all samples. Since the substrate was saturating in our study, results corresponded to potential activity rates. The fluorescence was measured using a Varian Cary Eclipse spectrofluorometer (excitation/emission of 380/440 nm) and transformed to hydrolysis activity using a standard curve established with different concentrations of the fluorochrome MCA.

Organic carbon (DOC and POC) was measured at the Institut de Recherche pour le Développement in Nouméa (New Caledonia) with a Shimadzu® TOC-L series analyser using a 680°C combustion catalytic oxidation method. The analyser was combined with a solid sample

module (SSM-5000A) when POC was measured, and a 40% glucose standard was used for calibrations. Repeated measurements of the standard at different concentrations indicated a measurement deviation < 2%.

3.4. Data analyses

We performed univariate multiple comparisons using non-parametric Kruskal-Wallis rank sum test due to variance heterogeneity and we identified groups of samples differing from one another using Wilcoxon pairwise comparisons (α = 5%, modified by Holm correction for multiple analysis). Seasonal comparisons were performed using Student test and using the Welch correction due to variance heterogeneity. Linear models were constructed to seek for variables controlling EPA and prokaryotic abundances but none of the measured physical (temperature, pH, salinity, dissolved oxygen, alkalinity) or biological (DOC, POC, SPM, δ^{13}C-POC, δ^{15}N-POC, C/N ratio) parameters were significantly limiting prokaryotic compartments (data from Chapter 1 and Chapter 2). However, EPA variability could be linked to the variation in OM composition (seasonal variability) and a probable particle-associated behaviour of prokaryotes in the bottom layer. Statistical analyses and graphical representations were performed using R (R Core Team 2017).

4. Results

4.1. Environmental parameters

Water column parameters at the sites located on the main estuarine channel (sites A to D) were described in Chapter 1 and parameters of the mangrove tidal creek (site E) were described in Taillardat et al. (in prep.). Salinity along the monitored 40 km of the Can Gio mangrove estuary ranged from 0 to 26, water temperature ranged from 26 to 31°C, dissolved oxygen (DO) saturation ranged from 17 to 83% and pH ranged from 6.5 to 7.8. All parameters were linearly correlated to salinity, which increased from site A to site D and was roughly similar to that of site C at site E. DO saturation and pH increased with salinity, and water temperature decreased. Higher salinity, higher DO saturation, higher pH and lower temperature were observed at each site during the dry season due to higher mixing with marine waters.

4.2. Prokaryotic compartment

Average prokaryotic abundance per sampling event ranged from 1.2 to 5.7 x 10^9 cells L^{-1} and average cell size ranged from 0.28 to 0.45 µm, considering both sampling periods, whatever the site, the layer and tidal time. Highest prokaryotic abundance was measured in sub-surface water at site C during the wet season and lowest value was recorded at site D in SML during the dry season. No significant difference in prokaryotic abundance was observed between the 3 water layers during the dry season (Kruskal-Wallis rank sum test; χ^2 = 1.70, df = 2, p-value = 0.43, n = 24 for each group; Figure 3-2a). Differences were not tested between sites and tidal stages whatever the season due to low amount of data per group (n = 3). Prokaryotic abundance in sub-surface waters was very similar between all sites and whatever the tidal stage during the dry season and on average 2-3 times higher at sites C and D compared to the other sites during the wet season (Figure 3-3a and Figure 3-3d). No significant difference was measured between seasons in sub-surface waters (Welch t-test; t = -1.72, df = 15.1, p-value = 0.11, n = 24 and 15 for the dry and the wet season, respectively; Figure 3-4a).

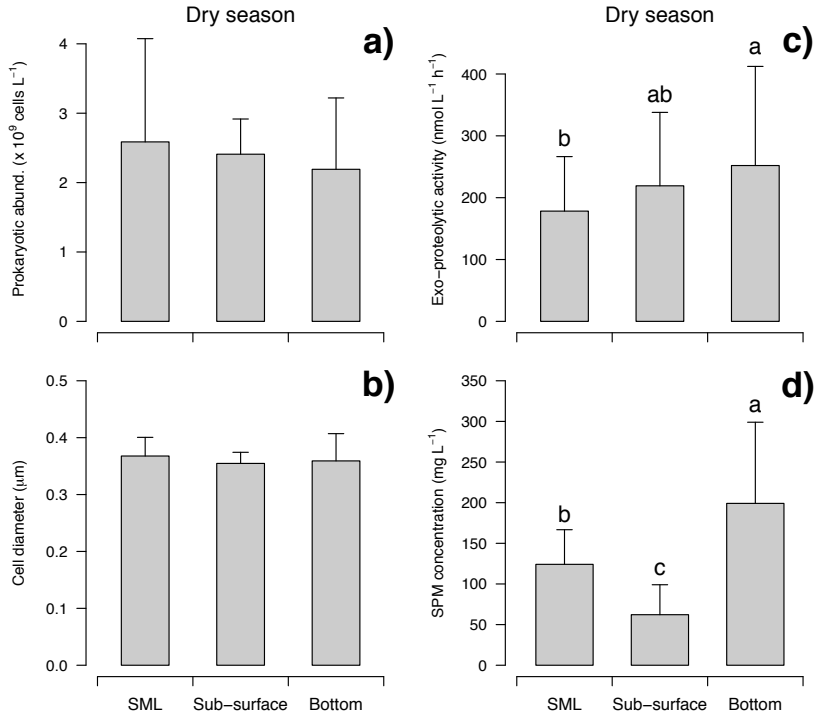

Figure 3-2: Vertical variability in a) prokaryotic abundance b) cell diameter c) leucine-aminopeptidase exo-proteolytic activity and c) suspended particulate matter concentration in the 3 water layers of the Can Gio mangrove during the dry season. For a) and b), n = 24 for each bar, and for c) and d), n = 32 for each bar. Letters indicate significant differences at α = 5% (Kruskal-Wallis rank sum test plus Wilcoxon pairwise comparisons with Holm-corrected α).

Highest cell size was measured in bottom waters at site A during the dry season and lowest values was recorded at site E in SML during the wet season. No significant difference in cell size was observed between the 3 water layers during the dry season (Kruskal-Wallis rank sum test; χ^2 = 2.61, df = 2, p-value = 0.27, n = 24 for each group; Figure 3-2b). Differences were not tested between sites and tidal stages. Cell size remained very stable among sites, seasons and tidal stages in sub-surface waters (Figure 3-3b and Figure 3-3e). Seasonal comparison in sub-surface waters revealed higher values during the dry season (Welch t-test; t = 2.63, df = 18.6, p-value = 0.02, n = 24 and 15 for the dry and the wet season, respectively; Figure 3-4b).

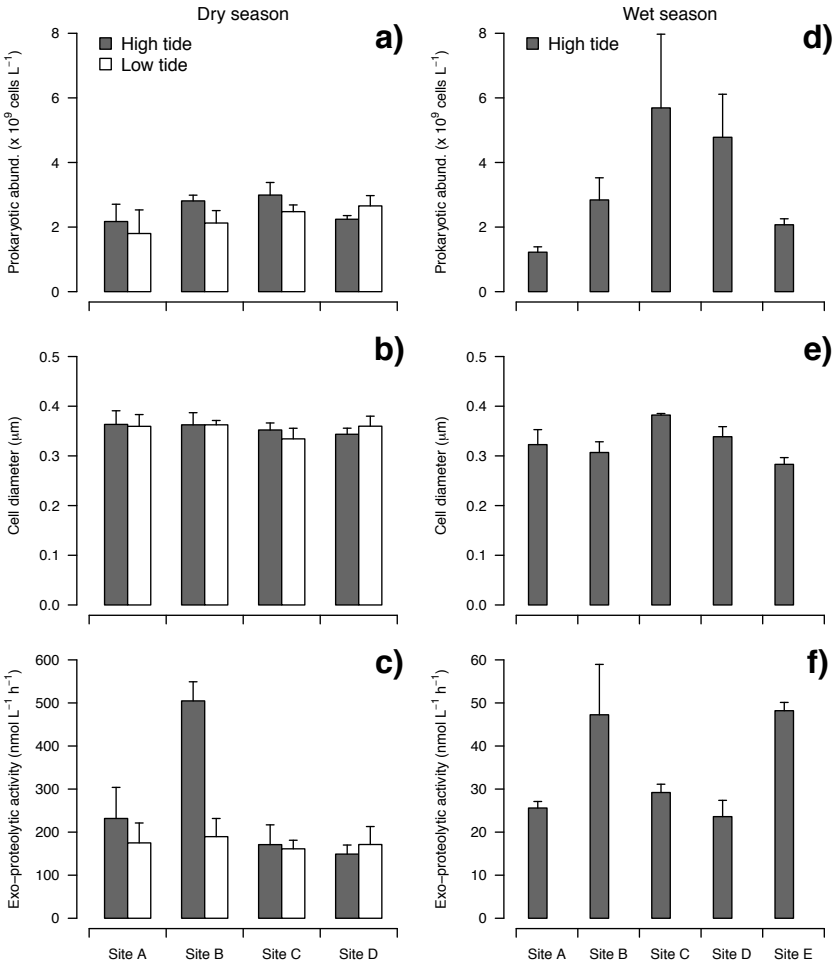

Figure 3-3: Spatial variability in a) prokaryotic abundance b) cell diameter c) leucine-aminopeptidase exo-proteolytic activity and d) suspended particulate matter concentration in the sub-surface water layer of the Can Gio mangrove. For a), b), d) and e) n = 3 for each bar; for c), n = 4 for each bar; and for f), n = 5 for each bar. Statistical differences between groups were not tested given the low amount of data.

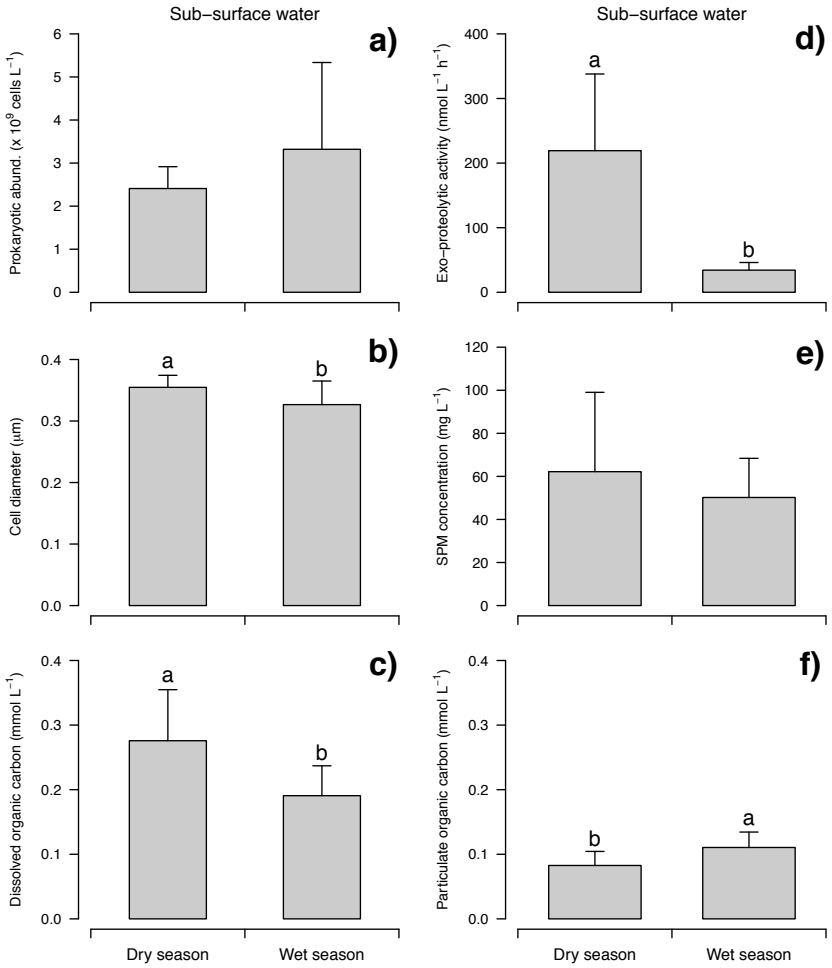

Figure 3-4: Seasonal variability in a) prokaryotic abundance b) cell diameter c) dissolved organic carbon concentration d) leucine-aminopeptidase exo-proteolytic activity e) suspended particulate matter concentration and f) particulate organic carbon concentration in the sub-surface water layer of the Can Gio mangrove. For a) and b), n = 24 and 15, respectively for the dry and the wet season; for d) and e), n = 32 and 25; for c), n = 24 and 12; and for f), n = 10 and 12. Letters indicate significant differences at α = 5% (Welch t-test).

Average leucine-aminopeptidase exo-proteolytic activity per sampling event ranged from 24 to 505 nmol L^{-1} h^{-1}. Highest activity was measured in sub-surface waters at site B during the dry season and lowest value was recorded in SML at site A during the dry season. A significant difference in EPA was observed between the 3 water layers during the dry season, highlighting higher values in bottom layer and lower values in SML (Kruskal-Wallis rank sum test; χ^2 = 9.32, df = 2, p-value = 0.009, n = 32 for each group; Wilcoxon pairwise comparisons: p-value (SML-bottom) = 0.006, p-value (surface-bottom) = 0.069, p-value (surface-SML) = 0.825; Figure 3-2c). Differences were not tested between sites and tidal stages. EPA was on average 2-3 times higher at site B during high tide compared to the other sites during the dry season and on average 2 times higher at sites B and E compared to the other sites during the

wet season (Figure 3-3c and Figure 3-3f). Seasonal comparison in sub-surface waters revealed higher EPA during the dry season (Welch t-test; t = 8.75, df = 31.8, p-value < 0.001, n = 32 and 25 for the dry and the wet season, respectively; Figure 3-4d).

4.3. Organic carbon pools

POC concentration ranged from 0.6 to 1.8 mg L^{-1} and DOC concentration ranged from 1.6 to 5.4 mg L^{-1}. SPM concentration ranged from 20 to 433 mg L^{-1} and greatly varied during tidal cycles, whatever the site. Variations were attributed to important changes in current velocity, which induced a cycle of flocculation, settling, deposition, erosion, and resuspension of particles (Verney et al. 2009). SPM however significantly differed among water layers (Figure 3-2d), with higher values in the bottom layer and lower values in the sub-surface water (Kruskal-Wallis rank sum test χ^2 = 46.408, df = 2, p-value < 0.001, n = 32 for each group; Wilcoxon pairwise comparisons: p-value (SML-bottom) = 0.005, p-value (surface-bottom) < 0.001, p-value (surface-SML) < 0.001). No seasonal difference was measured in SPM concentration in sub-surface waters (Welch t-test; t = 1.60, df = 47.6, p-value = 0.12, n = 32 and 25; Figure 3-4e). Seasonal comparisons however revealed higher DOC concentration (Welch t-test; t = 4.06, df = 33.0, p-value < 0.001, n = 24 and 12; Figure 3-4c) and lower POC concentration (t = -2.86, df = 19.8, p-value < 0.01, n = 10 and 12; Figure 3-4f) during the dry season.

5. Discussion

Prokaryotic abundance, ranging from 1.2 to 5.7 x 10^9 cells L^{-1}, was in the same order of magnitude than previously observed in other tropical and sub-tropical mangroves. In tidal creeks of the Indus River delta, Bano et al. (1997) measured a prokaryotic abundance ranging from 1 to 4 x 10^9 cells L^{-1}, while Bhaskar and Bhosle (2008) counted 0.6 to 3.5 x 10^9 cells L^{-1} in a mangrove dominated estuary from the west coast of India, thus suggesting that the prokaryotic compartment of the Can Gio mangrove estuary is relatively similar to that of other mangrove ecosystems.

To our best knowledge, there has been no record of EPA in mangrove waters. The activities we measured, on average 219 nmol L^{-1} h^{-1} during the dry season and 34 nmol L^{-1} h^{-1}

during the wet season (Figure 3-4d), were similar to that observed in bottom waters of the semi-enclosed eutrophic Uranouchi Inlet (Japan) by Patel et al. (2000), but much lower than the values they observed in surface waters, reaching 1,170 nmol L^{-1} h^{-1}. Converted to cell-specific activity, the exoproteolytic activities we measured in sub-surface waters ranged from 4.9 to 237.5 amol $cell^{-1}$, which is roughly similar to the values reported by Lamy et al. (2009) during a *Phaeocystis globosa* bloom in the eastern English Channel (50 to 239.1 amol $cell^{-1}$). These results suggest that the prokaryotic compartment of the Can Gio mangrove estuary is relatively active and thus able to efficiently mineralise proteins and make nitrogen available for primary producers.

5.1. Stratification effects on the prokaryotic compartment

The main objective of this study was to explore the EPA variability in a tropical mangrove ecosystem, and link it to the variability of OM composition and quality. The absence of significant differences in prokaryote abundance (Figure 3-2a) and cell size (Figure 3-2b) between the 3 water layers suggests that the prokaryotic compartment is poorly stratified in the water column, contrary to our hypothesis. The Can Gio mangrove estuary is highly hydrodynamic, with current velocity reaching 1.5 m s^{-1} during ebb and 1.3 m s^{-1} in the opposite direction during flood (data not provided). A strong vertical mixing is thus to be expected and probably inhibits the establishment of a prokaryote-enriched SML, as previously observed in a highly hydrodynamic estuary of Portugal (Santos et al. 2011). In their study, Santos et al. (2011) compared the SML and the sub-surface water of the most hydrodynamic zone of the Ria de Aveiro estuary (Portugal). They measured a similar abundance of prokaryotes between water layers but a higher proportion of particle-attached cells and a lower prokaryotic productivity in the SML. In our study we did not differentiate free cells from particle-attached cells but we measured a lower EPA in the SML compared to the bottom layer (Figure 3-2c), suggesting that despite similar cells number (Figure 3-2a), the functioning of the prokaryotic compartment is different among water layers.

Similar prokaryotic abundance measured between water layers (Figure 3-2a), despite different SPM concentrations (Figure 3-2d), suggest that a larger fraction of cells are attached to particles in the bottom layer compared to the sub-surface water, while SML is intermediate. It has previously been observed that particle-attached prokaryotes were more

active than free-living cells (Grossart et al. 2007a, 2007b, Schapira et al. 2012). The higher EPA in the bottom layer (Figure 3-2c) might be due to a higher proportion of particle-attached prokaryotes compared to the sub-surface water, while SML is enriched in SPM compared to the sub-surface water (Figure 3-2d) but without comprising a more active prokaryotic compartment. Thus, contrary to our hypothesis, prokaryotes were not more active in the SML (Figure 3-2c). Our postulate was however validated for the bottom layer of the estuary, where prokaryotes were indeed more active (Figure 3-2c). In this system, prokaryotic numbers and EPA were not directly correlated to SPM, suggesting that other factors than the availability of colonisation sites regulate the prokaryotic abundance and activity (Friedrich et al. 1999).

Prokaryotic cells are influenced by the presence of organic and inorganic particles in the water column, creating patches, or "hotspots" of biomass where OM is intensely recycled (Long and Azam 2001, Simon et al. 2002), especially in a tidal estuary exhibiting high load of suspended matter where they can reach up to 80% of total abundance (De Souza et al. 2003). Particle-attached prokaryotes might be larger in size than free-living cells, probably due to better nutritive conditions (organic and inorganic nutrients) in aggregates compared to the surrounding waters (Cho and Azam 1988, Simon et al. 2002). In our study, we did not measure any difference in cell sizes among water layers (Figure 3-2b). However, such metabolically induced differences are subject to controversy. Despite studies have shown that particle-attached cells are more active than free cells (Grossart et al. 2007a, 2007b, Schapira et al. 2012), differences in prokaryotic activity might be due to the quality of OM used by both fractions rather than different cell sizes (Lyons and Dobbs 2012, Schapira et al. 2012). In the Can Gio mangrove estuary, we showed that the distribution of carbon and the quality of OM varied at both seasonal and at short spatial scales (see Chapter 1 and Chapter 2) and we thus hypothesised that EPA also varied according to these variables.

5.2. Relation of the prokaryotic compartment with OM quality

During the dry season, EPA was roughly 10 times higher than during the wet season (Figure 3-4d), while prokaryotic abundance did not differ (Figure 3-4a) and cell size was only slightly lower (Figure 3-4b), suggesting that the prokaryotic biomass did not change according to the season. EPA is usually closely related to the prokaryotic abundance (Cunha et al. 2000, Patel et al. 2000) and thus, the observed stability in bacterial stock and size was unexpected.

Intense top-down pressure (grazing or virus mortality) could explain such decoupling between prokaryotic standing stock and activity (Fuhrman and Noble 1995, De Souza et al. 2003). High EPA levels could also be sustained by a large fraction of free enzymes released far from the cells. These free enzymes are susceptible to be degraded by physical (temperature, pH, UV…) and chemical factors or transported far away from the producing cells that cannot directly benefit from hydrolysis products (Chróst 1991). Free enzymes production would be a benefit for the cells if the distance with the substrate to hydrolyse is less than 10 µm (Vetter et al. 1998).

Lower POC and higher DOC concentrations measured during the dry season indicate that the nature of OM differed among seasons (Figure 3-4c and Figure 3-4f). Indeed, OM exhibited higher freshness during the wet season, with higher proportion of polyunsaturated fatty acids, indicative of phytoplankton, and branched fatty acids, indicative of bacteria (see Chapter 2). In their study, Baltar et al. (2017) hypothesised that the macromolecules composing DOC (i.e. carbohydrates, proteins, lipids, etc.) and their palatability for heterotrophic prokaryotes may influence microbial degradation processes. They fuelled prokaryotes with mangrove-derived DOC and observed an increase in EPA up to 400 nmol L^{-1} h^{-1} after 4 days of incubation. In our study, the renewal of water in the mangrove was probably higher during the wet season compared to the dry season, due to rain inputs and higher discharge of the estuary. Thus, DOC released by mangrove leaves could be more rapidly diluted during the wet season. As a consequence, the prokaryotic compartment activity did not increased to the same levels as during the dry season, when higher quantities of DOC originated from mangrove leaves. Similarly, high EPA at site E during the wet season in comparison to the other sites (Figure 3-3f) was most likely due to the high concentration of mangrove-derived DOC close to the mangrove forest.

We expected EPA to vary as a function of salinity in the estuary, as a response to the mixing of fresh and marine waters, but no clear relation between the prokaryotic compartment and salinity was evidenced (Figure 3-3c and Figure 3-3f). The high EPA at site B in sub-surface water during both seasons at high tide (Figure 3-3c and Figure 3-3f) was unexpected given its relative stability in other sites whatever the tidal stage considered (Figure 3-3c). Site B is located down the area dedicated to shrimp farming (Figure 3-1) and the intensive shrimp production requires punctual water renewal in ponds, releasing wastewaters loaded with organic matter and nutrients to adjacent ecosystems (Anh et al. 2010). Shrimp

pond effluents are characterised by intense biological activity and might contain elevated concentrations of protein degrading enzymes, such as the leucine-aminopeptidase. However, another sampling strategy or lab experiments would be required to trace the influence of such effluents and confirm that such releases could affect EPA in the estuary.

Our results suggest that both mangrove-derived DOC and shrimp pond effluents increase the release of extracellular enzymes by prokaryotes. The aim of such enzymes is to convert compounds of high molecular weight into monomeric substances, allowing them to be transported through the cytoplasmic membrane. It is thus to be expected that a higher degree of macromolecules polymerisation or organically less labile OM would lead to a higher release of extracellular enzymes by prokaryotes. Baltar et al. (2017) rather suggested that it is the high palatability (that is probably linked to easier assimilation) of mangrove-derived DOC that enhances extracellular enzymes production. According to Findlay et al. (1991), autochthonously produced organic matter, including exudates, intracellular contents and biomass of primary producers are easily degraded by prokaryotes, while allochthonous sources are relatively more complex and refractory to prokaryote degradation. In ecological studies, it is generally assumed that mangrove leaves are poorly nutritive and hardly consumed by living organisms (Harada and Lee 2016). In addition, a substantial fraction of OM in shrimp pond effluents is autochthonously produced given the high level of nutrients provided to phytoplankton (Anh et al. 2010), but unconsumed food pellets and faeces may also fuel effluents with elevated amounts of highly-polymerised OM resistant to degradation. We thus suggest that EPA is enhanced in environments where OM is composed of high amounts of macromolecules resistant to degradation.

6. Conclusions

To our best knowledge, this study is the first to determine the leucine-aminopeptidase activity in mangrove waters. Our results suggest that particles are preferential sites for macromolecules hydrolysis, and that their vertical movements due to water current play a substantial role in OM cycling. The surface micro-layer of the estuary, that we expected to serve as a receptacle for anthropogenic pollutants, do not seem to be well structured because of high water turbulence. Finally, the nature of OM transported by the Can Gio mangrove estuary affect the ability of prokaryotes to degrade organic matter and recycle

nitrogen, despite abundance of prokaryotic cells did not vary. Thus, spatial and temporal changes in OM quality influence prokaryotes extracellular enzymes production, leading to higher exo-proteolytic activity, most likely due to high load resuspended particles and to a higher degree of macromolecules polymerisation.

7. Acknowledgments

The authors would like to thank Xavier Mari from the French IRD for providing the glass plate sampler during field trips and Vietnamese students for their help during samplings.

Chapter 4: Particulate organic matter decomposition in shrimp pond effluents and mangrove water: a laboratory experiment

VIVIER Baptiste, DAVID Frank, MARCHAND Cyril, NGUYỄN THÀNH Nho and MEZIANE Tarik

1. Abstract

Intensive shrimp farming is strongly criticized for its negative environmental impacts. In the present study, we used an experimental approach to study changes in SPOM nutritional quality during decomposition of shrimp pond effluents after being released in the Can Gio Mangrove Biosphere Reserve (Southern Vietnam). Water samples were taken in Can Gio, separated in 3 conditions (shrimp pond effluents, river water and a mixture of both) and then incubated in a dark room for 16 days. Water parameters, nutrients, stable isotopes and fatty acids were measured regularly. Total concentrations of FA rapidly decreased in shrimp pond effluents, with a 50% loss of FA during the first 24 h of the experiment and a 75% loss after 4 days of incubation. Phytoplanktonic cells immediately died after mixing both water sources, probably because of the brutal change in environment characteristics (i.e. pH, salinity). Microbial degradation of algal organic matter was accompanied by a strong increase in relative proportions of the FA 18:1ω7, which is supposedly an indicator of aerobic denitrifying bacteria. This FA can thus be used to trace the influence of shrimp pond effluents release on the ecosystem. In addition, our study suggests that aerobic denitrification may occur during shrimp pond effluents decomposition, thus releasing N_2 and N_20, the latter being a strong greenhouse gaz.

2. Introduction

Shrimp farming has grown explosively in the last decades. Global shrimp production was 1.1 billion tons in 2000, 3.4 billion tons in 2008 and reached 4.9 billion tons in 2015 (FAO 2017). Although shrimp farming generates important social and economic benefits (Primavera 1997), its huge development is strongly criticized for its negative environmental impacts (Primavera 2006, Anh et al. 2010). Intensive shrimp farming is characterized by high shrimp density, high amounts of inputs (food pellets, fertilizers and antibiotics) and high water renewal rate in ponds (15% every two weeks in Vietnam; Anh et al. 2010). This leads to high effluent releases associated with a highly degraded water quality close to shrimp farming areas (Páez-Osuna 2001, Trott et al. 2004, Lemonnier and Faninoz 2006) that may stimulate algal blooms and create anoxic water conditions (Naylor et al. 1998, Smith et al. 1999).

However, despite potential negative impacts of shrimp pond effluents discharges in estuarine waters are recognized, their effect is mostly investigated regarding nutrients (Trott and Alongi 2000, Páez-Osuna and Ruiz-Fernández 2005, Molnar et al. 2013) and other parameters, such as the nutritional quality of impacted water suspended particulate organic matter (SPOM), are poorly documented. In a recent study, Aschenbroich et al. (2015) have shown that the nutritional quality of mangrove surface sediments was affected by shrimp pond effluents releases. Indeed, sediments integrate chronic disturbances on a relatively long-time basis (Molnar al. 2013), while SPOM naturally varies at short spatial scales in the Can Gio mangrove estuary (see Chapter 2), making difficult to differentiate changes induced by environmental parameters from those due to shrimp pond effluent releases.

In the present study, we used an experimental approach to constrain natural short-time changes in SPOM nutritional quality and study the effect of shrimp pond effluent releases on estuarine SPOM in the Can Gio Mangrove Biosphere Reserve (Southern Vietnam). The mangrove is located approximately 50 km south of Ho Chi Minh City and covers an area of 75,740 ha. In 2000, the UNESCO designated Can Gio as the first mangrove Biosphere Reserve in Vietnam (Nam et al. 2014). At the northeast border of the mangrove forest, a transition area covers 29,880 ha where intensive shrimp farming is the main economic activity, releasing wastewaters in the nearby waterways, with potential negative impacts on the ecosystem (Anh et al. 2010). We expected to measure elevated phytoplanktonic abundance in effluents that can induce a strong bacterial development when they are being

decomposed in mangrove waters. We chose three categories of water quality indicators to follow shrimp pond effluents SPOM degradation: fatty acids (FA), stable isotopes and nutrients. FA biomarkers successfully detailed the organic matter composition of marine ecosystems (Parrish et al. 2000). They are good indicators of microalgae and bacteria relative abundances (Meziane and Tsuchiya 2000, Canuel 2001) and allow to evaluate the physiological state of phytoplankton cells (Pan et al. 2014, 2017). In complement to fatty acids, stable isotopes and C/N ratio enable to assess relative contributions of multiple organic matter sources to the bulk SPOM (Dunn et al. 2008, Volkman et al. 2008, Bouillon et al. 2011). Finally, nutrients are the building blocks of OM and are made available for primary producers after OM has been degraded, thus release ammonia in the surrounding waters and fueling the nitrification cycle (Pauer and Auer 2000).

We sampled water from shrimp ponds and a nearby mangrove channel to study the degradation processes of SPOM in the absence of light (thus imitating natural conditions in the estuary). Pure shrimp pond effluents, pure river water and a combination of both were incubated in controlled conditions during 16 days (Image 4-1). We hypothesized that (1) algal cells were rapidly decomposed after being released in mangrove waters, (2) specific degradation pathways were favored in a mix of shrimp pond effluents with river water compared to both waters taken in isolate (3) specific fatty acids could be used as tracers of shrimp pond effluents release in natural ecosystems.

Image 4-1: Dark room used to incubate water samples during the decomposition experiment

3. Materials and methods

3.1. Water collection

Water samples were collected in shrimp ponds (Image 4-2a) and a nearby mangrove channel (Image 4-2b) from the Can Gio mangrove Biosphere Reserve in February 2017. Surface estuarine water (river water; RV) was collected from the middle of the Rung Sat bridge (10° 35' 2.94'' N; 106° 49' 32.68'' E) at the beginning of the ebb tide, while a composite sample of shrimp pond effluents (EF) was made using water from three different intensive shrimp ponds (40-60 shrimps m^2) located close to the river water sampling point.

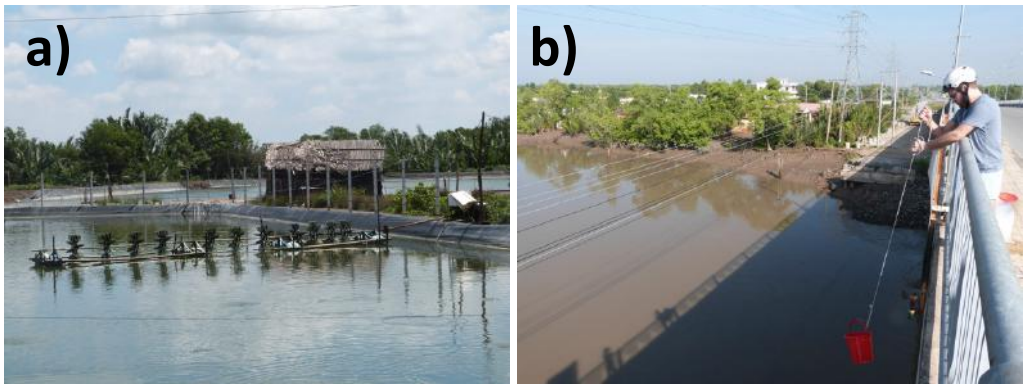

Image 4-2: a) Shrimp pond and b) Rung Sat bridge in the Can Gio mangrove Biosphere Reserve

3.2. Experimental design

Water samples were brought to the CARE (Centre Asiatique de Recherche sur l'Eau) in Ho Chi Minh City and disseminated in 14 L plastic buckets. These buckets were meant to test three conditions: (1) pure shrimp pond effluents (EF), (2) pure river water (RV) and, (3) a combination of both waters (mixed water; MI: 90% river water + 10% shrimp pond effluents). These 3 conditions were tested in 4 replicates each (12 buckets). The exact amount of wastewaters released from shrimp farming production and the ratio between effluents release and river discharge is unknown and thus, proportion of river water and effluents in the MI condition (90/10) were chosen in a way to place shrimp pond effluents SPOM in the environmental conditions found in river waters, while keeping a sufficient proportion of effluents SPOM in the mix condition to allow a correct differentiation between the 3 conditions, especially regarding FA. All buckets were incubated in a dark room at 30°C and continuously homogenized with 200 L h^{-1} aquarium pumps during 16 days. Samples were

taken at short intervals at the beginning of the experiment and more spaced thereafter (Marty et al. 1996). Samplings were performed at T0 and after 8 h, 16 h, 24 h, 2 days, 3 days, 4 days, 8 days, 12 days and 16 days of incubation (T8, T16, T24, D2, D4, D8, D12 and D16). Dark conditions are meant to simulate the high turbidity of mangrove waters, although we are aware that it does not perfectly represent natural conditions where SPOM may reach the photic zone from time to time due to elevated water turbulence.

Water subsamples from the 12 buckets were regularly filtered during the 16 days of the experiment for further analysis of fatty acids and stable isotope signatures of SPOM. Filtrations were performed using pre-combusted and pre-weighed (4 h at 450°C) 0.7 µm Whatman® GF/F glass microfiber filters and filtered water was kept for dissolved nutrients analysis. All filters were kept at -25°C before analysis.

3.3. Sample processing

Salinity, dissolved oxygen and pH were measured at the beginning of the experiment (T0) using a multi-parameter probe (WTW 3420®). Dissolved nutrients (NO_2^-, NO_3^-) were measured only at T0, T8, T24, D2, D4, D8 and D16, using a Hach-Lang kit photolab DR 1900 employing standard colorimetric methods (APHA 1995, Strady et al. 2017). Reproducibility for replicated measurements was better than 5%.

Lipids were extracted following a slightly modified method of Bligh and Dyer (1959) as described in Meziane et al. (2006). An internal standard (23:0) was added to the samples prior to extraction. Lipids were first extracted using a methanol:water:chloroform mixture (2:1:2 v:v:v). Chloroform, containing lipid extracts, was isolated and evaporated under nitrogen (N_2) flux. Dried lipid extracts were then saponified with a solution of methanol and sodium hydroxide (NaOH, 2N) (2:1, v:v) at 90°C for 1 h 30 min. Subsequently, methylation was performed, transforming all fatty acid esters into fatty acid methyl esters (FAME) using methanolic boron trifluoride (BF3—CH_3OH). FAMEs were quantified by gas chromatography analysis (Varian 3800), using a flame ionization detector. Identification of fatty acids was performed using coupled gas chromatography mass spectrometry (Varian 450-GC; Varian 220-MS), as well as by comparison of gas chromatography retention times with those of standards (Supelco®). The internal standard (23:0) was used to determine the concentration of each fatty acid (C_{FA}) in µg FA per mg SPOM.

Stable isotopes were determined only at T0, T24, D4 and D16. SPOM samples were fumigated for 4 h using 35% HCl to remove all carbonates. Samples were prepared in tin capsules and analyzed at the University of California Davis Stable Isotope Facility (Department of Plant Sciences, UC Davis, Davis, California), using a Vario EL Cube elemental analyzer (Elementar Analysensysteme GmbH, Hanau, Germany) interfaced to a PDZ Europa 20–20 isotope ratio mass spectrometer (Sercon Ltd., Cheshire, U.K.). During analysis, replicates of compositionally similar laboratory standards previously calibrated against international standard reference materials were interspersed with samples. Carbon and nitrogen stable isotope results were reported in parts per thousand (‰), using standard delta notation ($\delta^{13}C$ and $\delta^{15}N$) and are relative to V-PDB (Vienna PeeDee Belemnite) and atmospheric air, respectively. C/N_m ratio was calculated as the molar ratio of particulate organic carbon (POC) vs. particulate organic nitrogen (PON).

4. Results

4.1. Water parameters

Salinity was lower in EF (10.1 ± 0.0) compared to RV (13.2 ± 0.0) and pH was higher in EF (8.35 ± 0.01) compared to RV (7.45 ± 0.01) (Table 4-1). As intended, the MI condition almost kept the conditions displayed by RV (salinity = 12.8 ± 0.0 and pH = 7.53 ± 0.00). SPM concentration was about twice lower in EF (91.2 ± 10.3 mg L^{-1}) compared to RV (204.6 ± 4.3 mg L^{-1}). Shrimp pond effluents were enriched in dissolved nutrients (NO_2^- and NO_3^-) compared to RV. N-NO_2 concentrations in EF varied between 0.25 ± 0.00 and 0.45 ± 0.05 mmol L^{-1} and dropped near zero at D16 (Figure 4-1a) while in MI and RV it remained close to zero during the entire experiment (Figure 4-1a). N-NO_3 concentrations rose from 0.85 ± 0.04 to 1.36 ± 0.10 mmol L^{-1} in EF between T0 and D8, and dropped to 0.21 ± 0.04 mmol L^{-1} at D16, while it ranged between 0.11 ± 0.05 and 0.20 ± 0.02 mmol L^{-1} in MI and slightly under in RV, except at D16 were N-NO_3 concentration increased to 0.37 ± 0.08 mmol L^{-1} (Figure 4-1b).

Table 4-1: Water parameters at T0 in each experimental condition

Parameter	Shrimp pond effluents (EF) (n = 4)	Mixed water (MI) (n = 4)	River water (RV) (n = 4)
Salinity	10.1 ± 0.0	12.8 ± 0.0	13.2 ± 0.0
pH	8.35 ± 0.01	7.53 ± 0.00	7.45 ± 0.01
SPM (mg/L)	91.2 ± 10.3	175.3 ± 3.7	204.6 ± 4.3
C/N (mol/mol)	7.0 ± 0.0	9.0 ± 0.4	9.7 ± 1.4

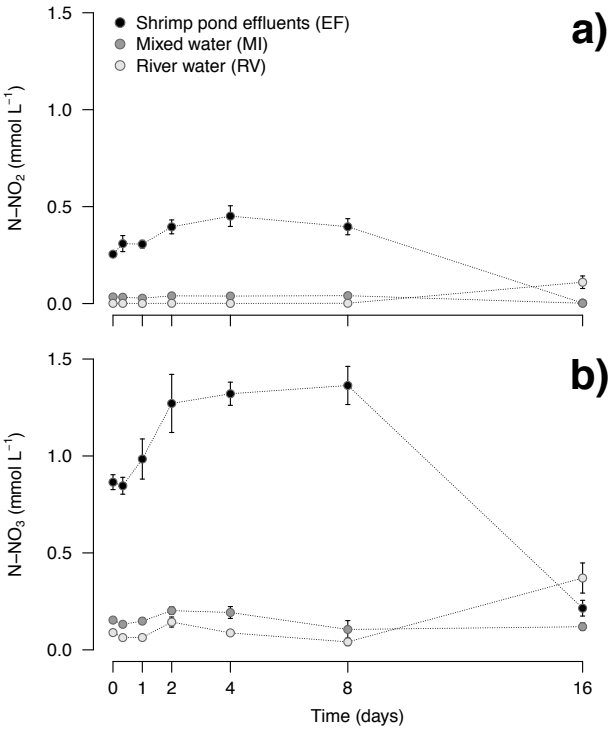

Figure 4-1: Concentration of a) N-NO_2 (mmol L^{-1}) and b) N-NO_3 (mmol L^{-1}) in water samples according to the incubating time (days)

4.2. Fatty acids

Identified FA in SPOM samples include saturated fatty acids (SAFA; e.g. 16:0 and 18:0), polyunsaturated fatty acids (PUFA; e.g. 18:2ω6 and 20:5ω3), monounsaturated fatty acids (MUFAs; e.g. 16:1ω7 and 18:1ω9), and branched fatty acids (BrFA; e.g. iso-15:0 and anteiso-15:0) (Table 2). Total concentration of FA at T0 was about 15 times higher in EF (1.00 ± 0.16 mg L^{-1}) compared to RV (0.067 ± 0.020 mg L^{-1}) (Figure 4-2b). High proportions of PUFA were identified in EF (32.9 ± 1.1%), with a dominant contribution of C_{16} PUFA, 18:3ω3 and 20:5ω3 (Table 4-2). In contrast, RV was dominated by SFAs (56.8 ± 4.1%) and PUFA proportions were low (8.8 ± 0.7%) (Table 4-2).

Total concentrations of FA exponentially decreased during the entire experiment in EF, with a 50% loss of FA during the first 24 h of the experiment and a 75% loss at D4, while it remained almost stable in MI and RV during the entire experiment (Figure 4-2b). Concentrations of total PUFA, 18:3ω3 and 20:5ω3 followed the same trend as total concentrations (Figure 4-3), while relative contributions remained almost stable between T0 and T24 in EF, and dropped rapidly after T24 (Figure 4-3). In contrast, total PUFAs and 18:3ω3 relative proportions decreased since the first hours of the experiment in MI (Figure 4-3) and

almost did not changed in RV during the entire experiment. Concentrations of BrFA and 18:1ω7 remained almost stable during the entire experiment, while relative proportions increased in all conditions (Figure 4-3). Relative proportions of 18:1ω7 showed a sharp increase in MI from 5.3 ± 0.3% at T0 to a maximum of 23.6 ± 0.8% at D4, reaching values higher than in EF (12.8 ± 1.1%) and RV (15.8 ± 2.4%) at the same moment (Figure 4-3).

Table 4-2: Relative proportions of main FA in SPOM in each experimental condition at T0 (mean ± SD). Only FA with proportions > 0.5% in at least one condition are displayed

Fatty acids (%)	Shrimp pond effluents (EF) (n = 4)	Mixed water (MI) (n = 4)	River water (RV) (n = 4)
Saturated			
12:0	0.2 ± 0.1	0.3 ± 0.1	0.6 ± 0.8
14:0	9.7 ± 0.3	6.8 ± 1.4	4.7 ± 1.4
15:0	0.9 ± 0.1	1.3 ± 0.2	2.4 ± 0.5
16:0	22.2 ± 0.6	28.3 ± 1.4	33.9 ± 1.4
17:0	0.4 ± 0.1	0.9 ± 0.2	1.3 ± 0.4
18:0	1.9 ± 0.3	4.6 ± 0.8	9.6 ± 1.2
19:0	0.0 ± 0.0	0.3 ± 0.1	0.8 ± 0.6
20:0	0.2 ± 0.1	0.4 ± 0.1	0.8 ± 0.1
22:0	0.2 ± 0.0	0.6 ± 0.1	1.3 ± 0.2
24:0	0.1 ± 0.0	0.9 ± 0.4	1.0 ± 0.5
∑SFA	**35.9 ± 1.3**	**44.6 ± 1.6**	**56.8 ± 4.1**
Monounsaturated			
16:1ω9	2.9 ± 0.1	2.9 ± 0.4	3.6 ± 1.3
16:1ω7	15.4 ± 0.2	13.1 ± 0.4	9.3 ± 1.3
16:1ω5	0.4 ± 0.0	0.5 ± 0.0	0.8 ± 0.2
17:1ω9	0.1 ± 0.0	0.2 ± 0.1	0.6 ± 0.3
18:1ω11	0.3 ± 0.0	0.2 ± 0.1	1.2 ± 1.3
18:1ω9	3.6 ± 0.1	5.0 ± 0.7	5.7 ± 0.5
18:1ω7	3.7 ± 0.2	5.3 ± 0.3	7.3 ± 2.4
∑MUFA	**27.2 ± 0.1**	**28.2 ± 1.1**	**29.5 ± 3.7**
Polyunsaturated			
16:2ω6	1.1 ± 0.2	0.5 ± 0.1	0.4 ± 0.2
16:2ω4	2.3 ± 0.1	1.6 ± 0.1	0.6 ± 0.1
16:3ω4	2.5 ± 0.1	1.6 ± 0.1	0.5 ± 0.1
16:3ω3	2.4 ± 0.2	1.4 ± 0.1	0.2 ± 0.0
16:4ω3	1.3 ± 0.1	0.9 ± 0.2	0.3 ± 0.2
18:2ω9	tr.	tr.	0.7 ± 0.1
18:2ω6	3.4 ± 0.1	3.2 ± 0.3	1.1 ± 0.2
18:3ω3	7.3 ± 0.4	5.2 ± 0.6	0.6 ± 0.1
18:4ω3	2.6 ± 0.1	1.8 ± 0.1	0.5 ± 0.2
20:2ω9	tr.	tr.	0.8 ± 0.4
20:4ω6	1.4 ± 0.1	1.2 ± 0.1	0.5 ± 0.1
20:5ω3	5.0 ± 0.3	3.4 ± 0.2	1.6 ± 0.3
22:6ω3	1.5 ± 0.2	0.3 ± 0.4	0.4 ± 0.4
∑PUFA	**32.9 ± 1.1**	**22.3 ± 0.6**	**8.8 ± 0.7**
Branched			
15:0iso	1.6 ± 0.0	1.6 ± 0.2	1.5 ± 0.2
15:0anteiso	0.5 ± 0.0	0.8 ± 0.1	1.2 ± 0.1
16:0iso	0.4 ± 0.0	0.5 ± 0.0	0.7 ± 0.1
17:0iso	1.0 ± 0.2	1.5 ± 0.2	0.8 ± 0.1
∑BrFA	**4.0 ± 0.1**	**4.9 ± 0.3**	**4.9 ± 0.4**
Others	3.7 ± 0.4	3.0 ± 0.8	3.0 ± 1.6

tr. = traces

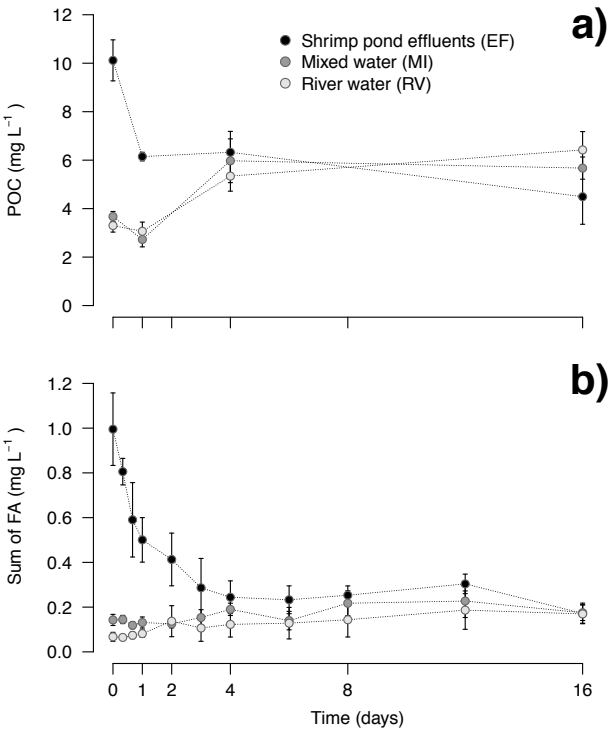

Figure 4-2: a) particulate organic carbon (POC; mg L^{-1}) and b) total FA concentrations (mg L^{-1}) in SPOM according to the incubating time (days)

4.3. Stable isotopes $\delta^{13}C$ and $\delta^{15}N$

POC concentrations were about 3 times higher in EF (10.1 ± 0.8 mg L^{-1}) compared to RV (3.3 ± 0.3 mg L^{-1}) (Figure 4-2a). It rapidly decreased during the first 24 h of the experiment in EF, while it increased in MI and RV, reaching values almost similar in all conditions at D4 and remaining stable until the end of the experiment (Figure 4-2a).

$\delta^{13}C$ signatures of SPOM at T0 were lower in EF (-27.89 ± 0.15‰) compared to RV (-25.66 ± 0.04‰) (Figure 4-4a). It decreased in EF from T0 to T24 (-38.35 ± 0.09‰) and then increased until the end of the experiment, while it slightly increased during the entire experiment in MI and RV (Figure 4-4a). $\delta^{15}N$ signatures of SPOM were higher in EF (9.14 ± 0.07‰) compared to RV (5.16 ± 0.73‰) (Figure 4-4b). It increased until D4 up to 14.2 ± 0.3‰ in EF, and then decreased to 10.0 ± 0.6‰ at D16, while it oscillated roughly between 4.7‰ and 8.4‰ in MI and RV during the entire experiment.

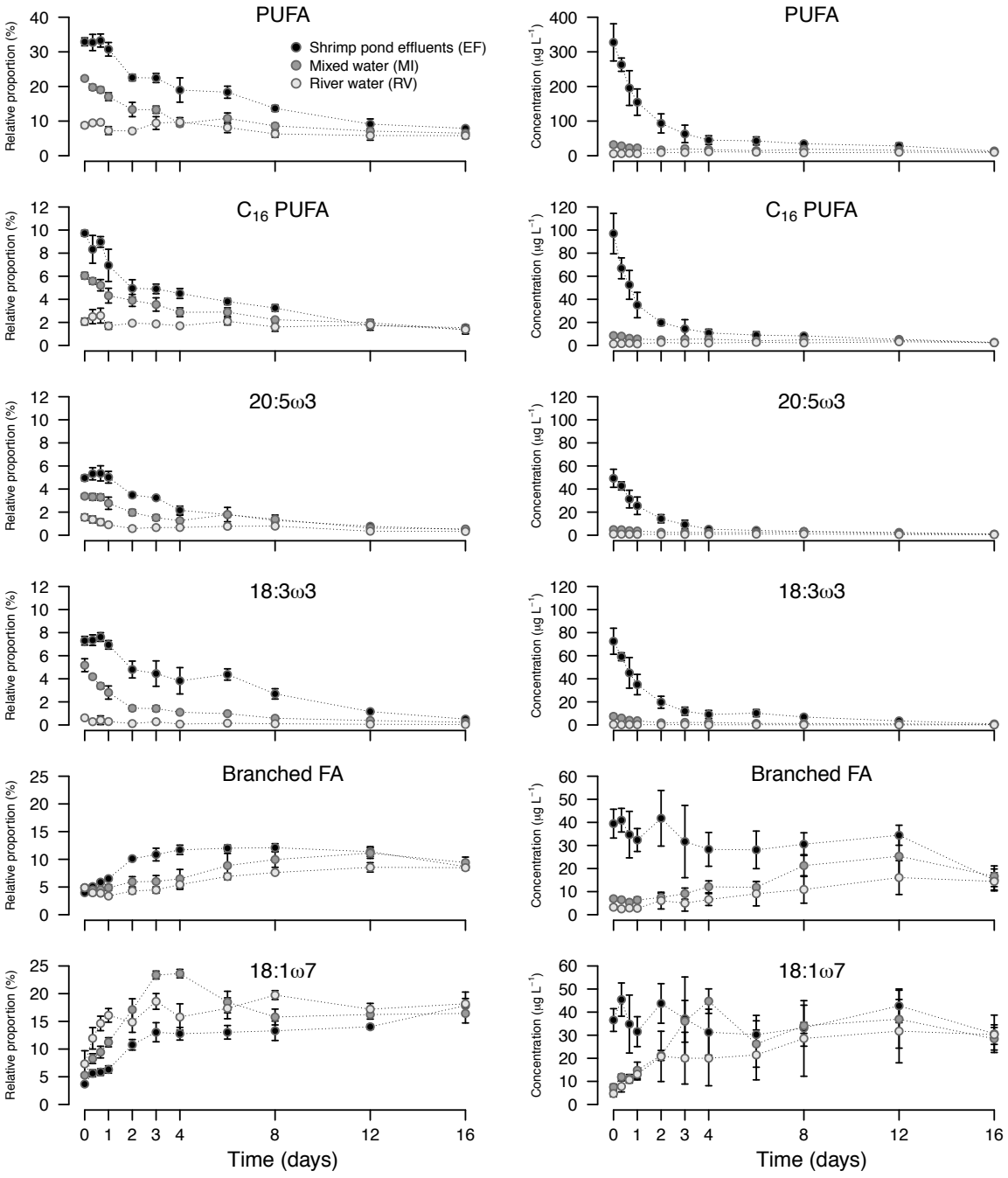

Figure 4-3: Relative proportions (%) and concentrations (µg L^{-1}) of specific fatty acids (20:5ω3, 18:3ω3 and 18:1ω7) and FA groups (polyunsaturated FA - PUFA, C_{16} PUFA and Branched FA) in SPOM according to the incubating time (days)

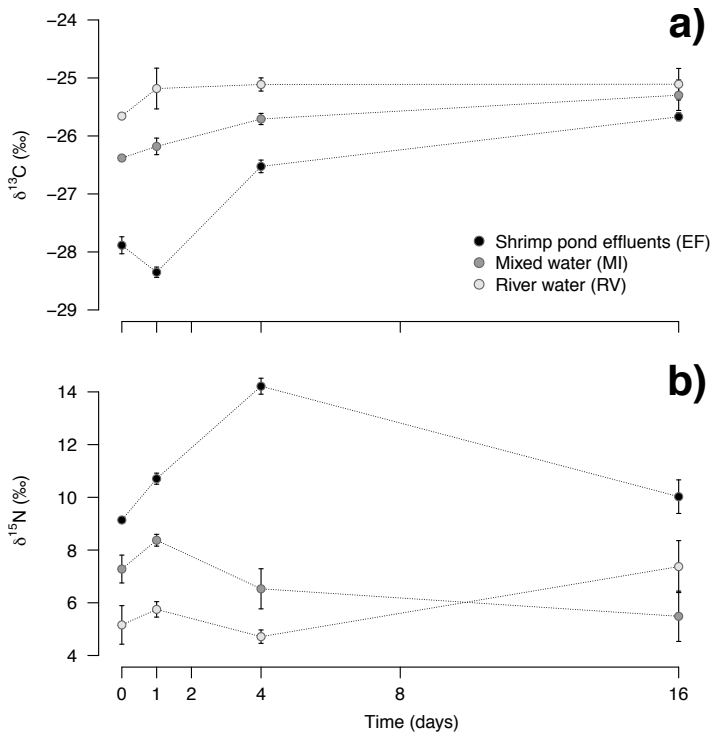

Figure 4-4: a) $\delta^{13}C$ (‰) and b) $\delta^{15}N$ (‰) stable isotopes ratios of SPOM according to the incubating time (days)

5. Discussion

5.1. Composition of SPOM sources at T0

In shrimp pond effluents (EF), high PUFA relative proportions (32.9 ± 1.1%; Table 4-2), indicative of phytoplankton in natural environments (Napolitano et al. 1997, Canuel 2001, Moynihan et al. 2016), and C/N_m ratio close to the Redfield ratio (6.6) (Table 1), show that a substantial fraction of SPOM is constituted by living phytoplankton. Shrimp ponds generally exhibit high primary production (Burford et al. 2003) and the elevated level of nutrients we measured in EF (Figure 4-1) provides ideal conditions for phytoplankton growth. In our experiment, dominant algal cells were diatoms and green algae, as observed with microscope (unpublished data) and confirmed by the high proportions of PUFA 20:5ω3, C_{16} PUFAs, and PUFA 18:3ω3, indicative, respectively for the two first of Bacillariophyceae, and for the latter of Chlorophyceae (Dalsgaard et al. 2003). In contrast, low POC concentrations (Figure 4-2a) and low PUFA relative proportions in river water (RV) (8.79 ± 0.7%, Table 4-2) show that SPOM was highly degraded (Jaffé et al. 1995, Canuel 2001), as we observed in the main branch of the Can Gio mangrove estuary (see Chapter 2).

5.2. Degradation of shrimp pond effluents

The high decomposition rate of FA in EF indicates that algal lipids were rapidly degraded once photoautotrophic production was stopped (in the absence of light in experimental conditions). However, the upholding of PUFA relative proportions during the first 24 h of the experiment (from T0 to T24) followed by their gradual decay from T24 to D16 (Figure 4-3) suggests that two different processes are successively involved in FA degradation. In complete darkness, living algal cells consume lipids from intracellular storage compartments (Brown et al. 1996, Eltgroth et al. 2005), possibly allowing them to survive during a few days using triacylglycerols and galactolipids as an energy source (Manoharan et al. 1999). In the present study, phytoplankton from shrimp pond effluents survived during the first 24 h of the experiment (from T0 to T24), leading to the upholding of PUFA relative proportions. In contrast, cells death after T24 led to the decrease of PUFA relative proportions, as usually observed during microbial degradation of phytoplankton (Ding and Sun 2005, Pan et al. 2014, 2017). $\delta^{13}C$ dynamics confirm the succession of these two processes, with decreasing values during the first 24 h of the experiment and increasing values thereafter (Figure 4-4a). Pan et al. (2014) measured that during cell respiration, the $\delta^{13}C$ of phytoplankton FA decreased, while it increased during microbial degradation. In our experiment, cell respiration thus decreased the $\delta^{13}C$ of SPOM between T0 and T24, while microbial degradation increased the $\delta^{13}C$ of SPOM between T24 and D16 (Figure 4-4a).

The increase of BrFA and FA 18:1ω7 relative proportions, indicative of bacteria (Kaneda 1991, Meziane and Tsuchiya 2000, Dalsgaard et al. 2003), along with the upholding of their concentrations (Figure 4-3), indicate that the bacterial compartment remained active during the entire experiment. The increase of nitrates from T0 to D8 and the increase of nitrites from T0 to T4 in EF shows that OM in being degraded and ammonia is transformed to nitrate though nitrification, which occurs in aerobic conditions and darkness (Smith et al. 2014). In addition, we observed an increase of $\delta^{15}N$ in shrimp pond effluents SPOM during the experiment (Figure 4-4b), which is most probably induced by the nitrification process (Caraco et al. 1998, De Brabandere et al. 2002). However, the strong decrease of nitrate concentrations at the end of the experiment (Figure 4-1b) was unexpected since denitrification, that could eventually convert NO_3^- into N_2, generally occurs in anaerobic condition (Chen et al. 2012), and should not have happened in our experiment in which water

was continuously mixed with pumps. Nevertheless, aerobic denitrification may not be uncommon since aerobic denitrifiers tend to work efficiently under similar conditions to our experiment (T°C = 25-37°C; pH = 7-8; dissolved oxygen concentration = 3-5 mg/L and C/N ratio = 5-10; Ji et al. 2015). We suggest that the high levels of nitrate in EF led to the growth of aerobic denitrifying bacteria and thus to the denitrification of nitrate, leading to the release of N_2 and N_2O to the atmosphere (Hu et al. 2012).

5.3. Mixing of shrimp pond effluents with river water

Conversely to shrimp pond effluents, the relative stability of nutrient concentrations (Figure 4-1), FA relative proportions (Figure 4-3) and isotopic ratios (Figure 4-4) in river water SPOM indicates that organic matter is poorly processed during the experiment, which is to be expected since mangrove channels SPOM is assumed to be in an advanced state of decomposition (see Chapter 2). The RV condition in our experiment can thus serve as a baseline to be compared with river water in which shrimp pond effluents were released (MI condition). The sum of FA was about 15 times higher in EF compared to RV and thus, the volume ratio used to produce the MI condition (10% EF and 90% RV) is supposed to have added almost the same quantity of both sources SPOM to the overall SPOM pool. In the absence of interaction effect between EF and RV, we expect measured SPOM variables (FA and stable isotopes) to be in MI roughly equal to the mean of EF and RV.

In MI, no upholding of PUFA relative proportions was measured during the first 24 h of the experiment, conversely to EF and RV (Figure 4-3), suggesting that phytoplankton cells immediately died and started to decompose just after water mixing. This is confirmed by the $\delta^{13}C$ of SPOM, which immediately increased in MI due to microbial degradation, unlike in EF where cell respiration and microbial degradation occurred successively and showed two different trends in SPOM $\delta^{13}C$ variation (Figure 4-4a). The complete darkness in our study may have induced phytoplankton cells death in EF, but only after 24 h. We thus suggest that immediate cell death in MI was not due to light depletion but rather to the mixing of the two different water masses, possibly because of the difference in pH or salinity between EF and RV (Table 4-1), or any other sudden environmental stress induced by the water mixing (Bidle and Falkowski 2004). The volumes of shrimp pond effluents released in the environment are most probably much lower than 10% (the ratio used in our experiment), and thus, change in

environmental conditions for phytoplankton cells released in mangrove channels is at least as brutal as in our experiment. Indeed, cell death and variations in FA and stable isotopes of SPOM in the MI condition of our experiment were most likely representative of the processes that could happen in natural conditions.

The FA 18:1ω7 showed an interesting dynamic in MI since its relative proportion increased between T0 and D4 up to values that exceed proportions measured in both EF and RV (Figure 4-3). Its dynamics was different from that of the BrFA's one, which never exceeded that of both EF and RV, suggesting that specific bacterial strains have grown in MI, probably as a result of substrate availability brought by shrimp pond effluents and/or bacterial inoculum brought by mangrove channel waters. This FA is commonly used as a bacterial biomarker in natural environments (Meziane and Tsuchiya 2000, Dalsgaard et al. 2003). However, it has been found in such elevated proportions only in phospholipids of alphaproteobacteria, such as *Paracoccus denitrificans*, which are involved in aerobic denitrification (Zelles 1997), thus reinforcing our suggestion that aerobic denitrifying bacteria may grow in shrimp pond effluents. In a recent study, Aschenbroich et al. (2015), found a higher concentration of FA 18:1ω7 in mangrove sediments receiving shrimp pond effluents during the active farm period compared to the non-active period. We thus suggest that FA 18:1ω7 could be used as an indicator of shrimp pond effluent releases in mangrove waters, and that found in high proportions, it may indicate aerobic denitrification processes.

6. Conclusions

Our study confirms that shrimp pond effluents are enriched in phytoplankton and nutrients compared to mangrove waters. Placed in dark conditions, such effluents begin to decompose after 24 h, leading to a 50% loss of FA during the first 24 h of the experiment and a 75% loss after 4 days of incubation. The proportion of PUFA in SPOM simultaneously decreased and nutrients concentration increased. In contrast to shrimp pond effluents alone, the mixture of shrimp pond effluents + river water (MI condition) induced immediate phytoplankton cells decomposition, most likely due to the brutal change in environmental conditions and representative of the processes that could happen in natural conditions. Then, microbial degradation of phytoplankton shifts microbial communities' composition, which could be traced using the relative proportion of FA 18:1ω7 in SPOM. Theses microbial

communities may be responsible for the aerobic production of N_2O that was released in the atmosphere.

7. Acknowledgments

The authors would like to thank the researchers of the Centre Asiatique de Recherche sur l'Eau, in the University of Technology of Ho Chi Minh City for their warm welcome in their laboratory during the experiment, especially Emilie Strady, Julien Némery and Nicolas Gratiot.

PARTIE 2 :

Structure et fonctionnement du réseau trophique

Résumé

Les mangroves sont à la fois considérées comme des nurseries, des zones d'alimentation pour de nombreuses espèces marines et des écosystèmes à partir desquels la nourriture est exportée vers l'océan, soutenant ainsi les réseaux trophiques côtiers. Cela suggère que les mangroves produisent de la nourriture (ou des nutriments) en grande quantité, mais aussi de bonne qualité nutritionnelle et assimilables par les organismes y ayant accès. Par ailleurs, le carbone présent dans cette nourriture transite nécessairement par les estuaires afin de relier les zones intérieures des mangroves aux écosystèmes côtiers, que ce soit une fois assimilée par des organismes (micro ou macroscopiques), ou sous une forme minérale ou organique détritique. La qualité nutritionnelle de la matière organique accessible aux organismes vivants est susceptible de changer le long d'un gradient depuis les zones intérieures des mangroves vers l'océan, ainsi qu'en réponse aux perturbations anthropiques, et donc d'affecter le régime alimentaire et le métabolisme des individus.

Le chapitre 5 s'intéresse aux variations de la qualité nutritionnelle de la matière organique particulaire au cours d'un cycle tidal dans un chenal de vidange situé au cœur de la mangrove. Les résultats présentés ont été acquis au cours de la mission d'échantillonnage en milieu naturel de la saison humide (septembre-octobre 2015). De même que pour les chapitres 1 et 2, cette approche nous a permis d'obtenir des séries de données continues (paramètres physico-chimiques de la masse d'eau) et discrètes selon un pas de temps de 2 h (acides gras de la matière particulaire, carbone organique particulaire et signature isotopique de ce carbone). Nous avons émis l'hypothèse que des quantités importantes de carbone sous une forme nutritive et directement assimilable par les organismes vivants étaient exportées depuis le chenal de vidange lors de la descente de la marée, alors que la remontée des eaux apportait peu de matière nutritive, en raison de la dilution par les eaux estuariennes transportant une matière organique essentiellement détritique. La qualité nutritive de la matière organique est évaluée dans cette étude par sa composition en acides gras, et essentiellement les acides gras polyinsaturés, indicateurs de biomasse « fraiche » et rapidement décomposés après la mort cellulaire. Les résultats obtenus confirment partiellement cette hypothèse. En effet, les plus fortes concentrations de carbone particulaire dans la colonne d'eau sont mesurées lors du jusant, du fait de l'érosion des sols. Cependant, la matière organique dans laquelle ce carbone est piégé est nutritionnellement pauvre,

contenant seulement 7,5 à 11,7% d'acides gras polyinsaturés. Les eaux provenant de l'estuaire transportent elles aussi une matière organique nutritionnellement pauvre, contenant en moyenne 11,3% d'acides gras polyinsaturés. En revanche, sur un court intervalle de temps au début du flot, la matière apportée à l'écosystème est bien plus nutritive, contenant 21,8% d'acides gras polyinsaturés et une concentration en acides gras à la fois par volume d'eau et par masse de matière en suspension largement supérieure aux autres phases de la marée. Cette matière est constituée de phytoplancton ayant vraisemblablement utilisé pour sa croissance le CO_2 libéré par les sols de mangrove lors du jusant par le mécanisme de « tidal pumping ». Ainsi, notre étude confirme que le carbone fixé par les palétuviers constitue une source importante de nourriture pour les organismes vivants. Cependant, sa qualité nutritionnelle est grandement améliorée lorsqu'il est minéralisé en CO_2 puis réintégré par le phytoplancton des cours d'eaux de faible profondeur situés entre les chenaux de vidange et l'estuaire.

Le chapitre 6 s'intéresse au régime alimentaire des espèces les plus communes vivant dans le chenal de vidange étudié, au cours de la saison humide. Les résultats présentés s'appuient sur la composition en acides gras et isotopes stables du carbone et de l'azote de 16 organismes, et des sources de nourriture de base prélevés dans le chenal de vidange et dans la zone intertidale adjacente. L'identification des ressources alimentaires de chacune des espèces se base dans cette étude sur le principe d'assimilation à moindre coût énergétique des ressources nutritives. Ainsi, il est plus intéressant pour un organisme vivant de fixer dans ses tissus les composés assimilés avec le minimum de remaniement métabolique possible, conduisant au concept de « you are what you eat ». Ce principe a été vérifié et maintes fois utilisé à la fois pour les acides gras et pour les isotopes stables ($\delta^{13}C$ et $\delta^{15}N$**)**. Nous avons émis l'hypothèse que la matière organique particulaire, en partie composée de phytoplancton et constituant un compartiment de transfert entre les zones intérieures des mangroves et les écosystèmes côtiers, était une source de nourriture privilégiée pour de nombreuses espèces, de même que les feuilles d'arbres, dont l'abondance suggère que certaines espèces ont développé des adaptations permettant leur consommation. Les résultats révèlent que les espèces les plus mobiles (poissons et crevettes) se nourrissent essentiellement de matière organique particulaire ou d'animaux ayant consommé cette ressource, tandis que les feuilles d'arbres sont en effet une ressource importante, mais principalement consommées par des crabes et des escargots moins

capables de connecter par leurs déplacements les écosystèmes côtiers aux mangroves. Cependant, notre étude suggère que ces organismes agissent comme des minéralisateurs, libérant ainsi du CO_2 et des nutriments par la suite réintégrés par la production primaire du phytoplancton. Ainsi, cette réintégration par les microalgues constitue le lien trophique entre les espèces mobiles et prédatrices venant se nourrir dans la mangrove et le carbone fixé par les palétuviers et autres végétaux associés.

Enfin, le chapitre 7 explore la variabilité du régime alimentaire et du remaniement métabolique des acides gras d'espèces cible largement répandues dans la mangrove afin de mettre en évidence des différences liées à un éloignement depuis la côte océanique ou à des perturbations anthropiques. Les résultats présentés sont issus d'individus de 4 espèces macrobenthiques prélevés au niveau des 3 sites de l'estuaire bordés par la mangrove au cours des deux saisons d'échantillonnage, et complétés par ces mêmes espèces prélevées dans la zone du chenal de vidange au cours de la saison humide, considérée comme non impactée par les activités humaines. Le crabe *Metaplax elegans*, consommateur de microphytobenthos, présente des différences temporelles et spatiales significatives de sa composition en acides gras, notamment de l'abondance relative du 16:1ω7 qui est un biomarqueur de la présence dominante de diatomées dans le bol alimentaire. Cette abondance relative diminue avec le gradient de salinité, qui correspond aussi à un gradient de pression anthropique, et est corrélée à la diminution de productivité primaire benthique du sédiment de surface sur lequel vit l'espèce. Cette dernière pourrait être due à la dilution des apports de nutriments depuis l'amont au fur et à mesure du rapprochement vers l'océan. L'escargot *Chicoreus capucinus* présente des différences similaires malgré son régime de prédateur, et indique que les différences de régime alimentaire observées pour un consommateur primaire peuvent être transmises aux échelons trophiques supérieurs. Par ailleurs, les deux espèces présentent des différences de rapport du 20:5ω3/20:4ω6, deux acides gras précurseurs des défenses immunitaires. Ces différences montrent toutes deux un ratio plus bas (en faveur du 20:4ω6) dans la zone du chenal de vidange. Enfin, les espèces *Nerita balteata* et *Metapenaeus ensis*, respectivement consommatrices de feuilles d'arbres et de matière particulaire fraichement déposée, ne montrent pas de différence de leur composition en acides gras, ni selon la saison ni selon le site de prélèvement. Dans le cas de *Nerita balteata*, cette absence pourrait être due à la synthèse d'acides gras NMI (non-methylene-interrupted) conférant aux cellules une meilleure résistance aux processus

oxydatifs et aux lipases microbiennes que les acides gras polyinsaturés communs. Ainsi, certaines espèces semblent plus aptes à résister aux variations environnementales et aux pressions anthropiques, notamment grâce à des voies métaboliques spécifiques.

Chapter 5: Nutritional composition of suspended particulate matter in a tropical mangrove creek during a tidal cycle (Can Gio, Vietnam)

DAVID Frank, MARCHAND Cyril, TAILLARDAT Pierre, NGUYỄN THÀNH Nho and MEZIANE Tarik

Accepted for publication in Estuarine, Coastal and Shelf Science

1. Abstract

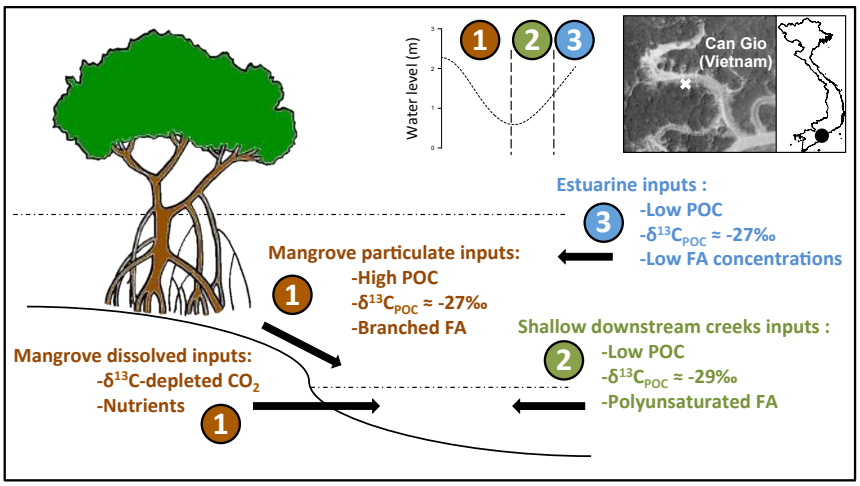

Mangrove forests are highly productive ecosystems and mangrove-derived organic matter has generally been assumed to play a basal role in sustaining coastal food webs. However, the mechanisms of mangrove-derived organic matter utilisation by consumers are not fully understood. In this study, we were interested in hourly changes in the nutritional quality of suspended particulate matter (SPM) entering and departing a mangrove creek during a tidal cycle. We determined the fatty acid composition and $\delta^{13}C$ stable isotope signature of SPM during a 26 h tidal cycle in a creek of the Can Gio Mangrove Biosphere Reserve (Southern Vietnam). Regarding fatty acids, the nutritional quality of SPM was low during most of the tidal cycle. However, it greatly increased during the first part of the strongest flood tide, occurring during daytime. The pulse of highly nutritive organic matter brought to the ecosystem was mostly composed of algal cells growing in specific shallow zones of the mangrove, that use nutrients and CO_2 exported during the preceding ebb tide and originating from the mineralisation of mangrove-derived organic matter, as evidenced by

their $\delta^{13}C$ signatures. This study confirms that mangrove-derived carbon plays a basal role in sustaining trophic webs of mangrove tidal creeks, but that its nutritive value is greatly enhanced when a first step of mineralisation is achieved and CO_2 is photosynthesised by algal cells.

2. Introduction

Mangrove forests are highly productive ecosystems and various authors have suggested that mangrove-derived organic matter (OM) via tidal export plays a significant role in carbon budgets along tropical and subtropical coastlines (Jennerjahn and Ittekkot 2002, Dittmar et al. 2006), as well as in sustaining trophic webs in coastal waters (Odum and Heald 1975, Lee 1995). Substantial amounts of suspended particulate matter (SPM), particulate organic carbon (POC) and dissolved inorganic carbon (DIC) are exported to tidal creeks and adjacent ecosystems during ebb tide, notably through tidal pumping which allows mangrove pore-water to circulate (Bouillon et al. 2007, Maher et al. 2013). OM sources in SPM have historically been traced using $\delta^{13}C$ stable isotope signature (Bouillon et al. 2008b), however little attention has been paid to the nutritional quality of SPM entering and departing mangrove ecosystems during a tidal cycle.

The processes allowing mangrove-derived OM utilisation by consumers is not fully understood, either in mangrove tidal creeks or in adjacent waters (Lee 1995, Bouillon et al. 2008b). While quantitative information on carbon flows is necessary to construct carbon budgets, evaluating the nutritional quality of the carbon associated with each of these flows is perhaps as important to evaluate its possible trophic assimilation (Canuel 2001). Fatty acids (FA) constitute only a small fraction of SPM but their contribution to trophic webs can be important nutritionally and they are organically traceable (Meziane and Tsuchiya 2000, Dalsgaard et al. 2003, Alfaro et al. 2006).

Within this context, our objective was to determine the evolution of the composition of SPM during a tidal cycle, using fatty acids and $\delta^{13}C$ stable isotope, in a mangrove creek located in the Can Gio Mangrove Biosphere Reserve (Southern Vietnam). We hypothesised that mangrove-derived OM was mainly exported during ebb tide, increasing the nutritional quality of SPM, while flood tide brings diluted water.

3. Materials and methods

3.1. Study site

We conducted our study during the monsoon season in 2015 (19-20 October) in a 1,400 m long mangrove tidal creek (10°30'24"N 106°52'57"E; Figure 5-1), located in the core zone of the Can Gio Mangrove Biosphere Reserve (UNESCO/MAB Project 2000). This creek does not receive any upstream freshwater inputs. Can Gio mangrove is formed by the deltaic confluence of the Saigon, Dong Nai and Vam Co Rivers, which drain into the South China Sea, and covers an area of 720 km^2. The tidal regime is semidiurnal and tidal amplitude was 2.1 m during our study, with maximum and minimum water levels of 2.8 m and 0.7 m, respectively. The tidal cycle of low amplitude occurred at night and will be referred to as the weak tide and that of high amplitude occurring during day will be referred to as the strong tide. The forest is largely dominated by the species *Rhizophora apiculata* and our study creek is bordered by a 30 m wide fringe hosting seaward species such as *Avicennia alba* and *Sonneratia alba*.

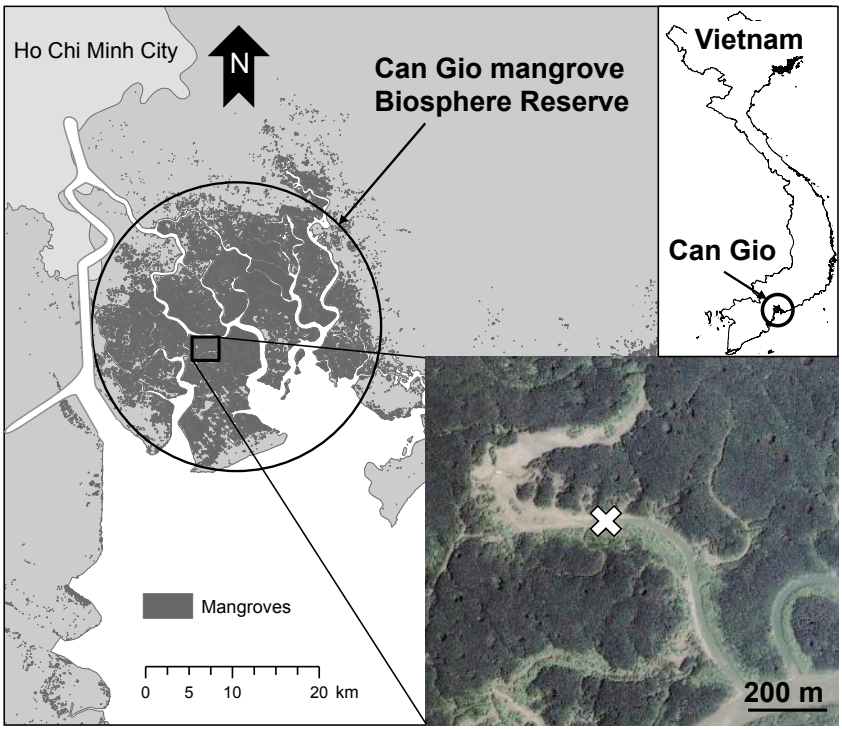

Figure 5-1: Map of the sampling site in Can Gio Mangrove Biosphere Reserve (Southern Vietnam). The white × on the aerial picture marks the spot where samples were taken

3.2. Data collection

We collected SPM during a 26 h asymmetric tidal cycle. Four samples of surface water were taken at two minutes interval every two hours (14 samplings; 56 samples) using a 10 L bucket. They were immediately vacuum-filtered through pre-combusted and pre-weighted glass fibre filters (Whatman® GF/F 0.7 µm) until clogging (requiring 250 mL to 1.2 L of water). They were freeze-dried and weighted for SPM determination. Then, one filter of SPM per sample was used for the analysis of fatty acids and two filters per sampling event were used for $\delta^{13}C$ and particulate organic carbon (POC) determination. Dissolved oxygen (DO) was measured continuously using a Hobo® data logger (HOBO U26-001) immersed 30 cm below water surface. Water depth was measured with a Plastimo® Echotest II depth sounder directed towards the creek bottom.

3.3. Sample processing

We extracted lipids following a slightly modified protocol of Bligh and Dyer (1959), as described in Meziane et al. (2007). Briefly, we quantified fatty acid methyl esters (FAME) using a GC-FID (Varian 3800-GC). Tricosanoic acid (23:0) was used as an internal standard. FA identification was performed using a GC-MS (Varian 450-GC; Varian 220-MS), and comparison of GC retention times with commercial standards (Supelco® 37 component FAME mix and marine source polyunsaturated FAME n°1 mix).

Isotopic analyses and POC determination were performed after filters fumigation for 16 h using HCl 37% to remove all carbonates. Analyses were done at the GEOTOP research centre, Université du Québec (Montréal, Canada). Unexpected $\delta^{13}C$ values were obtained, and thus another set of samples were analysed at the University of California Davis Stable Isotope Facility (Department of Plant Sciences, UC Davis, Davis, California). Results were similar to the first set of samples. Carbon stable isotope ratios were reported in parts per thousand (‰), using standard delta notation ($\delta^{13}C$) and POC concentrations were reported in mg L^{-1}.

4. Results and Discussion

4.1. FA biomarkers

A total of 51 FA were determined in the SPM of the mangrove tidal creek. Complete list of FA and absolute concentrations are provided in supplementary material (Appendix 5-1). Based on literature data, C_{18} polyunsaturated FA (PUFA), essentially 18:2ω6 and 18:3ω3, were attributed to mangrove-derived OM (Alfaro et al. 2006, Meziane et al. 2007). These biomarkers are also detected in high proportions in seagrasses (Kharlamenko et al. 2001, Alfaro et al. 2006, Dubois et al. 2014) and macroalgae (Nelson et al. 2002). However, such plants were not observed in any area of the Can Gio mangrove, indicating that the sum of C_{18} PUFA is a reliable biomarker for mangrove-derived OM in the present study. Regarding other sources, highly unsaturated FA (HUFA ≥ 20 carbons and 2 double bounds) were considered as good indicators of microalgae, phytoplankton or microphytobenthos (Canuel 2001, Dalsgaard et al. 2003). Such FA are absent from mangrove leaves (Meziane et al. 2007) and rapidly degraded in decaying material (Wakeham 1995). Their presence can thus be attributed to living algal cells. However, algal cells also synthesise other PUFA (C_{16} and C_{18}; Daalsgard et al. 2003) and the sum of PUFA rather than just HUFA has generally been used to trace fresh and nutritive algal OM (Canuel 2001). Branched FA (BrFA) are exclusively synthesised by bacteria (Kaneda 1991, Dalsgaard et al. 2003) and are found in high proportions in mangrove sediments (Meziane and Tsuchiya 2000, Aschenbroich et al. 2015). They were considered here as reliable biomarkers for sediment resuspension.

4.2. Dynamics of SPM during the weak tide

During the weak tide of the asymmetric cycle (between T0 and T18), SPM composition remained stable without any specific tidal variation. We measured low concentrations of SPM (45.5 ± 15.0 mg L^{-1}), POC (0.74 ± 0.33 mg L^{-1}) and FA (40.1 ± 13.6 µg L^{-1}), and $\delta^{13}C$ values were close to -27‰ (Table 5-1 and Figure 5-2). There have been very few studies on FA in mangrove creeks SPM and none are reporting absolute FA concentrations. Regarding other ecosystems, concentrations of FA were in the low range of the values obtained by Bodineau et al. (1998) in the macrotidal Seine estuary (France), and about 3 to 5 times lower than FA concentrations reported by Boëchat et al. (2014) in a large Brazilian tropical River. Regarding

its composition, the dominant contributions of FA 16:0 + 18:0 and FA 16:1 + 18:1 during this period (35.0% and 36.6%, respectively; Table 5-1) and the low PUFA contribution (5.9%; Table 5-1) indicate that the organic fraction of SPM was mainly constituted by highly degraded OM (Wakeham 1995). We thus suggest that during night and in the absence of strong tidal variations, the nutritional quality of SPM is relatively low and its role in supporting high trophic level and intermittent species in the Can Gio mangrove creek was most likely minor.

Table 5-1: Fatty acid composition of SPM during the 26 h tidal cycle in the Can Gio mangrove creek

Fatty acids (µg gSPM^{-1} (%) ± SD)	T0-T18 - Weak tide (n = 56)	T20 - Ebb tide (n = 4)	T22 - Low tide (n = 4)	T24 - Flood tide (n = 4)	T26 - High tide (n = 4)
∑ Branched FA	52.1 (5.7) ± 16.0	36.5 (6.3) ± 3.2	38.0 (7.1) ± 8.2	94.6 (3.6) ± 13.8	53.9 (4.9) ± 5.8
∑ 16:0 + 18:0 FA	321.3 (35.0) ± 107.9	181.4 (31.2) ± 29.4	186.6 (35.2) ± 35.1	882.1 (33.8) ± 160.7	415.3 (37.3) ± 51.9
∑ 16:1 + 18:1 FA	341.6 (36.6) ± 113.9	177.5 (30.7) ± 21.4	182.7 (34.4) ± 38.5	770.9 (29.6) ± 140.7	353.6 (31.9) ± 13.5
∑ PUFA	53.9 (5.9) ± 27.3	68.4 (11.7) ± 12.9	40.7 (7.5) ± 14.0	568.4 (21.8) ± 105.4	124.9 (11.3) ± 10.6
∑ C_{16} PUFA	11.3 (1.3) ± 7.1	21.3 (3.7) ± 2.7	12.5 (2.3) ± 3.6	140.2 (5.4) ± 29.8	28.4 (2.6) ± 2.6
∑ C_{18} PUFA	20.0 (2.1) ± 12.3	16.4 (2.8) ± 4.3	9.7 (1.8) ± 3.9	203.0 (7.8) ± 25.9	50.9 (4.6) ± 12.3
∑ HUFA	22.5 (2.5) ± 10.8	30.6 (5.3) ± 6.0	18.5 (3.4) ± 6.9	225.2 (8.6) ± 59.5	45.7 (4.1) ± 2.2
∑ Other FA	164.7 (16.8) ± 134.3	117.3 (20.1) ± 40.3	84.6 (15.8) ± 22.7	292.3 (11.3) ± 43.7	162.3 (14.6) ± 12.7
∑ FA (µg L^{-1})	40.1 ± 13.6	122.8 ± 18.1	131.8 ± 33.4	187.9 ± 34.9	44.0 ± 3.2
∑ FA (µg g^{-1})	933.7 ± 338.4	581.0 ± 77.2	532.6 ± 116.8	2608.3 ± 443.8	1109.9 ± 78.0

PUFA = Polyunsaturated fatty acids; HUFA = Highly unsaturated fatty acids

4.3. Dynamics of SPM during the strong ebb tide

During the strong ebb tide of the asymmetric cycle (between T18 and T22), the water level in the creek dropped sharply to a minimum of 0.6 m (Image 5-1a), compared to 1.8m during the weak ebb tide. As a result, SPM and POC concentrations significantly increased due to particle resuspension, either from mangrove soils or creek bottom, which is a general feature in mangrove tidal creeks (Bouillon et al., 2007). During the first part of the ebb tide, at T20, SPM mainly originated from mangrove soils erosion, with slight increases in HUFA, C_{18} PUFA and BrFA proportions (Table 5-1), which are typical of mangrove sediment samples and their associated microalgae (Meziane and Tsuchiya 2000, Aschenbroich et al. 2015). Both POC and the total FA concentrations per L of water were about 3 times above the values measured during the weak tide (from T0 to T18; Table 5-1, Figure 5-2b and Figure 5-2c), supporting our hypothesis that mangrove-derived OM is mainly exported during ebb tides.

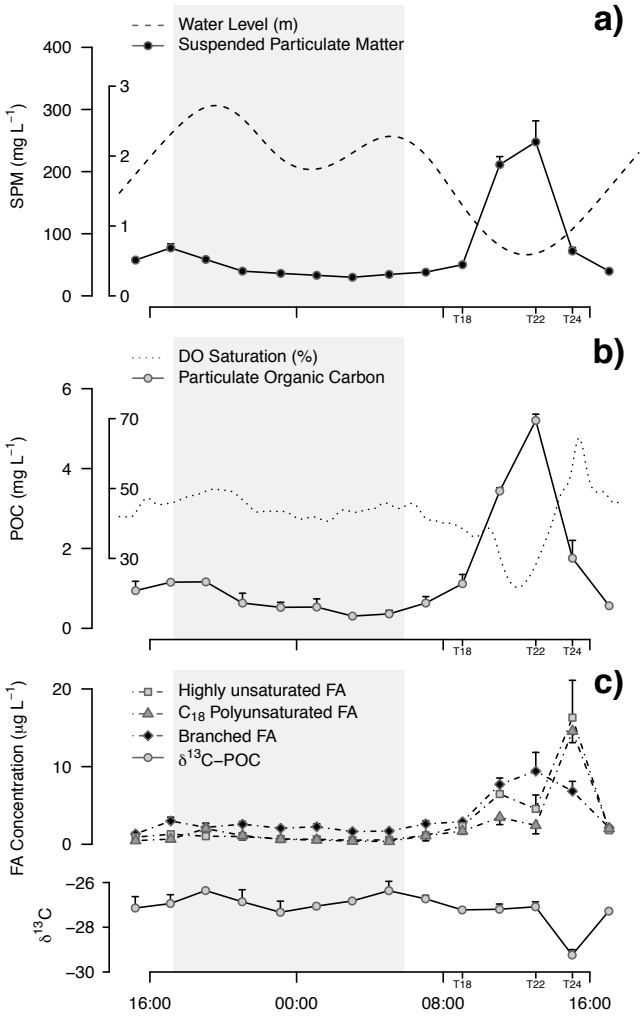

Figure 5-2: Dynamics of a) suspended particulate matter and water level b) particulate organic carbon and dissolved oxygen saturation and c) SPM fatty acids and $\delta^{13}C$ during the 26 h tidal cycle in the Can Gio mangrove creek. Grey shaded zones indicate night-time.
For SPM and FA n = 4 and for POC and $\delta^{13}C$ n = 2

The Can Gio mangrove is of type overwash forest, according to the classification of Odum et al. (1982), and the minimum water level to flood the tree roots was ~1.2 m relatively to the sampling point. Consequently, during the second part of the ebb tide, at T22, adjacent soils were completely emerged, and thus SPM originated mostly from the creek bottom (Image 5-1a). As a result, the nutritional quality of SPM dropped to its lowest with total FA concentrations of 532.6 ± 116.8 µg $gSPM^{-1}$. Conversely, BrFA proportions were at the maximum (7.1%; Table 5-1), confirming the sedimentary origin of SPM. Thus, our hypothesis of increased nutritional quality of SPM in the tidal creek during ebb due to the export of mangrove-derived particulate OM was invalidated.

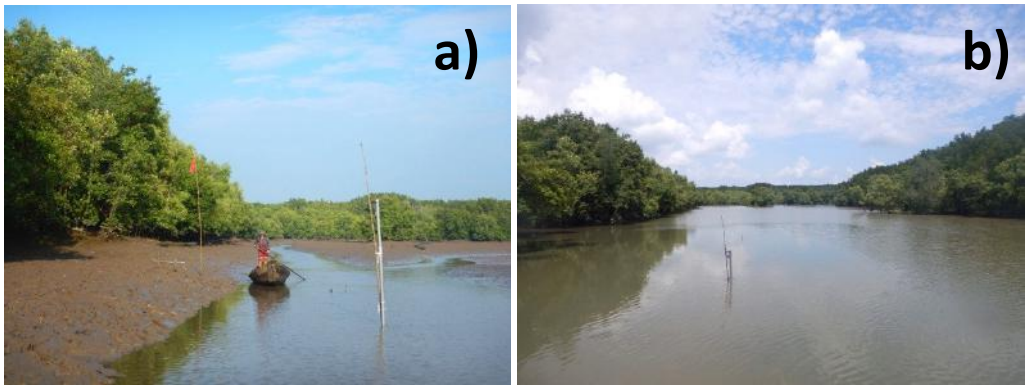

Image 5-1: Sampled tidal creek at a) low and b) high tide. Note the presence of the wood stick that may serve as a visual water level reference. Pictures from Pierre Taillardat.

4.4. Dynamics of SPM during the strong flood tide

During the strong flood tide of the asymmetric cycle (from T22 to T24), both FA composition and $\delta^{13}C$ of POC significantly varied, indicating a substantial change in SPM nutritional quality (Figure 5-2c). The PUFA proportions reached their maximum values at T24 (21.8%; Table 5-1), along with the maximum values of total FA concentrations (2,608.2 ± 443.8 µg $gSPM^{-1}$; Table 5-1), indicating a significant increase in SPM nutritional quality. This PUFA proportions remain much lower than the maximum values measured by Canuel (2001) during phytoplankton blooms in two temperate estuaries (~50%). On the contrary, PUFA concentrations in Can Gio (41.0 ± 7.6 µg L^{-1}; Figure 5-2c) were above the highest values Canuel (2001) measured in Chesapeake and San Francisco Bays during highly productive periods (~30 µg L^{-1}), and 8 to 10 times above values reported by Boëchat et al. (2014) in a Brazilian large tropical River. Total FA concentrations during the strong flood tide (187.9 ± 34.9 µg L^{-1}; Table 5-1) were higher than maximum values measured during the strong ebb tide (131.8 ± 33.4 µg L^{-1}; Table 5-1) and with higher nutritional quality. POC was mainly exported during the strong ebb tide (Figure 5-2b), as observed elsewhere (Bouillon et al. 2007, Maher et al. 2013), but we highlight here that the quality of OM exchanged in mangrove creeks and its possible inclusion in the food chain does not necessarily reflects its abundance. Changes in SPM nutritional quality may originate from organic matter inputs of different origins: mangrove-derived OM, phytoplankton or resuspended microphytobenthos. The $\delta^{13}C$ of POC dropped to -29.2‰ at T24, suggesting that decomposing mangrove leaves, with highly depleted $\delta^{13}C$ (Bouillon et al. 2008b), increasingly contributed to the POC pool during the strong flood tide (Figure 5-2c). We rather expected this $\delta^{13}C$ drop to occur during

ebb tide, when decomposing mangrove leaf particles are washed off by the water current. However, no $\delta^{13}C$ drop of SPM was observed at this period (Figure 5-2c). A substantial HUFA increase at T24 in SPM concomitant to a $\delta^{13}C$ drop could rather be caused by microalgae biomass during the strong flood tide. In addition, DO saturation reached 65% at T24, suggesting increased photosynthetic activity, which may include both phytoplankton and resuspended microphytobenthos, while it remained between 40 and 50 % during the weak flood tide (from T0 to T18; Figure 5-2b). Highly $\delta^{13}C$-depleted values were previously measured in phytoplankton sampled in tidal channels (down to -35.2‰; Cloern et al. 2002), but not in mangrove microphytobenthos, which $\delta^{13}C$ signature never drops under -25‰ and is usually ranging from -18 to -23‰ (Bouillon et al. 2008b, 2011). Consequently, we suggest that nutritional quality changes of SPM during strong flood tides were mostly related to living phytoplankton in the creeks.

This phytoplankton most likely uses nutrients brought by tidal pumping during the strong ebb tide. Mangrove pore water actually provides ideal conditions for phytoplankton growth, with high levels of nutrients and CO_2 (Tanaka and Choo 2000, Gleeson et al. 2013, Maher et al. 2015). Phytoplankton $\delta^{13}C$ in estuaries depends on the forms of carbon available (CO_2 or HCO_3^-), and its isotopic composition (Fogel et al. 1992). In experimental conditions, increasing levels of water CO_2 conducted to more depleted phytoplankton $\delta^{13}C$ compared to natural waters (Biswas et al. 2015). A carbon isotope fractionation of -30‰ relative to CO_2 was determined by in vitro experiment (Roeske and O'Leary 1984). In mangrove ecosystems, $\delta^{13}C$ of CO_2 can drop to -20‰ during ebb due to mangrove pore water inputs (Maher et al., 2015). It is thus not surprising to measure highly $\delta^{13}C$-depleted for phytoplankton having grown in exported mangrove pore waters. Since our mangrove creek was almost entirely flushed at low tide (T22; Image 5-1a), we suggest that the phytoplankton grew downstream our study site in larger channels fuelled by small creeks during the preceding ebb tide (T20 and T22), and was then brought back to the mangrove creek during the strong flood tide (T24; Image 5-1b).

During the second part of the strong flood tide, between T24 and T26, SPM and POC concentrations, FA composition and $\delta^{13}C$ of POC returned to values nearly similar to those measured during the weak tide (from T0 to T18; Figure 5-2). Tide was still rising at this moment and it was still the day (Image 5-1b). The steep decrease in FA concentrations at high tide (T26), especially PUFA, thus indicates that highly nutritive OM was brought to the creek

as a pulse. It was not related to algal cells brought from the ocean but rather from specific zones of the mangrove ecosystem receiving high loads of nutrients and CO_2 during strong ebb tides. These zones are most probably characterised by relatively shallow and clear waters allowing light penetration and thus phytoplankton blooming.

5. Conclusions

Our study highlights the influence of tides on the nutritional quality of SPM in a tropical mangrove tidal creek. The highest load of POC was exported from the creek during ebb tide, as previously observed in other mangrove ecosystems (Bouillon et al. 2007, Maher et al. 2013). However, this mangrove-derived organic matter was of poor nutritional quality. On the contrary, OM entering the tidal creek during the first part of the flood was of high nutritional quality and might provide a pulse to the mangrove ecosystem once it has reached the forest floor. The algal cells that mostly constitute this highly nutritive OM is suggested to have grown using nutrients and CO_2 provided by the tidal pumping of mangrove pore water, and thus originating from the mineralisation of mangrove-derived OM. Further studies would however need to be conducted to evaluate how variable can be this phenomenon across days, season, tidal range and sampling location. In addition, the fate of this nutritionally rich OM in the mangrove ecosystem remains to be understood. Our results are consistent with the hypothesis of Odum and Heald (1975) that mangrove-derived carbon plays a basal role in sustaining trophic webs of mangrove tidal creeks and coastal ecosystems, but after a first step of carbon mineralisation, that could be achieved by the microbial loop (Azam 1998) and by leaf shredders such as sesarmid crabs (Lee 1995, Ólafsson et al. 2002, Werry and Lee 2005). We suggest that this carbon mineralisation is a key step to explain how OM of originally poor nutritional quality (i.e. mangrove leaves) can maintain a high animal biodiversity in mangrove ecosystems.

Chapter 6: Trophic relationships and basal resources utilisation in the Can Gio Mangrove Biosphere Reserve (Southern Vietnam)

DAVID Frank, MARCHAND Cyril, TAILLARDAT Pierre, NGUYỄN THÀNH Nho, TRUONG VAN Vinh and MEZIANE Tarik

Submitted for publication in Journal of Sea Research

1. Abstract

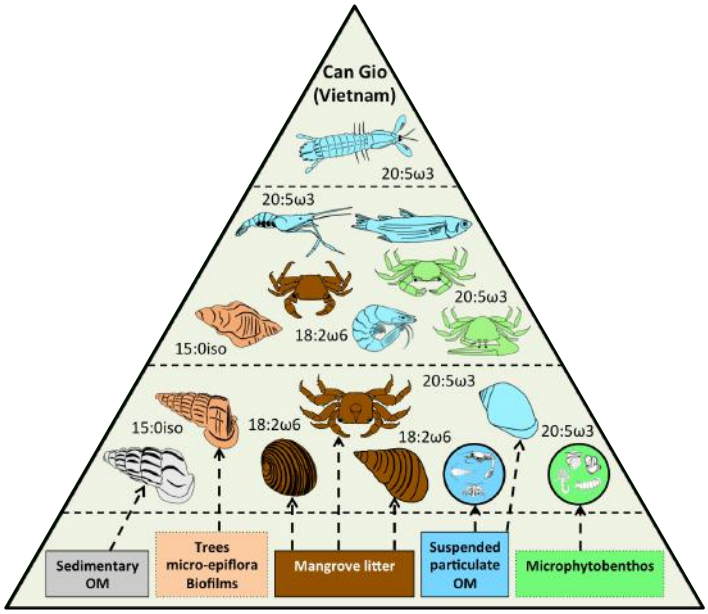

Fatty acid biomarkers and dual stable isotopes ($\delta^{13}C$ and $\delta^{15}N$) were used to identify the preferred food sources of consumers in a mangrove tidal creek and nearby unforested (mud bank) and forested areas located in the Can Gio Mangrove Biosphere Reserve (Southern Vietnam). We analysed 15 macro-invertebrates and 1 fish species representing the basal resources' consumers and their immediate predators in this area. Specific groups of fatty acids were used to trace the fate of these resources in the food web (i.e., suspended particulate organic matter, mangrove litter and sedimentary organic matter). The $\delta^{13}C$ and $\delta^{15}N$ of consumers ranged from -26.9 to -18.8‰ and from 1.1 to 9.9‰, respectively.

The trophic pathway based on mangrove litter, characteristic of mangrove ecosystems, is nutritionally sustaining various crab and snail species, whereas it appears that the most mobile species, fish and shrimps, are mostly feeding on suspended particulate

organic matter, suggesting that this trophic pathway is of great importance for connectivity among ecosystems. Our study suggests that ecosystem engineers, mostly snails and crabs, mainly act as mineralisers, processing high quantities of detrital material to meet their nutritional needs and thus releasing nutrients. Meanwhile, autochthonous phytoplankton feeds mobile species and links mangrove litter and nutrients to coastal food webs.

2. Introduction

Despite numerous studies on macrofauna diet in mangrove forests (Rodelli et al., 1984; Abrantes and Sheaves, 2009; Nordhaus et al., 2011; Tue et al., 2012), the role of faunal species on organic matter (OM) cycling in mangrove ecosystems still remains not fully understood (Sousa and Dangremond, 2011), notably with regard to the contribution of mangrove litter (i.e. senescent leaves, propagules, stems, flowers, etc.) to coastal food webs (Claudino et al., 2015; Abrantes et al. 2015). Since, measuring the ability of mangrove soils to store OM and determining the balance between forest production and exports is a key issue in mangrove carbon budget studies (Bouillon et al., 2008b; Alongi, 2014), it is therefore crucial to explore the role of faunal communities on the processing and/or the export of OM between mangroves and adjacent ecosystems. Early studies by Odum and Heald (1975) lead to a schematic representation of mangrove food webs emphasizing the basal role of leaf litter. The flow of energy was assumed to go from leaf litter to predators through bacterial and fungal conditioning and detritus consumers. This model was later enlarged to include the inputs of phytoplankton, benthic algae, roots epiphytes and seagrasses (Odum et al., 1982).

Later, Robertson and Blaber (1992) hypothesised that phytoplankton production plays an important role in supporting temporary and high trophic level species in estuarine mangrove ecosystems. Stable isotope studies confirmed this hypothesis and showed that various organisms, including shrimps (Dittel et al., 1997; Willems et al., 2016), gastropods (Bouillon et al., 2002) and fiddler crabs (France, 1998; Vermeiren et al., 2015) derive their carbon and nitrogen from phytoplankton and/or benthic algae to a much greater extent than from mangrove detritus. Meanwhile, the use of lipid biomarkers (i.e. fatty acids), which can clarify trophic web relationships in aquatic environments (Meziane and Tsuchiya, 2000; Dalsgaard et al., 2003; Kelly and Scheibling, 2012), was able to trace phytoplankton in estuarine food chains through abundance of the highly unsaturated FA (HUFA ≥ 20 carbons

and 2 double bounds) 20:5ω3 and 22:6ω3 (Alfaro et al., 2006), to measure mangrove litter contribution using the C_{18} polyunsaturated FA (C_{18} PUFA) 18:2ω6 and 18:3ω3 (Hall et al., 2006) and to highlight the importance of bacteria in the diet of shrimp post-larvae, gastropods and fiddler crabs using relative proportion of odd-branched FA (iso and anteiso, BrFA) in consumer tissues (Meziane and Tsuchiya, 2000; Gatune et al., 2014).

Both stable isotope and FA biomarker tools are based on the assumption that the composition of organism tissues reflects the food they assimilate, but each has its own limitations. On one hand, tracing consumers diet using stable isotope analysis requires non-overlapping signatures of available food sources (Bouillon et al., 2008b) and a good knowledge of the trophic enrichment factor, which corresponds to the isotopic shift of a consumer relative to its diet but may be highly variable among both organisms and food sources (Vanderklift and Ponsard, 2003; Bui and Lee, 2014). It also requires an exhaustive sampling of potential food sources while some food sources that may be difficult or impossible to sample have shown to play important roles in mangroves ecosystems, such as surface biofilms (Lee et al., 2001), trees micro-epiflora (Bouillon et al., 2004; Alfaro 2008) or leaf-shredder faeces (Camilleri, 1992; Werry and Lee, 2005). On the other hand, FA are rarely produced by only one group of organisms, and relative proportions rather than absolute abundances might be considered. FA composition of consumers depends on the metabolic processing of absorbed FA, including deposition in adipose tissue without modification, specific transformations between absorption and deposition and *de novo* synthesis in the consumer, which may vary among taxonomic groups (Budge et al., 2006). Combination of stable isotope signatures and FA biomarkers has the promising ability to refine our understanding of trophic web relationships in mangrove ecosystems (Bouillon et al., 2008b; Vermeiren et al., 2015), as previously done in temperate seagrasses (Kharlamenko et al., 2001; Alfaro et al., 2006; Dubois et al., 2014).

Our study aims to identify the role of 16 abundant animal species on OM cycling in a mangrove tidal creek and nearby unforested (mud bank) and forested areas located in the Can Gio Mangrove Biosphere Reserve (Southern Vietnam). We hypothesised that phytoplankton inputs play a substantial role in supporting the basal food chain in this tropical mangrove ecosystem, thus reinforcing the hypothesis of Robertson and Blaber (1992). Our study combines FA biomarkers and stable isotopes ($\delta^{13}C$ and $\delta^{15}N$) to refine organisms' diet and to understand the patterns of basal resources utilisation in this tropical mangrove.

3. Materials and methods

3.1. Study site

The study was conducted during the monsoon season in 2015 (19-20 October) in a 1.4 km long mangrove tidal creek (10°30'24"N 106°52'57E; Figure 6-1). The mangrove creek is located in the core zone of the Can Gio Mangrove Biosphere Reserve (UNESCO/MAB Project, 2000) and receives no freshwater upstream input. The mangrove is formed by the deltaic confluence of the Saigon, Dong Nai and Vam Co Rivers, which drain into the South China Sea. It covers an area of 720 km^2 (Nam et al., 2014). The forest is largely dominated by the species *Rhizophora apiculata*, massively replanted after Vietnam War conflict (1955-1975) and our study creek is bordered by a 30 m wide fringe hosting seaward species such as *Avicennia alba* and *Sonneratia alba*. Water salinity ranged from 16 to 23 during our study and tidal amplitude was 2.1 m, with maximum and minimum water levels of 2.8 m and 0.7 m, respectively.

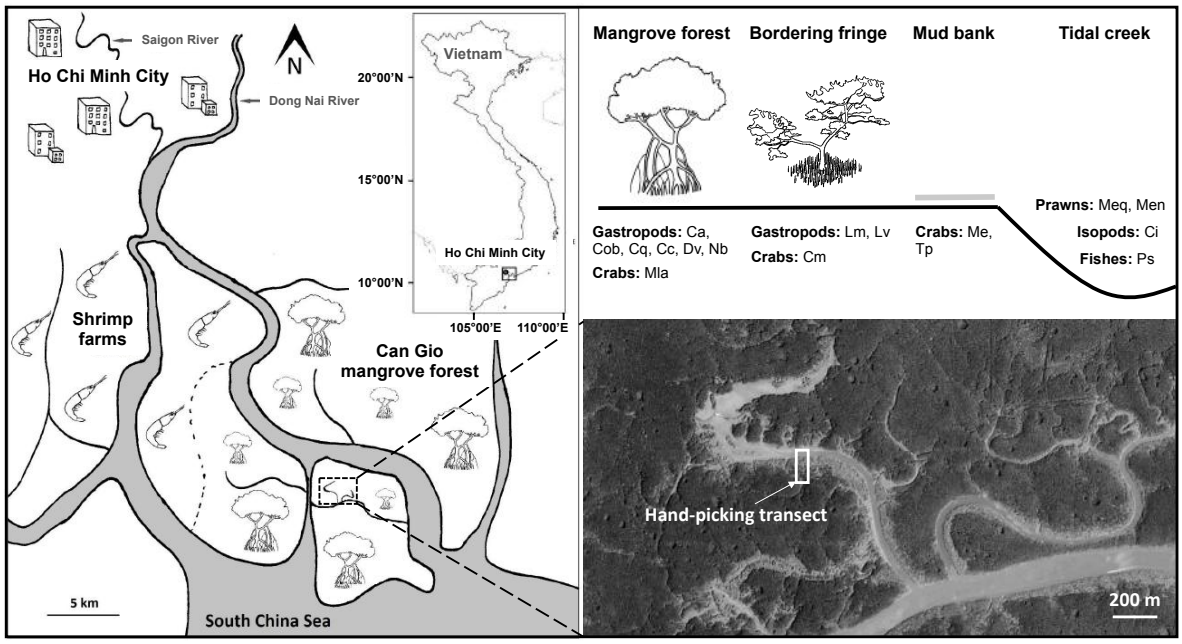

Figure 6-1: Sampling site in the mangrove tidal creek of the Can Gio Mangrove Biosphere Reserve (Southern Vietnam). Habitats and animal samples are placed on the transect schema. Acronyms are similar to those of Tue et al. (2012) when the same species were sampled.

Ca = *Cassidula aurisfelis*; Cc = *Chicoreus capucinus*; Cm = *Clistocoeloma merguiense*; Ci = *Cloridopsis immaculata*; Cob = *Cerithidea obtusa*; Cq = *Cerithidea quoyii*; Dv = *Neripteron (Dostia) violaceum*; Lm = *Littoraria melanostoma*; Lv = *Littoraria vespacea*; Me = *Metaplax elegans*; Men = *Metapenaeus ensis*; Meq = *Macrobrachium equidens*; Mla = *Metopograpsus latifrons*; Nb = *Nerita balteata*; Tp = *Tubuca (Uca) paradussumieri*; Ps = *Planiliza sp. B*

3.2. Sample collection

Flora, fauna and sediments were collected during low tide in four replicates/species-samples along a transect perpendicular to the mangrove tidal creek (Figure 6-1). Freshly fallen tree leaves, crabs and gastropods were hand-picked, while local fishermen caught for us fishes, prawns and stomatopods using fishing nets. We collected 16 animal species (Image 6-1) that are mainly the most abundant in the mangrove creek and are widely distributed in South East Asian mangroves (Rodelli et al., 1984; Tan, 2008; Nordhaus et al., 2011; Tue et al., 2012; Diele et al., 2013). We considered that they were representative of the basal resources consumers and their immediate predators in the mangroves of this region. Sediment cores (1 cm depth × 2 cm Ø) were randomly sampled in the three vegetation zones: *Rhizophora*, *Avicennia* and mudflat. Microphytobenthos could not be isolated from sediments and was not analysed. Suspended particulate organic matter (SPOM) was monitored during a 26 h asymmetric neap tidal cycle. Surface water was taken every two hours (14 samplings) and immediately vacuum-filtered through pre-combusted and pre-weighted glass fibre filters (Whatman® GF/F 0.7 µm) until clogging (requiring 250 mL to 1.2 L of water). All samples were kept on ice during sampling and stored at -25°C until analysis.

3.3. Sample processing and analysis

Animal species were measured and then identified by taxonomists from the Muséum National d'Histoire Naturelle (MNHN, Paris, France) and from other institutions (see acknowledgments). The collected material were freeze-dried and powdered before fatty acids and stable isotopes were analysed. Individual samples consisted in one sediment core or one SPOM filter or one tree leave or one animal. For crab species, we analysed muscles from the claw, for shrimp species we used muscles from the abdomen and for the fish we took white muscles from the flank. Tissues of gastropods could not be isolated. The entire organism was removed from its shell, tissues were homogenised and the pooled material was used. Four samples were analysed for each species and food source, except for the less frequent species *Cassidula aurisfelis* and *Cloridopsis immaculata* for those only 2 and 3 individuals could be sampled, respectively.

We extracted lipids following a slightly modified protocol of Bligh and Dyer (1959), as described in Meziane and Tsuchiya (2000) and using 100 mg of dry material for tree leave, 30 mg for animal tissue (except for the small species *Littoraria vespacea* and *Metaplax elegans* for those down to 5 mg was used), 1 g for sediments and 20 to 70 mg of suspended matter for SPOM (corresponding to the weight difference between pre-weighted filter and freeze-dried filter after sampling). Tricosanoic acid (23:0) was used as an internal standard to measure the absolute samples FA concentration. We quantified fatty acid methyl esters (FAME) by gas chromatography analysis (Varian 3800-GC), using a flame ionisation detector. Identification of fatty acids was performed using coupled gas chromatography mass spectrometry (Varian 450-GC; Varian 220-MS), and comparison of GC retention times with commercial standards (Supelco® 37 component FAME mix and marine source polyunsaturated FAME n°1 mix). We reported values as % of total FA or absolute concentrations (µg g^{-1} or mg g^{-1}).

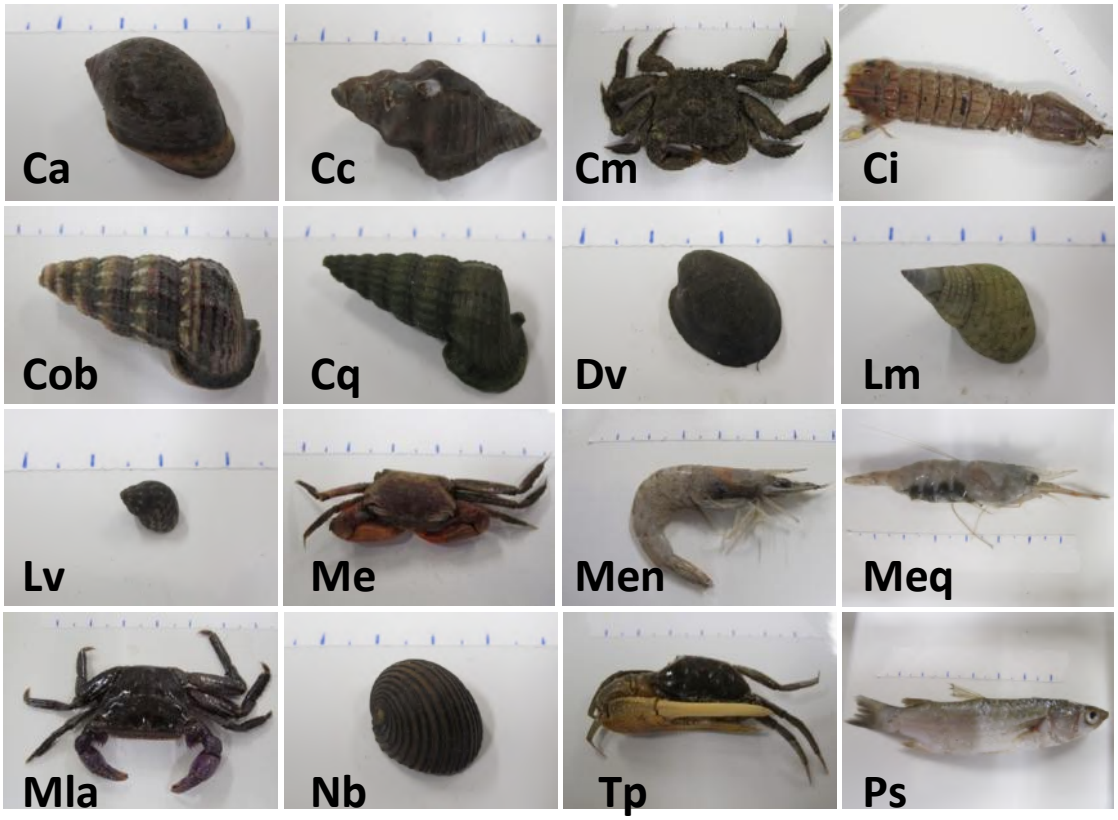

Image 6-1: Organisms sampled in the tidal creek and nearby areas of the Can Gio Mangrove Biosphere Reserve. The space between the thick lines represents 1 cm and the fine line 0.5 cm.
Ca = *Cassidula aurisfelis*; Cc = *Chicoreus capucinus*; Cm = *Clistocoeloma merguiense*; Ci = *Cloridopsis immaculata*; Cob = *Cerithidea obtusa*; Cq = *Cerithidea quoyii*; Dv = *Neripteron (Dostia) violaceum*; Lm = *Littoraria melanostoma*; Lv = *Littoraria vespacea*; Me = *Metaplax elegans*; Men = *Metapenaeus ensis*; Meq = *Macrobrachium equidens*; Mla = *Metopograpsus latifrons*; Nb = *Nerita balteata*; Tp = *Tubuca (Uca) paradussumieri*; Ps = *Planiliza sp. B*

We performed isotopic analyses on the same samples that were powdered for lipid extractions, except for SPOM analyses for which a whole filter was used. Flora and fauna samples were prepared without pre-treatment, while sediment and SPOM samples were fumigated for 16h using HCl 37% to remove all carbonates. All samples were prepared in tin capsules. Stable isotopes were analysed at the University of California Davis Stable Isotope Facility (Department of Plant Sciences, UC Davis, Davis, California) using a Vario EL Cube elemental analyser interfaced to a PDZ Europa 20–20 isotope ratio mass spectrometer. Carbon and nitrogen stable isotope ratios were reported in parts per thousand (‰), using standard delta notation ($\delta^{13}C$ and $\delta^{15}N$), and are relative to Vienna PeeDee Belemnite and atmospheric air, respectively.

3.4. Data analysis

The isotopic signatures of potential food sources overlapped each other, and thus we could not appropriately estimate sources contribution to the animals' diet using Bayesian mixing models such as SIAR or MixSIR. Stable isotope results were interpreted individually for each species, taking into account available literature on species and their supposed food sources. Trophic level of animals was determined according to their $\delta^{15}N$ signature, assuming a $\Delta\delta^{15}N \sim 2.8‰$ between trophic level (Vanderklift and Ponsard, 2003) and corrected using conclusions from diets analysis.

We visualised the underlying structure of both food sources and consumers fatty acid profiles using non-standardised principal component analysis (PCA) on relative contribution data matrices. The number of replicates per species-samples (n = 4) was enough to highlight meaningful significant differences among species taking into account natural intraspecific variability in both food sources and consumers. An initial data square root transformation was performed to alleviate variance heteroscedasticity (Legendre and Gallagher, 2001). Principal components were calculated using the whole fatty acid profiles, and relevant indicators were posteriorly positioned as supplementary rows. All statistical analyses and graphical representations were performed using R 3.3.2 (R Core Team 2017).

4. Results

4.1. Stable isotope compositions

The potential food sources' $\delta^{13}C$ ranged from -33.9 to -26.1‰ (Figure 6-2). Mangrove leaves of the species *Rhizophora apiculata* exhibited the lowest average $\delta^{13}C$ (-31.1 ± 2.0‰) and bordering fringe sediment exhibited the highest average $\delta^{13}C$ (-26.7 ± 0.1‰), while other food sources were encompassed between these two extremum (Table 6-1). Potential food sources' $\delta^{15}N$ ranged between 1.4 and 5.0‰ and the three groups of food sources (i.e. SPOM, mangrove leaves and sediments) greatly overlapped each other (Table 6-1 and Figure 6-2).

Table 6-1: Isotopic values ($\delta^{13}C$ and $\delta^{15}N$ in ‰) of the food web components in the Can Gio mangrove tidal creek and nearby areas. Sizes refer to total length for gastropods, prawns, isopods and fishes, and carapace width for crabs.

Food webs components	Acronym	Size (mm)	$\delta^{13}C$ Mean ± SD	$\delta^{15}N$ Mean ± SD	n
Sources					
Sediments	Sed				
Mud bank	Mub	-	-26.8 ± 0.1	3.8 ± 0.0	4
Bordering fringe	Bof	-	-26.7 ± 0.1	4.0 ± 0.1	4
Mangrove forest	Maf	-	-28.6 ± 0.3	3.4 ± 0.1	4
Mangrove leaves	Mang				
Avicennia alba	Ava	-	-27.6 ± 1.1	3.7 ± 1.2	4
Sonneratia alba	Soa	-	-29.5 ± 0.5	4.5 ± 0.5	4
Rhizophora apiculata	Rha	-	-31.1 ± 2.0	4.8 ± 0.1	4
Suspended Particulate Organic Matter	SPOM	-	-27.1 ± 0.7	4.6 ± 0.9	14
Consumers					
Gastropods					
Cassidula aurisfelis	Ca	20-25	-26.9 ± 0.1	4.8 ± 0.3	2
Cerithidea obtusa	Cob	45-60	-25.9 ± 0.5	6.0 ± 0.5	4
Cerithidea quoyii	Cq	40-55	-25.5 ± 0.4	1.1 ± 0.7	4
Chicoreus capucinus	Cc	25-40	-23.1 ± 0.3	7.8 ± 0.6	4
Littoraria melanostoma	Lm	16-20	-25.2 ± 1.2	1.8 ± 1.1	4
Littoraria vespacea	Lv	7-11	-22.7 ± 1.1	2.8 ± 1.0	4
Neripteron (Dostia) violaceum	Dv	12-18	-23.2 ± 0.1	4.4 ± 1.0	4
Nerita balteata	Nb	15-20	-23.3 ± 0.4	4.0 ± 0.9	4
Crabs					
Clistocoeloma merguiense	Cm	30-35	-26.1 ± 0.1	6.5 ± 0.3	4
Metaplax elegans	Me	13-20	-20.1 ± 0.9	7.8 ± 0.4	4
Metopograpsus latifrons	Mla	25-35	-23.3 ± 0.6	5.3 ± 2.0	4
Tubuca (Uca) paradussumieri	Tp	35-45	-18.8 ± 1.4	8.0 ± 0.3	4
Prawns					
Macrobrachium equidens	Meq	55-65	-25.7 ± 0.8	8.1 ± 0.4	4
Metapenaeus ensis	Men	50-65	-26.7 ± 1.3	7.8 ± 0.6	4
Isopods					
Cloridopsis immaculata	Ci	80-100	-23.2 ± 0.5	9.9 ± 0.7	3
Fishes					
Planiliza sp. B	Ps	80-110	-21.6 ± 0.7	9.3 ± 0.4	4

The average consumers' $\delta^{13}C$ ranged from -26.9 to -18.8‰ (Table 6-1 and Figure 6-2). Lowest $\delta^{13}C$ values were found in the pulmonate snail *Cassidula aurisfelis* (-26.9 ± 0.1‰) and highest values were measured in the ocypodid crab *Tubuca paradussumieri* (-18.8 ± 1.4‰). The average consumers' $\delta^{15}N$ ranged from 1.1 to 9.9‰ (Table 6-1 and Figure 6-2). Lowest $\delta^{15}N$ were measured in the potamid snail *Cerithidae quoyii* (1.1 ± 0.7‰) and highest values were found in the stomatopod *Cloridopsis immaculata* (9.9 ± 0.7‰). Among snail species, the mangrove murex snail *Chicoreus capucinus* exhibited the highest $\delta^{15}N$ (7.8 ± 0.6‰). The sesarmid crab *Metopograpsus latifrons* exhibited the highest intra-specific $\delta^{15}N$ variability (Figure 6-2), with values ranging from 3.4 to 8.1‰.

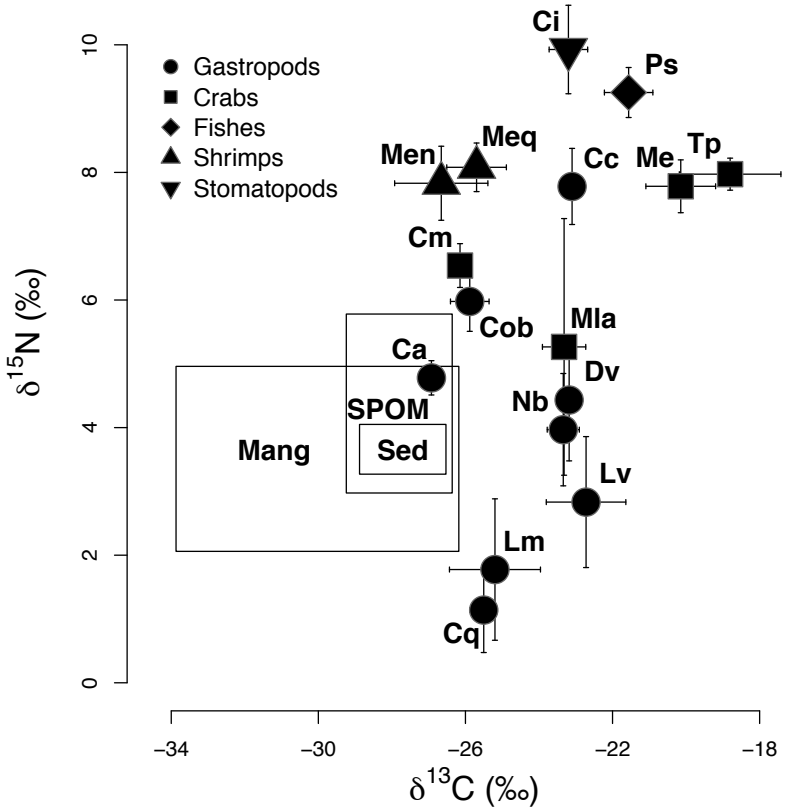

Figure 6-2: Isotopic signatures ($\delta^{13}C$ and $\delta^{15}N$) of the food web components in the Can Gio mangrove tidal creek and nearby areas. Boxes correspond to the range of potential food sources. Consumer symbols represent averaged data (± SD). Acronyms are fully displayed in Table 1

4.2. Fatty acid composition of potential food sources

A total of 51 FA were identified in the basal food resources (i.e. SPOM, mangrove leaves and sediments). Absolute concentrations of FA are provided in Appendix 6-1. Mangrove leaves contained higher concentrations of total FA than sediments and SPOM, but they did not contain C_{16} polyunsaturated FA and highly unsaturated FA (C_{16} PUFA and HUFA; Table 6-2). The PCA revealed strong dissimilarities between the three sources sampled, with high C_{18} PUFA values correlated to the 1st axis and high values of branched FA (BrFA) correlated to the 2nd axis (Figure 6-3). Dominant FA in mangrove leaves were C_{18} PUFA (Table 6-2 and Figure 6-3). Sediments were characterised by low FA concentrations, but proportions highlighted substantial relative abundance of BrFA (Figure 6-3). SPOM was dominated by C_{16} and C_{18} saturated (C_{16} + C_{18} SFA) and monounsaturated FA (C_{16} + C_{18} MUFA), and contained the highest HUFA concentration (Table 6-2). Concentration of FA substantially changed during the tidal cycle (see Chapter 5) but relative proportions remained relatively similar and well differentiated from other food sources (Figure 6-3).

Table 6-2: Fatty acid composition in µg g^{-1} (%) ± SD of potential food sources in the Can Gio mangrove tidal creek and nearby areas

Fatty acids (µg g^{-1} (%) ± SD)	Suspended matter (n = 56)	Sedimentary OM (n = 12)	Mangrove leaves (n = 12)
∑ Branched FA	53.2 (5.7) ± 19.0	44.9 (24.0) ± 17.9	-
∑ 16:0 + 18:0 FA	348.5 (34.8) ± 188.2	45.2 (25.0) ± 11.9	3048.0 (36.0) ± 534.2
∑ 16:1 + 18:1 FA	350.1 (35.2) ± 165.9	33.8 (19.0) ± 7.2	634.7 (7.4) ± 175.0
∑ C_{16} PUFA	22.6 (1.9) ± 34.6	1.2 (0.7) ± 0.2	-
∑ C_{18} PUFA	34.3 (2.7) ± 49.6	3.2 (1.7) ± 1.6	3732.4 (43.7) ± 773.8
∑ HUFA	38.9 (3.3) ± 55.1	3.1 (1.8) ± 0.7	-
∑ Other FA	164.5 (16.4) ± 121.8	52.2 (27.7) ± 21.9	1075.6 (12.8) ± 204.5
∑ FA (µg L^{-1})	63.4 ± 49.2	-	-
∑ FA (µg g^{-1})	1012.1 ± 560.4	183.6 ± 59.3	8489.7 ± 1484.1

PUFA = Polyunsaturated FA; HUFA = Highly unsaturated FA

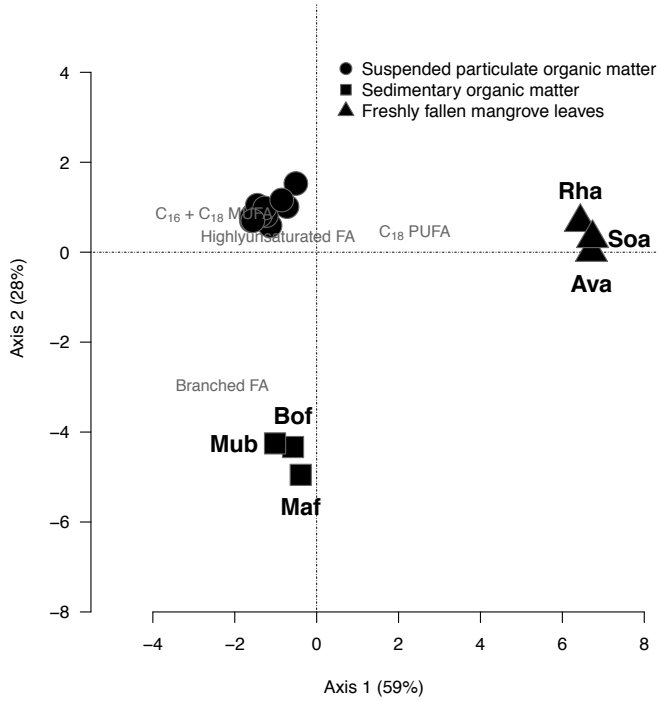

Figure 6-3: Mean score of potential food sources on the two first axes of principal component analysis (SD were smaller than symbols size). Texts in grey represent the position of FA biomarkers on the axis. Acronyms are fully displayed in Table 1

4.3. Fatty acid composition of consumers

A total of 59 FA were found in the fauna samples of the Can Gio mangrove creek and nearby areas. Relative proportions of FA are provided in Appendices 6-2 and 6-3. We detected strong differences between the FA profiles of organisms analysed whole (gastropods) and those analysed only as muscle tissues. Gastropod tissues exhibited fatty acids that are barely detected in other organisms (e.g. 20:1ω9, 22:2ω9, 22:2ω6), while they displayed low proportions of ω3 HUFA (e.g. 20:5ω3, 22:6ω3; see Appendices 6-2 and 6-3 for details). The exploration of such differences and whether they are due to the mixing of tissues or to taxonomic specificities goes beyond the objectives of our study and thus, organisms analysed whole (gastropods) were considered separately from others. For both groups, the PCA revealed dissimilarities between species, with opposite trends of C_{18} PUFA and HUFA, correlated with the 1st axis, and similar trends of BrFA and C_{16} + C_{18} MUFA, correlated to the 2nd axis (Figure 6-4).

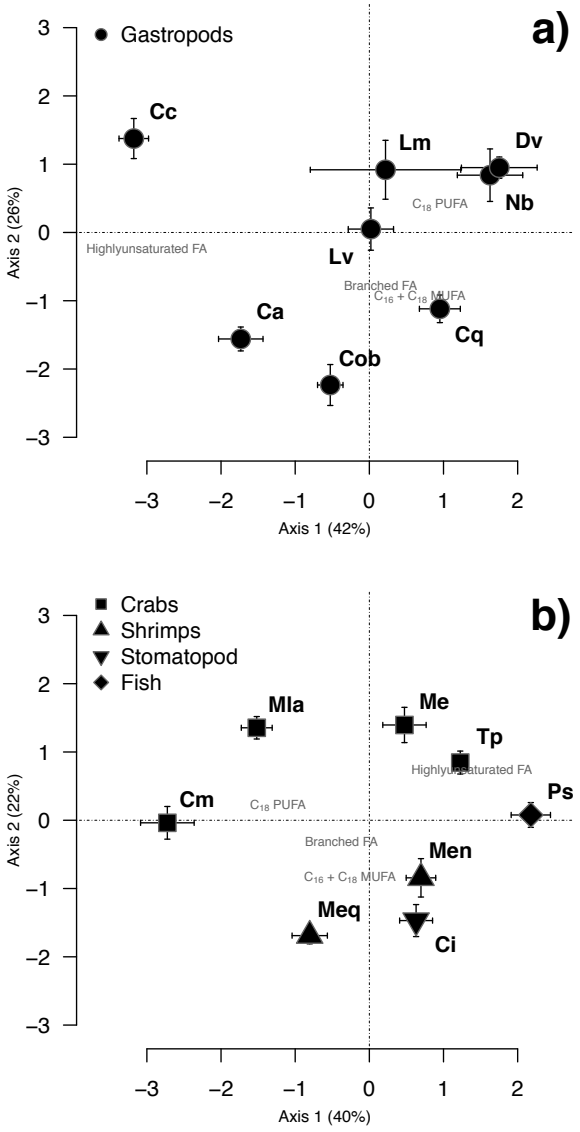

Figure 6-4: Mean score of a) gastropod and b) crustacean and fish species on the two first axes of principal component analysis (± SD). Text in grey represents position of FA biomarkers on the axis. Acronyms are fully displayed in Table 1

Gastropod analysis showed high HUFA proportions in *Chicoreus capucinus* tissues compared to other species, while littorinid and neritid snails exhibited high C_{18} PUFA relative abundances. Potamids and the species *Cassidula aurisfelis* exhibited high BrFA and C_{16} + C_{18} MUFA proportions (Table 6-3 and Figure 6-4a). In other consumers' analysis, high HUFA proportions were measured in the sesarmid crab *Metaplax elegans*, the ocypodid crab *Tubuca paradussumieri* and the mullet *Planiliza sp. B*, while the grapsid crab *Metopograpsus latifrons* and the sesarmid crab *Clistocoeloma merguiense* exhibited high C_{18} PUFA proportions. Prawns and the stomatopod *Cloridopsis immaculata* showed high relative abundances of branched FA and C_{16} + C_{18} MUFA (Table 6-3 and Figure 6-4b).

Table 6-3: Fatty acid composition (%) of consumers in the Can Gio mangrove tidal creek and nearby areas

Fatty acids (%)	Cassidula aurisfelis (n = 2)	Cerithidea obtusa (n = 4)	Cerithidea quoyii (n = 4)	Chicoreus capucinus (n = 4)	Littoraria melanostoma (n = 4)	Littoraria vespacea (n = 4)	Neripteron violaceum (n = 4)	Nerita balteata (n = 4)
∑ Branched FA	5.3 ± 1.5	6.1 ± 0.2	4.9 ± 0.4	2.4 ± 1.4	3.1 ± 0.6	2.2 ± 0.4	3.2 ± 0.5	3.4 ± 0.2
∑ 16:0 + 18:0 FA	22.3 ± 0.7	29.0 ± 1.3	31.8 ± 2.8	17.4 ± 1.3	28.5 ± 3.3	27.2 ± 4.5	25.0 ± 1.1	24.5 ± 0.9
∑ 16:1 + 18:1 FA	14.7 ± 0.2	18.0 ± 2.2	16.9 ± 1.5	6.2 ± 1.9	12.0 ± 3.0	10.4 ± 1.2	14.8 ± 0.8	15.8 ± 2.6
∑ 20:1 + 22:1 FA	6.3 ± 0.3	5.0 ± 0.3	5.5 ± 0.8	10.9 ± 0.6	6.1 ± 0.2	6.1 ± 1.2	7.1 ± 0.4	6.6 ± 1.0
∑ C16 PUFA	0.3 ± 0.1	0.4 ± 0.1	1.3 ± 0.3	0.3 ± 0.0	1.1 ± 0.4	1.5 ± 0.6	2.8 ± 0.8	2.5 ± 0.4
∑ C18 PUFA	4.9 ± 0.2	4.7 ± 0.4	10.0 ± 1.4	4.7 ± 0.5	10.8 ± 1.7	14.9 ± 2.2	19.3 ± 2.5	19.2 ± 2.5
∑ HUFA	37.5 ± 3.0	26.6 ± 2.4	20.5 ± 2.2	49.8 ± 1.9	27.5 ± 0.5	29.4 ± 8.4	18.6 ± 2.4	21.1 ± 3.2
∑ Other FA	8.9 ± 1.1	10.1 ± 0.7	9.1 ± 0.8	8.2 ± 1.0	11.0 ± 1.4	8.3 ± 3.0	9.3 ± 0.7	6.9 ± 0.3
∑ FA (mg g^{-1})	25.0 ± 6.1	40.6 ± 3.3	68.6 ± 21.4	14.3 ± 3.5	44.1 ± 7.8	48.1 ± 32.7	54.3 ± 17.7	72.5 ± 27.5

Fatty acids (%)	Clistocoeloma merguiense (n = 4)	Metaplax elegans (n = 4)	Metopograpsus latifrons (n = 4)	Tubuca paradussumieri (n = 4)	Macrobrachium equidens (n = 4)	Metapenaeus ensis (n = 4)	Cloridopsis immaculata (n = 3)	Planiliza sp. B (n = 4)
∑ Branched FA	0.7 ± 0.2	1.3 ± 0.3	0.7 ± 0.1	1.1 ± 0.4	1.5 ± 0.2	3.6 ± 0.7	1.9 ± 0.3	0.9 ± 0.1
∑ 16:0 + 18:0 FA	25.9 ± 1.3	29.2 ± 1.2	25.6 ± 0.7	27.5 ± 1.0	32.1 ± 1.3	27.3 ± 0.7	34.4 ± 0.6	36.4 ± 0.2
∑ 16:1 + 18:1 FA	21.2 ± 1.1	14.0 ± 1.0	13.9 ± 1.6	17.1 ± 2.1	28.7 ± 2.3	16.0 ± 1.8	20.5 ± 0.9	11.7 ± 0.4
∑ 20:1 + 22:1 FA	0.4 ± 0.2	1.7 ± 0.3	0.5 ± 0.1	1.5 ± 0.1	0.5 ± 0.0	1.6 ± 0.2	1.4 ± 0.5	1.0 ± 0.1
∑ C16 PUFA	0.0 ± 0.0	1.4 ± 1.0	0.2 ± 0.1	0.9 ± 0.1	0.1 ± 0.0	0.2 ± 0.0	1.0 ± 0.4	1.0 ± 0.5
∑ C18 PUFA	22.6 ± 2.8	6.7 ± 1.7	16.9 ± 2.6	4.5 ± 0.3	8.2 ± 1.8	4.7 ± 0.7	5.7 ± 0.7	1.7 ± 0.1
∑ HUFA	23.3 ± 1.7	39.3 ± 4.2	38.1 ± 2.7	36.1 ± 2.0	21.6 ± 0.6	36.9 ± 1.9	22.8 ± 1.9	41.8 ± 1.5
∑ Other FA	5.8 ± 0.6	6.5 ± 1.3	4.1 ± 0.3	11.2 ± 1.8	7.3 ± 0.4	9.8 ± 0.6	12.3 ± 0.6	5.6 ± 1.0
∑ FA (mg g^{-1})	19.8 ± 3.7	26.6 ± 21.4	18.2 ± 3.6	17.0 ± 2.8	49.1 ± 5.4	29.7 ± 3.0	73.0 ± 10.7	29.7 ± 1.5

PUFA = Polyunsaturated FA; HUFA = Highly unsaturated FA

5. Discussion

5.1. Isotopic and fatty acid composition of potential food sources

The core zone of Can Gio Mangrove Biosphere Reserve is a relatively preserved mangrove ecosystem that hosts a high diversity of species and habitats (Tuan and Kuenzer, 2012). There is no abundant presence of macroalgae or seagrasses in any area of the mangrove, contrary to other areas in the Indo-Pacific where such food sources were shown to play a crucial role in food web interactions (Meziane and Tsuchiya, 2000; Alfaro et al., 2006; Abrantes and Sheaves, 2009). In the tidal creek studied, the basal food sources are assumed to derive mostly from decomposing mangrove leaves, but we hypothesised that estuarine phytoplankton inputs and benthic microalgae are also important basal resources.

The $\delta^{13}C$ of SPOM was depleted compared to the results of Tue et al. (2012), who studied a mangrove ecosystem in the Red River Delta in northern Vietnam (-27.1 ± 0.7 vs. -23.9 ± 0.8 ‰), while sediment and mangrove leaves exhibited relative similar values than in the Tue et al.'s (2012) study and others in the Indo-Pacific (Rodelli et al. 1984, Abrantes and Sheaves 2009, Alfaro et al. 2006). In addition, the consumer species assemblage of Tue et al. (2012) was relatively similar to ours and thus, exploring the differences between our $\delta^{13}C$

dataset with theirs offers an opportunity to assess the contribution of SPOM to the diet of organisms which are common to both the Red River Delta and the Can Gio mangroves.

C_{18} PUFA in mangrove leaves are mostly constituted by the FA 18:2ω6 and 18:3ω3 (Appendix 6-1). These biomarkers have also been detected in high proportions in seagrasses (Kharlamenko et al., 2001; Alfaro et al., 2006; Dubois et al. 2014) and macroalgae (Nelson et al., 2002) but since such food sources were not observed in any area of the Can Gio mangrove, the sum of C_{18} PUFA is a good biomarker for mangrove leaves in this ecosystem. More widely, C_{18} PUFA are also important components of mangrove propagules and pneumatophores (Wanningama et al., 1981; Xu et al., 1997), which can constitute substantial food sources in mangrove food webs (Sousa and Dangremond, 2011), along with stems, flowers, etc. We were not able to differentiate such components in this study and thus we will group all these basal food sources under the term "mangrove litter".

Elevated proportions of BrFA in sediments are consistent with previous observations in mangrove ecosystems (Meziane and Tsuchiya, 2000; Aschenbroich et al., 2015). BrFA are exclusively synthesised by bacteria (Kaneda, 1991), which are actually abundant in sediments, but might also be found in any decaying material transported as SPOM, and in basal resources that could not be sampled in this study, such as biofilms or tree micro-epiflora (Alfaro, 2008).

Highly unsaturated FA in SPOM are mostly constituted by the FA 20:5ω3 (Appendix 6-1), which is essentially synthesised either by planktonic or benthic diatoms (Dalsgaard et al., 2003; Kelly and Scheibling, 2012). These FA can be transferred to higher trophic levels through meiofauna consumption but can also derive from the ingestion of ω3 C_{18} PUFA (Monroig et al., 2013).

C_{16} and C_{18} MUFA are ubiquitous FA found in any kind of organic matter and can be synthesised *de novo* by animals (Dalsgaard et al., 2003), originate from PUFA degradation (Aschenbroich et al., 2015) or be produced by diatoms and other algae (Kelly and Scheibling, 2012). They can hardly be used as liable tracers of specific organic matter sources in this ecosystem but were nevertheless more abundant in SPOM.

These specific FA biomarkers were used to identify the preferred food sources of consumers, with a particular emphasize on C_{18} PUFA relative abundance as a tracer of mangrove litter and HUFA relative abundance as a tracer of microalgae-derived OM.

5.2. Identification of consumers' diet

The two potamid snails sampled in the Can Gio mangrove creek exhibited high BrFA and C_{16} + C_{18} MUFA proportions (Table 6-3 and Figure 6-4a), suggesting that they feed on unselected sediment particles, which is consistent with previous findings (Meziane and Tsuchiya, 2000; Bouillon et al., 2002; Tue et al., 2012). The low $\delta^{15}N$ signature of C*erithidea quoyii* may be due to the scraping of tree micro-epiflora with highly depleted $\delta^{15}N$ values, similarly to the littorinid snails studied by Bouillon et al. (2004). In addition, the species *C. quoyii* exhibited higher C_{18} PUFA proportion than *C. obtusa* (10.0% for *C. quoyii* and 4.9% for *C. obtusa*; Table 6-3), which may originate from this micro-epiflora (Alfaro, 2008). We suggest that *C. obtusa* feeds exclusively on sediment particles, while *C. quoyii* includes in its diet a substantial proportion of tree micro-epiflora.

The pulmonate snail *Cassidula aurisfelis* FA profiles exhibited relatively high HUFA and BrFA concentrations (mean %HUFA = 37.5% and mean %BrFA = 5.3%; Table 6-3 and Figure 6-4a), consistent with a diet mainly constituted by SPOM and conversely to the potamid snails, despite both groups are deposit feeders. The study of Tue et al. (2012) indicated a $\delta^{13}C$ signature of -22.8‰ for *C. aurisfelis*, consistent with a potential feeding on creek SPOM with $\delta^{13}C$ values averaging -23.9‰. In our study, SPOM exhibited a mean $\delta^{13}C$ of -27.1‰ and values down to -29.2‰ when abundance of FA in SPOM was the highest (Table 6-1 and Chapter 5), while *C. aurisfelis* had an average $\delta^{13}C$ signature of -26.9‰. Thus, the difference between their $\delta^{13}C$ measurements and ours on both SPOM and *C. aurisfelis*, combined to the constancy of the isotopic shift between the source and the consumer strongly suggests that *C. aurisfelis* feeds on SPOM. The snail most probably scraps the SPOM that is deposited in thin layer on wood bark and pneumatophores during flood.

The mangrove murex snail *Chicoreus capucinus* is a predator that feeds on a variety of bivalves and gastropods, drilling holes in their shell (Tan, 2008). Its $\delta^{15}N$ signature is higher than the theoretical trophic shift that would be observed if *C. capucinus* was feeding on littorinids or *Cerithidea quoyii* (considering an isotopic $\delta^{15}N$ shift of ~2.8‰ for carnivorous species; Vanderklift and Ponsard, 2003). However, isotopic signatures suggest that *C. capucinus* could feed on a combination of neritid snails and *C. obtusa* (Figure 6-2), which is consistent with observed populations preying on other potamid and neritid snails in Thailand (Tan, 2008). In addition, *C. capucinus* has a high HUFA content (mean %HUFA = 49.8; Table

6-3), suggesting that its trophic regime originates from microalgae. HUFA tend to accumulate with increasing trophic level in aquatic food webs (Kainz et al., 2006; Hall et al., 2006) and thus, *C. capucinus* FA profiles are consistent with a predatory behaviour of the species.

Neritid snails FA profiles indicate that they mainly feed on tree leaves (high C_{18} PUFA content; Table 6-3 and Figure 6-4a), despite previous studies generally indicate that they feed on microalgae (mostly diatoms) or sedimentary organic matter (Bouillon et al., 2002; Eichhorst, 2016). The low HUFA proportion (Table 6-3), especially FA 20:5ω3 (Appendix 6-3), which is considered a diatom biomarker, found in *Neripteron violaceum* and *Nerita balteata* tissues indicate that microalgae is not their primary food source. In addition, low BrFA proportions indicate a weak contribution of sediments to the neritid snails diet (Table 6-3). Their $\delta^{13}C$ signature (~ -23‰; Table 6-1 and Figure 6-2) suggests that they feed on a combination of highly $\delta^{13}C$-depleted mangrove leaves, and a $\delta^{13}C$-enriched food source, that could be other microalgae than diatoms or a non-sampled source.

Littorinid snails exhibited slightly lower C_{18} PUFA proportions than neritid snails but still higher than most organisms (Table 6-3 and Figure 6-4a). Their $\delta^{15}N$ signature was particularly low, which is consistent with previous observations by Christensen et al. (2001), Bouillon et al. (2002, 2004) and Alfaro (2008). These $\delta^{15}N$-depleted signatures are likely to be due to the ingestion of tree micro-epiflora, usually exhibiting negative $\delta^{15}N$ values (Bouillon et al., 2004). We suggest that the littorinid snails in our mangrove creek feed on a combination of mangrove litter and other scrapable items available on trees, such as micro-epiflora. These results are consistent with the observations of Lee et al. (2001) in Hong Kong mangroves.

The FA profiles and isotopic compositions of the sesarmid crab *Clistocoeloma merguiense* is consistent with a leaf litter-based diet. This feeding behaviour was previously observed in various species of grapsoid crabs from Australia (Bui and Lee, 2014) or Indonesia (Nordhaus et al., 2011). In contrast, analysis of the sesarmid crab *Metaplax elegans* and the ocypodid crab *Tubuca paradussumieri* suggest that both species diet is essentially based on microphytobenthos, as generally observed for both *M. elegans* and most ocypodid crabs (Bouillon et al., 2002, 2004; Tue et al., 2012; Vermeiren et al., 2015). The relatively high $\delta^{15}N$ values of both crabs (~ 8‰; Table 6-1 and Figure 6-2) indicate that they might obtain a non-negligible proportion of their nitrogen from a predator/scavenger behaviour. FA profiles and $\delta^{13}C$ values of the sesarmid crab *Metopograpsus latifrons* were intermediate compared to the other crab species (Table 6-2 and Figure 6-4b) and suggest an omnivorous behaviour

including highly $\delta^{13}C$ depleted mangrove material, and a more $\delta^{13}C$-enriched food source, such as microphytobenthos (Vermeiren et al., 2015). The high inter-individual $\delta^{13}C$ signature variability of *M. latifrons* was previously observed and attributed to its opportunistic predator/scavenger behaviour (Nordhaus et al., 2011; Vermeiren et al., 2015).

The two prawn species FA profiles indicate that they feed on SPOM (Figure 6-4b). The SPOM $\delta^{13}C$ values (mean $\delta^{13}C$ = -27.1‰ and values down to -29.2‰; Table 6-1 and Chapter 5) are consistent with these results (mean $\delta^{13}C$ of shrimps ~ -27‰). In addition, prawns were particularly $\delta^{13}C$-depleted compared to previous studies (~ -15-23‰; Rodelli et al., 1984; Stoner and Zimmerman, 1988; Abrantes and Sheaves, 2009; Tue et al., 2012) suggesting a similar effect than for *C. aurisfelis*, with exceptionally low SPOM $\delta^{13}C$ values responsible for $\delta^{13}C$-depleted consumers. The relatively high $\delta^{15}N$ values of both prawn species (~ 8‰; Table 6-1 and Figure 6-2) indicate that they might exhibit a predator/scavenger behaviour. This behaviour was previously evidenced in various penaeid species (Stoner and Zimmerman, 1988; Willems et al. 2016). We suggest that an intermediate trophic level, not sampled in our study and potentially constituted by pericarid crustaceans, macrobenthos larvae and other meiofauna (Bouillon et al., 2008b; Abrantes and Sheaves, 2009; Willems et al., 2016) is sustained by SPOM and serve as trophic link between SPOM and higher tropic level species such as crabs and prawns.

The high $\delta^{15}N$ signature of *Cloridopsis immaculata* indicates that the species is a predator, as previously observed morphologically (Dingle and Caldwell, 1975; Prasad and Yedukondala Rao, 2015). FA composition of *C. immaculata* was relatively similar to that of the two prawn species (Figure 6-4b), indicating that the species probably feeds on such food sources. The isotopic shift between *C. immaculata* and both prawn species confirm that prawns could be their primary food source ($\Delta\delta^{15}N$ ~ 2‰; Figure 6-2) but that other organisms probably also contribute to its diet due to the high shift in $\delta^{13}C$ signature between *C. immaculata* and prawns ($\Delta\delta^{13}C$ ~ 3‰ vs. usually ~ 1‰ between the food source and the consumer, although possibly highly variable; Figure 6-2 and Bui and Lee 2014).

The mullet *Planiliza sp. B* (see species details in Durand et al., 2017) FA profiles and isotopic signatures indicate that the fish feeds on microalgae and/or exhibit a predatory behaviour (Figure 6-2 and Figure 6-4b). These results are in accordance with previous studies that usually described mullets as non-specialised consumers feeding on microalgae,

zooplankton and a variety of benthic organisms (Abrantes and Sheaves, 2009; Tue et al., 2014).

5.3. Trophic web structure

According to the results of FA and stable isotopes, it is difficult to precisely define the contribution of each food source to the diet of the different species. However, our study highlights the dominant food source of each species. Clearly, the food web of the Can Gio mangrove creek and nearby areas relies on mangrove litter, SPOM (notably through phytoplankton), microphytobenthos, and tree micro-epiflora and biofilms (Figure 6-5).

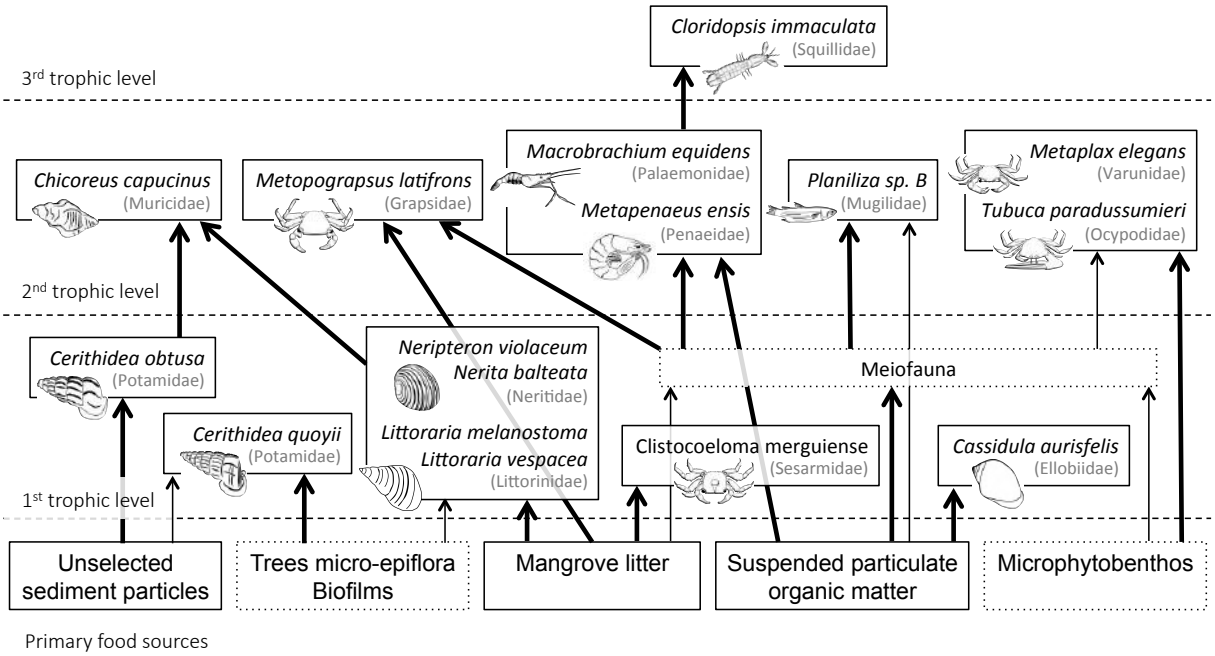

Figure 6-5: Representation of the food web structure in the Can Gio mangrove tidal creek and nearby areas based on fatty acid biomarkers, stable isotopes, and field observations. Dot line boxes represent theoretic food web components that were not sampled in our study

The trophic pathway based on mangrove litter, characteristic of mangrove ecosystems, is nutritionally sustaining the sesarmid crab *Clistocoeloma merguiense*, the littorinid snails and to a lesser extent, the grapsid crab *Metopograpsus latifrons* and neritid snails (Figure 6-5). Our results also highlight trophic pathways based on microalgae. The sesarmid crab *Metaplax elegans* and the ocypodid crab *Tubuca paradussumieri* dominantly feed on microphytobenthos, while the pulmonate snail *Cassidula aurisfelis*, the two prawn species and the mullet *Planiliza sp. B* rather feed on SPOM (Figure 6-5) wherein the most

nutritive fraction is phytoplankton. Other species feed on unselected sediment particles, mostly composed of bacteria, tree micro-epiflora and biofilms, which are probably highly $\delta^{15}N$-depleted (Bouillon et al., 2004) given the isotopic signatures of their consumers, mostly snails.

Given the elevated $\delta^{15}N$ signatures of the prawn and crabs species, we suggest that an intermediate trophic level serve as link between SPOM and higher tropic level species (Bouillon et al., 2008b; Abrantes and Sheaves, 2009; Willems et al., 2016). In our study we believe that this trophic link is constituted by pericarid crustaceans and other meiofauna, as observed in Australian mangroves (Abrantes and Sheaves 2009). The prawns benefiting on this trophic link are themselves consumed by the stomatopod *C. immaculata* and thus, at least three trophic levels are partly sustained by SPOM in the Can Gio mangrove creek.

Our study was not meant to be quantitative and further researches on species biomass and nutrient budgets should be conducted to evaluate the importance of each basal food source on the entire ecosystem. Despite this, it appears that the most mobile species found in our mangrove creek (fish and shrimps) are mainly feeding on SPOM, suggesting that this trophic pathway is of great importance for connectivity among ecosystems. Nevertheless, we suggest that given the low $\delta^{13}C$ value of SPOM in our mangrove creek, it does not originate from the ocean but rather from autochthonous primary production, using nutrients and carbon released by the mangrove forest (Abrantes and Sheaves, 2009). Thus, our study supports the hypothesis that tropical mangroves fuel coastal food webs, not necessarily by the direct consumption of mangrove tree leaves after bacterial and fungal conditioning, but rather through the local production of phytoplankton using nutrients released by mangrove soils (see Chapter 5). In this representation, ecosystem engineers, mostly snails and crabs, would mainly act as mineralisers, processing high quantities of detrital material to meet their nutritional needs (Lee, 2008; Harada and Lee, 2016), and thus releasing carbon and nutrients. The reintegration of these compounds into algal cells then constitutes a mechanism linking mobile and/or high trophic level species to mangrove litter (i.e. leaves, propagules, stems, flowers, etc.) in tidal creeks and coastal food webs.

6. Acknowledgments

We would particularly like to thank Dr. David Reid, from the British Museum, for snail species identification, Dr. Joseph Poupin, from the Ecole Navale of Brest (France), Pr. Danièle Guinot, from the Museum National d'Histoire Naturelle (MNHN), and Dr. Diem My Tran Ngoc, from the University of Science of Ho Chi Minh City, for crab species identification, Dr. Jean-Dominique Durand, from the Institut de Recherche pour le Développement (IRD), and Dr. Agnès Dettai, from the MNHN, for fish species identification. We would also like to thank the Vietnamese students for their crucial help with fieldwork and Marine Fuhrman, from the Institut Français de Recherche pour l'Exploitation de la Mer (IFREMER) of Brest for her drawings of the animal species.

Chapter 7: Fatty acid composition of four benthic species along the salinity gradient of a human impacted and mangrove dominated tropical mangrove (Can Gio, Vietnam)

DAVID Frank, MARCHAND Cyril, TAILLARDAT Pierre, NGUYỄN THÀNH Nho, TRUONG VAN Vinh and MEZIANE Tarik

1. Abstract

Mangrove ecosystems are characterised by high spatial and temporal variability in the conditions they provide for living organisms, which in turn may affect their biochemical composition. In addition, anthropogenic contaminants such as nutrients, antibiotics, pesticides and trace metals may also affect biochemical composition of living organisms, notably with regard to fatty acids, of which optimal species-specific polyunsaturated fatty acid ratios are required to maintain healthy conditions. The objective of this study is to evidence changes in the FA profile of four ubiquist benthic species in relation to the salinity gradient of the human impacted and mangrove dominated Can Gio mangrove tropical estuary (Southern Vietnam). Among the four benthic species studied, two exhibited spatial and seasonal changes in their fatty acid composition, with higher proportions of FA 16:1ω7, lower proportions of highly unsaturated FA and higher ratios of eicosapentanoic acid/arachidonic acid, that can be related to anthropogenic wastewater releases influence. The varunid crab *Metaplax elegans* might be affected because of changes in its diet induced by high relative abundance of benthic microalgae due to nutrient inputs, while the predatory mangrove murex snail *Chicoreus capucinus* shows that the very likely influence of anthropogenic pressures is transferred within trophic webs. Finally, some species, such as *Nerita balteata* and *Metapenaeus ensis* might have more adaptive capacities, because of their mobility, or because of their specific metabolic pathways, allowing them to be poorly effected by anthropogenic stressors.

2. Introduction

Mangrove ecosystems are characterised by high spatial and temporal variability in the conditions they provide for living organisms, such as temperature or salinity (Sousa and Dangremond 2011), which in turn may affect their biochemical composition (Frolov et al. 1991, Romano et al. 2014). Besides, Southeast Asian mangroves are threatened by demographic pressure and land area requirements for food production, leading to their conversion into urban areas, aquaculture ponds, paddy rice fields or oil palm plantations (Richards and Friess 2016). Human activities associated to these conversions release wastewaters loaded with contaminants such as nutrients, antibiotics, pesticides or trace metals (Gräslund and Bengtsson 2001, Marcotullio 2007, Strady et al. 2017). Such compounds may also affect the biochemical composition of exposed living organisms, with contrasting response depending on the stressor and the species considered (Filimonova et al. 2016, Kowalczyk-Pecka et al. 2016). Mangrove ecosystems are assumed to act as powerful biofilters, trapping these elements before the water is being transferred into the ocean (Robertson and Philips 1995, Marchand et al. 2012). However, how anthropogenic pressures (i.e. wastewater releases) affect faunal communities of exposed mangrove ecosystems and the benefits they provide is yet to be explored.

Fatty acids (FA) are ubiquitous compounds that play major roles in the metabolism of living organisms; being used as energy storage forms, membranes constituents and immune system precursors (Budge et al. 2006, Bergé and Barnathan 2005). It can thus be expected that perturbations in the FA profile of organisms, induced by diet shift or diverse stressors, have implications on their metabolic functioning (Ahlgren et al. 2009). The FA composition of benthic organisms is affected by the nutritional composition of available food sources in aquatic ecosystems, allowing them to be used as trophic biomarkers in benthic food webs (Meziane and Tsuchiya 2000, Kelly and Scheibling 2012). In studies conducted for aquaculture purpose, alterations to dietary ω3 polyunsaturated fatty acids (PUFA)/ω6 PUFA ratios and, particularly dietary eicosapentanoic/arachidonic (EPA/ARA) ratios, have strong consequences for eicosanoids metabolism, themselves implied in ionic regulation of cells, stress response and immune system functioning (Tocher and Glencross 2015). These conclusions suggest that optimal species-specific PUFA ratios are required to maintain organisms in healthy conditions (Sargent et al. 1995, Ahlgren et al. 2009).

The Can Gio mangrove receives wastewaters from Ho Chi Minh City (HCMC), the biggest city of Vietnam (~13 million inhabitants) (Strady et al. 2017), and from an intense shrimp farming activity located at the upstream border of the mangrove (Anh et al. 2010). The present study aims to examine the FA profiles of four benthic species widely distributed within the Can Gio mangrove and belonging to different trophic groups, the microphytobenthos consumer crab *Metaplax elegans* (Varunidae), the predator snail *Chicoreus capucinus* (Muricidae), the particulate organic matter feeding shrimp *Metapenaeus ensis* (Penaeidae) and the leaf litter consuming snail *Nerita balteata* (Neritidae) (see Chapter 6). We postulated that (1) organisms' diet was affected by the distance to the ocean coast and the season, due to changing organic matter quality (2) the fatty acid composition of their tissues was varying according to such changes and as a response to human pressures. Organisms were sampled along the salinity gradient of the Can Gio mangrove estuary, from the downstream end of HCMC to the South China Sea coast, and around a tidal creek located in the core protected zone of the mangrove, taken as a reference site preserved from human pressures. In addition, for one species (*Nerita balteata*), which did not exhibit any specific spatial or temporal variability in its FA profiles, we were interested in retracing biosynthetic pathways of FA doing a starvation experiment. Studying FA metabolism will contribute to understand organisms' vulnerability to external stressors, such as changes in food resources, varying environmental parameters or exposition to contaminants.

3. Materials and methods

3.1. Study site

The Can Gio mangrove (Southern Vietnam, 10°N) is formed by the deltaic confluence of the Saigon, Dong Nai and Vam Co Rivers. It covers an area of 720 km^2, accounting for 20% of Vietnam's mangroves (Tuan and Kuenzer 2012). Its high biodiversity and its social importance, being considered as the "green lung" of Ho Chi Minh City, conducted UNESCO to designate Can Gio as the first mangrove biosphere reserve in Vietnam (UNESCO/MAB Project 2000). Due to massive replanting after Vietnam War conflict (1955-1975), the forest is dominated by mature trees of the species *Rhizophora apiculata*, providing relatively homogeneous habitats and promoting a wide spatial distribution of benthic animal species.

Study sites were selected to cover a gradient of anthropogenic pressures on the ecosystem and to allow comparisons with a remote near-pristine area (Figure 7-1). The four sites were located: 1) at the upstream end of the mangrove forest (10°34'19"N 106°50'11"E); 2) in the centre of the mangrove protected core (10°31'04"N 106°53'13"E); 3) near the outlet to the South China Sea (10°29'32"N 106°56'55"E); R) at the end of a 1,400 m long mangrove tidal creek (10°30'24"N 106°52'57E) not directly connected to the main estuarine channel.

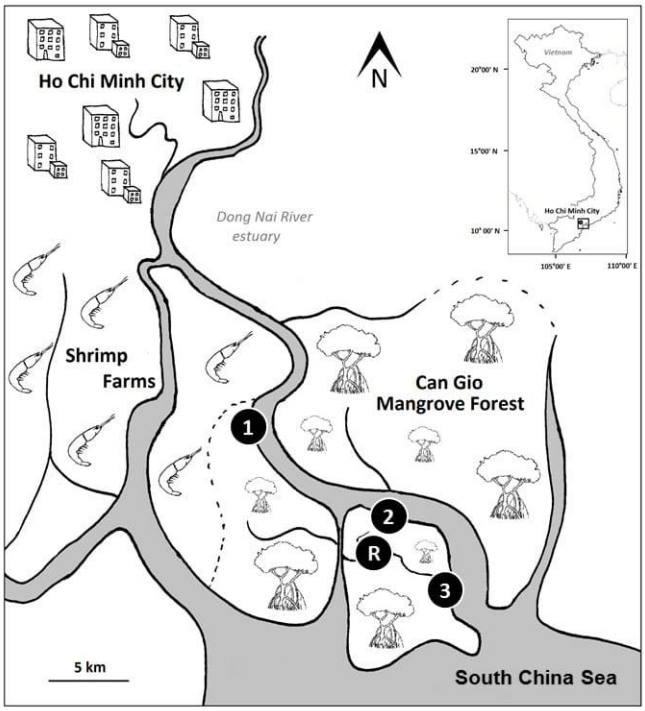

Figure 7-1: Map of the sampling area in Can Gio mangrove (Southern Vietnam). 1, 2 and 3 indicate the sampling sites along the main channel of the estuary and R indicates the reference site located in a near-pristine area

3.2. Field collections

Flora, fauna and sediment were collected during dry (January-February) and monsoon (September-October) periods in 2015 at site 1, 2 and 3, and only during the monsoon period at the reference site (R). At site R, the salinity range (16-23) was between that of site 2 (13-19) and site 3 (17-25) (see Chapter 1 and Chapter 5). Samples were collected in four replicates within 60 m from the estuarine channel in a daily flooded zone. Freshly fallen tree leaves and crabs were handpicked on the sediment, gastropods were gathered on mangrove tree roots and shrimps were caught with fishing nets. Sediments were taken from two distinct zones, the flat flooded mangrove forest, overwashed during high tide, and the vertical

bordering fringe, eroded by the estuarine water current and retained by mangrove lateral roots. The varunid crab *Metaplax elegans* was caught on this latter sediment and is known to feed essentially on microphytobenthos (Bouillon et al. 2002, Tue et al. 2012, see Chapter 6). The mangrove murex snail *Chicoreus capucinus* is a predator feeding on other molluscs (Tan 2008, see Chapter 6), the neritid snail *Nerita balteata* has been identified as feeding on a combination of mangrove tree leaves and biofilms (see Chapter 6) and the penaeid shrimp *Metapenaeus ensis* is mostly feeding on particulate organic matter and meiofauna (Stoner and Zimmerman 1988, see Chapter 6). Samples were not available at all sites for all species, but species sampling was not exhaustive and the absence of data for one species at a given site does not necessarily signify that the species was absent from the site. Sediment cores (1 cm depth × 2 cm Ø) were sampled on the same habitat where crabs were found. All samples were kept on ice during sampling and stored at -25°C until analysis.

3.3. Starvation experiment

A group of neritid snails *Nerita balteata* gathered at site 1 during monsoon period was kept alive for the starvation experiment. Snails were placed at dark without food sources in a plastic container filled with 1 cm of 0.7 µm filtered estuarine water. After 6, 12 and 20 days of starvation, four individuals were frozen for further analysis of FA. Water was regularly changed and vacuum-filtered through pre-combusted and pre-weighted glass fibre filters (Whatman® GF/F 0.7 µm) to recover snail faeces.

3.4. Sample processing

Collected material was freeze-dried and powdered before analysis. Each sample consisted in one sediment core, one tree leave, tissues of one animal or one filter with snail faeces. For crabs, both hepatopancreas and muscles taken from the claw were analysed, for shrimps only muscles were taken and for gastropods, the entire organism was removed from its shell and homogenised. Additionally, only male crabs were analysed to avoid risks of variability in fatty acid composition due to egg development.

Lipids were extracted following a slightly modified protocol of Bligh and Dyer (1959), as described in Meziane et al. (2007). Lipids were extracted using 100 mg of dry material for

tree leaves, 30 mg for animal tissues, 3 to 15 mg for snail faeces and 1 g for sediments. Tricosanoic acid (23:0) was used as an internal standard to measure the absolute FA concentration of samples. Fatty Acid Methyl Esters (FAME) were quantified by gas chromatography analysis (Varian 3800-GC), using a flame ionization detector. Identification of fatty acids was performed using coupled gas chromatography mass spectrometry (Varian 450-GC; Varian 220-MS), and comparison of GC retention times with commercial standards (Supelco® 37 component FAME mix and marine source polyunsaturated FAME n°1 mix). Values were reported as % of total FA or absolute concentrations (µg mg^{-1}).

3.5. Data analysis

The FA proposed as biomarkers of anthropogenic influence were selected according to their prevalence in tissues, their known significant role in physiological processes and their biological relevance as indicating alterations of the ecosystem related to anthropogenic pressures. Despite various biomarkers were tested for their ability to evidence spatial and seasonal difference in FA profiles of the four studied organisms, only most relevant indicators are presented, comprising proportion of the FA 16:1ω7, proportion of highly unsaturated FA (HUFA), ratio of ω3 PUFA/ω6 PUFA, ratio of EPA/ARA and total sum of FA.

Proportions and ratios of FA biomarkers in field-collected animals were compared using non-parametric Kruskal-Wallis rank tests due to low amount of data (usually 4 per group). When significant p-value was found, differences between groups were assessed using Wilcoxon pairwise comparisons (α = 5%). Temporal variations in single FA of snails submitted to starvation experiment were assessed using linear regression analysis and residuals distributions were tested by Shapiro-Wilk normality test (α = 5%). Full FA profiles of snails submitted to starvation experiment and their faeces were compared using non-metric multi-dimensional scaling (NMDS) based on Bray–Curtis similarity matrix. All statistical analyses and graphical representations were performed using R 3.3.3 (R Core Team 2017).

4. Results

4.1. Fatty acids in potential food sources

Fatty acid profiles of freshly fallen tree leaves reveal a dominant contribution of saturated fatty acids (SFA = 50.6%) and polyunsaturated FA (PUFA = 40.0%), essentially C_{18} PUFA (18:2ω6 + 18:3ω3 = 39.5%) (Table 7-1). Sediment samples are also dominated by SFA (55.4 and 46.9%, respectively for bordering fringe and mangrove forest zones) but highlight lower contribution of PUFA (6.8 and 5.8%). Branched FA and the FA 16:1ω7 are found in important proportions in sediments (BrFA = 16.6 and 23.8%; 16:1ω7 = 8.1 and 5.5%) while they are absent or nearly absent from tree leaves (Table 7-1). Complete fatty acid compositions of potential food sources are provided in Appendices 7-1, 7-2 and 7-3.

Table 7-1: FA compositions of potential food sources and organisms sampled for the study

Fatty acids (%)	Sediment Bordering fringe (n = 28)	Sediment Mangrove forest (n = 28)	*Rhizophora a.* Brown leaves (n = 28)	*Chicoreus c.* (n = 20)	*Metapenaeus e.* (n = 20)	*Metaplax e.* Claw muscle (n = 20)	*Metaplax e.* Hepatopancreas (n = 20)	*Nerita b.* (n = 24)
∑ Saturated FA	55.4 ± 6.6	46.9 ± 3.7	50.6 ± 4.7	28.8 ± 3.9	36.1 ± 2.5	36.3 ± 2.9	41.8 ± 3.5	30.3 ± 1.6
∑ Monounsaturated FA	21.2 ± 5.1	23.5 ± 3.1	9.4 ± 3.4	24.7 ± 6.1	19.8 ± 2.0	17.3 ± 1.7	21.6 ± 1.8	23.5 ± 3.6
16:1ω7	8.1 ± 3.5	5.5 ± 1.5	0.3 ± 0.1	4.8 ± 2.9	4.5 ± 1.3	6.6 ± 2.6	14.0 ± 4.4	1.8 ± 0.7
∑ Polyunsaturated FA	6.8 ± 2.7	5.8 ± 2.0	40.0 ± 4.4	45.5 ± 8.8	40.9 ± 2.4	44.4 ± 3.8	34.8 ± 4.4	43.3 ± 3.2
∑ C18 PUFA	2.1 ± 0.9	2.1 ± 0.8	39.5 ± 4.6	4.5 ± 1.1	5.7 ± 1.9	4.2 ± 1.5	4.7 ± 2.0	16.5 ± 4.2
∑ Highlyunsaturated FA	2.6 ± 1.4	2.5 ± 1.1		40.9 ± 7.9	35.0 ± 2.4	38.3 ± 4.3	22.2 ± 4.8	25.5 ± 4.8
20:4ω6 (ARA)	0.8 ± 0.4	1.3 ± 0.6		14.4 ± 5.2	13.8 ± 3.2	6.2 ± 2.2	5.4 ± 3.1	13.0 ± 3.8
20:5ω3 (EPA)	1.8 ± 1.1	1.2 ± 0.7		1.4 ± 0.3	10.2 ± 2.4	20.1 ± 2.4	12.2 ± 1.9	2.0 ± 0.7
∑ Branched FA	16.6 ± 3.8	23.8 ± 2.5		1.0 ± 1.0	3.2 ± 1.0	0.8 ± 0.3	1.8 ± 0.8	2.9 ± 0.7
∑ Fatty Acids (mg g^{-1})	0.3 ± 0.1	0.3 ± 0.1	3.7 ± 2.4	25.5 ± 10.1	31.3 ± 5.8	20.4 ± 7.3		54.4 ± 21.8

Proportions of the FA 16:1ω7 in bordering fringe sediment is significantly affected by site location while no difference is observed in mangrove forest sediment and *Rhizophora* tree leaves (Table 7-2). The ω3/ω6 ratios in *Rhizophora* tree leaves are not affected by site location but significant differences are observed in total concentration of FA (Table 7-2). Other FA biomarkers in sediments are significantly affected by site location but their response does not show a trend related to the salinity gradient (Table 7-2). These differences are essentially due to FA concentrations 2-3 times higher during wet season (unpublished data).

Table 7-2: Significance of spatial and seasonal differences on selected FA biomarkers on potential food sources and organisms sampled for the study. Differences that were considered as biologically relevant are highlighted in bold

Kruskal-Wallis significance test	FA 16:1ω7	HUFA	ω3/ω6	EPA/ARA	Sum of FA
Sediment (Bordering fringe)	**< 0.01**	< 0.05	< 0.05	< 0.05	< 0.05
Sediment (Mangrove forest)	0.16	< 0.05	< 0.05	< 0.05	0.10
Rhizophora a. (Brown leaves)	0.05		0.69		< 0.01
Chicoreus c.	**< 0.05**	**< 0.05**	0.13	**< 0.05**	0.05
Metapenaeus e.	0.32	0.06	0.31	0.09	0.33
Metaplax e. (Claw muscle)	**< 0.01**	0.07	**< 0.01**	**< 0.01**	0.10
Metaplax e. (Hepatopancreas)	**< 0.01**	0.08	**< 0.01**	**< 0.01**	-
Nerita b.	0.24	0.30	0.27	0.84	0.66

HUFA = Highlyunsaturated fatty acids; EPA = Eicosapentanoic acid; ARA = Arachidonic acid

4.2. Fatty acids in consumers

Fatty acid profiles of consumers reveal a dominant contribution of PUFA in all species except in the hepatopancreas of the varunid crab *Metaplax elegans*, dominated by SFA (Table 7-1). The highest proportions of FA 16:1ω7 are found in the hepatopancreas of *M. elegans* (14.0%) and the highest proportions of C_{18} PUFA are found in the neritid snail *Nerita balteata* (16.5%; Table 7-1). Important differences are observed in the EPA/ARA ratio of consumers, with high values in *M. elegans* (2.3 and 3.2, respectively for hepatopancreas and claw muscles), low values in snails (0.10 and 0.15, respectively for the mangrove murex *Chicoreus capucinus* and *N. balteata*) and intermediate values in the penaeid shrimp *Metapenaeus ensis* (0.74; Table 7-1). Complete fatty acid compositions of consumers are provided in Appendices 7-4, 7-5, 7-6 and 7-7.

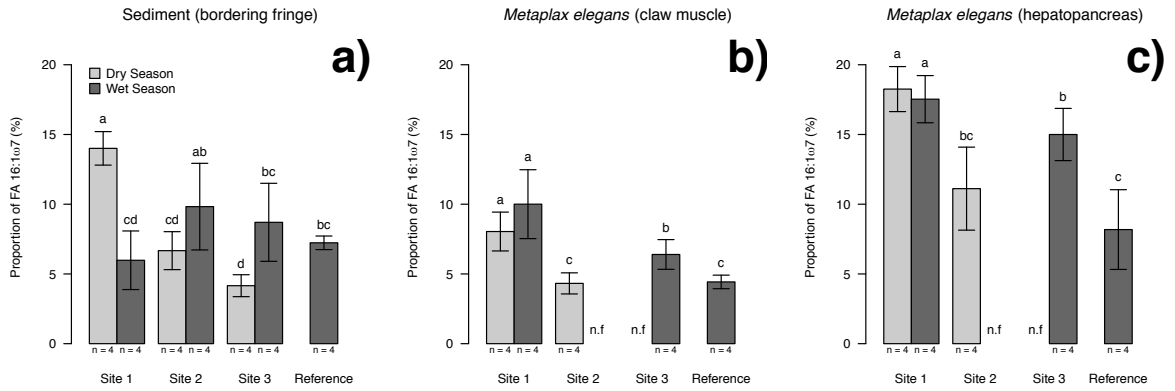

Figure 7-2: Proportions of a) FA 16:1ω7 in sediments and tissues of the sesarmid crab *Metaplax elegans*, b) claw muscles and c) hepatopancreas. Letters indicate significant differences as revealed by pairwise Wilcoxon comparisons after Kruskal-Wallis significance test (α = 5%). n.f = species not found

Proportions of the FA 16:1ω7 in *C. capucinus* and both tissues of *M. elegans* is significantly affected by site location while no difference is observed in *M. ensis* and *N. balteata* (Table 7-2). Differences show a similar significant trend in both affected species with higher proportions of the FA 16:1ω7 close to the upstream end of the mangrove forest (Site 1) and lower values close to the South China Sea (Site 3) or at the Reference site (Figure 7-2b, Figure 7-2c and Figure 7-3a). Both proportions of HUFA and EPA/ARA ratios are affected by sampling site location in *C. capucinus* (Table 7-2). Lower HUFA proportions and higher EPA/ARA ratios are observed at the impacted sites compared to the Reference site, with significant differences only highlighted during wet season (Figure 7-3b and Figure 7-3c). Ratios of ω3/ω6 FA and EPA/ARA are affected by site location in both tissues of *M. elegans*, with a similar trend than observed for the EPA/ARA ratios in *C. capucinus,* showing increasing values from the upstream end of the mangrove to the outlet to the South China Sea or at the Reference site (Figure 7-4). No FA biomarkers exhibit significant difference according to season or sampling site location in the species *M. ensis* and *N. balteata* (Table 7-2).

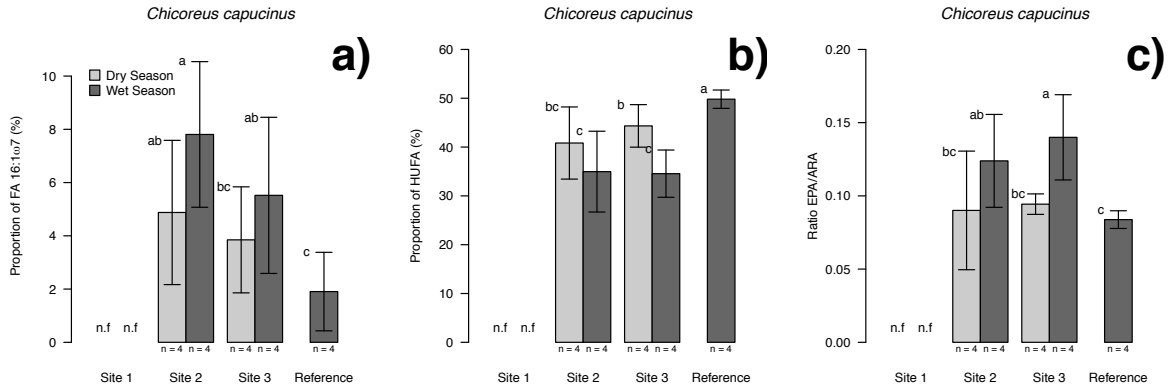

Figure 7-3: Proportions of a) FA 16:1ω7, b) proportions of highly unsaturated fatty acids (HUFA), and c) ratios of eicosapentanoic acid/arachidonic acid (EPA/ARA) in tissues of the mangrove murex snail *Chicoreus capucinus*. Letters indicate significant differences as revealed by pairwise Wilcoxon comparisons after Kruskal-Wallis significance test (α = 5%). n.f = species not found

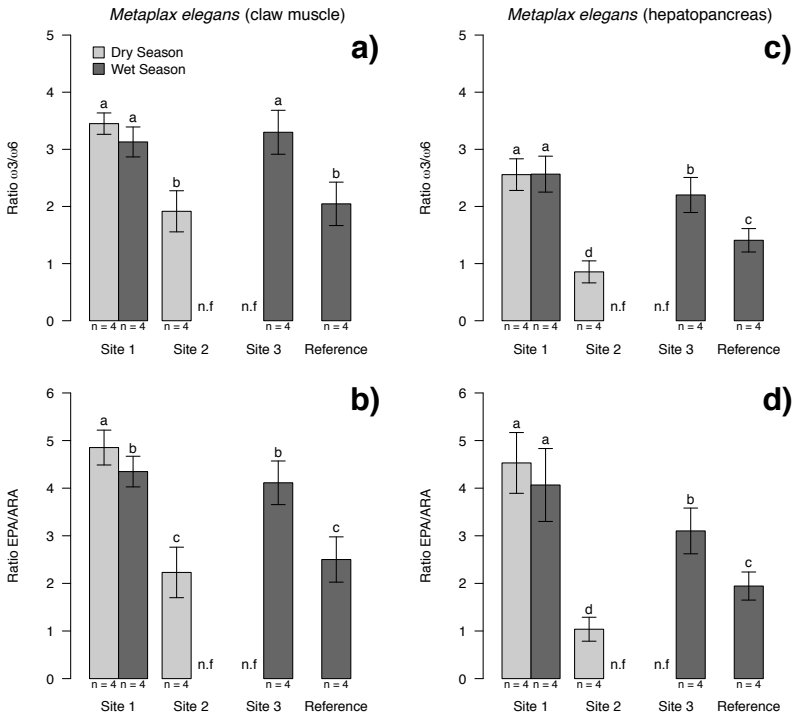

Figure 7-4: Ratios of ω3/ω6 FA in a) claw muscles and b) hepatopancreas of the sesarmid crab *Metaplax elegans*. Ratios of eicosapentanoic acid/arachidonic acid (EPA/ARA) in c) claw muscles and d) hepatopancreas of the sesarmid crab *Metaplax elegans* Letters indicate significant differences as revealed by pairwise Wilcoxon comparisons after Kruskal-Wallis significance test (α = 5%). n.f = species not found

4.3. *Nerita balteata* starvation experiment

Fatty acid profiles of faeces of the neritid snail *Nerita balteata* show a dominant contribution of SFA and low proportions of PUFA in comparison to snail tissues (<20% vs. >40%; Table 7-3). The proportions of BrFA are particularly higher in faeces compared to snail tissues (>12.8% vs. <3.4%; Table 7-3). During starvation, total concentration of FA rapidly drop from 44.6 ± 16.9 mg g^{-1} at T0 to 26.5 ± 8.8 mg g^{-1} at T6 and remain roughly constant until the end of the experiment, reaching 25.2 ± 10.8 mg g^{-1} at T20 (Table 7-3). Composition of snail tissues display increasing proportions of FA 18:0, 20:1ω11, 20:4ω6 and 22:2ω9, while it exhibit decreasing proportions of FA 16:0, 18:1ω9, 18:2ω6, 20:2ω6 and 20:3ω6 (Table 7-4). Faeces display increasing proportions of FA 16:1ω5 and 18:1ω7 during starvation, and decreasing proportions of FA 24:0, sum of SFA, 17:1ω9, 20:1ω9, 18:2ω6, 18:3ω3 and 20:2ω9 (Table 7-4).

Table 7-3: FA compositions of tissues and faeces of the neritid snail *Nerita balteata* during the starving experiment. Only FA displaying an average proportion greater than 0.8% within at least one group of samples are presented

Fatty acids (%)	*Nerita b.* D00 (n = 4)	*Nerita b.* D06 (n = 4)	*Nerita b.* D12 (n = 4)	*Nerita b.* D20 (n = 4)	Faeces D02 - D03 (n = 2)	Faeces D06 - D07 (n = 2)	Faeces D11 - D20 (n = 3)
Saturated							
12:0	0.2 ± 0.2	0.1 ± 0.0	0.0 ± 0.0	0.0 ± 0.0	0.8 ± 0.0	0.4 ± 0.1	0.2 ± 0.2
14:0	2.6 ± 0.4	1.9 ± 0.7	1.8 ± 0.3	2.2 ± 0.5	4.5 ± 0.8	7.8 ± 0.7	7.1 ± 2.3
15:0	1.1 ± 0.3	1.6 ± 0.4	1.7 ± 0.3	1.8 ± 0.8	1.8 ± 0.5	2.2 ± 0.4	2.1 ± 0.1
16:0	20.4 ± 2.1	16.5 ± 5.5	15.1 ± 3.4	14.9 ± 2.3	22.2 ± 0.2	19.0 ± 1.7	17.2 ± 1.4
17:0	1.3 ± 0.1	1.4 ± 0.2	1.3 ± 0.2	1.4 ± 0.1	1.3 ± 0.2	1.1 ± 0.0	1.3 ± 0.4
18:0	4.7 ± 0.2	6.0 ± 0.9	6.7 ± 0.4	6.1 ± 0.7	5.3 ± 0.0	4.7 ± 0.0	5.1 ± 1.7
24:0	0.2 ± 0.1	0.2 ± 0.1	0.2 ± 0.1	0.1 ± 0.1	0.9 ± 0.1	0.5 ± 0.1	0.2 ± 0.1
∑SFA	**30.7 ± 1.8**	**27.9 ± 5.6**	**27.1 ± 3.6**	**26.9 ± 1.0**	**37.9 ± 1.7**	**36.8 ± 3.1**	**33.9 ± 4.6**
Monounsaturated							
16:1ω7	1.8 ± 0.9	1.2 ± 0.7	0.8 ± 0.3	1.0 ± 0.4	5.5 ± 0.3	3.6 ± 0.3	4.6 ± 3.4
16:1ω5	0.3 ± 0.0	0.2 ± 0.1	0.1 ± 0.1	0.2 ± 0.1	0.2 ± 0.0	0.4 ± 0.1	1.1 ± 1.0
17:1ω9	0.1 ± 0.0	0.1 ± 0.1	0.0 ± 0.0	0.1 ± 0.1	0.8 ± 0.3	0.6 ± 0.3	0.2 ± 0.1
18:1ω11	2.3 ± 2.0	2.0 ± 2.4	1.3 ± 1.4	3.8 ± 2.4	0.7 ± 0.1	0.4 ± 0.1	0.4 ± 0.0
18:1ω9	4.4 ± 0.4	3.2 ± 1.0	2.5 ± 0.5	3.0 ± 0.6	5.4 ± 0.7	4.5 ± 0.9	5.1 ± 0.3
18:1ω7	5.9 ± 0.7	5.7 ± 0.9	4.4 ± 0.9	4.6 ± 1.5	9.6 ± 0.1	11.5 ± 0.7	15.0 ± 3.8
20:1ω11	5.1 ± 0.8	9.1 ± 2.2	10.2 ± 1.9	9.2 ± 2.0	5.5 ± 0.8	3.5 ± 0.3	3.7 ± 0.5
20:1ω9	1.3 ± 0.2	1.0 ± 0.2	0.9 ± 0.2	1.0 ± 0.3	1.2 ± 0.4	0.7 ± 0.0	0.5 ± 0.2
20:1ω7	0.5 ± 0.2	0.5 ± 0.2	0.6 ± 0.1	0.7 ± 0.2	0.6 ± 0.2	0.9 ± 0.4	0.5 ± 0.0
∑MUFA	**22.2 ± 2.6**	**23.6 ± 2.6**	**21.4 ± 1.6**	**24.4 ± 3.8**	**30.6 ± 0.3**	**27.1 ± 0.2**	**31.8 ± 7.5**
Polyunsaturated							
18:2ω6	15.6 ± 3.9	9.9 ± 1.5	8.3 ± 1.5	7.2 ± 1.4	7.8 ± 0.9	3.3 ± 0.6	2.0 ± 0.5
18:3ω3	2.1 ± 1.2	1.3 ± 0.8	1.2 ± 0.7	0.8 ± 0.5	0.8 ± 0.3	0.3 ± 0.1	0.2 ± 0.1
20:2ω9	0.9 ± 0.8	0.6 ± 0.8	0.4 ± 0.4	1.2 ± 0.8	0.5 ± 0.1	0.3 ± 0.0	0.2 ± 0.0
20:2ω6	1.5 ± 0.3	1.3 ± 0.3	1.3 ± 0.5	0.9 ± 0.2	0.9 ± 0.4	0.7 ± 0.3	0.5 ± 0.2
20:3ω6	0.9 ± 0.2	0.7 ± 0.2	0.6 ± 0.1	0.4 ± 0.1	0.3 ± 0.1	0.3 ± 0.1	0.3 ± 0.2
20:4ω6	12.4 ± 1.6	18.9 ± 5.5	22.7 ± 5.1	20.4 ± 5.3	3.0 ± 0.1	3.2 ± 0.8	3.7 ± 0.5
20:5ω3	2.1 ± 0.4	2.2 ± 0.9	2.5 ± 0.7	2.1 ± 0.5	0.8 ± 0.4	1.0 ± 0.7	0.7 ± 0.3
22:2ω9 (NMI)	2.5 ± 0.8	4.1 ± 1.3	4.5 ± 1.4	5.1 ± 1.1	2.1 ± 0.6	1.5 ± 0.1	1.6 ± 0.2
22:3ω6	0.5 ± 0.2	1.0 ± 0.4	1.1 ± 0.3	1.0 ± 0.3	0.3 ± 0.0	0.2 ± 0.0	0.2 ± 0.0
22:4ω6	2.7 ± 0.5	3.1 ± 0.7	3.3 ± 0.9	3.5 ± 0.6	0.4 ± 0.0	0.6 ± 0.3	0.6 ± 0.3
22:5ω3	0.6 ± 0.4	0.6 ± 0.1	0.9 ± 0.5	0.6 ± 0.1	0.2 ± 0.2	0.4 ± 0.4	0.2 ± 0.1
∑PUFA	**44.2 ± 3.0**	**45.6 ± 5.9**	**48.2 ± 4.3**	**45.3 ± 3.9**	**18.7 ± 1.7**	**13.8 ± 4.1**	**11.9 ± 1.7**
Branched							
15:0iso	0.5 ± 0.3	0.7 ± 0.3	0.7 ± 0.2	0.7 ± 0.4	5.8 ± 1.2	16.5 ± 0.7	16.7 ± 3.4
15:0anteiso	0.1 ± 0.0	0.1 ± 0.0	0.1 ± 0.0	0.1 ± 0.1	1.0 ± 0.1	1.3 ± 0.2	1.0 ± 0.2
16:0iso	0.9 ± 0.1	1.0 ± 0.4	1.2 ± 0.4	1.1 ± 0.4	3.1 ± 1.2	2.0 ± 0.1	2.0 ± 0.6
17:0iso	0.8 ± 0.1	0.7 ± 0.1	0.8 ± 0.1	0.9 ± 0.1	1.7 ± 0.2	1.8 ± 0.1	2.0 ± 0.6
∑BrFA	**2.9 ± 0.2**	**3.0 ± 0.6**	**3.3 ± 0.4**	**3.4 ± 1.0**	**12.8 ± 0.2**	**22.4 ± 0.8**	**22.4 ± 2.6**
Other minor FA	4.0 ± 1.6	3.1 ± 1.9	2.7 ± 1.3	3.5 ± 1.5	5.0 ± 2.1	4.8 ± 1.8	3.5 ± 1.5
∑FA (mg g^{-1})	**44.6 ± 16.9**	**26.5 ± 8.8**	**24.0 ± 6.1**	**25.2 ± 10.8**	**6.2 ± 2.3**	**13.5 ± 1.6**	**14.3 ± 7.1**

The MDS ordination of FA composition of snail faeces and tissues separates both materials on the first axis of the analysis and reveals temporal trends on the second axis (Figure 7-5). Scores of FA on the first axis confirms the higher proportions of SFA and BrFA in snail faeces and the higher proportions of PUFA in snail tissues. Scores of FA on the second axis reveals higher proportions of C_{16} and C_{18} PUFA at the beginning of the starvation experiment and higher proportions of longer chain PUFA (C_{20} and C_{22}) at the end of the experiment (Figure 7-5).

Table 7-4 : Significance of the linear relationship between FA proportions in tissues and faeces of the nertid snail *Nerita balteata* and starving duration. n.n.d = not normally distributed model residuals

Linear Model	*Nerita b.* Tissues (n = 16)		*Nerita b.* Faeces (n = 7)	
	p.value	Estimate	p.value	Estimate
Saturated				
12:0	0.16		0.10	
14:0	0.43		0.79	
15:0	0.05		0.46	
16:0	< 0.05	-0.26	n.n.d	
17:0	0.43		0.32	
18:0	< 0.05	0.07	n.n.d	
24:0	0.08		< 0.01	-0.04
∑SFA	0.13		< 0.05	-0.44
Monounsaturated				
16:1ω7	0.10		0.47	
16:1ω5	0.27		< 0.01	0.10
17:1ω9	0.28		< 0.05	-0.04
18:1ω11	n.n.d		0.09	
18:1ω9	< 0.05	-0.07	0.82	
18:1ω7	0.05		< 0.001	0.51
20:1ω11	< 0.05	0.19	0.09	
20:1ω9	0.13		< 0.05	-0.04
20:1ω7	0.10		n.n.d	
∑MUFA	0.43		0.15	
Polyunsaturated				
18:2ω6	< 0.001	-0.39	< 0.05	-0.35
18:3ω3	n.n.d		< 0.05	-0.04
20:2ω9	n.n.d		< 0.05	-0.02
20:2ω6	< 0.05	-0.03	0.07	
20:3ω6	< 0.001	-0.02	0.44	
20:4ω6	< 0.05	0.40	0.05	
20:5ω3	0.94		0.98	
22:2ω9 (NMI)	< 0.01	0.12	0.24	
22:3ω6	0.11		0.38	
22:4ω6	0.08		0.72	
22:5ω3	n.n.d		0.89	
∑PUFA	0.61		0.05	
Branched				
15:0iso	0.23		0.23	
15:0anteiso	0.30		0.86	
16:0iso	0.27		0.62	
17:0iso	0.38		n.n.d	
∑BrFA	0.16		n.n.d	
∑FA (mg g^{-1})	< 0.05	-0.88	0.21	

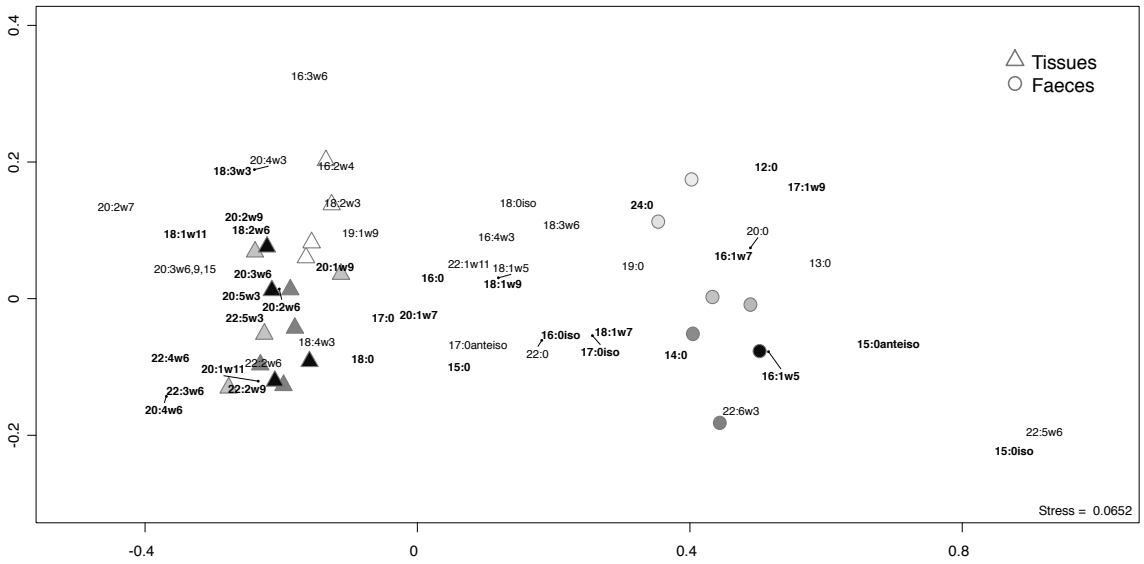

Figure 7-5 : Non-metric multidimensional scaling of individual fatty acid proportions (%) in tissues and faeces of *Nerita balteata*. FA displaying an average proportion greater than 0.8% within at least one group of samples are highlighted in bold

5. Discussion

5.1. Spatial differences in relative abundance of benthic microalgae

Diatoms strongly contribute to microphytobenthos assemblages in the Can Gio mangrove (Costa-Böddeker et al. 2017). Thus, different contributions of FA 16:1ω7, a diatom biomarker, in mangrove sediments may be used as a proxy for relative abundance of benthic microalgae (Aschenbroich et al. 2015). During the dry season, the higher proportions of this FA at site 1 in bordering fringe sediments suggest enhanced autotrophic production compared to sites 2 and 3 (Figure 7-2a). This higher microalgae relative abundance is likely to be induced by the uptake of nutrients originating from upstream wastewater discharges, whether they were released from shrimp farms (Anh et al. 2010), as observed in New Caledonia (Molnar et al. 2013), or from Ho Chi Minh City urban canals (Strady et al. 2017). The absence of such trend during the wet season suggests that inputs were more homogeneously distributed due to higher water discharge. Within the mangrove forest, the absence of spatial and seasonal differences in relative proportions of FA 16:1ω7 is probably due to high toxic tannin content of litter and light limitation (Alongi 1994). In addition, biofilm development at sediment surface, in which diatoms can grow, is linked to the position of the mangrove stand, leading to different canopy characteristics, soil water content, and nutrient

inputs, leading to high short scale heterogeneity in benthic primary production (Leopold et al. 2013).

Proportions of FA 16:1ω7 in tissues of the varunid crab *Metaplax elegans*, a direct consumer of microphytobenthos (see Chapter 6), reflect the observations made for bordering fringe sediments, with significant spatial differences between all sites, highest proportions at site 1 and lowest proportions at the reference site (Figure 7-2b and Figure 7-2c). In addition, differences were more significant during the dry season, in accordance with a more heterogeneous distribution of inputs during this season. It confirms the trophic transfer of FA from sediments to the crab hepatopancreas, and their storage into consumer muscles. Finally, it suggests that consumers may be more integrative and discriminating in tracking anthropogenic influence on trophic webs than food sources. Differences in relative contribution of FA 16:1ω7 are also observed in the mangrove murex snail *Chicoreus capucinus* (Figure 7-3a) despite it does not feed on microphytobenthos or on *M. elegans* (see Chapter 6). It indicates that anthropogenic pressures similarly affect other consumers than *M. elegans* and that this effect is transferred within trophic chains.

5.2. Metabolically implied fatty acids in consumers

Differences in both ω3/ω6 and EPA/ARA ratios of *M. elegans* and *C. capucinus* indicate that both species are subject to metabolic differences related to the salinity gradient (Figure 7-3c and Figure 7-4). In studies comparing fatty acid composition of wild vs. cultured aquatic species, it has generally been observed that EPA/ARA ratios were higher in cultured species compared to their wild counterparts (Dunstan et al. 1996, Ouraji et al. 2011). Such differences are essentially due to low proportions of ARA in cultured species (Ahlgren et al. 2009). They might be attributed to food sources, generally enriched in EPA and DHA compared to ARA (Ahlgren et al. 2009), but also induced by the release of ARA from phospholipids for the synthesis and secretion of prostaglandins in response to a stressor (Van Anholt et al. 2004). Most studies have been conducted on fishes and little is known regarding invertebrates species. However, this phenomenon has been suggested to happen in shrimps and a diet supplemented with ARA could minimise stress response and enhance some effectors of the immune system, such as clotting and respiratory burst (Aguilar et al. 2012). Higher EPA/ARA ratios in tissues of the varunid crab *M. elegans* in sites closer to the anthropogenic influence

suggest that differences may be caused as a response to stressors, even though it is not possible to link this response to a particular stressor, which would require experimental trials.

Higher proportions of HUFA in tissues of *C. capucinus* sampled in the more preserved mangrove zone (R) traduce the anthropogenic pressures on the food web on the main estuarine channel. Indeed, in an experimental study involving terrestrial snails *Helix pomatia* exposed to microdoses of molluscicides, Kowalczyk-Pecka et al. (2016) showed that proportions of HUFA in tissues decreased with increasing concentrations of the stressor. Since salinity at site R is between that of sites 2 and 3, such differences could not be related to salinity in our study, as previously observed in other species (Frolov et al. 1991, Romano et al. 2014), and might thus be induced by anthropogenic stressors, whether they are directly affecting *C. capucinus*, or the organisms these snails are feeding on. In addition, seasonal differences suggest that the influence of anthropogenic stressors was lower during the dry season, with lower proportions of FA 16:1ω7, higher proportions of HUFA and lower EPA/ARA ratios during this season.

5.3. Biosynthetic pathways of fatty acids in *Nerita balteata*

The absence of salinity gradient related alterations in the fatty acid profiles of the penaeid shrimps *Metapenaeus ensis* may be due to their mobility within the mangrove and their known seasonal changes in food resources (Stoner and Zimmerman 1988), allowing them to easily adapt their FA composition to stressors. The neritid snail *Nerita balteata* also have its fatty acid profile unaffected by external stressors despite its low mobility. However, changes in the FA composition of *N. balteata* during starvation may explain such stability.

The step decrease of the FA 18:2ω6 in both tissues and faeces during the first days of starvation indicates that this FA is an important component of the snail food resources and that it is rapidly excreted or converted after ingestion. This decrease, associated to a diminution of the FA 20:2ω6 and 20:3ω6 and an increase of the FA 20:4ω6 (ARA) highlight a biosynthetic pathway previously identified in other molluscs such as clams or cephalopods (Monroig et al. 2013). High relative proportions and rapid increase of ARA during starvation suggest that this metabolic pathway is particularly important in *N. balteata* (Table 7-3 and Figure 7-6).

Other pathways are highlighted using temporal variations in FA profiles during starvation. The FA 20:1ω11 is produced as a result of the elongation of saturated fatty acids to 18:0 or 20:0, and desaturation using the enzyme Δ9 desaturase (Figure 7-6). However, this FA is not further elongated to 22:1ω11 in *N. balteata*, unlike it has been observed in calanoid copepods (Kattner and Hagen 1995). The biosynthesis of FA 22:2ω9 has been evidenced in marine bivalves using 18:1ω9 as precursor, further chain elongation, and desaturation using the enzyme Δ5 desaturase (Zhukova 1991). This pathway leads to the production of non-methylene interrupted FA (NMI), which are unusual unsaturated fatty acids in that their double bonds are separated by more than one methylene group. The unusual double bond positions in NMI FA are considered to confer to cell membranes a higher resistance to oxidative processes and microbial lipases than the common PUFA (Barnathan 2009, Zhukova 2014). Thus, gastropods might be more resistant to anthropogenic stressors than other groups of invertebrates because of specific biosynthesis pathways of FA with protective function.

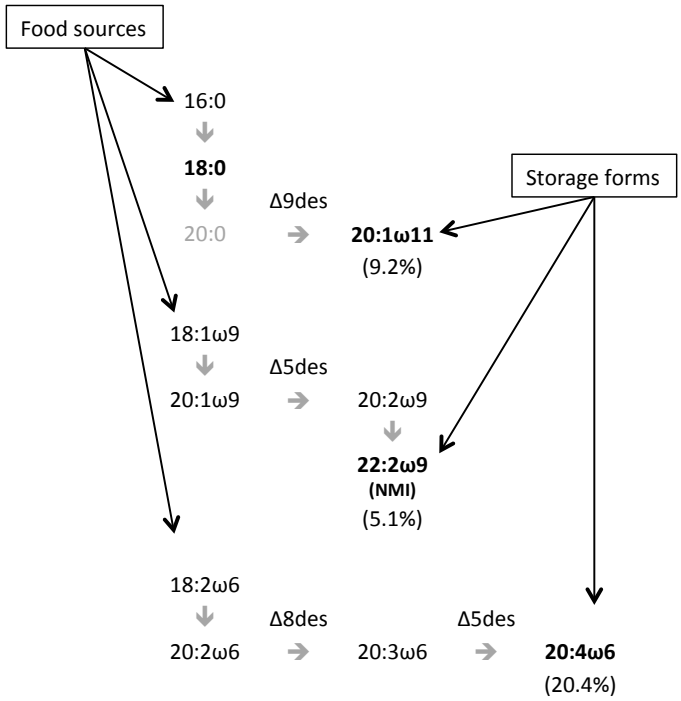

Figure 7-6: Major metabolic pathways for the synthesis of FA in the neritid snail *Nerita balteata*. Vertical arrows represent elongation and horizontal arrows correspond to desaturation processes with corresponding Δ desaturase enzyme. FA in bold showed increasing contributions to the pool of FA during starvation. The proportion of FA in grey was lower than 0.5% in both muscles and faeces and non-bold FA showed decreasing contributions to the pool of FA during starvation. Value between parentheses indicates the average proportion of corresponding FA measured in snail tissues after 20 days of starvation

6. Conclusion

Among the four benthic species studied, two exhibited spatial changes in their fatty acid composition that can be related to the intensity of anthropogenic pressures. The varunid crab *M. elegans* might be affected because of changes in its diet induced by higher relative abundance of benthic microalgae close to the inputs of anthropogenic wastewaters, thus enhancing the proportions of FA 16:1ω7 in both its hepatopancreas and muscles. The mangrove murex snail *C. capucinus* shows that predators are affected by the studied gradient, with increasing proportions of FA 16:1ω7 in its tissues, decreasing proportions of HUFA and increasing EPA/ARA ratios. Thus, the very likely influence of anthropogenic pressures on organisms' FA composition is transferred within trophic webs. The penaeid shrimp *Metapenaeus ensis* is poorly affected by the anthropogenic pressures probably because of its mobility within the mangrove and its seasonal changes in food resources. Finally, the neritid snail *Nerita balteata* might be less sensitive to anthropogenic stressors due to the synthesis of non-methylene interrupted FA, conferring to cell membranes a higher resistance to external stressors. Nevertheless, further studies would be required to evaluate in which terms changes in their FA ratios affect health condition of organisms and how these changes may affect the mangrove food web.

Conclusion et perspectives

1. Emissions de CO_2 des estuaires à mangrove

1.1. Quantification

Dans le chenal principal de l'estuaire à mangrove de la province de Can Gio, les émissions de CO_2 à l'interface eau/air varient de 74 à 876 mmolCO_2/m^2/j (voir chapitre 1). Recalculées sur une base annuelle, ces valeurs correspondent à des émissions de 27 à 320 molCO_2/m^2/an, avec une moyenne sur l'ensemble de l'estuaire estimée à 142 molCO_2/m^2/an. Ces valeurs sont très largement supérieures à celles rapportées par Chen et Borges (2009) dans leur synthèse bibliographique sur les émissions de CO_2 des estuaires à mangrove (5 à 56,5 molCO_2/m^2/an). Ainsi, il convient de se demander si cette différence provient d'une méthodologie inadaptée, ou si l'estuaire de Can Gio présente des émissions particulièrement élevées.

La différence majeure entre notre étude et celles compilées par Chen et Borges (2009) ou par Chen et al. (2013), qui présente une synthèse des émissions de CO_2 dans des estuaires de toute latitude, est l'approche méthodologique. La plupart des données ayant servi à la rédaction de ces articles de synthèse sont issues de mesures *in situ* de pCO_2, ou de mesures de pH et d'alcalinité permettant par la suite d'estimer la pCO_2 à l'aide des équations de Park (1969) et des constantes de solubilité de Millero et al. (2006) et Millero (2010). Les émissions de CO_2 sont ensuite calculées à partir d'équations établies pour les systèmes tempérés (Raymond and Cole 2001, Borges et al. 2004) ou pour l'interface entre l'océan et l'air (Wanninkhof et al. 1992). Les valeurs de pCO_2 mesurées dans notre étude sont élevées (voir chapitre 1), mais restent dans la gamme de valeurs observée dans les estuaires à mangrove (Chen et Borges 2009). Ainsi, ces émissions élevées semblent principalement dues au coefficient de transfert du CO_2, plus élevé dans notre étude que celui estimé par les équations théoriques.

Dans l'une des rares études ayant utilisé une chambre d'incubation flottante dans un estuaire à mangrove d'Asie du sud Est (Malaisie), Müller et al. (2016) ont mesuré des émissions de CO_2 de 268 ± 166 molCO_2/m^2/an dans l'estuaire le plus comparable à celui de la mangrove de Can Gio. Par ailleurs, en aval du barrage de petit saut, en Guyane, Guérin et al. (2007) ont aussi mesuré des émissions de CO_2 comparables aux nôtres, avec des valeurs moyennes autour de 295 molCO_2/m^2/an. En tenant compte de certaines précautions relatives

à leur utilisation (Vachon et al. 2010, Lorke et al. 2015), il semble donc approprié et recommandé d'utiliser des chambres d'incubation flottantes afin de mieux estimer les émissions de CO_2 dans les estuaires à mangrove. Par ailleurs, laisser dériver les chambres d'incubation au gré du courant permettrait d'obtenir des données continues et non plus uniquement aux étals comme nous avons été contraints de le faire. Ainsi, les mangroves sont certes parmi les écosystèmes ayant la plus forte productivité primaire, mais les estuaires les traversant sont quant à eux parmi les milieux les plus émetteurs de CO_2 par unité de surface.

1.2. Origine du CO_2 émis

Dans le chenal principal de l'estuaire à mangrove de la province de Can Gio, la pression partielle en CO_2 atteint ses valeurs maximales (5 000 µatm) au niveau du site le plus en amont et diminue avec le gradient de salinité, en étant toutefois fortement influencée par le stade de la marée (voir chapitre 1). Les quantités élevées de CO_2 entrant dans le système estuarien sont en partie dues aux rejets anthropiques, comme le montre aussi le taux de saturation en oxygène exceptionnellement bas (jusqu'à 17% en saison humide) et la proportion élevée de carbone organique dans la matière particulaire en suspension (jusqu'à 5,1%). Ces apports sont plus élevés en saison humide, certainement en raison du lessivage des sols qui apporte de la matière organique labile à l'écosystème. Pour une même salinité, le taux d'oxygène est alors plus bas et la pCO_2 plus élevée (voir chapitre 1). Dans l'estuaire, la proportion de matière organique dans la matière particulaire en suspension diminue de manière exponentielle au cours du transit estuarien, reflétant ainsi sa décomposition, tandis que les variations à court terme de pCO_2 liées au cycle tidal montrent qu'une proportion non négligeable du carbone émis vers l'atmosphère provient de la mangrove (voir chapitre 1).

Les estuaires tropicaux transportent de grandes quantités de carbone provenant de l'ensemble des bassins versants environnants (Huang et al. 2012). Toutefois, Cai (2011) suggère que les émissions de CO_2 importantes observées depuis les eaux côtières proviennent du transport latéral de carbone depuis les écosystèmes intertidaux, tels que les mangroves, plutôt que de la décomposition du carbone plus âgé et réfractaire provenant des zones en amont. La matière particulaire transportée par l'estuaire de Can Gio est en effet de nature principalement détritique, malgré des variations jour/nuit traduisant une production autotrophe durant la journée (voir chapitre 2).

En conditions expérimentales, la quantité de carbone organique particulaire présente dans l'eau de l'estuaire au début de la zone couverte par la forêt de mangrove reste stable (voire en légère augmentation) même après 16 jours d'incubation dans des conditions permettant sa décomposition aérobie (voir chapitre 4). Dans les effluents d'élevage crevetticoles, au contraire, 40% du carbone particulaire est minéralisé au cours des premières 24 h d'incubation, puis la quantité reste stable les 15 jours suivants (voir chapitre 4). De même, dans les eaux résiduelles urbaines, Marty et al. (1996) ont mesuré une perte d'environ 50% du carbone particulaire après 5 jours d'incubation puis une concentration restant relativement stable au cours des 55 jours restants de leur expérience. Ainsi, ces résultats suggèrent que le CO_2 émis par l'estuaire de Can Gio proche du site le plus en amont provient essentiellement de la minéralisation rapide des rejets anthropiques, qui sont les sources les plus proches, tandis qu'au cœur de la mangrove la pression partielle en CO_2 de l'estuaire est maintenue à un niveau élevé en raison des apports latéraux induits par le mécanisme de « tidal pumping » (Atkins et al. 2013, Call et al. 2015).

1.3. Rôle dans la régulation du climat

Les émissions de CO_2 mesurées dans l'estuaire de la mangrove de Can Gio suggèrent un rôle plus important des estuaires à mangrove dans le bilan global du carbone que précédemment établi. Dans la synthèse publiée par Chen et al. (2013), les émissions de CO_2 des estuaires à mangroves sont responsables de 8 à 10% des émissions de CO_2 de l'ensemble des estuaires, tandis qu'ils représentent 10 à 15% en superficie (Borges 2005, Borges et al. 2005, Chen et Borges 2009). En valeur absolue, ces émissions représentent 33 à 50 Tg C/an. Si l'ensemble des estuaires à mangroves étaient aussi émetteurs de CO_2 que celui de la province de Can Gio, cette valeur pourrait atteindre 273 Tg C/an (142 mol/m^2/an ramenés à une superficie de 160 000 km^2, les auteurs cités dans la synthèse de Chen et al. 2013 ayant assimilé la superficie des estuaires à mangroves à la superficie des écosystèmes de mangrove). Ces valeurs suggèrent aussi qu'une fraction des émissions de CO_2 des estuaires tropicaux, jusqu'à il y a peu prise en compte dans les bilans globaux comme d'origine naturelle (Ciais et al. 2014, Regnier et al. 2013), est en réalité induite par les rejets anthropiques. Cette « pollution cachée » et ce qu'elle implique seront discutées plus en détails dans la partie 3 : « influence des activités humaines sur l'écosystème ».

Afin d'évaluer le rôle des mangroves dans la régulation du climat, il est nécessaire d'établir des bilans de masse entre le carbone fixé par la mangrove et son devenir à différentes échelles temporelles, approximé par les formes sous lesquelles il est exporté/enfoui. Pour la mangrove de Can Gio, une partie du « carbone manquant » du bilan proposé par Bouillon et al. (2008a) est à rajouter dans le compartiment « émissions de CO_2 ». En effet, Bouillon et al. (2008a) ont considéré des émissions de CO_2 à l'interface eau/air égales aux émissions sédiment/air (21,9 mol CO_2/m^2/an), ceci en raison de la similitude des données de la littérature entre ces deux zones d'échange et de la difficulté à quantifier la proportion relative de l'une et de l'autre dans les mangroves, en raison de l'alternance des marées couvrant et découvrant les sols. Dans la mangrove de Can Gio, Nam et al. (2014) ont évalué la superficie couverte en permanence par les cours d'eau à 31% du total. En remplaçant 31% du flux de CO_2 estimé par Bouillon et al. (2008a) par les valeurs obtenues dans le chapitre 1 et en recalculant ces flux sur la base de la superficie mondiale des mangroves pour faciliter la comparaison, la fraction du carbone retournée à l'atmosphère serait de 85 Tg C/an, au lieu de 42 Tg C/an, pouvant ainsi expliquer le devenir de 38% du « carbone manquant » (112 Tg C/an). La mangrove de Can Gio est cependant située en zone tropicale et les émissions de CO_2 sont probablement au dessus des moyennes mondiales calculées par Bouillon et al. (2008) (tout comme la productivité primaire nette, plus importantes aux basses latitudes). Par ailleurs, les émissions ont été mesurées au niveau de l'estuaire et sont potentiellement plus faibles dans les chenaux intérieurs où le temps de résidence de l'eau est plus long. Ainsi, des données supplémentaires intégrant des mangroves de différentes latitudes et des chenaux de tailles diverses seraient nécessaires pour mieux affiner la proportion de « carbone manquant » émise sous forme de CO_2 à l'interface eau-air.

2. Rôle des organismes dans le cycle du carbone

2.1. Fixation du carbone minéral

Dans un chenal de vidange de la mangrove de Can Gio et la zone intertidale qui lui est adjacente, le carbone est premièrement fixé depuis l'atmosphère par les plantes aériennes (palétuviers et végétaux associés), puis il est libéré dans l'eau par le mécanisme de « tidal pumping » et de nouveau fixé, pour une partie au moins, par le phytoplancton (voir chapitre

5). Ainsi, la productivité du phytoplancton est soutenue par la présence de la mangrove environnante. Dans les estuaires à mangrove, la valeur moyenne de la productivité primaire du phytoplancton est faible (100 à 500 g C/m^2/an ; Cloern et al. 2014) en comparaison des zones couvertes par la forêt (1 362,5 ± 450 g C/m2/an ; Bouillon et al. 2008a). Cette productivité est probablement supérieure dans certaines zones de faible profondeur situées entre les chenaux de vidange et l'estuaire (voir chapitre 5), mais à l'échelle de l'ensemble de l'écosystème, la superficie couverte par ces zones reste faible. Ainsi, même si cette fixation secondaire joue un rôle important dans la couverture des besoins nutritionnels de certaines espèces vivant dans la mangrove, elle paraît peu impliquée dans le cycle du carbone.

2.2. Export de carbone vers l'océan

Bien que les feuilles de palétuviers constituent la principale source de matière organique disponible pour le vivant dans les mangroves, les espèces les plus mobiles semblent plutôt s'alimenter de matière particulaire en suspension dans la colonne d'eau (voir chapitre 6). Cette dernière est particulièrement nutritive proche des chenaux de vidange en raison des concentrations élevées de nutriments et de la faible hauteur d'eau (suffisamment transparente pour permettre la pénétration de la lumière) qui fournissent des conditions idéales pour la croissance du phytoplancton (voir chapitre 5). Ainsi, il est probable que les organismes côtiers (principalement crevettes, poissons et crabes nageurs) viennent dans la mangrove pour se nourrir de la matière particulaire qui y est présente et qu'ils soient accompagnés de prédateurs (espèces différentes appartenant aux mêmes groupes). Ces derniers suivent les consommateurs primaires mais sont aussi certainement capables de consommer des espèces peu mobiles se nourrissant de feuilles de palétuviers (crabes, escargots, zooplancton, méiofaune).

La méthode de pêche traditionnelle employée au Vietnam (et très certainement ailleurs), permettant la capture des crevettes, crabes et poissons de petite taille, consiste à tendre un filet maillant parallèlement à la bordure de la mangrove lors du flot puis à piéger les organismes lors de leur sortie de la mangrove au cours du jusant. C'est cette méthode qui a permis la capture des crevettes *Metapenaeus ensis*, *Macrobrachium equidens*, *Cloridopsis immaculata* et du poisson *Planiliza sp. B*. L'analyse des tissus de ces espèces montre cependant qu'elles consomment soit de la matière organique particulaire en suspension, soit

des organismes qui ont eux-mêmes consommé cette matière en suspension (voir chapitre 6). Ces espèces pourraient éventuellement ne rentrer dans la mangrove que pour se protéger des prédateurs, mais il semble tout de même difficile de n'avoir besoin de se cacher qu'à marée haute et il est donc probable qu'elles rentrent plutôt dans la mangrove pour s'alimenter. Les racines de palétuviers et l'ensemble des éléments augmentant la complexité structurelle du milieu agissent très certainement comme un peigne et fixent une très fine pellicule de matière en suspension à leur surface lors du flot. Cette matière devient ainsi accessible pour les organismes ramasseurs (« deposit-feeders ») tels que la crevette *Metapenaeus ensis*.

Quantifier l'export de carbone de ces organismes depuis les mangroves vers les écosystèmes côtiers est cependant très difficile car il est peu probable qu'ils soient répartis de manière homogène dans la colonne d'eau, comme cela est généralement admis en ce qui concernent le carbone dissous et particulaire. Pour cela, il faudrait arriver à quantifier la biomasse d'organismes entrant dans la mangrove lors du flot puis celle ressortant lors du jusant, ce qui paraît peu réalisable. Dans le bilan de masse entre le carbone fixé par la mangrove et son devenir, proposé par Bouillon et al. (2008a), l'export par le vivant est envisagé, comme le soutien l'hypothèse d' « outwelling » (Odum et Heald 1975, Lee 1995), mais non quantifié. La totalité du « carbone manquant » du bilan (112 Tg C/an) correspond à un export de 1,9 g C/m^2/j, soit environ la moitié de la productivité primaire des mangroves, estimée à 3,7 g C/m^2/j (Bouillon et al. 2008a). En considérant un taux de consommation de 2% par jour, correspondand au poids sec de matière consommé par poids vif d'un crabe consommateur de feuilles d'arbres (Olafsson et al. 2002), et 50% de carbone dans la matière organique, il faudrait 190 g d'organismes par m^2 entrant dans la mangrove lors du flot et en repartant lors du jusant pour exporter la totalité du « carbone manquant », soit 29 crevettes de 6-7 g chacune telles que *Metapenaeus ensis* (Chu et al. 1995). Abordé du point de vue d'une seule espèce, cet export paraît très invraisemblable, mais en considérant l'ensemble des espèces susceptibles d'entrer dans la mangrove lors du flot, y compris les prédateurs d'espèces consommant des feuilles d'arbres, il est possible qu'il ne soit pas négligeable. Ainsi, ce calcul suggère fortement que l'export par le vivant doit être considéré dans le bilan de carbone des mangroves.

3. Influence des activités humaines sur l'écosystème

3.1. Modification des flux et stocks de carbone

Le chapitre 1 suggère qu'une fraction des émissions de CO_2 des estuaires tropicaux, encore récemment prise en compte dans les bilans globaux comme d'origine naturelle (Ciais et al. 2014, Regnier et al. 2013), est en réalité induite par les rejets anthropiques. Ces rejets entrent ainsi dans la catégorie des « pollutions cachées », dont l'homme est responsable mais sans en être conscient, et dont les conséquences sont autant difficiles à appréhender que le problème est ignoré. Ces émissions représentent au moins 40 à 50% du carbone organique particulaire rejeté par les activités humaines (voir chapitre 4), qui est principalement contenu dans les eaux résiduelles urbaines et les effluents de crevetticulture dans cette région du monde (Lee 2016). A l'échelle globale, ces rejets ont été récemment estimés à 1,0 Pg C/an de plus qu'au cours de l'ère préindustrielle, dont ~0,5 Pg C/an sont rapidement réémis vers l'atmosphère, ce qui concorde avec nos observations (voir chapitre 4), ~0,4 Pg C/an sont stockés dans les sédiments et seulement ~0,1 Pg C/an arrivent jusqu'à l'océan (Regnier et al. 2013). Ces rejets de matière organique labile induisent aussi un effet « priming » qui pourrait contribuer de manière significative à la modification des flux de carbone dans les estuaires tropicaux et les océans côtiers (Guenet et al. 2010). En effet, dans les systèmes pélagiques, une augmentation de 10% de la quantité de matière organique labile induit une augmentation de 50 à 500% de la dégradation du carbone récalcitrant (Guenet et al. 2010). Le mécanisme responsable de cette augmentation n'a pas encore été identifié en milieu aquatique mais cette décomposition semble due à une stimulation du métabolisme microbien (Guenet et al. 2010).

Au delà de l'effet sur les masses d'eau, cet effet « priming » pourrait induire la minéralisation de la matière organique stockée dans les sédiments de mangrove. En effet, 49 à 98% du carbone des mangroves est stocké dans les sols, sous une forme récalcitrante (Donato et al. 2011). Ce phénomène de « priming » ayant été premièrement mis en évidence dans des sols, bien que non-inondés, il est possible qu'il soit aussi présent dans les sédiments de mangrove. Ainsi, il est possible qu'une partie des variations de pCO_2 observées dans l'estuaire de Can Gio et liées aux exports depuis la mangrove soit due à un effet accélérateur du « priming » et à la décomposition de matière organique récalcitrante.

3.2. Impact sur les réseaux trophiques

Le chapitre 7 suggère que le régime alimentaire et le métabolisme de certaines espèces vivant dans la mangrove de Can Gio sont affectés par la pression anthropique. Cependant, notre étude ne permet pas de savoir si ces espèces sont affectées positivement ou négativement. Le fait que la production primaire benthique soit augmentée par les rejets anthropiques de nutriments indique plutôt que la nourriture est plus abondante, et donc que l'écosystème est capable de nourrir une plus grande biomasse de consommateurs, tandis que l'augmentation du ratio 20:5ω3/20:4ω6 dans les zones sous pression anthropique va dans le même sens que les différences observées pour une espèce de crevettes en conditions d'élevage et sauvage (Ouraji et al. 2011). Cette différence est susceptible de modifier la réponse immunitaire des organismes. En effet, ces deux acides gras entrent en compétition pour l'accès à la même enzyme permettant leur oxydation en eicosanoïdes, qui sont des hormones à courte durée de vie intervenant dans divers processus physiologiques dont la régulation de la coagulation du sang, la reproduction, les fonctions rénales ou les processus inflammatoires (Tocher et Glencross 2015). La survie des organismes en cas d'infection virale ou bactérienne pourrait ainsi en être affectée, de même que leur succès de reproduction, mais sans que l'on puisse à ce jour prévoir dans quel sens.

D'autres études mettent en avant une modification de la stœchiométrie des éléments chimiques de la matière organique dissoute, principalement C, N et P, due au changement d'occupation des sols et pouvant induire des modifications du fonctionnement de la boucle microbienne (Gücker et al. 2016). Par ailleurs, Lee (2016) suggère qu'un remplacement des apports de « blue carbon » provenant des mangroves par du « black carbon » provenant des rejets anthropiques, ainsi que des apports supplémentaires de nutriments, pourrait conduire à des impacts négatifs sur les écosystèmes peu tolérants à des charges élevés de nutriments tels que les coraux. Si dans ce dernier cas, le dépassement d'un seuil de tolérance à des conséquences facilement imaginables pour certaines espèces, l'effet du changement de ratio d'un élément par rapport à un autre sur un écosystème est quant à lui bien plus difficile à appréhender (Sardans et al. 2012). Il est généralement admis qu'un écosystème non soumis à la pression anthropique est dans un bon état de santé. Mais est-ce réellement le cas replacé à la lumière de l'évolution et de la lutte pour la survie ? Et reste encore des écosystèmes « référence » non soumis aux perturbations humaines ?

Bibliographie

- A -

Abrantes, K., Sheaves, M., 2009. Food web structure in a near-pristine mangrove area of the Australian wet tropics. Estuarine, Coastal and Shelf Science 82, 597–607.

Abrantes, K., Johnston, R., Connolly, R.M., Sheaves, M., 2015. Importance of mangrove carbon for aquatic food webs in wet–dry tropical estuaries. Estuaries and Coasts 38, 383–399.

Abril, G., Bouillon, S., Darchambeau, F., Teodoru, C.R., Marwick, T.R., Tamooh, F., Ochieng Omengo, F., Geeraert, N., Deirmendjian, L., Polsenaere, P., Borges, A.V., 2015. Technical note: large overestimation of pCO_2 calculated from pH and alkalinity in acidic, organic-rich freshwaters. Biogeosciences 12, 67–78.

Abril, G., Commarieu, M.-V., Sottolichio, A., Bretel, P., Guérin, F., 2009. Turbidity limits gas exchange in a large macrotidal estuary. Estuarine, Coastal and Shelf Science 83, 342–348.

Abril, G., Deborde, J., Savoye, N., Mathieu, F., Moreira-Turcq, P., Artigas, F., Meziane, T., Takiyama, L.R., de Souza, M.S., Seyler, P., 2013. Export of ^{13}C-depleted dissolved inorganic carbon from a tidal forest bordering the Amazon estuary. Estuarine, Coastal and Shelf Science 129, 23–27.

Adame, M.F., Reef, R., Herrera-Silveira, J.A., Lovelock, C.E., 2012. Sensitivity of dissolved organic carbon exchange and sediment bacteria to water quality in mangrove forests. Hydrobiologia 691, 239–253.

Aguilar, V., Racotta, I.S., Goytortúa, E., Wille, M., Sorgeloos, P., Civera, R., Palacios, E., 2012. The influence of dietary arachidonic acid on the immune response and performance of Pacific whiteleg shrimp, *Litopenaeus vannamei*, at high stocking density: ARA influences response to stocking density in shrimp. Aquaculture Nutrition 18, 258–271.

Ahlgren, G., Vrede, T., Goedkoop, W., 2009. Fatty Acid Ratios in Freshwater Fish, Zooplankton and Zoobenthos – Are There Specific Optima?, in: Kainz, M., Brett, M.T., Arts, M.T. (Eds.), Lipids in Aquatic Ecosystems. Springer New York, pp. 147–178.

Al-Ahmad, A., Daschner, F.D., Kümmerer, K., 1999. Biodegradability of cefotiam, ciprofloxacin, meropenem, penicillin G, and sulfamethoxazole and inhibition of waste water bacteria. Archives of Environmental Contamination and toxicology 37, 158–163.

Alfaro, A.C., 2008. Diet of *Littoraria scabra*, while vertically migrating on mangrove trees: Gut content, fatty acid, and stable isotope analyses. Estuarine, Coastal and Shelf Science 79, 718–726.

Alfaro, A.C., Thomas, F., Sergent, L., Duxbury, M., 2006. Identification of trophic interactions within an estuarine food web (northern New Zealand) using fatty acid biomarkers and stable isotopes. Estuarine, Coastal and Shelf Science 70, 271–286.

Alongi, D.M., 1994. Zonation and seasonality of benthic primary production and community respiration in tropical mangrove forests. Oecologia 98, 320–327.

Alongi, D.M., 2008. Mangrove forests: resilience, protection from tsunamis, and responses to global climate change. Estuarine, Coastal and Shelf Science 76, 1–13.

Alongi, D.M., 2009. The energetics of mangrove forests. Springer, S.l.

Alongi, D.M., 2014. Carbon cycling and storage in mangrove forests. Annual Review of Marine Science 6, 195–219.

Amorocho, J., DeVries, J.J., 1980. A new evaluation of the wind stress coefficient over water surfaces. Journal of Geophysical Research: Oceans 85 : 433–442.

Anh, P.T., Kroeze, C., Bush, S.R., Mol, A.P.J., 2010. Water pollution by intensive brackish shrimp farming in south-east Vietnam: causes and options for control. Agricultural Water Management 97, 872–882.

Antonio, E.S., Richoux, N.B., 2016. Tide-induced variations in the fatty acid composition of estuarine particulate organic matter. Estuaries and Coasts 39, 1072–1083.

Arnaud-Haond, S., Duarte, C.M., Teixeira, S., Massa, S.I., Terrados, J., Tri, N.H., Hong, P.N. and Serrão, E.A., 2009. Genetic recolonization of mangrove: genetic diversity still increasing in the Mekong Delta 30 years after Agent Orange. Marine Ecology Progress Series 390, 129-135.

Arnosti, C., 2011. Microbial extracellular enzymes and the marine carbon cycle. Annual Review of Marine Science 3, 401–425.

Aschenbroich, A., Marchand, C., Molnar, N., Deborde, J., Hubas, C., Rybarczyk, H., Meziane, T., 2015. Spatio-temporal variations in the composition of organic matter in surface sediments of a mangrove receiving shrimp farm effluents (New Caledonia). Science of The Total Environment 512–513, 296–307.

Atkins, M.L., Santos, I.R., Ruiz-Halpern, S., Maher, D.T., 2013. Carbon dioxide dynamics driven by groundwater discharge in a coastal floodplain creek. Journal of Hydrology 493, 30–42.

Avnimelech, Y., Ritvo, G., 2003. Shrimp and fish pond soils: processes and management. Aquaculture 220, 549–567.

Azam, F., 1998. Microbial control of oceanic carbon flux: the plot thickens. Science 280, 694–696.

- B -

Baltar, F., Morán, X.A.G., Lønborg, C., 2017. Warming and organic matter sources impact the proportion of dissolved to total activities in marine extracellular enzymatic rates. Biogeochemistry 133, 307–316.

Bano, N., Nisa, M.-U., Khan, N., Saleem, M., Harrison, P.J., Ahmed, S.I., Azam, F., 1997. Significance of bacteria in the flux of organic matter in the tidal creeks of the mangrove ecosystem of the Indus River delta, Pakistan. Marine Ecology Progress Series 1–12.

Barnathan, G., 2009. Non-methylene-interrupted fatty acids from marine invertebrates: occurrence, characterization and biological properties. Biochimie 91, 671–678.

Beck, M.W., Heck, K.L., Able, K.W., Childers, D.L., Eggleston, D.B., Gillanders, B.M., Halpern, B., Hays, C.G., Hoshino, K., Minello, T.J., Orth, R.J., Sheridan, P.F., Weinstein, M.P., 2001. The identification, conservation, and management of estuarine and marine nurseries for fish and invertebrates. BioScience 51, 633.

Becquevort, S., Rousseau, V., Lancelot, C., 1998. Major and comparable roles for free-living and attached bacteria in the degradation of *Phaeocystis*-derived organic matter in Belgian coastal waters of the North Sea. Aquatic Microbial Ecology 14, 39–48.

Benson, B.B., Krause, D., 1984. The concentration and isotopic fractionation of oxygen dissolved in freshwater and seawater in equilibrium with the atmosphere. Limnology and oceanography 29, 620–632.

Bergamino, L., Dalu, T., Richoux, N.B., 2014. Evidence of spatial and temporal changes in sources of organic matter in estuarine sediments: stable isotope and fatty acid analyses. Hydrobiologia 732, 133–145.

Bergé, J.-P., Barnathan, G., 2005. Fatty acids from lipids of marine organisms: molecular biodiversity, roles as biomarkers, biologically active compounds, and economical aspects, in: Ulber, R., Le Gal, Y. (Eds.), Marine Biotechnology I. Springer Berlin Heidelberg, Berlin, Heidelberg, pp. 49–125.

Bhaskar, P.V., Bhosle, N.B., 2008. Bacterial production, glucosidase activity and particle-associated carbohydrates in Dona Paula bay, west coast of India. Estuarine, Coastal and Shelf Science 80, 413–424.

Bianchi, T.S., Bauer, J.E., 2011. Particulate organic carbon cycling and transformation, in: Treatise on Estuarine and Coastal Science. Elsevier, pp. 69–117.

Bidle, K.D., Falkowski, P.G., 2004. Cell death in planktonic, photosynthetic microorganisms. Nature Reviews Microbiology 2, 643–655.

Biswas, H., Jie, J., Li, Y., Zhang, G., Zhu, Z.-Y., Wu, Y., Zhang, G.-L., Li, Y.-W., Liu, S.M., Zhang, J., 2015. Response of a natural Phytoplankton community from the Qingdao coast (Yellow Sea, China) to variable CO_2 levels over a short-term incubation experiment. Current Science.

Bligh, E.G., Dyer, W.J., 1959. A rapid method of total lipid extraction and purification. Canadian Journal of Biochemistry and Physiology 37, 911–917.

Bodineau, L., Thoumelin, G., Béghin, V., Wartel, M., 1998. Tidal time-scale changes in the composition of particulate organic matter within the estuarine turbidity maximum zone in the macrotidal Seine Estuary, France: the use of fatty acid and sterol biomarkers. Estuarine, Coastal and Shelf Science 47, 37–49.

Boëchat, I.G., Krüger, A., Chaves, R.C., Graeber, D., Gücker, B., 2014. Land-use impacts on fatty acid profiles of suspended particulate organic matter along a larger tropical river. Science of The Total Environment 482–483, 62–70.

Borges, A.V., 2005. Do we have enough pieces of the jigsaw to integrate CO_2 fluxes in the Coastal Ocean? Estuaries 28.

Borges, A.V., Abril, G., 2011. 5.04-Carbon dioxide and methane dynamics in estuaries. Treatise on Estuarine and Coastal Science, Volume 5: Biogeochemistry 119–161.

Borges, A.V., Delille, B., Frankignoulle, M., 2005. Budgeting sinks and sources of CO_2 in the coastal ocean: diversity of ecosystems counts. Geophysical Research Letters 32.

Borges, A.V., Vanderborght, J.-P., Schiettecatte, L.-S., Gazeau, F., Ferrón-Smith, S., Delille, B., Frankignoulle, M., 2004. Variability of the gas transfer velocity of CO_2 in a macrotidal estuary (the Scheldt). Estuaries 27, 593–603.

Bouchez, A., Pascault, N., Chardon, C., Bouvy, M., Cecchi, P., Lambs, L., Herteman, M., Fromard, F., Got, P., Leboulanger, C., 2013. Mangrove microbial diversity and the impact of trophic contamination. Marine Pollution Bulletin 66, 39–46.

Bouillon, S., Borges, A.V., Castañeda-Moya, E., Diele, K., Dittmar, T., Duke, N.C., Kristensen, E., Lee, S.Y., Marchand, C., Middelburg, J.J., Rivera-Monroy, V.H., Smith, T.J., Twilley, R.R., 2008a. Mangrove production and carbon sinks: a revision of global budget estimates. Global Biogeochemical Cycles 22.

Bouillon, S., Connolly, R.M., Gillikin, D.P., 2011. Use of stable isotopes to understand food webs and ecosystem functioning in estuaries, in: Treatise on Estuarine and Coastal Science. Elsevier, pp. 143–173.

Bouillon, S., Connolly, R.M., Lee, S.Y., 2008b. Organic matter exchange and cycling in mangrove ecosystems: Recent insights from stable isotope studies. Journal of Sea Research 59, 44–58.

Bouillon, S., Koedam, N., Raman, A., Dehairs, F., 2002. Primary producers sustaining macro-invertebrate communities in intertidal mangrove forests. Oecologia 130, 441–448.

Bouillon, S., Middelburg, J.J., Dehairs, F., Borges, A.V., Abril, G., Flindt, M.R., Ulomi, S., Kristensen, E., 2007. Importance of intertidal sediment processes and porewater exchange on the water column biogeochemistry in a pristine mangrove creek (Ras Dege, Tanzania). Biogeosciences 4, 311–322.

Bouillon, S., Moens, T., Overmeer, I., Koedam, N., Dehairs, F., 2004. Resource utilization patterns of epifauna from mangrove forests with contrasting inputs of local versus imported organic matter. Marine Ecology Progress Series 278, 77–88.

Brown, M.R., Dunstan, G.A., Norwood, S., Miller, K.A., others, 1996. Effects of harvest stage and light on the biochemical composition of the diatom *Thalassiosira pseudonana*. Journal of phycology 32, 64–73.

Budge, S.M., Iverson, S.J., Koopman, H.N., 2006. Studying trophic ecology in marine ecosystems using fatty acids: a primer on analysis and interpretation. Marine Mammal Science 22, 759–801.

Budge, S.M., Parrish, C.C., 1998. Lipid biogeochemistry of plankton, settling matter and sediments in Trinity Bay, Newfoundland. II. Fatty acids. Organic Geochemistry 29, 1547–1559.

Budge, S.M., Parrish, C.C., Mckenzie, C.H., 2001. Fatty acid composition of phytoplankton, settling particulate matter and sediments at a sheltered bivalve aquaculture site. Marine Chemistry 76, 285–303.

Bui, T.H.H., Lee, S.Y., 2014. Does “You Are What You Eat” Apply to Mangrove Grapsid Crabs? PLoS ONE 9, e89074.

Burford, M.A., Costanzo, S.D., Dennison, W.C., Jackson, C.J., Jones, A.B., McKinnon, A.D., Preston, N.P., Trott, L.A., 2003. A synthesis of dominant ecological processes in intensive shrimp ponds and adjacent coastal environments in NE Australia. Marine Pollution Bulletin 46, 1456–1469.

- C -

Cabaniss, S.E., Madey, G., Leff, L., Maurice, P.A., Wetzel, R., 2005. A Stochastic Model for the Synthesis and Degradation of Natural Organic Matter. Part I. Data Structures and Reaction Kinetics. Biogeochemistry 76, 319–347.

Cai, W.-J., 2011. Estuarine and coastal ocean carbon paradox: CO_2 sinks or sites of terrestrial carbon incineration? Annual Review of Marine Science 3, 123–145.

Call, M., Maher, D.T., Santos, I.R., Ruiz-Halpern, S., Mangion, P., Sanders, C.J., Erler, D.V., Oakes, J.M., Rosentreter, J., Murray, R., Eyre, B.D., 2015. Spatial and temporal variability of carbon dioxide and methane fluxes over semi-diurnal and spring–neap–spring timescales in a mangrove creek. Geochimica et Cosmochimica Acta 150, 211–225.

Camilleri, J.C., 1992. Leaf-litter processing by invertebrates in a mangrove forest in Queensland. Marine Biology 114, 139–145.

Cannicci, S., Bartolini, F., Dahdouh-Guebas, F., Fratini, S., Litulo, C., Macia, A., Mrabu, E.J., Penha-Lopes, G., Paula, J., 2009. Effects of urban wastewater on crab and mollusc assemblages in equatorial and subtropical mangroves of East Africa. Estuarine, Coastal and Shelf Science 84, 305–317.

Canuel, E.A., 2001. Relations between river flow, primary production and fatty acid composition of particulate organic matter in San Francisco and Chesapeake Bays: a multivariate approach. Organic Geochemistry 32, 563–583.

Caraco, N.F., Lampman, G., Cole, J.J., Limburg, K.E., Pace, M.L., Fischer, D., 1998. Microbial assimilation of DIN in a nitrogen rich estuary: implications for food quality and isotope studies. Marine Ecology Progress Series 167, 59–71.

Chen, C.-T.A., Borges, A.V., 2009. Reconciling opposing views on carbon cycling in the coastal ocean: continental shelves as sinks and near-shore ecosystems as sources of atmospheric CO_2. Deep Sea Research Part II: Topical Studies in Oceanography 56, 578–590.

Chen, C.-T.A., Huang, T.-H., Chen, Y.-C., Bai, Y., He, X., Kang, Y., 2013. Air–sea exchanges of CO_2 in the world's coastal seas. Biogeosciences 10, 6509–6544.

Chen, G.C., Tam, N.F.Y., Ye, Y., 2012. Spatial and seasonal variations of atmospheric N_2O and CO_2 fluxes from a subtropical mangrove swamp and their relationships with soil characteristics. Soil Biology and Biochemistry 48, 175–181.

Cho, B.C., Azam, F., 1990. Biogeochemical significance of bacterial biomass in the ocean's euphotic zone. Marine Ecology Progress Series 253–259.

Chouvelon, T., Schaal, G., Grall, J., Pernet, F., Perdriau, M., A-Pernet, E.J., Le Bris, H., 2015. Isotope and fatty acid trends along continental shelf depth gradients: inshore versus offshore hydrological influences on benthic trophic functioning. Progress in Oceanography 138, 158–175.

Christensen, J.T., Sauriau, P.-G., Richard, P., Jensen, P.D., 2001. Diet in mangrove snails: preliminary data on gut contents and stable isotope analysis. Journal of Shellfish Research 20, 423–426.

Chu, K.H., Chen, Q.C., Huang, L.M., Wong, C.K., 1995. Morphometric analysis of commercially important penaeid shrimps from the Zhujiang estuary, China. Fisheries Research 23, 83–93.

Chróst, R.J., 1991. Environmental control of the synthesis and activity of aquatic microbial ectoenzymes, in: Chróst, R.J. (Ed.), Microbial Enzymes in Aquatic Environments. Springer New York, New York, NY, pp. 29–59.

Ciais, P., Sabine, C., Bala, G., Bopp, L., Brovkin, V., Canadell, J., Chhabra, A., DeFries, R., Galloway, J., Heimann, M., others, 2014. Carbon and other biogeochemical cycles, in: Climate Change 2013: The Physical Science Basis. Contribution of Working Group I to the Fifth Assessment Report of the Intergovernmental Panel on Climate Change. Cambridge University Press, pp. 465–570.

Claudino, M.C., Pessanha, A.L.M., Araújo, F.G., Garcia, A.M., 2015. Trophic connectivity and basal food sources sustaining tropical aquatic consumers along a mangrove to ocean gradient. Estuarine, Coastal and Shelf Science 167, 45–55.

Cloern, J.E., 2001. Our evolving conceptual model of the coastal eutrophication problem. Marine ecology progress series 210, 223–253.

Cloern, J.E., Canuel, E.A., Harris, D., 2002. Stable carbon and nitrogen isotope composition of aquatic and terrestrial plants of the San Francisco Bay estuarine system. Limnology and oceanography 47, 713–729.

Cloern, J.E., Foster, S.Q., Kleckner, A.E., 2014. Phytoplankton primary production in the world's estuarine-coastal ecosystems. Biogeosciences 11, 2477–2501.

Connelly, T., McClelland, J., Crump, B., Kellogg, C., Dunton, K., 2015. Seasonal changes in quantity and composition of suspended particulate organic matter in lagoons of the Alaskan Beaufort Sea. Marine Ecology Progress Series 527, 31–45.

Costa-Böddeker, S., Thuyên, L.X., Schwarz, A., Huy, H.Đ., Schwalb, A., 2017. Diatom assemblages in surface sediments along nutrient and salinity gradients of Thi Vai estuary and Can Gio mangrove forest, Southern Vietnam. Estuaries and Coasts 40, 479–492.

Cunha, A., Almeida, A., 2006. Influence of an estuarine plume and marine sewage outfall on the dynamics of coastal bacterioplankton communities. Aquatic microbial ecology 44, 253–262.

Cunha, M.A., Almeida, M.A., Alcântara, F., 2000. Patterns of ectoenzymatic and heterotrophic bacterial activities along a salinity gradient in a shallow tidal estuary. Marine Ecology Progress Series 204, 1–12.

Cunliffe, M., Engel, A., Frka, S., Gašparović, B., Guitart, C., Murrell, J.C., Salter, M., Stolle, C., Upstill-Goddard, R., Wurl, O., 2013. Sea surface microlayers: a unified physicochemical and biological perspective of the air–ocean interface. Progress in Oceanography 109, 104–116.

Currie, B.R., Johns, R.B., 1988. Lipids as indicators of the origin of organic matter in fine marine particulate matter. Marine and Freshwater Research 39, 371–383.

- D -

Dalsgaard, J., St. John, M., Kattner, G., Müller-Navarra, D., Hagen, W., 2003. Fatty acid trophic markers in the pelagic marine environment, in: Advances in Marine Biology. Elsevier, pp. 225–340.

De Brabandere, L., Dehairs, F., Van Damme, S., Brion, N., Meire, P., Daro, N., 2002. $\delta^{15}N$ and $\delta^{13}C$ dynamics of suspended organic matter in freshwater and brackish waters of the Scheldt estuary. Journal of Sea Research 48, 1–15.

De Souza, M.-J.B., Nair, S., Bharathi, P.L., Chandramohan, D., 2003. Particle-associated bacterial dynamics in a tropical tidal plain (Zuari estuary, India). Aquatic microbial ecology 33, 29–40.

Diele, K., Tran Ngoc, D.M., Geist, S.J., Meyer, F.W., Pham, Q.H., Saint-Paul, U., Tran, T., Berger, U., 2013. Impact of typhoon disturbance on the diversity of key ecosystem engineers in a monoculture mangrove forest plantation, Can Gio Biosphere Reserve, Vietnam. Global and Planetary Change 110, 236–248.

Ding, H., Sun, M.-Y., 2005. Biochemical degradation of algal fatty acids in oxic and anoxic sediment–seawater interface systems: effects of structural association and relative roles of aerobic and anaerobic bacteria. Marine Chemistry 93, 1–19.

Dingle, H., Caldwell, R.L., 1975. Distribution, abundance, and interspecific agonistic behavior of two mudflat stomatopods. Oecologia 20, 167–178.

Dittel, A.I., Epifanio, C.E., Cifuentes, L.A., Kirchman, D.L., 1997. Carbon and nitrogen sources for shrimp postlarvae fed natural diets from a tropical mangrove system. Estuarine, Coastal and Shelf Science 45, 629–637.

Dittmar, T., Hertkorn, N., Kattner, G., Lara, R.J., 2006. Mangroves, a major source of dissolved organic carbon to the oceans. Global Biogeochemical Cycles 20.

Donato, D.C., Kauffman, J.B., Murdiyarso, D., Kurnianto, S., Stidham, M., Kanninen, M., 2011. Mangroves among the most carbon-rich forests in the tropics. Nature Geoscience 4, 293–297.

Droppo, I.G., 2001. Rethinking what constitutes suspended sediment. Hydrological Processes 15, 1551–1564.

Dubois, S., Blanchet, H., Garcia, A., Massé, M., Galois, R., Grémare, A., Charlier, K., Guillou, G., Richard, P., Savoye, N., 2014. Trophic resource use by macrozoobenthic primary consumers within a semi-enclosed coastal ecosystem: stable isotope and fatty acid assessment. Journal of Sea Research 88, 87–99.

Duke, N.C., 2016. Oil spill impacts on mangroves: recommendations for operational planning and action based on a global review. Marine Pollution Bulletin 109, 700–715.

Duke, N.C., Ball, M.C., Ellison, J.C., 1998. Factors influencing biodiversity and distributional gradients in mangroves. Global Ecology and Biogeography Letters 7, 27.

Duke, N.C., Bochove, J.-W. van, United Nations Environment Programme, 2014. The importance of mangroves to people: a call to action.

Dung, L.V., Tue, N.T., Nhuan, M.T. and Omori, K., 2016. Carbon storage in a restored mangrove forest in Can Gio Mangrove Forest Park, Mekong Delta, Vietnam. Forest Ecology and Management 380, 31-40.

Dunn, R.J.K., Welsh, D.T., Teasdale, P.R., Lee, S.Y., Lemckert, C.J., Meziane, T., 2008. Investigating the distribution and sources of organic matter in surface sediment of Coombabah Lake (Australia) using elemental, isotopic and fatty acid biomarkers. Continental Shelf Research 28, 2535–2549.

Dunstan, G.A., Baillie, H.J., Barrett, S.M., Volkman, J.K., 1996. Effect of diet on the lipid composition of wild and cultured abalone. Aquaculture 140, 115–127.

Durand, J.-D., Hubert, N., Shen, K.-N., Borsa, P., 2017. DNA barcoding grey mullets. Reviews in Fish Biology and Fisheries 27, 233–243.

- E -

Eichhorst, T.E., 2016. Neritidae of the World. ConchBooks.

Eisma, D., 1986. Flocculation and de-flocculation of suspended matter in estuaries. Netherlands Journal of Sea Research 20, 183–199.

Eltgroth, M.L., Watwood, R.L., Wolfe, G.V., 2005. Production and cellular localization of neutral long-chain lipids in the haptophyte algae *Isochrysis galbana* and *Emiliania huxleyi*. Journal of Phycology 41, 1000–1009.

- F -

FAO, 2007. The World's Mangroves, 1980-2005: a thematic study prepared in the framework of the global forest resources assessment 2005. Food and Agriculture Organization of the United Nations.

FAO Fisheries and Aquaculture Department, 2017. Statistics and Information Service FishStatJ: Universal software for fishery statistical time series.

Fernandes, L., 2011. Origin and biochemical cycling of particulate nitrogen in the Mandovi estuary. Estuarine, Coastal and Shelf Science 94, 291–298.

Filimonova, V., Gonçalves, F., Marques, J.C., De Troch, M., Gonçalves, A.M.M., 2016. Fatty acid profiling as bioindicator of chemical stress in marine organisms: a review. Ecological Indicators 67, 657–672.

Findlay, S., Pace, M.L., Lints, D., Cole, J.J., Caraco, N.F., Peierls, B., 1991. Weak coupling of bacterial and algal production in a heterotrophic ecosystem: the Hudson River estuary. Limnology and Oceanography 36, 268–278.

Finlay, J.C., 2003. Controls of streamwater dissolved inorganic carbon dynamics in a forested watershed. Biogeochemistry 62, 231–252.

Fischer, A.M., Ryan, J.P., Levesque, C., Welschmeyer, N., 2014. Characterizing estuarine plume discharge into the coastal ocean using fatty acid biomarkers and pigment analysis. Marine Environmental Research 99, 106–116.

Fogel, M.L., Cifuentes, L.A., Velinsky, D.J., Sharp, J.H., 1992. Relationship of carbon availability in estuarine phytoplankton to isotopic composition. Marine Ecology Progress Series 82, 291–300.

France, R., 1998. Estimating the assimilation of mangrove detritus by fiddler crabs in Laguna Joyuda, Puerto Rico, using dual stable isotopes. Journal of Tropical Ecology 14, 413–425.

Frankignoulle, M., Borges, A., Biondo, R., 2001. A new design of equilibrator to monitor carbon dioxide in highly dynamic and turbid environments. Water Research 35, 1344–1347.

Friedrich, U., Schallenberg, M., Holliger, C., 1999. Pelagic bacteria–particle interactions and community-specific growth rates in four lakes along a trophic gradient. Microbial ecology 37, 49–61.

Froelich, P., Klinkhammer, G.P., Bender, M.L., Luedtke, N.A., Heath, G.R., Cullen, D., Dauphin, P., Hammond, D., Hartman, B., Maynard, V., 1979. Early oxidation of organic matter in pelagic sediments of the eastern equatorial Atlantic: suboxic diagenesis. Geochimica et cosmochimica acta 43, 1075–1090.

Frolov, A.V., Pankov, S.L., Geradze, K.N., Pankova, S.A., 1991. Influence of salinity on the biochemical composition of the rotifer *Brachionus plicatilis* (Muller). Aspects of adaptation. Comparative Biochemistry and Physiology Part A: Physiology 99, 541–550.

Fromard, F., Kiet, L. K., 2002. Les mangroves du Vietnam du Sud : histoire récente, dynamique actuelle et perspectives Bois et Forêts des tropiques, 2002, N° 273 (3), Dossier Vietnam du Sud/Mangrove.

Fry, B., 2006. Stable isotope ecology. Springer, New York, NY.

Fry, B., Cormier, N., 2011. Chemical Ecology of Red Mangroves, *Rhizophora mangle*, in the Hawaiian Islands 1. Pacific Science 65, 219–234.

Fuhrman, J.A., Noble, R.T., 1995. Viruses and protists cause similar bacterial mortality in coastal seawater. Limnology and Oceanography 40, 1236–1242.

- G -

Gatune, W., Vanreusel, A., Ruwa, R., Bossier, P., De Troch, M., 2014. Fatty acid profiling reveals a trophic link between mangrove leaf litter biofilms and the post-larvae of giant tiger shrimp *Penaeus monodon*. Aquaculture Environment Interactions 6, 1–10.

Ghaderpour, A., Ho, W.S., Chew, L.-L., Bong, C.W., Chong, V.C., Thong, K.-L., Chai, L.C., 2015. Diverse and abundant multi-drug resistant *E. coli* in Matang mangrove estuaries, Malaysia. Frontiers in Microbiology 6.

Gleeson, J., Santos, I.R., Maher, D.T., Golsby-Smith, L., 2013. Groundwater–surface water exchange in a mangrove tidal creek: evidence from natural geochemical tracers and implications for nutrient budgets. Marine Chemistry 156, 27–37.

Gonsalves, M., Nair, S., Loka Bharathi, P., Chandramohan, D., 2009. Abundance and production of particle-associated bacteria and their role in a mangrove-dominated estuary. Aquatic Microbial Ecology 57, 151–159.

Gräslund, S., Bengtsson, B.-E., 2001. Chemicals and biological products used in south-east Asian shrimp farming, and their potential impact on the environment - a review. Science of the Total Environment 280, 93–131.

Gräslund, S., Holmström, K., Wahlström, A., 2003. A field survey of chemicals and biological products used in shrimp farming. Marine Pollution Bulletin 46, 81–90.

Grossart, H., Engel, A., Arnosti, C., De La Rocha, C., Murray, A., Passow, U., 2007. Microbial dynamics in autotrophic and heterotrophic seawater mesocosms. III. Organic matter fluxes. Aquatic Microbial Ecology 49, 143–156.

Grossart, H.-P., Tang, K.W., Kiørboe, T., Ploug, H., 2007. Comparison of cell-specific activity between free-living and attached bacteria using isolates and natural assemblages. FEMS Microbiology Letters 266, 194–200.

Gücker, B., Silva, R.C.S., Graeber, D., Monteiro, J.A.F., Boëchat, I.G., 2016. Urbanization and agriculture increase exports and differentially alter elemental stoichiometry of dissolved organic matter (DOM) from tropical catchments. Science of The Total Environment 550, 785–792.

Guenet, B., Danger, M., Abbadie, L., Lacroix, G., 2010. Priming effect: bridging the gap between terrestrial and aquatic ecology. Ecology 91, 2850–2861.

Guérin, F., Abril, G., Serça, D., Delon, C., Richard, S., Delmas, R., Tremblay, A., Varfalvy, L., 2007. Gas transfer velocities of CO_2 and CH_4 in a tropical reservoir and its river downstream. Journal of Marine Systems 66, 161–172.

Guo, X., Cai, W.-J., Zhai, W., Dai, M., Wang, Y., Chen, B., 2008. Seasonal variations in the inorganic carbon system in the Pearl River (Zhujiang) estuary. Continental Shelf Research 28, 1424–1434.

- H -

Ha, T.T.T., Bush, S.R., 2010. Transformations of Vietnamese Shrimp Aquaculture Policy: Empirical Evidence from the Mekong Delta. Environment and Planning C: Government and Policy 28, 1101–1119.

Hall, D., Lee, S.Y., Meziane, T., 2006. Fatty acids as trophic tracers in an experimental estuarine food chain: Tracer transfer. Journal of Experimental Marine Biology and Ecology 336, 42–53.

Halsey, K.H., Jones, B.M., 2015. Phytoplankton strategies for photosynthetic energy allocation. Annual Review of Marine Science 7, 265–297.

Harada, Y., Lee, S.Y., 2016. Foraging behavior of the mangrove sesarmid crab *Neosarmatium trispinosum* enhances food intake and nutrient retention in a low-quality food environment. Estuarine, Coastal and Shelf Science 174, 41–48.

Harvey, G.W., Burzell, L.A., 1972. A simple microlayer method for small samples. Limnology and Oceanography 17, 156–157.

Harvey, H.R., 2006. Sources and cycling of organic matter in the marine water column, in: Volkman, J.K. (Ed.), Marine Organic Matter: Biomarkers, Isotopes and DNA. Springer-Verlag, Berlin/Heidelberg, pp. 1–25.

Herteman, M., Fromard, F., Lambs, L., 2011. Effects of pretreated domestic wastewater supplies on leaf pigment content, photosynthesis rate and growth of mangrove trees: a field study from Mayotte Island, SW Indian Ocean. Ecological Engineering 37, 1283–1291.

Ho, D.T., Coffineau, N., Hickman, B., Chow, N., Koffman, T., Schlosser, P., 2016. Influence of current velocity and wind speed on air-water gas exchange in a mangrove estuary: gas exchange in a mangrove estuary. Geophysical Research Letters 43, 3813–3821.

Hofmann, E.E., Cahill, B., Fennel, K., Friedrichs, M.A.M., Hyde, K., Lee, C., Mannino, A., Najjar, R.G., O'Reilly, J.E., Wilkin, J., Xue, J., 2011. Modeling the dynamics of continental shelf carbon. Annual Review of Marine Science 3, 93–122.

Hogarth, P.J., 2015. The biology of mangroves and seagrasses, Third Edition. ed, Biology of Habitats Series. Oxford University Press, Oxford, New York.

Hoppe, H.-G., 1993. Use of fluorogenic model substrates for extracellular enzyme activity (EEA) measurement of bacteria. Handbook of methods in aquatic microbial ecology 423–431.

Houlihan, D.F., 1979. Respiration in air and water of three mangrove snails. Journal of Experimental Marine Biology and Ecology 41, 143–161.

Howard, J., Sutton-Grier, A., Herr, D., Kleypas, J., Landis, E., Mcleod, E., Pidgeon, E., Simpson, S., 2017. Clarifying the role of coastal and marine systems in climate mitigation. Frontiers in Ecology and the Environment 15, 42–50.

Hu, Z., Lee, J.W., Chandran, K., Kim, S., Khanal, S.K., 2012. Nitrous oxide (N_2O) emission from aquaculture: a review. Environmental Science & Technology 46, 6470–6480.

Huang, T.-H., Fu, Y.-H., Pan, P.-Y., Chen, C.-T.A., 2012. Fluvial carbon fluxes in tropical rivers. Current Opinion in Environmental Sustainability 4, 162–169.

Huotari, J., Haapanala, S., Pumpanen, J., Vesala, T., Ojala, A., 2013. Efficient gas exchange between a boreal river and the atmosphere: Efficient gas exchange of a large river. Geophysical Research Letters 40, 5683–5686.

- I -

- J -

Jacquet, S., Partensky, F., Lennon, J.-F., Vaulot, D., 2001. Diel patterns of growth and division in marine picoplankton in culture. Journal of Phycology 37, 357–369.

Jaffé, R., Wolff, G.A., Cabrera, A., Chitty, H.C., 1995. The biogeochemistry of lipids in rivers of the Orinoco Basin. Geochimica et Cosmochimica Acta 59, 4507–4522.

Jennerjahn, T.C., Ittekkot, V., 2002. Relevance of mangroves for the production and deposition of organic matter along tropical continental margins. Naturwissenschaften 89, 23–30.

Ji, B., Yang, K., Zhu, L., Jiang, Y., Wang, H., Zhou, J., Zhang, H., 2015. Aerobic denitrification: a review of important advances of the last 30 years. Biotechnology and Bioprocess Engineering 20, 643–651.

- K -

Kainz, M., Telmer, K., Mazumder, A., 2006. Bioaccumulation patterns of methyl mercury and essential fatty acids in lacustrine planktonic food webs and fish. Science of The Total Environment 368, 271–282.

Kaneda, T., 1991. Iso-and anteiso-fatty acids in bacteria: biosynthesis, function, and taxonomic significance. Microbiological reviews 55, 288–302.

Kathleen, M.M., Samuel, L., Felecia, C., Reagan, E.L., Kasing, A., Lesley, M., Toh, S.C., 2016. Antibiotic resistance of diverse bacteria from aquaculture in Borneo. International Journal of Microbiology 2016, 1–9.

Kattner, G., Hagen, W., 1995. Polar herbivorous copepods–different pathways in lipid biosynthesis. ICES Journal of Marine Science: Journal du Conseil 52, 329–335.

Kelly, J., Scheibling, R., 2012. Fatty acids as dietary tracers in benthic food webs. Marine Ecology Progress Series 446, 1–22.

Kharlamenko, V.I., Kiyashko, S.I., Imbs, A.B., Vyshkvartzev, D.I., 2001. Identification of food sources of invertebrates from the seagrass *Zostera marina* community using carbon and sulfur stable isotope ratio and fatty acid analyses. Marine Ecology Progress Series 220, 103–117.

Kowalczyk-Pecka, D., Pecka, S., Kowalczuk-Vasilev, E., 2017. Selected fatty acids as biomarkers of exposure to microdoses of molluscicides in snails *Helix pomatia* (Gastropoda Pulmonata). Environmental Pollution 222, 138–145.

Kristensen, E., Bouillon, S., Dittmar, T., Marchand, C., 2008. Organic carbon dynamics in mangrove ecosystems: a review. Aquatic Botany 89, 201–219.

- L -

Laegdsgaard, P., Johnson, C., 2001. Why do juvenile fish utilise mangrove habitats? Journal of experimental marine biology and ecology 257, 229–253.

Lamy, D., Obernosterer, I., Laghdass, M., Artigas, F., Breton, E., Grattepanche, J., Lecuyer, E., Degros, N., Lebaron, P., Christaki, U., 2009. Temporal changes of major bacterial groups and bacterial heterotrophic activity during a *Phaeocystis globosa* bloom in the eastern English Channel. Aquatic Microbial Ecology 58, 95–107.

Lancelot, C., Muylaert, K., 2011. 7.02 Trends in estuarine phytoplankton ecology, in: Treatise on Estuarine and Coastal Science, Academic Press, Waltham. pp. 5–15.

Le, T., Munekage, Y., Kato, S., 2005. Antibiotic resistance in bacteria from shrimp farming in mangrove areas. Science of The Total Environment 349, 95–105.

Le, T.P.Q., Dao, V.N., Rochelle-Newall, E., Garnier, J., Lu, X., Billen, G., Duong, T.T., Ho, C.T., Etcheber, H., Nguyen, T.M.H., Nguyen, T.B.N., Nguyen, B.T., Da Le, N., Pham, Q.L., 2017. Total organic

carbon fluxes of the Red River system (Vietnam): TOC fluxes of the Red River. Earth Surface Processes and Landforms.

Le, T.X., Munekage, Y., 2004. Residues of selected antibiotics in water and mud from shrimp ponds in mangrove areas in Viet Nam. Marine Pollution Bulletin 49, 922–929.

Lee, O.H.K., Williams, G.A., Hyde, K.D., 2001. The diets of *Littoraria ardouiniana* and *L. melanostoma* in Hong Kong mangroves. Journal of the Marine Biological Association of the UK 81, 967–973.

Lee, S.Y., 1995. Mangrove outwelling: a review. Hydrobiologia 295, 203–212.

Lee, S.Y., 2008. Mangrove macrobenthos: assemblages, services, and linkages. Journal of Sea Research 59, 16–29.

Lee, S.Y., 2016. From blue to black: Anthropogenic forcing of carbon and nitrogen influx to mangrove-lined estuaries in the South China Sea. Marine Pollution Bulletin 109, 682–690.

Lee, S.Y., Primavera, J.H., Dahdouh-Guebas, F., McKee, K., Bosire, J.O., Cannicci, S., Diele, K., Fromard, F., Koedam, N., Marchand, C., Mendelssohn, I., Mukherjee, N., Record, S., 2014. Ecological role and services of tropical mangrove ecosystems: a reassessment of mangrove ecosystem services. Global Ecology and Biogeography 23, 726–743.

Legendre, P., Gallagher, E., 2001. Ecologically meaningful transformations for ordination of species data. Oecologia 129, 271–280.

Lemonnier, H., Faninoz, S., 2006. Effect of water exchange on effluent and sediment characteristics and on partial nitrogen budget in semi-intensive shrimp ponds in New Caledonia. Aquaculture Research 37, 938–948.

Leopold, A., Marchand, C., Deborde, J., Allenbach, M., 2017. Water biogeochemistry of a mangrove-dominated estuary under a semi-arid climate (New Caledonia). Estuaries and Coasts 40, 773–791.

Leopold, A., Marchand, C., Deborde, J., Chaduteau, C., Allenbach, M., 2013. Influence of mangrove zonation on CO_2 fluxes at the sediment–air interface (New Caledonia). Geoderma 202-203, 62–70.

Lewis, M., Pryor, R., Wilking, L., 2011. Fate and effects of anthropogenic chemicals in mangrove ecosystems: A review. Environmental Pollution 159, 2328–2346.

Li, S., Lu, X.X., Bush, R.T., 2013. CO_2 partial pressure and CO_2 emission in the Lower Mekong River. Journal of Hydrology 504, 40–56.

Loferer-Kröbbacher, M., Klima, J., Psenner, R., 1998. Determination of bacterial cell dry mass by transmission electron microscopy and densitometric image analysis. Applied and Environmental Microbiology 64, 688–694.

Long, R.A., Azam, F., 2001. Microscale patchiness of bacterioplankton assemblage richness in seawater. Aquatic Microbial Ecology 26, 103.

Lorke, A., Bodmer, P., Noss, C., Alshboul, Z., Koschorreck, M., Somlai-Haase, C., Bastviken, D., Flury, S., McGinnis, D.F., Maeck, A., Müller, D., Premke, K., 2015. Technical note: drifting versus anchored flux chambers for measuring greenhouse gas emissions from running waters. Biogeosciences 12, 7013–7024.

Lovelock, C.E., Ball, M.C., Martin, K.C., Feller, I.C., 2009. Nutrient enrichment increases mortality of mangroves. PLoS One 4, e5600.

Luyssaert, S., Inglima, I., Jung, M., Richardson, A.D., Reichstein, M., Papale, D., Piao, S.L., Schulze, E.-D., Wingate, L., Matteucci, G., Aragao, L., Aubinet, M., Beer, C., Bernhofer, C., Black, K.G., Bonal, D., Bonnefond, J.-M., Chambers, J., Ciais, P., others, 2007. CO_2 balance of boreal, temperate, and tropical forests derived from a global database. Global Change Biology 13, 2509–2537.

Lyons, M.M., Dobbs, F.C., 2012. Differential utilization of carbon substrates by aggregate-associated and water-associated heterotrophic bacterial communities. Hydrobiologia 686, 181–193.

- M -

Madariaga, I., 2002. Short-term variations in the physiological state of phytoplankton in a shallow temperate estuary, in: Orive, E., Elliott, M., Jonge, V.N. de (Eds.), Nutrients and Eutrophication in Estuaries and Coastal Waters, Developments in Hydrobiology. Springer Netherlands, pp. 345–358.

Maher, D.T., Cowley, K., Santos, I.R., Macklin, P., Eyre, B.D., 2015. Methane and carbon dioxide dynamics in a subtropical estuary over a diel cycle: Insights from automated in situ radioactive and stable isotope measurements. Marine Chemistry 168, 69–79.

Maher, D.T., Santos, I.R., Golsby-Smith, L., Gleeson, J., Eyre, B.D., 2013. Groundwater-derived dissolved inorganic and organic carbon exports from a mangrove tidal creek: the missing mangrove carbon sink? Limnology and Oceanography 58, 475–488.

Mannino, A., Harvey, H.R., 2000. Biochemical composition of particles and dissolved organic matter along an estuarine gradient: Sources and implications for DOM reactivity. Limnology and Oceanography 45, 775–788.

Manoharan, K., Lee, T.K., Cha, J.M., Kim, J.H., Lee, W.S., Chang, M., Park, C.W., Cho, J.H., 1999. Acclimation of *Prorocentrum minimum* (Dinophyceae) to prolonged darkness by use of an alternative carbon source from triacylglycerides and galactolipids. Journal of phycology 35, 287–292.

Marchand, C., 2017. Soil carbon stocks and burial rates along a mangrove forest chronosequence (French Guiana). Forest Ecology and Management 384, 92–99.

Marchand, C., Fernandez, J.-M., Moreton, B., Landi, L., Lallier-Vergès, E., Baltzer, F., 2012. The partitioning of transitional metals (Fe, Mn, Ni, Cr) in mangrove sediments downstream of a ferralitized ultramafic watershed (New Caledonia). Chemical Geology 300–301, 70–80.

Marchand, C., Lallier-Verges, E., Allenbach, M., 2011. Redox conditions and heavy metals distribution in mangrove forests receiving effluents from shrimp farms (Teremba Bay, New Caledonia). Journal of Soils and Sediments 11, 529–541.

Marcotullio, P.J., 2007. Urban water-related environmental transitions in Southeast Asia. Sustainability Science 2, 27–54.

Mari, X., Passow, U., Migon, C., Burd, A.B., Legendre, L., 2017. Transparent exopolymer particles: Effects on carbon cycling in the ocean. Progress in Oceanography 151, 13–37.

Marty, Y., Quéméneur, M., Aminot, A., Le Corre, P., 1996. Laboratory study on degradation of fatty acids and sterols from urban wastes in seawater. Water Research 30, 1127–1136.

Matthews, C.J.D., St.Louis, V.L., Hesslein, R.H., 2003. Comparison of three techniques used to measure diffusive gas exchange from sheltered aquatic surfaces. Environmental Science & Technology 37, 772–780.

Mazda, Y., Magi, M., Kogo, M., Hong, P.N., 1997. Mangroves as a coastal protection from waves in the Tong King delta, Vietnam. Mangroves and Salt Marshes 1, 127–135.

McCallister, S.L., Bauer, J.E., Ducklow, H.W., Canuel, E.A., 2006. Sources of estuarine dissolved and particulate organic matter: a multi-tracer approach. Organic Geochemistry 37, 454–468.

McClelland, J.W., Valiela, I., 1998. Linking nitrogen in estuarine producers to land-derived sources. Limnology and Oceanography 43, 577–585.

McCutchan, J.H., Lewis, W.M., Kendall, C., McGrath, C.C., 2003. Variation in trophic shift for stable isotope ratios of carbon, nitrogen, and sulfur. Oikos 102, 378–390.

Mcleod, E., Chmura, G.L., Bouillon, S., Salm, R., Björk, M., Duarte, C.M., Lovelock, C.E., Schlesinger, W.H., Silliman, B.R., 2011. A blueprint for blue carbon: toward an improved understanding of

the role of vegetated coastal habitats in sequestering CO_2. Frontiers in Ecology and the Environment 9, 552–560.

Merkus, H.G., 2009. Particle size measurements: fundamentals, practice, quality. Springer Science & Business Media.

Meybeck, M., 1982. Carbon, nitrogen, and phosphorus transport by world rivers. American Journal of Science 282, 401–450.

Meziane, T., Bodineau, L., Retiere, C., Thoumelin, G., 1997. The use of lipid markers to define sources of organic matter in sediment and food web of the intertidal salt-marsh-flat ecosystem of Mont-Saint-Michel Bay, France. Journal of Sea Research 38, 47–58.

Meziane, T., d'Agata, F., Lee, S.Y., 2006. Fate of mangrove organic matter along a subtropical estuary: small-scale exportation and contribution to the food of crab communities. Marine Ecology Progress Series 312, 15–27.

Meziane, T., Lee, S.Y., Mfilinge, P.L., Shin, P.K.S., Lam, M.H.W., Tsuchiya, M., 2007. Inter-specific and geographical variations in the fatty acid composition of mangrove leaves: implications for using fatty acids as a taxonomic tool and tracers of organic matter. Marine Biology 150, 1103–1113.

Meziane, T., Tsuchiya, M., 2000. Fatty acids as tracers of organic matter in the sediment and food web of a mangrove/intertidal flat ecosystem, Okinawa, Japan. Marine Ecology Progress Series 200, 49–57.

Meziane, T., Tsuchiya, M., 2002. Organic matter in a subtropical mangrove-estuary subjected to wastewater discharge: origin and utilisation by two macrozoobenthic species. Journal of Sea Research 47, 1–11.

Middelburg, J.J., Herman, P.M.J., 2007. Organic matter processing in tidal estuaries. Marine Chemistry 106, 127–147.

Millero, F.J., 2010. Carbonate constants for estuarine waters. Marine and Freshwater Research 61, 139.

Millero, F.J., Graham, T.B., Huang, F., Bustos-Serrano, H., Pierrot, D., 2006. Dissociation constants of carbonic acid in seawater as a function of salinity and temperature. Marine Chemistry 100, 80–94.

Minh, N.H., Minh, T.B., Iwata, H., Kajiwara, N., Kunisue, T., Takahashi, S., Viet, P.H., Tuyen, B.C., Tanabe, S., 2007. Persistent organic pollutants in sediments from Sai Gon–Dong Nai River

basin, Vietnam: levels and temporal trends. Archives of Environmental Contamination and Toxicology 52, 458–465.

Miyajima, T., Tsuboi, Y., Tanaka, Y., Koike, I., 2009. Export of inorganic carbon from two Southeast Asian mangrove forests to adjacent estuaries as estimated by the stable isotope composition of dissolved inorganic carbon. Journal of Geophysical Research 114.

Molnar, N., Marchand, C., Deborde, J., Patrona, L.D., Meziane, T., 2014. Seasonal pattern of the biogeochemical properties of mangrove sediments receiving shrimp farm effluents (New Caledonia). Journal of Aquaculture Research & Development 5, 262.

Molnar, N., Welsh, D.T., Marchand, C., Deborde, J., Meziane, T., 2013. Impacts of shrimp farm effluent on water quality, benthic metabolism and N-dynamics in a mangrove forest (New Caledonia). Estuarine, Coastal and Shelf Science 117, 12–21.

Monroig, Ó., Tocher, D., Navarro, J., 2013. Biosynthesis of polyunsaturated fatty acids in marine invertebrates: Recent advances in molecular mechanisms. Marine Drugs 11, 3998–4018.

Mortillaro, J.M., Abril, G., Moreira-Turcq, P., Sobrinho, R.L., Perez, M., Meziane, T., 2011. Fatty acid and stable isotope ($\delta^{13}C$, $\delta^{15}N$) signatures of particulate organic matter in the lower Amazon River: seasonal contrasts and connectivity between floodplain lakes and the mainstem. Organic Geochemistry 42, 1159–1168.

Mortillaro, J.M., Passarelli, C., Abril, G., Hubas, C., Alberic, P., Artigas, L.F., Benedetti, M.F., Thiney, N., Moreira-Turcq, P., Perez, M.A.P., Vidal, L.O., Meziane, T., 2016. The fate of C4 and C3 macrophyte carbon in central Amazon floodplain waters: Insights from a batch experiment. Limnologica - Ecology and Management of Inland Waters 59, 90–98.

Moynihan, M.A., Barbier, P., Olivier, F., Toupoint, N., Meziane, T., 2016. Spatial and temporal dynamics of nano- and pico-size particulate organic matter (POM) in a coastal megatidal marine system: Dynamics of nano- and pico- POM. Limnology and Oceanography 61, 1087–1100.

Müller, D., Warneke, T., Rixen, T., Müller, M., Mujahid, A., Bange, H.W., Notholt, J., 2016. Fate of terrestrial organic carbon and associated CO_2 and CO emissions from two Southeast Asian estuaries. Biogeosciences 13, 691–705.

- N -

Nagelkerken, I., Blaber, S.J.M., Bouillon, S., Green, P., Haywood, M., Kirton, L.G., Meynecke, J.-O., Pawlik, J., Penrose, H.M., Sasekumar, A., Somerfield, P.J., 2008. The habitat function of mangroves for terrestrial and marine fauna: a review. Aquatic Botany 89, 155–185.

Nam, V.N., Sinh, L.V., Miyagi, T., Baba, S., Chan, H.T., 2014. An overview of Can Gio district and mangrove biosphere reserve, in: Studies in Can Gio Mangrove Biosphere Reserve, Ho Chi Minh City, Vietnam. Tohoku Gakuin University, Japan.

Napolitano, G.E., Pollero, R.J., Gayoso, A.M., Macdonald, B.A., Thompson, R.J., 1997. Fatty acids as trophic markers of phytoplankton blooms in the Bahía Blanca estuary (Buenos Aires, Argentina) and in Trinity Bay (Newfoundland, Canada). Biochemical Systematics and Ecology 25, 739–755.

Naylor, R.L., Goldburg, R.J., Mooney, H., Beveridge, M., Clay, J., Folke, C., Kautsky, N., Lubchenco, J., Primavera, J., Williams, M., 1998. Nature's subsidies to shrimp and salmon farming. Science 282, 883–884.

Nelson, M.M., Phleger, C.F., Nichols, P.D., 2002. Seasonal lipid composition in macroalgae of the northeastern pacific ocean. Botanica Marina 45, 58–65.

Ng, P.K.L., Wang, L.K., Lim, K.K.P., Research, R.M. of B., 2007. Private lives: an exposé of Singapore's mangroves. Raffles Museum of Biodiversity Research, National University of Singapore.

Nippon Koei, 1996. The master plan study on Dong Nai River and surrounding basins water resources development. Final Report. Vol. IX. Appendix VIII. Flood mitigation and urban drainage. Tokyo, Japan: Nippon Koei.

Nordhaus, I., Salewski, T., Jennerjahn, T.C., 2011. Food preferences of mangrove crabs related to leaf nitrogen compounds in the Segara Anakan Lagoon, Java, Indonesia. Journal of Sea Research 65, 414–426.

Noriega, C.E.D., Araujo, M., Lefèvre, N., 2013. Spatial and temporal variability of the CO_2 fluxes in a tropical, highly urbanized estuary. Estuaries and Coasts 36, 1054–1072.

Norton, T.A., Hawkins, S.J., Manley, N.L., Williams, G.A., Watson, D.C., 1990. Scraping a living: a review of littorinid grazing, in: Progress in Littorinid and Muricid Biology. Springer, pp. 117–138.

- O -

Odum, W.E., Heald, E.J., 1975. The detritus-based food web of an estuarine mangrove community, in: Estuarine Research: Chemistry, Biology, and the Estuarine System. Elsevier.

Odum, W.E., McIvor, C.C., Smith III, T.J., 1982. The ecology of the mangroves of South Florida: a community profile (Federal Government Series No. 81/24), FWS/OBS. U.S. Fish and Wildlife Service.

Ólafsson, E., Buchmayer, S., Skov, M.W., 2002. The east african decapod crab *Neosarmatium meinerti* (De Man) sweeps mangrove floors clean of leaf litter. Ambio 31, 569–573.

Ouraji, H., Fereidoni, A.E., Shayegan, M., Asil, S.M., 2011. Comparison of fatty acid composition between farmed and wild indian white shrimps, *Fenneropenaeus indicus*. Food and Nutrition Sciences 02, 824–829.

- P -

Páez-Osuna, F., 2001. The environmental impact of shrimp aquaculture: a global perspective. Environmental pollution 112, 229–231.

Páez-Osuna, F., Ruiz-Fernández, A.C., 2005. Environmental load of nitrogen and phosphorus from extensive, semiintensive, and intensive shrimp farms in the Gulf of California ecoregion. Bulletin of Environmental Contamination and Toxicology 74, 681–688.

Pan, H., Culp, R.A., Noakes, J.E., Sun, M.-Y., 2014. Effects of growth stages, respiration, and microbial degradation of phytoplankton on cellular lipids and their compound-specific stable carbon isotopic compositions. Journal of Experimental Marine Biology and Ecology 461, 7–19.

Pan, H., Culp, R.A., Sun, M.-Y., 2017. Influence of physiological states of *Emiliania huxleyi* cells on their lipids and associated molecular isotopic compositions during microbial degradation. Journal of Experimental Marine Biology and Ecology 488, 1–9.

Park, P.K., 1969. Oceanic CO_2 system: an evaluation of ten methods of investigation. Limnology and Oceanography 14, 179–186.

Parnell, A.C., Inger, R., Bearhop, S., Jackson, A.L., 2010. Source partitioning using stable isotopes: coping with too much variation. PLoS ONE 5, e9672.

Parrish, C.C., Abrajano, T.A., Budge, S.M., Helleur, R.J., Hudson, E.D., Pulchan, K., Ramos, C., 2000. Lipid and phenolic biomarkers in marine ecosystems: analysis and applications, in: Marine Chemistry. Springer, pp. 193–223.

Passow, U., 2002. Transparent exopolymer particles (TEP) in aquatic environments. Progress in Oceanography 55, 287–333.

Patel, A.B., Fukami, K., Nishijima, T., 2000. Regulation of seasonal variability of aminopeptidase activities in surface and bottom waters of Uranouchi Inlet, Japan.

Pauer, J.J., Auer, M.T., 2000. Nitrification in the water column and sediment of a hypereutrophic lake and adjoining river system. Water Research 34, 1247–1254.

Popp, M., Larher, F., Weigel, P., 1985. Osmotic adaption in Australian mangroves. Vegetatio 61, 247–253.

Porter, K.G., Feig, Y.S., 1980. The use of DAPI for identifying and counting aquatic microflora. Limnology and oceanography 25, 943–948.

Prasad, R., Yedukondala Rao, P., 2015. Studies on food and feeding habits of *Oratosquilla anomala* (Tweedie, 1935) (Crustacea: Stomatopoda) represented in the shrimp trawl net by-catches off Visakhapatnam, east coast of India. European Journal of Experimental Biology 5, 43–48.

Primavera, J.H., 1997. Socio-economic impacts of shrimp culture. Aquaculture research 28, 815–827.

Primavera, J.H., 2006. Overcoming the impacts of aquaculture on the coastal zone. Ocean & Coastal Management 49, 531–545.

- Q -

Quéméneur, M., Marty, Y., 1994. Fatty acids and sterols in domestic wastewaters. Water Research 28, 1217–1226.

- R -

R Core Team, 2017. R: A language and environment for statistical computing. R Foundation for Statistical Computing, Vienna, Austria. URL https://www.R-project.org/.

Raymond, P.A., Cole, J.J., 2001. Gas exchange in rivers and estuaries: choosing a gas transfer velocity. Estuaries and Coasts 24, 312–317.

Reef, R., Lovelock, C.E., 2015. Regulation of water balance in mangroves. Annals of Botany 115, 385–395.

Regnier, P., Friedlingstein, P., Ciais, P., Mackenzie, F.T., Gruber, N., Janssens, I.A., Laruelle, G.G., Lauerwald, R., Luyssaert, S., Andersson, A.J., Arndt, S., Arnosti, C., Borges, A.V., Dale, A.W., Gallego-Sala, A., Goddéris, Y., Goossens, N., Hartmann, J., Heinze, C., Ilyina, T., Joos, F., LaRowe, D.E., Leifeld, J., Meysman, F.J.R., Munhoven, G., Raymond, P.A., Spahni, R., Suntharalingam, P., Thullner, M., 2013. Anthropogenic perturbation of the carbon fluxes from land to ocean. Nature Geoscience 6, 597–607.

Richards, D.R., Friess, D.A., 2016. Rates and drivers of mangrove deforestation in Southeast Asia, 2000–2012. Proceedings of the National Academy of Sciences 113, 344–349.

Riera, P., Montagna, P.A., Kalke, R.D., Richard, P., 2000. Utilization of estuarine organic matter during growth and migration by juvenile brown shrimp *Penaeus aztecus* in a South Texas estuary. Marine Ecology Progress Series 205–216.

Ringler, C., Cong, N.C., Huy, N.V., 2002. Water allocation and use in the Dong Nai River Basin in the context of water institution strengthening. Integrated Water-resources Management in a River-basin Context: Institutional Strategies for Improving the Productivity of Agricultural Water Management 215.

Robertson, A. I., Blaber, S. J. M., 1992. Plankton, epibenthos and fish communities, in: Robertson, A.I., Alongi, D.M. (Eds.), Tropical Mangrove Ecosystems. American Geophysical Union, pp. 173–224.

Robertson, A.I., Phillips, M.J., 1995. Mangroves as filters of shrimp pond effluent: predictions and biogeochemical research needs. Hydrobiologia 295, 311–321.

Rodelli, M.R., Gearing, J.N., Gearing, P.J., Marshall, N., Sasekumar, A., 1984. Stable isotope ratio as a tracer of mangrove carbon in Malaysian ecosystems. Oecologia 61, 326–333.

Roeske, C.A., O'Leary, M.H., 1984. Carbon isotope effects on enzyme-catalyzed carboxylation of ribulose bisphosphate. Biochemistry 23, 6275–6284.

Romano, N., Wu, X., Zeng, C., Genodepa, J., Elliman, J., 2014. Growth, osmoregulatory responses and changes to the lipid and fatty acid composition of organs from the mud crab, *Scylla serrata*, over a broad salinity range. Marine Biology Research 10, 460–471.

Rosentreter, J.A., Maher, D.T., Ho, D.T., Call, M., Barr, J.G., Eyre, B.D., 2017. Spatial and temporal variability of CO_2 and CH_4 gas transfer velocities and quantification of the CH_4 microbubble flux in mangrove dominated estuaries: Gas transfers in estuaries. Limnology and Oceanography 62: 561–578.

- S -

Sakdullah, A., Tsuchiya, M., 2009. The origin of particulate organic matter and the diet of tilapia from an estuarine ecosystem subjected to domestic wastewater discharge: fatty acid analysis approach. Aquatic Ecology 43, 577–589.

Santos, I.R., Maher, D.T., Eyre, B.D., 2012. Coupling automated radon and carbon dioxide measurements in coastal waters. Environmental Science & Technology 46, 7685–7691.

Santos, L., Santos, A.L., Coelho, F.J.R.C., Gomes, N.C.M., Dias, J.M., Cunha, Â., Almeida, A., 2011. Relation between bacterial activity in the surface microlayer and estuarine hydrodynamics:

Bacterial activity in the SML and estuarine hydrodynamics. FEMS Microbiology Ecology 77, 636–646.

Sardans, J., Rivas-Ubach, A., Peñuelas, J., 2012. The elemental stoichiometry of aquatic and terrestrial ecosystems and its relationships with organismic lifestyle and ecosystem structure and function: a review and perspectives. Biogeochemistry 111, 1–39.

Sargent, J.R., Bell, J.G., Bell, M.V., Henderson, R.J., Tocher, D.R., 1995. Requirement criteria for essential fatty acids. Journal of applied Ichthyology 11, 183–198.

Schapira, M., McQuaid, C.D., Froneman, P.W., 2012. Free-living and particle-associated prokaryote metabolism in giant kelp forests: Implications for carbon flux in a sub-Antarctic coastal area. Estuarine, Coastal and Shelf Science 106, 69–79.

Scribe, P., Fillaux, J., Laureillard, J., Denant, V., Saliot, A., 1991. Fatty acids as biomarkers of planktonic inputs in the stratified estuary of the Krka River, Adriatic Sea: relationship with pigments. Marine Chemistry 32, 299–312.

Scully, N.M., Cooper, W.J., Tranvik, L.J., 2003. Photochemical effects on microbial activity in natural waters: the interaction of reactive oxygen species and dissolved organic matter. FEMS Microbiology Ecology 46, 353–357.

Sherr, E., Sherr, B., 1988. Role of microbes in pelagic food webs: a revised concept. Limnology and Oceanography 33, 1225–1227.

Shilla, D.J., Tsuchiya, M., Shilla, D.A., 2011. Terrigenous nutrient and organic matter in a subtropical river estuary, Okinawa, Japan: origin, distribution and pattern across the estuarine salinity gradient. Chemistry and Ecology 27, 523–542.

Simon, M., Grossart, H.-P., Schweitzer, B., Ploug, H., 2002. Microbial ecology of organic aggregates in aquatic ecosystems. Aquatic microbial ecology 28, 175–211.

Smith, D.C., Simon, M., Alldredge, A.L., Azam, F., 1992. Intense hydrolytic enzyme activity on marine aggregates and implications for rapid particle dissolution. Nature 359, 139–142.

Smith, J.M., Chavez, F.P., Francis, C.A., 2014. Ammonium uptake by phytoplankton regulates nitrification in the sunlit ocean. PLoS ONE 9, e108173.

Smith, V.H., Tilman, G.D., Nekola, J.C., 1999. Eutrophication: impacts of excess nutrient inputs on freshwater, marine, and terrestrial ecosystems. Environmental pollution 100, 179–196.

Sousa, W.P., Dangremond, E.M., 2011. Trophic interactions in coastal and estuarine mangrove forest ecosystems, in: Treatise on Estuarine and Coastal Science. Elsevier, pp. 43–93.

Stoner, A.W., Zimmerman, R.J., 1988. Food pathways associated with penaeid shrimps in a mangrove-fringed estuary. Fishery Bulletin 86, 543–552.

Strady, E., Dang, V.B.H., Némery, J., Guédron, S., Dinh, Q.T., Denis, H., Nguyen, P.D., 2017. Baseline seasonal investigation of nutrients and trace metals in surface waters and sediments along the Saigon River basin impacted by the megacity of Ho Chi Minh (Vietnam). Environmental Science and Pollution Research 24, 3226–3243.

Suárez-Abelenda, M., Ferreira, T.O., Camps-Arbestain, M., Rivera-Monroy, V.H., Macías, F., Nóbrega, G.N., Otero, X.L., 2014. The effect of nutrient-rich effluents from shrimp farming on mangrove soil carbon storage and geochemistry under semi-arid climate conditions in northern Brazil. Geoderma 213, 551–559.

- T -

Takahashi, T., Sutherland, S.C., Chipman, D.W., Goddard, J.G., Ho, C., Newberger, T., Sweeney, C., Munro, D.R., 2014. Climatological distributions of pH, pCO_2, total CO_2, alkalinity, and $CaCO_3$ saturation in the global surface ocean, and temporal changes at selected locations. Marine Chemistry 164, 95–125.

Tan, K.S., 2008. Mudflat predation on bivalves and gastropods by *Chicoreus capucinus* (Neogastropoda: Muricidae) at Kungkrabaen Bay, Gulf of Thailand. Raffles Bulletin of Zoology Supplement 18, 235–245.

Tanaka, K., Choo, P.-S., 2000. Influences of nutrient outwelling from the mangrove swamp on the distribution of phytoplankton in the Matang Mangrove Estuary, Malaysia. Journal of oceanography 56, 69–78.

Tocher, D.R., Glencross, B.D., 2015. Lipids and fatty acids, in: Lee, C.-S., Lim, C., III, D.M.G., Webster, C.D. (Eds.), Dietary Nutrients, Additives, and Fish Health. John Wiley & Sons, Inc, pp. 47–94.

Trott, L.A., Alongi, D.M., 2000. The impact of shrimp pond effluent on water quality and phytoplankton biomass in a tropical mangrove estuary. Marine Pollution Bulletin 40, 947–951.

Trott, L.A., McKinnon, A.D., Alongi, D.M., Davidson, A., Burford, M.A., 2004. Carbon and nitrogen processes in a mangrove creek receiving shrimp farm effluent. Estuarine, Coastal and Shelf Science 59, 197–207.

Tuan, L. D., Oanh, T.K., Thành, C.V., Qui, N., 2002. Can Gio Mangrove Biosphere Reserve. Eds. Nha Xuat Ban. Ho Chi Minh. 311pp.

Tuan, V.Q., Kuenzer, C., 2012. Can Gio mangrove biosphere reserve evaluation, 2012: current status, dynamics, and ecosystem services. IUCN Viet Nam Country Office, Hanoi, Vietnam.

Tue, N.T., Hamaoka, H., Quy, T.D., Nhuan, M.T., Sogabe, A., Nam, N.T., Omori, K., 2014. Dual isotope study of food sources of a fish assemblage in the Red River mangrove ecosystem, Vietnam. Hydrobiologia 733, 71–83.

Tue, N.T., Hamaoka, H., Sogabe, A., Quy, T.D., Nhuan, M.T., Omori, K., 2012. Food sources of macro-invertebrates in an important mangrove ecosystem of Vietnam determined by dual stable isotope signatures. Journal of Sea Research 72, 14–21.

- U -

Underwood, J.C., Harvey, R.W., Metge, D.W., Repert, D.A., Baumgartner, L.K., Smith, R.L., Roane, T.M., Barber, L.B., 2011. Effects of the antimicrobial sulfamethoxazole on groundwater bacterial enrichment. Environmental Science & Technology 45, 3096–3101.

UNESCO / MAB Project, 2000. Valuation of the mangrove ecosystem in Can Gio mangrove biosphere reserve, Vietnam. The Vietnam MAB National Committee.

- V -

Vachon, D., Prairie, Y.T., Cole, J.J., 2010. The relationship between near-surface turbulence and gas transfer velocity in freshwater systems and its implications for floating chamber measurements of gas exchange. Limnology and Oceanography 55, 1723–1732.

Van Anholt, R.D., Spanings, F.A.T., Koven, W.M., Wendelaar Bonga, S.E., 2004. Dietary supplementation with arachidonic acid in tilapia (*Oreochromis mossambicus*) reveals physiological effects not mediated by prostaglandins. General and Comparative Endocrinology 139, 215–226.

Vanderklift, M.A., Ponsard, S., 2003. Sources of variation in consumer-diet $\delta^{15}N$ enrichment: a meta-analysis. Oecologia 136, 169–182.

Vermeiren, P., Abrantes, K., Sheaves, M., 2015. Generalist and specialist feeding crabs maintain discrete trophic niches within and among estuarine locations. Estuaries and Coasts 38, 2070–2082.

Verney, R., Lafite, R., Brun-Cottan, J.-C., 2009. Flocculation potential of estuarine particles: the importance of environmental factors and of the spatial and seasonal variability of suspended particulate matter. Estuaries and Coasts 32, 678–693.

Vetter, Y.A., Deming, J.W., Jumars, P.A., Krieger-Brockett, B.B., 1998. A predictive model of bacterial foraging by means of freely released extracellular enzymes. Microbial ecology 36, 75–92.

Volkman, J.K., Revill, A.T., Holdsworth, D.G., Fredericks, D., 2008. Organic matter sources in an enclosed coastal inlet assessed using lipid biomarkers and stable isotopes. Organic Geochemistry 39, 689–710.

Volkman, J.K., Tanoue, E., 2002. Chemical and biological studies of particulate organic matter in the ocean. Journal of Oceanography 58, 265–279.

- W -

Wafar, S., Untawale, A.G., Wafar, M., 1997. Litter fall and energy flux in a mangrove ecosystem. Estuarine, Coastal and Shelf Science 44, 111–124.

Wakeham, S.G., 1995. Lipid biomarkers for heterotrophic alteration of suspended particulate organic matter in oxygenated and anoxic water columns of the ocean. Deep Sea Research Part I: Oceanographic Research Papers 42, 1749–1771.

Wang, S., Jin, B., Qin, H., Sheng, Q., Wu, J., 2015. Trophic dynamics of filter feeding bivalves in the Yangtze estuarine intertidal marsh: stable isotope and fatty acid analyses. PLOS ONE 10, e0135604.

Wang, Y.P., Voulgaris, G., Li, Y., Yang, Y., Gao, J., Chen, J., Gao, S., 2013. Sediment resuspension, flocculation, and settling in a macrotidal estuary: flocculation and settling in estuary. Journal of Geophysical Research: Oceans 118, 5591–5608.

Wannigama, G.P., Volkman, J.K., Gillan, F.T., Nichols, P.D., Johns, R.B., 1981. A comparison of lipid components of the fresh and dead leaves and pneumatophores of the mangrove *Avicennia marina*. Phytochemistry 20, 659–666.

Wanninkhof, R., 1992. Relationship between wind speed and gas exchange over the ocean. Journal of Geophysical Research: Oceans 97, 7373–7382.

Webb, J.R., Maher, D.T., Santos, I.R., 2016. Automated, in situ measurements of dissolved CO_2, CH_4, and $\delta^{13}C$ values using cavity enhanced laser absorption spectrometry: comparing response times of air-water equilibrators. Limnology and Oceanography: Methods 14, 323–337.

Weiss, R.F., 1974. Carbon dioxide in water and seawater: the solubility of a non-ideal gas. Marine Chemistry 2, 203–215.

Werry, J., Lee, S.Y., 2005. Grapsid crabs mediate link between mangrove litter production and estuarine planktonic food chains. Marine Ecology Progress Series 293, 165–176.

Willems, T., De Backer, A., Kerkhove, T., Dakriet, N.N., De Troch, M., Vincx, M., Hostens, K., 2016. Trophic ecology of Atlantic seabob shrimp *Xiphopenaeus kroyeri*: intertidal benthic microalgae support the subtidal food web off Suriname. Estuarine, Coastal and Shelf Science 182, 146–157.

Wollast, R., 2003. Biogeochemical processes in estuaries, in: Wefer, P.D.G., Lamy, D.F., Mantoura, P.D.F. (Eds.), Marine Science Frontiers for Europe. Springer Berlin Heidelberg, pp. 61–77.

Woodroffe, C., 1992. Mangrove Sediments and Geomorphology, in: Robertson, A.I., Alongi, D.M. (Eds.), Tropical Mangrove Ecosystems. American Geophysical Union, pp. 7–41.

Wu, Y., Bao, H.-Y., Unger, D., Herbeck, L.S., Zhu, Z.-Y., Zhang, J., Jennerjahn, T.C., 2013. Biogeochemical behavior of organic carbon in a small tropical river and estuary, Hainan, China. Continental Shelf Research 57, 32–43.

- X -

Xu, J., Lin, P., Meguro, S., Kawachi, S., 1997. Phytochemical research on mangrove plants. I. Lipids and carbohydrates in propagules of ten mangrove species of China. Mokuzai Gakkaishi 43, 875–881.

Xu, Y., Jaffé, R., 2007. Lipid biomarkers in suspended particles from a subtropical estuary: assessment of seasonal changes in sources and transport of organic matter. Marine Environmental Research 64, 666–678.

- Y -

Yin, K., Lin, Z., Ke, Z., 2004. Temporal and spatial distribution of dissolved oxygen in the Pearl River Estuary and adjacent coastal waters. Continental Shelf Research 24, 1935–1948.

Yoon, T.K., Jin, H., Oh, N.-H., Park, J.-H., 2016. Technical note: assessing gas equilibration systems for continuous pCO_2 measurements in inland waters. Biogeosciences 13, 3915–3930.

- Z -

Zelles, L., 1997. Phospholipid fatty acid profiles in selected members of soil microbial communities. Chemosphere, Experimental and Theoretical Approaches in Environmental Chemistry 35, 275–294.

Zhang, K., Liu, H., Li, Y., Xu, H., Shen, J., Rhome, J., Smith, T.J., 2012. The role of mangroves in attenuating storm surges. Estuarine, Coastal and Shelf Science 102–103, 11–23.

Zhukova, N., 2014. Lipids and fatty acids of nudibranch mollusks: potential sources of bioactive compounds. Marine Drugs 12, 4578–4592.

Zhukova, N.V., 1991. The pathway of the biosynthesis of non-methylene-interrupted dienoic fatty acids in molluscs. Comparative Biochemistry and Physiology Part B: Comparative Biochemistry 100, 801–804.

Annexes

Appendix 5-1: Complete fatty acid compositions of suspended particulate matter during the 26 h tidal cycle in the Can Gio mangrove creek

Fatty acids (µg gSPM^{-1} ± SD)	T00 (n = 4)	T02 (n = 4)	T04 (n = 4)	T06 (n = 4)	T08 (n = 4)	T10 (n = 4)	T12 (n = 4)	T14 (n = 4)	T16 (n = 4)	T18 (n = 4)	T20 (n = 4)	T22 (n = 4)	T24 (n = 4)	T26 (n = 4)
Saturated														
12:0	9.8 ± 10.6	9.3 ± 5.6	20.7 ± 15.8	32.0 ± 22.2	24.3 ± 22.8	11.3 ± 6.2	13.5 ± 2.3	28.0 ± 10.4	144.4 ± 245.7	26.4 ± 18.1	25.5 ± 29.8	9.7 ± 5.1	15.8 ± 4.5	11.3 ± 2.4
13:0	0.9 ± 0.6	2.6 ± 0.6	3.5 ± 0.9	5.0 ± 1.0	3.9 ± 0.7	5.1 ± 2.6	5.8 ± 1.0	4.8 ± 1.1	3.9 ± 2.0	3.2 ± 1.4	1.8 ± 0.9	2.7 ± 1.5	2.5 ± 0.7	4.7 ± 0.7
14:0	34.0 ± 8.0	39.7 ± 6.1	53.2 ± 10.8	84.2 ± 18.4	69.1 ± 15.1	66.1 ± 18.9	59.8 ± 8.8	65.5 ± 2.5	146.3 ± 144.7	79.3 ± 15.4	57.9 ± 13.9	35.1 ± 8.3	182.8 ± 28.6	82.1 ± 8.5
15:0	9.2 ± 1.3	13.5 ± 1.7	18.2 ± 5.5	33.5 ± 8.7	26.5 ± 1.9	32.9 ± 11.4	26.0 ± 3.6	23.5 ± 4.2	25.5 ± 4.0	20.1 ± 0.5	13.8 ± 1.8	16.6 ± 2.9	40.0 ± 6.3	23.7 ± 2.9
16:0	127.2 ± 13.0	166.2 ± 30.0	244.4 ± 44.6	359.6 ± 93.1	273.0 ± 26.1	327.8 ± 70.4	251.1 ± 24.5	221.3 ± 30.8	323.8 ± 91.9	252.9 ± 24.0	153.5 ± 20.7	151.8 ± 27.3	781.6 ± 132.9	333.2 ± 37.0
17:0	4.3 ± 0.7	6.4 ± 1.7	10.1 ± 3.7	15.6 ± 5.3	12.3 ± 1.0	16.1 ± 5.4	13.0 ± 2.5	11.4 ± 1.5	13.0 ± 3.3	9.9 ± 0.6	6.1 ± 1.2	7.2 ± 1.8	16.8 ± 3.0	11.9 ± 1.8
18:0	42.2 ± 9.5	43.5 ± 15.3	80.1 ± 22.1	103.1 ± 43.6	63.9 ± 15.8	79.5 ± 16.7	63.3 ± 11.1	54.6 ± 8.9	83.0 ± 38.6	52.5 ± 4.7	27.9 ± 9.7	34.8 ± 8.7	100.6 ± 28.8	82.1 ± 15.8
19:0	2.3 ± 0.5	3.0 ± 0.7	4.4 ± 0.9	3.9 ± 1.4	5.1 ± 1.4	5.8 ± 1.2	6.1 ± 1.4	4.2 ± 0.7	3.8 ± 1.0	3.0 ± 0.4	2.1 ± 0.7	2.6 ± 1.2	3.4 ± 1.4	5.2 ± 2.4
20:0	2.8 ± 0.6	2.2 ± 0.5	3.6 ± 1.1	5.7 ± 2.7	4.1 ± 0.8	4.9 ± 1.1	3.2 ± 0.7	3.2 ± 1.0	3.5 ± 1.2	2.2 ± 0.6	1.7 ± 0.7	2.0 ± 0.8	6.5 ± 0.8	4.5 ± 1.0
22:0	2.6 ± 0.6	2.1 ± 0.4	3.0 ± 1.0	5.6 ± 2.2	3.7 ± 0.7	3.6 ± 0.5	3.1 ± 0.6	3.2 ± 1.0	2.9 ± 0.6	2.6 ± 0.3	1.8 ± 0.3	2.3 ± 0.6	4.2 ± 0.8	2.6 ± 0.6
∑SFA	**235.4 ± 24.1**	**288.5 ± 55.8**	**441.2 ± 81.6**	**648.3 ± 186.3**	**485.9 ± 66.2**	**553.1 ± 127.2**	**444.8 ± 52.8**	**419.7 ± 41.0**	**750.2 ± 500.3**	**452.1 ± 52.5**	**292.3 ± 51.2**	**264.6 ± 55.6**	**1154.0 ± 199.0**	**561.2 ± 60.0**
Monounsaturated														
14:1ω5	0.7 ± 0.5	1.2 ± 0.5	1.4 ± 0.9	4.2 ± 2.6	3.4 ± 0.8	3.6 ± 3.0	2.3 ± 0.4	2.4 ± 0.6	3.7 ± 0.7	3.7 ± 1.1	2.3 ± 0.7	2.1 ± 0.5	8.3 ± 1.6	3.3 ± 0.7
16:1ω9	2.9 ± 0.8	6.8 ± 2.0	15.2 ± 9.2	28.5 ± 11.0	24.8 ± 3.6	30.3 ± 20.5	20.3 ± 5.1	16.9 ± 2.1	16.6 ± 1.1	18.1 ± 4.1	12.9 ± 4.1	7.7 ± 3.9	65.7 ± 22.2	15.5 ± 3.1
16:1ω7	50.6 ± 6.7	81.8 ± 8.3	76.6 ± 16.7	146.5 ± 21.5	153.6 ± 6.7	177.7 ± 45.3	129.4 ± 17.3	115.8 ± 20.7	158.7 ± 6.9	151.2 ± 15.4	70.8 ± 4.3	75.2 ± 14.7	367.5 ± 82.8	137.7 ± 4.9
17:1ω9	0.5 ± 0.3	0.6 ± 0.2	1.4 ± 0.6	3.7 ± 1.7	4.9 ± 2.2	3.3 ± 3.1	1.9 ± 0.4	1.8 ± 0.2	1.6 ± 0.2	1.9 ± 1.6	1.1 ± 0.7	1.2 ± 0.6	1.9 ± 0.7	2.5 ± 0.4
17:1ω7	2.5 ± 0.5	5.5 ± 0.7	5.5 ± 1.2	8.0 ± 2.2	8.4 ± 0.2	10.9 ± 2.8	9.7 ± 0.6	9.3 ± 1.6	8.7 ± 1.2	6.1 ± 0.7	2.1 ± 0.4	2.0 ± 0.4	5.5 ± 1.1	9.3 ± 1.1
18:1ω9	22.4 ± 4.8	68.1 ± 8.3	139.3 ± 25.8	130.3 ± 39.0	115.7 ± 7.6	106.3 ± 17.0	114.9 ± 11.1	92.3 ± 12.4	138.8 ± 38.6	114.2 ± 26.8	55.2 ± 11.0	59.9 ± 11.7	153.8 ± 42.7	107.1 ± 8.2
18:1ω7	33.4 ± 5.1	61.9 ± 11.3	65.6 ± 13.3	122.8 ± 5.7	118.4 ± 4.0	133.1 ± 32.5	103.3 ± 12.3	91.3 ± 15.8	121.3 ± 12.2	101.1 ± 8.8	38.7 ± 3.1	39.9 ± 9.5	183.8 ± 34.1	93.4 ± 6.1
20:1ω9	0.3 ± 0.1	0.4 ± 0.5	0.7 ± 0.1	0.3 ± 0.3	0.3 ± 0.1	0.2 ± 0.1	0.0 ± 0.0	0.1 ± 0.1	0.5 ± 0.3	0.7 ± 0.5	0.2 ± 0.2	0.3 ± 0.3	2.6 ± 1.0	0.4 ± 0.3
22:1ω9	1.3 ± 1.7	1.1 ± 1.7	2.3 ± 1.2	3.2 ± 2.2	1.1 ± 0.8	0.9 ± 0.9	1.9 ± 2.3	1.0 ± 1.0	1.4 ± 1.4	0.7 ± 0.4	0.7 ± 0.8	1.0 ± 1.4	2.1 ± 1.2	0.8 ± 0.7
∑MUFA	**114.6 ± 14.2**	**227.4 ± 28.0**	**308.0 ± 60.5**	**447.6 ± 73.9**	**430.4 ± 18.7**	**466.2 ± 107.6**	**383.6 ± 23.8**	**330.8 ± 50.9**	**451.2 ± 45.1**	**397.6 ± 33.7**	**183.9 ± 23.8**	**189.3 ± 39.5**	**791.3 ± 144.0**	**369.9 ± 14.8**
Polyunsaturated														
16:2ω4	2.6 ± 0.6	3.3 ± 0.3	3.0 ± 0.6	3.6 ± 1.5	3.1 ± 0.4	2.7 ± 0.8	2.2 ± 0.2	2.1 ± 0.9	5.2 ± 0.5	9.4 ± 1.3	6.8 ± 0.7	3.8 ± 1.1	44.0 ± 10.8	9.1 ± 0.9
16:3ω4	3.3 ± 0.6	4.7 ± 0.7	4.0 ± 1.2	5.7 ± 3.3	4.2 ± 0.4	3.7 ± 1.3	3.4 ± 0.4	3.9 ± 0.8	7.5 ± 0.8	18.6 ± 2.3	12.7 ± 1.7	7.5 ± 2.6	73.5 ± 16.8	15.6 ± 1.9
16:4ω3	0.5 ± 0.3	1.0 ± 0.2	1.6 ± 0.5	1.9 ± 0.5	1.9 ± 0.8	2.4 ± 1.3	2.0 ± 0.9	1.3 ± 0.1	2.7 ± 0.8	2.1 ± 0.8	1.9 ± 0.3	1.2 ± 0.6	22.7 ± 2.6	3.7 ± 0.4
18:2ω6	5.2 ± 0.5	5.4 ± 1.7	28.7 ± 7.9	20.5 ± 11.3	11.6 ± 1.3	10.2 ± 3.2	9.5 ± 1.7	6.6 ± 1.2	20.4 ± 11.9	22.5 ± 5.3	7.0 ± 1.8	7.8 ± 3.2	48.8 ± 16.5	16.5 ± 2.5
18:3ω3	1.6 ± 0.1	1.5 ± 1.1	3.1 ± 1.3	5.1 ± 3.7	3.3 ± 0.9	3.5 ± 1.4	2.0 ± 0.8	2.3 ± 0.7	4.0 ± 2.3	5.4 ± 0.9	5.7 ± 1.5	0.9 ± 0.3	85.4 ± 7.5	17.7 ± 5.2
18:4ω3	1.4 ± 0.1	1.6 ± 1.1	2.5 ± 1.0	3.0 ± 1.4	2.6 ± 0.3	3.2 ± 1.5	2.0 ± 1.6	2.1 ± 0.6	4.2 ± 1.9	5.8 ± 1.2	3.7 ± 1.0	1.0 ± 0.4	68.7 ± 8.0	16.7 ± 4.9
20:4ω6	2.5 ± 0.5	3.4 ± 0.4	3.1 ± 0.9	4.7 ± 1.3	4.4 ± 0.4	4.0 ± 1.4	3.7 ± 0.6	3.7 ± 1.0	6.1 ± 0.8	6.8 ± 0.6	4.4 ± 0.4	3.9 ± 1.3	20.6 ± 5.0	5.4 ± 0.5
20:5ω3	8.7 ± 2.4	11.1 ± 1.2	11.1 ± 4.2	14.7 ± 5.3	11.3 ± 0.5	11.7 ± 4.3	10.7 ± 1.3	11.4 ± 3.0	19.9 ± 3.9	34.5 ± 5.6	22.7 ± 3.6	13.2 ± 4.6	149.0 ± 35.6	31.1 ± 0.8
22:6ω3	4.7 ± 1.2	2.2 ± 1.1	3.4 ± 2.7	5.6 ± 5.5	3.1 ± 1.5	3.7 ± 3.0	3.2 ± 0.3	1.8 ± 1.0	4.0 ± 2.0	5.7 ± 3.0	3.5 ± 2.2	1.5 ± 1.0	55.6 ± 21.0	9.2 ± 1.3
∑PUFA	**30.6 ± 2.7**	**34.2 ± 5.8**	**60.5 ± 18.7**	**64.9 ± 29.6**	**45.5 ± 4.4**	**45.1 ± 15.7**	**38.8 ± 5.8**	**35.1 ± 7.4**	**74.0 ± 21.9**	**110.8 ± 16.7**	**68.4 ± 12.9**	**40.7 ± 14.0**	**568.4 ± 105.4**	**124.9 ± 10.6**
Branched														
14:0iso	1.9 ± 1.3	3.9 ± 0.8	3.7 ± 0.6	7.0 ± 1.9	5.7 ± 0.9	5.9 ± 1.1	5.5 ± 0.7	5.1 ± 0.9	6.4 ± 0.7	7.1 ± 0.8	5.0 ± 0.4	4.6 ± 0.6	14.8 ± 1.8	5.2 ± 3.5
15:0iso	9.0 ± 1.3	14.1 ± 1.3	12.7 ± 3.0	23.4 ± 3.3	20.6 ± 3.0	23.8 ± 3.6	18.7 ± 2.1	18.5 ± 3.8	24.8 ± 1.7	19.7 ± 1.5	11.1 ± 0.6	11.8 ± 2.6	24.0 ± 5.4	17.0 ± 2.3
15:0anteiso	4.5 ± 0.3	7.8 ± 1.0	7.6 ± 1.6	13.8 ± 1.2	12.2 ± 1.5	15.9 ± 3.0	12.8 ± 2.2	10.4 ± 1.8	12.2 ± 1.0	10.6 ± 0.6	6.5 ± 0.7	7.6 ± 1.8	17.6 ± 3.8	9.8 ± 1.2
16:0iso	2.0 ± 0.3	4.2 ± 0.5	3.6 ± 0.7	6.9 ± 0.6	6.1 ± 0.4	6.8 ± 1.0	5.3 ± 0.8	4.4 ± 0.5	8.0 ± 4.4	5.7 ± 0.3	3.5 ± 0.5	4.2 ± 1.2	6.8 ± 1.3	5.3 ± 0.9
17:0iso	2.8 ± 0.2	4.3 ± 0.8	4.4 ± 1.4	7.0 ± 0.8	5.9 ± 0.9	7.7 ± 2.0	5.1 ± 0.5	4.9 ± 0.5	7.7 ± 0.9	9.3 ± 0.9	6.2 ± 0.8	4.7 ± 1.2	23.9 ± 2.3	10.3 ± 1.1
17:0anteiso	2.8 ± 0.4	4.4 ± 0.4	4.8 ± 0.9	7.1 ± 1.4	6.8 ± 0.8	8.3 ± 1.7	7.5 ± 1.2	6.3 ± 0.7	10.2 ± 6.4	5.6 ± 1.1	4.3 ± 1.1	5.1 ± 1.3	7.5 ± 2.1	6.3 ± 1.6
∑BrFA	**23.1 ± 3.1**	**38.8 ± 3.7**	**36.9 ± 7.9**	**65.1 ± 8.4**	**57.3 ± 6.6**	**68.3 ± 11.6**	**54.9 ± 7.2**	**49.6 ± 7.1**	**69.3 ± 12.4**	**58.0 ± 3.5**	**36.5 ± 3.2**	**38.0 ± 8.2**	**94.6 ± 13.8**	**53.9 ± 5.8**
∑FA (µg gSPM^{-1})	**403.7 ± 33.1**	**588.8 ± 87.7**	**846.6 ± 157.0**	**1225.8 ± 293.6**	**1019.0 ± 64.9**	**1132.7 ± 248.0**	**922.2 ± 87.0**	**835.2 ± 103.7**	**1344.7 ± 556.1**	**1018.5 ± 92.6**	**581.0 ± 77.2**	**532.6 ± 116.8**	**2608.3 ± 443.8**	**1109.9 ± 78.0**
∑FA (µg L^{-1})	**23.3 ± 2.3**	**45.5 ± 8.7**	**49.9 ± 11.2**	**48.6 ± 11.0**	**36.8 ± 1.8**	**37.4 ± 7.9**	**27.6 ± 2.9**	**28.7 ± 2.9**	**51.9 ± 23.9**	**51.1 ± 5.0**	**122.8 ± 18.1**	**131.8 ± 33.4**	**187.9 ± 34.9**	**44.0 ± 3.2**

Appendix 6-1: Complete fatty acid compositions in µg g^{-1} ± SD of potential food sources in the Can Gio mangrove tidal creek and nearby areas

Fatty acids (µg g^{-1})	Suspended matter (n = 56)	Sediment Maf (n = 4)	Sediment Bof (n = 4)	Sediment Mub (n = 4)	Leaves Ava (n = 4)	Leaves Soa (n = 4)	Leaves Rha (n = 4)
Saturated							
12:0	27.3 ± 67.7	3.6 ± 1.0	1.7 ± 0.7	1.8 ± 1.0	17.3 ± 2.1	11.0 ± 5.2	91.6 ± 24.0
13:0	3.6 ± 1.8	0.8 ± 0.2	0.4 ± 0.1	0.5 ± 0.2	-	-	-
14:0	75.4 ± 54.1	14.5 ± 0.6	7.5 ± 1.1	9.2 ± 1.9	348.1 ± 46.6	348.4 ± 125.3	427.2 ± 97.2
15:0	23.1 ± 9.4	6.5 ± 0.4	2.8 ± 0.6	4.6 ± 0.7	25.7 ± 6.5	31.9 ± 6.8	35.9 ± 8.8
16:0	283.4 ± 165.4	50.8 ± 2.1	30.0 ± 4.5	32.1 ± 4.1	2740.0 ± 281.1	2599.3 ± 348.2	2933.2 ± 746.5
17:0	11.0 ± 4.5	3.1 ± 0.3	1.5 ± 0.3	1.9 ± 0.2	49.2 ± 15.8	42.9 ± 9.5	93.9 ± 28.0
18:0	65.1 ± 29.5	9.4 ± 0.3	6.5 ± 0.7	6.7 ± 0.8	298.9 ± 35.2	261.1 ± 44.0	311.7 ± 91.4
19:0	3.9 ± 1.6	0.8 ± 0.1	0.5 ± 0.0	0.5 ± 0.0	25.7 ± 10.5	9.1 ± 2.7	6.7 ± 2.6
20:0	3.6 ± 1.7	3.6 ± 0.5	1.7 ± 0.3	1.6 ± 0.1	219.8 ± 34.5	187.7 ± 37.8	87.3 ± 20.1
21:0	0.0 ± 0.0	2.5 ± 0.5	0.4 ± 0.1	0.4 ± 0.0	33.2 ± 9.8	62.2 ± 15.1	16.4 ± 7.2
22:0	3.1 ± 1.2	5.0 ± 0.6	1.7 ± 0.3	1.6 ± 0.1	82.6 ± 12.2	179.7 ± 40.8	55.8 ± 17.0
24:0	-	8.6 ± 1.9	2.7 ± 0.3	2.7 ± 0.3	99.7 ± 12.3	53.0 ± 9.4	48.4 ± 9.6
25:0	-	1.0 ± 0.2	0.4 ± 0.1	0.5 ± 0.1	28.1 ± 7.7	12.9 ± 5.6	18.1 ± 3.2
26:0	-	8.5 ± 2.4	2.3 ± 0.1	2.3 ± 0.4	93.4 ± 13.1	26.3 ± 7.2	12.3 ± 5.8
27:0	-	0.4 ± 0.1	0.3 ± 0.0	0.3 ± 0.1	9.4 ± 1.3	6.1 ± 1.7	-
28:0	-	4.5 ± 1.1	2.0 ± 0.4	1.7 ± 0.5	80.4 ± 13.0	23.6 ± 4.1	-
29:0	-	0.2 ± 0.1	0.2 ± 0.1	0.2 ± 0.0	17.5 ± 19.4	-	-
30:0	-	1.2 ± 0.8	1.2 ± 0.5	0.8 ± 0.4	37.2 ± 13.3	-	-
∑SFA	**499.4 ± 273.3**	**125.0 ± 10.0**	**63.7 ± 9.5**	**69.3 ± 9.3**	**4206.3 ± 325.6**	**3855.4 ± 598.3**	**4138.4 ± 965.1**
Monounsaturated							
15:1ω1	-	-	-	-	41.0 ± 8.7	26.1 ± 3.9	23.3 ± 4.3
16:1ω7	135.2 ± 79.5	15.6 ± 1.8	10.0 ± 0.9	12.4 ± 1.4	72.7 ± 8.0	25.7 ± 6.6	22.1 ± 6.7
16:1ω5	-	3.1 ± 0.3	1.8 ± 0.2	2.0 ± 0.2	-	-	-
17:1ω9	2.0 ± 1.6	1.4 ± 0.3	0.7 ± 0.2	1.1 ± 0.2	-	-	-
17:1ω7	6.7 ± 3.1	3.1 ± 0.4	1.3 ± 0.2	1.3 ± 0.2	24.2 ± 7.9	15.2 ± 1.5	18.8 ± 6.4
18:1ω9	101.3 ± 41.6	7.6 ± 0.7	6.4 ± 1.8	5.5 ± 1.2	577.5 ± 196.4	557.3 ± 141.0	434.8 ± 117.8
18:1ω7	93.4 ± 43.4	15.9 ± 1.2	10.2 ± 1.0	10.7 ± 1.2	82.7 ± 8.6	49.9 ± 19.4	81.3 ± 24.1
19:1ω9	-	2.9 ± 0.3	2.4 ± 0.2	2.4 ± 0.4	-	-	-
20:1ω9	0.5 ± 0.7	0.4 ± 0.0	0.4 ± 0.2	0.3 ± 0.0	7.1 ± 1.9	8.6 ± 3.1	3.3 ± 0.5
22:1ω9	1.4 ± 1.4	8.0 ± 0.8	4.5 ± 1.9	3.8 ± 1.0	-	-	-
∑MUFA	**363.7 170.6**	**58.0 ± 3.8**	**37.8 ± 6.1**	**39.5 ± 4.2**	**805.4 ± 194.3**	**682.8 ± 171.9**	**583.6 ± 155.4**
Polyunsaturated							
16:2ω6	-	0.3 ± 0.0	0.2 ± 0.0	0.3 ± 0.1	-	-	-
16:2ω4	7.2 10.9	0.7 ± 0.1	0.5 ± 0.0	0.6 ± 0.2	-	-	-
16:3ω4	12.0 18.3	0.3 ± 0.1	0.3 ± 0.0	0.5 ± 0.1	-	-	-
16:4ω3	3.3 5.5	-	-	-	-	-	-
18:2ω6	15.8 13.2	3.0 ± 0.7	2.3 ± 1.0	1.4 ± 0.2	1048.8 ± 193.0	936.4 ± 216.8	1237.4 ± 449.6
18:3ω6	-	0.5 ± 0.1	0.2 ± 0.1	0.1 ± 0.1	-	-	-
18:3ω3	10.1 ± 21.6	1.3 ± 0.4	0.6 ± 0.4	0.3 ± 0.0	3047.5 ± 666.5	2506.6 ± 299.3	2420.2 ± 693.3
18:4ω3	8.5 ± 17.5	-	-	-	-	-	-
20:4ω6	5.5 ± 4.6	1.4 ± 0.1	1.3 ± 0.1	1.6 ± 0.3	-	-	-
20:5ω3	25.8 ± 36.4	1.7 ± 0.1	1.2 ± 0.2	2.1 ± 0.3	-	-	-
22:6ω3	7.7 ± 14.5	-	-	-	-	-	-
∑PUFA	**95.8 ± 137.9**	**9.1 ± 1.2**	**6.6 ± 1.6**	**6.8 ± 1.0**	**4096.3 ± 769.3**	**3443.1 ± 455.9**	**3657.7 ± 1049.0**
Branched							
13:0iso	-	0.6 ± 0.0	0.4 ± 0.1	0.4 ± 0.1	-	-	-
13:0anteiso	-	0.3 ± 0.0	0.1 ± 0.0	0.1 ± 0.0	-	-	-
14:0iso	5.8 ± 3.1	5.8 ± 0.7	2.4 ± 0.4	2.8 ± 0.5	-	-	-
15:0iso	17.8 ± 5.7	19.2 ± 1.8	9.1 ± 1.3	10.5 ± 1.4	-	-	-
15:0anteiso	10.7 ± 3.9	16.1 ± 1.8	5.4 ± 0.8	6.3 ± 0.9	-	-	-
16:0iso	5.2 ± 2.0	7.3 ± 1.2	3.3 ± 0.5	3.7 ± 0.5	-	-	-
10-methyl 16	-	10.6 ± 0.9	6.3 ± 0.5	6.4 ± 1.0	-	-	-
17:0iso	7.5 5.1	4.1 ± 0.3	2.4 ± 0.3	2.5 ± 0.3	-	-	-
17:0anteiso	6.2 2.6	3.9 ± 0.5	1.8 ± 0.2	2.0 ± 0.2	-	-	-
18:0iso	-	0.4 ± 0.1	0.2 ± 0.0	0.3 ± 0.0	-	-	-
∑BrFA	**53.2 ± 19.0**	**68.3 ± 6.7**	**31.5 ± 4.0**	**35.0 ± 4.6**	**-**	**-**	**-**
∑FA (µg g^{-1})	**1012.1 ± 560.4**	**260.5 ± 18.1**	**139.6 ± 19.3**	**150.6 ± 17.4**	**9108.0 ± 1250.2**	**7981.2 ± 1048.9**	**8379.7 ± 2131.3**

Appendix 6-2: Complete fatty acid compositions (% ± SD) of gastropods in the Can Gio mangrove tidal creek and nearby areas

Fatty acids (%)	Cassidula aurisfelis (n = 2)	Cerithidea obtusa (n = 4)	Cerithidea quoyii (n = 4)	Chicoreus capucinus (n = 4)	Littoraria melanostoma (n = 4)	Littoraria vespacea (n = 4)	Neripteron violaceum (n = 4)	Nerita balteata (n = 4)
Saturated								
12:0	0.0 ± 0.0	0.3 ± 0.4	0.1 ± 0.0	0.5 ± 0.5	0.2 ± 0.1	0.1 ± 0.1	0.1 ± 0.0	0.1 ± 0.1
13:0	0.1 ± 0.0	0.1 ± 0.0	0.2 ± 0.0	0.1 ± 0.0	0.2 ± 0.1	0.1 ± 0.1	0.1 ± 0.1	0.1 ± 0.0
14:0	2.2 ± 0.9	3.8 ± 0.3	4.2 ± 0.7	3.8 ± 0.7	6.4 ± 1.7	5.1 ± 2.9	5.6 ± 0.5	3.9 ± 0.3
15:0	2.1 ± 0.5	2.2 ± 0.3	1.4 ± 0.1	1.1 ± 0.5	1.3 ± 0.1	0.7 ± 0.3	1.1 ± 0.2	1.1 ± 0.1
16:0	13.6 ± 1.1	21.0 ± 0.9	24.4 ± 1.0	9.7 ± 1.5	21.2 ± 3.6	19.3 ± 5.7	20.5 ± 0.9	20.5 ± 1.4
17:0	3.4 ± 0.2	2.7 ± 0.2	2.5 ± 0.4	1.8 ± 0.2	1.9 ± 0.1	1.7 ± 0.3	1.4 ± 0.1	1.2 ± 0.2
18:0	8.6 ± 0.5	7.9 ± 0.8	7.4 ± 1.9	7.7 ± 0.6	7.3 ± 0.6	7.8 ± 1.3	4.5 ± 0.3	4.0 ± 0.7
19:0	0.2 ± 0.0	0.3 ± 0.0	0.3 ± 0.0	0.2 ± 0.1	0.2 ± 0.0	0.2 ± 0.0	0.1 ± 0.0	0.1 ± 0.0
20:0	0.3 ± 0.1	0.2 ± 0.0	0.2 ± 0.0	0.1 ± 0.0	0.2 ± 0.0	0.1 ± 0.0	0.1 ± 0.0	0.1 ± 0.0
22:0	0.2 ± 0.0	0.1 ± 0.0	0.0 ± 0.0	0.4 ± 0.2	0.1 ± 0.0	0.1 ± 0.1	0.1 ± 0.0	0.1 ± 0.0
24:0	0.1 ± 0.0	0.0 ± 0.0	0.0 ± 0.0	0.0 ± 0.0	0.2 ± 0.1	0.1 ± 0.1	0.3 ± 0.1	0.1 ± 0.1
26:0	0.0 ± 0.0	0.0 ± 0.0	0.0 ± 0.0	0.0 ± 0.0	0.2 ± 0.1	0.0 ± 0.0	0.1 ± 0.1	0.0 ± 0.0
∑SFA	**30.8 ± 1.8**	**38.7 ± 1.2**	**40.6 ± 2.6**	**25.5 ± 1.6**	**39.2 ± 4.6**	**35.3 ± 7.4**	**34.1 ± 1.8**	**31.1 ± 0.7**
Monounsaturated								
16:1ω7	2.6 ± 0.2	2.4 ± 0.2	1.8 ± 0.6	1.9 ± 1.5	1.1 ± 0.4	0.9 ± 0.2	1.6 ± 0.3	1.8 ± 0.8
16:1ω5	1.0 ± 0.1	1.6 ± 0.5	0.4 ± 0.2	0.1 ± 0.1	0.4 ± 0.1	0.3 ± 0.1	0.3 ± 0.1	0.3 ± 0.1
18:1ω11	0.2 ± 0.0	0.5 ± 0.1	0.2 ± 0.2	0.3 ± 0.2	0.2 ± 0.0	0.2 ± 0.1	0.2 ± 0.0	2.1 ± 1.8
18:1ω9	4.4 ± 0.2	5.0 ± 0.5	8.3 ± 0.8	2.3 ± 0.6	4.5 ± 1.2	5.1 ± 0.7	8.2 ± 1.4	5.5 ± 0.9
18:1ω7	6.1 ± 0.3	7.8 ± 1.7	6.0 ± 0.6	1.4 ± 0.6	5.6 ± 2.0	3.7 ± 0.7	4.6 ± 0.5	5.8 ± 0.9
18:1ω5	0.4 ± 0.0	0.7 ± 0.1	0.2 ± 0.0	0.1 ± 0.1	0.1 ± 0.0	0.1 ± 0.0	0.1 ± 0.0	0.3 ± 0.1
19:1ω9	0.2 ± 0.1	0.2 ± 0.0	0.2 ± 0.0	0.2 ± 0.0	0.2 ± 0.0	0.1 ± 0.0	0.2 ± 0.0	0.3 ± 0.1
20:1ω11	4.4 ± 0.4	3.9 ± 0.2	4.1 ± 0.8	9.5 ± 0.4	4.6 ± 0.1	4.3 ± 1.0	4.6 ± 0.7	4.2 ± 0.8
20:1ω9	0.8 ± 0.0	0.5 ± 0.1	0.9 ± 0.1	0.5 ± 0.1	0.5 ± 0.1	1.2 ± 0.2	1.9 ± 0.5	1.7 ± 0.4
20:1ω7	0.9 ± 0.1	0.5 ± 0.1	0.2 ± 0.0	0.3 ± 0.1	0.8 ± 0.2	0.4 ± 0.1	0.2 ± 0.1	0.4 ± 0.1
22:1ω11	0.4 ± 0.1	0.5 ± 0.1	0.3 ± 0.1	0.7 ± 0.2	0.4 ± 0.1	0.2 ± 0.1	0.2 ± 0.1	0.1 ± 0.0
∑MUFA	**21.4 ± 0.2**	**23.6 ± 2.1**	**22.7 ± 1.5**	**17.4 ± 2.2**	**18.5 ± 2.9**	**16.6 ± 1.2**	**22.0 ± 0.7**	**22.6 ± 2.0**
Polyunsaturated								
16:2ω6	0.0 ± 0.0	0.1 ± 0.0	0.6 ± 0.2	0.0 ± 0.0	0.4 ± 0.2	0.5 ± 0.3	0.9 ± 0.4	0.7 ± 0.1
16:2ω4	0.1 ± 0.0	0.2 ± 0.0	0.1 ± 0.1	0.0 ± 0.0	0.1 ± 0.0	0.0 ± 0.0	0.1 ± 0.0	0.2 ± 0.1
16:3ω6	0.1 ± 0.0	0.1 ± 0.0	0.6 ± 0.1	0.1 ± 0.1	0.4 ± 0.2	0.8 ± 0.3	1.6 ± 0.4	1.2 ± 0.2
16:4ω3	0.0 ± 0.0	0.1 ± 0.1	0.0 ± 0.0	0.1 ± 0.1	0.3 ± 0.1	0.3 ± 0.1	0.3 ± 0.1	0.4 ± 0.1
18:2ω6	3.8 ± 0.0	3.5 ± 0.6	8.9 ± 1.2	4.0 ± 0.4	8.9 ± 1.7	13.1 ± 1.9	18.3 ± 2.5	17.6 ± 2.3
18:2ω3	0.1 ± 0.0	0.2 ± 0.1	0.1 ± 0.0	0.0 ± 0.0	0.1 ± 0.1	0.0 ± 0.0	0.1 ± 0.1	0.0 ± 0.0
18:3ω6	0.1 ± 0.0	0.0 ± 0.0	0.1 ± 0.0	0.0 ± 0.0	0.0 ± 0.0	0.1 ± 0.0	0.1 ± 0.0	0.1 ± 0.0
18:3ω3	0.9 ± 0.2	0.8 ± 0.1	0.8 ± 0.2	0.6 ± 0.2	1.6 ± 0.3	1.6 ± 0.3	0.8 ± 0.0	1.5 ± 0.5
18:4ω3	0.0 ± 0.0	0.2 ± 0.0	0.1 ± 0.0	0.1 ± 0.0	0.1 ± 0.0	0.1 ± 0.0	0.1 ± 0.0	0.1 ± 0.0
20:2ω9 (NMI)	0.1 ± 0.0	0.4 ± 0.1	0.2 ± 0.1	0.2 ± 0.1	0.1 ± 0.0	0.2 ± 0.1	0.3 ± 0.1	1.1 ± 0.7
20:2ω7 (NMI)	0.1 ± 0.0	0.1 ± 0.1	0.0 ± 0.0	0.6 ± 0.4	0.2 ± 0.1	0.1 ± 0.0	0.0 ± 0.0	0.3 ± 0.3
20:2ω6	2.5 ± 0.5	2.4 ± 0.4	2.3 ± 0.3	2.0 ± 0.3	4.2 ± 0.6	3.7 ± 0.5	1.3 ± 0.2	1.1 ± 0.2
20:3ω6,9,15 (NMI)	0.2 ± 0.0	0.8 ± 0.3	0.7 ± 0.3	0.6 ± 0.2	0.6 ± 0.1	0.3 ± 0.1	0.2 ± 0.0	0.4 ± 0.3
20:3ω6	1.0 ± 0.1	1.0 ± 0.1	1.4 ± 0.7	0.3 ± 0.1	0.9 ± 0.0	1.1 ± 0.2	0.6 ± 0.1	0.7 ± 0.2
20:4ω6	8.5 ± 0.5	8.1 ± 1.2	7.0 ± 1.3	19.6 ± 0.8	9.9 ± 0.7	10.9 ± 2.7	9.3 ± 1.5	10.4 ± 2.1
20:4ω3	0.3 ± 0.0	0.1 ± 0.0	0.4 ± 0.0	0.1 ± 0.0	0.2 ± 0.0	0.2 ± 0.0	0.0 ± 0.0	0.0 ± 0.0
20:5ω3	5.7 ± 0.2	2.6 ± 0.3	2.0 ± 0.8	1.6 ± 0.1	2.4 ± 0.8	2.0 ± 0.8	0.7 ± 0.5	1.5 ± 0.6
22:2ω9 (NMI)	2.1 ± 0.1	1.3 ± 0.2	1.2 ± 0.3	7.2 ± 0.7	1.7 ± 0.2	3.6 ± 1.8	2.2 ± 1.6	2.2 ± 0.7
22:2ω6	0.9 ± 0.0	0.7 ± 0.1	0.2 ± 0.0	4.1 ± 1.2	1.0 ± 0.4	0.5 ± 0.1	0.8 ± 1.3	0.1 ± 0.0
22:3ω6	0.6 ± 0.1	0.8 ± 0.2	1.0 ± 0.1	2.8 ± 0.7	2.4 ± 0.3	0.9 ± 0.2	0.4 ± 0.1	0.3 ± 0.0
22:4ω6	8.0 ± 0.8	2.8 ± 0.6	1.8 ± 0.3	5.9 ± 0.6	1.7 ± 0.4	2.9 ± 1.0	2.3 ± 0.4	2.2 ± 0.6
22:5ω6	0.8 ± 0.2	2.0 ± 0.4	0.9 ± 0.6	0.2 ± 0.1	0.1 ± 0.0	0.0 ± 0.0	0.0 ± 0.0	0.0 ± 0.0
22:5ω3	3.6 ± 0.4	0.9 ± 0.1	0.4 ± 0.1	4.1 ± 0.9	1.9 ± 0.4	3.1 ± 1.9	0.3 ± 0.3	0.6 ± 0.5
22:6ω3	3.0 ± 0.1	2.5 ± 0.5	1.0 ± 0.7	0.6 ± 0.2	0.2 ± 0.2	0.1 ± 0.0	0.1 ± 0.1	0.0 ± 0.0
∑PUFA	**42.4 ± 3.1**	**31.6 ± 2.6**	**31.9 ± 2.6**	**54.8 ± 2.0**	**39.3 ± 1.6**	**45.8 ± 7.7**	**40.7 ± 1.9**	**42.9 ± 2.7**
Branched								
15:0iso	1.1 ± 0.3	1.1 ± 0.1	0.4 ± 0.1	0.3 ± 0.3	0.3 ± 0.1	0.2 ± 0.2	0.6 ± 0.3	0.6 ± 0.1
15:0anteiso	0.5 ± 0.0	0.3 ± 0.0	0.2 ± 0.1	0.1 ± 0.1	0.2 ± 0.1	0.1 ± 0.0	0.2 ± 0.0	0.1 ± 0.0
16:0iso	1.4 ± 0.3	0.7 ± 0.0	1.0 ± 0.2	0.3 ± 0.2	0.5 ± 0.1	0.3 ± 0.1	0.6 ± 0.1	0.9 ± 0.2
10-methyl 16	0.2 ± 0.1	0.2 ± 0.0	0.2 ± 0.0	0.0 ± 0.0	0.1 ± 0.0	0.1 ± 0.0	0.1 ± 0.0	0.1 ± 0.0
17:0iso	0.6 ± 0.9	2.7 ± 0.2	1.7 ± 0.3	0.8 ± 0.3	1.2 ± 0.2	1.0 ± 0.2	1.0 ± 0.0	0.9 ± 0.2
17:0anteiso	0.9 ± 0.0	0.7 ± 0.1	0.6 ± 0.1	0.7 ± 0.5	0.4 ± 0.1	0.2 ± 0.0	0.3 ± 0.1	0.3 ± 0.0
18:0iso	0.5 ± 0.0	0.2 ± 0.1	0.7 ± 0.3	0.2 ± 0.1	0.3 ± 0.1	0.3 ± 0.1	0.2 ± 0.0	0.4 ± 0.1
∑BrFA	**5.3 ± 1.5**	**6.1 ± 0.2**	**4.9 ± 0.4**	**2.4 ± 1.4**	**3.1 ± 0.6**	**2.2 ± 0.4**	**3.2 ± 0.5**	**3.4 ± 0.2**
∑FA (mg g^{-1})	**25.0 ± 6.1**	**40.7 ± 3.3**	**68.6 ± 21.4**	**14.3 ± 3.5**	**44.2 ± 7.8**	**48.1 ± 32.7**	**54.2 ± 17.6**	**72.3 ± 27.5**

Appendix 6-3: Complete fatty acid compositions (% ± SD) of crustaceans and fish in the Can Gio mangrove tidal creek and nearby areas

Fatty acids (%)	Clistocoeloma merguiense (n = 4)	Metaplax elegans (n = 4)	Metopograpsus latifrons (n = 4)	Tubuca paradussumieri (n = 4)	Macrobrachium equidens (n = 4)	Metapenaeus ensis (n = 4)	Cloridopsis immaculata (n = 3)	Planiliza sp. B (n = 4)
Saturated								
12:0	0.2 ± 0.1	0.1 ± 0.1	0.1 ± 0.1	0.2 ± 0.1	0.2 ± 0.1	0.1 ± 0.1	0.5 ± 0.1	0.1 ± 0.1
13:0	0.1 ± 0.0	0.0 ± 0.0	0.0 ± 0.0	0.1 ± 0.1	0.1 ± 0.0	0.1 ± 0.0	0.2 ± 0.0	0.0 ± 0.0
14:0	0.6 ± 0.2	0.5 ± 0.4	0.6 ± 0.2	1.2 ± 0.5	2.3 ± 0.3	1.5 ± 0.3	4.7 ± 0.7	1.5 ± 0.4
15:0	0.8 ± 0.1	1.6 ± 0.5	0.7 ± 0.1	2.3 ± 0.8	1.2 ± 0.1	2.1 ± 0.3	1.8 ± 0.1	1.2 ± 0.4
16:0	14.9 ± 1.2	17.2 ± 2.0	14.7 ± 0.4	15.9 ± 0.8	23.5 ± 0.9	16.2 ± 0.7	24.7 ± 0.9	26.1 ± 0.4
17:0	2.3 ± 0.1	1.6 ± 0.3	1.7 ± 0.1	2.1 ± 0.6	1.6 ± 0.4	3.6 ± 0.2	2.0 ± 0.3	0.7 ± 0.1
18:0	11.0 ± 0.3	12.0 ± 1.3	10.9 ± 0.4	11.6 ± 0.3	8.6 ± 0.9	11.1 ± 0.7	9.7 ± 0.5	10.3 ± 0.5
19:0	0.4 ± 0.1	0.3 ± 0.0	0.2 ± 0.1	0.2 ± 0.0	0.2 ± 0.0	0.4 ± 0.0	0.4 ± 0.0	0.3 ± 0.0
20:0	0.3 ± 0.1	0.5 ± 0.1	0.2 ± 0.0	0.2 ± 0.0	0.3 ± 0.0	0.3 ± 0.0	0.7 ± 0.1	0.2 ± 0.0
22:0	0.1 ± 0.0	0.5 ± 0.1	0.2 ± 0.1	0.4 ± 0.1	0.2 ± 0.0	0.5 ± 0.0	0.7 ± 0.2	0.2 ± 0.0
24:0	0.0 ± 0.0	0.1 ± 0.0	0.0 ± 0.0	0.0 ± 0.0	0.1 ± 0.0	0.1 ± 0.0	0.2 ± 0.0	0.3 ± 0.1
∑SFA	**30.9 ± 1.7**	**34.4 ± 0.6**	**29.3 ± 0.8**	**34.0 ± 0.7**	**38.3 ± 1.3**	**35.8 ± 0.9**	**45.4 ± 1.2**	**41.1 ± 0.9**
Monounsaturated								
16:1ω7	3.6 ± 0.6	4.4 ± 0.5	1.8 ± 0.5	8.8 ± 1.1	6.8 ± 1.2	3.9 ± 0.7	9.0 ± 1.1	4.0 ± 0.9
16:1ω5	0.1 ± 0.0	0.1 ± 0.1	0.1 ± 0.0	0.0 ± 0.0	0.2 ± 0.1	0.3 ± 0.2	0.2 ± 0.1	0.3 ± 0.1
17:1ω9	0.6 ± 0.2	1.1 ± 0.4	0.2 ± 0.1	4.4 ± 0.5	0.9 ± 0.2	1.0 ± 0.2	1.0 ± 0.3	0.6 ± 0.2
17:1ω7	0.1 ± 0.0	0.1 ± 0.1	0.1 ± 0.1	0.2 ± 0.1	0.1 ± 0.0	0.1 ± 0.0	0.1 ± 0.1	0.1 ± 0.0
18:1ω11	0.0 ± 0.0	0.0 ± 0.0	0.1 ± 0.0	0.0 ± 0.0	0.0 ± 0.0	0.2 ± 0.0	0.3 ± 0.2	0.0 ± 0.0
18:1ω9	13.9 ± 0.5	5.7 ± 0.6	8.2 ± 1.6	6.0 ± 1.2	18.1 ± 2.4	6.6 ± 0.9	7.0 ± 0.8	4.5 ± 0.9
18:1ω7	3.6 ± 0.4	3.6 ± 0.3	3.7 ± 1.0	2.2 ± 0.4	3.4 ± 0.6	4.7 ± 0.2	3.8 ± 0.2	2.7 ± 0.2
18:1ω5	0.1 ± 0.0	0.1 ± 0.0	0.1 ± 0.0	0.1 ± 0.0	0.2 ± 0.1	0.3 ± 0.1	0.2 ± 0.1	0.1 ± 0.0
19:1ω9	0.1 ± 0.0	0.1 ± 0.0	0.0 ± 0.0	0.1 ± 0.0	0.1 ± 0.0	0.1 ± 0.0	0.2 ± 0.0	0.2 ± 0.0
20:1ω11	0.1 ± 0.0	0.1 ± 0.0	0.1 ± 0.1	0.0 ± 0.0	0.2 ± 0.0	0.7 ± 0.1	0.6 ± 0.4	0.1 ± 0.0
20:1ω9	0.3 ± 0.1	1.1 ± 0.2	0.2 ± 0.0	1.1 ± 0.1	0.2 ± 0.0	0.6 ± 0.2	0.5 ± 0.0	0.6 ± 0.1
20:1ω7	0.0 ± 0.0	0.1 ± 0.0	0.0 ± 0.0	0.0 ± 0.0	0.1 ± 0.0	0.2 ± 0.1	0.2 ± 0.0	0.1 ± 0.0
22:1ω11	0.0 ± 0.0	0.0 ± 0.0	0.0 ± 0.0	0.0 ± 0.0	0.0 ± 0.0	0.1 ± 0.0	0.1 ± 0.0	0.0 ± 0.0
22:1ω9	0.0 ± 0.0	0.4 ± 0.0	0.0 ± 0.0	0.4 ± 0.0	0.0 ± 0.0	0.0 ± 0.0	0.0 ± 0.0	0.0 ± 0.0
∑MUFA	**22.5 ± 1.4**	**16.5 ± 1.2**	**14.7 ± 1.7**	**23.0 ± 2.1**	**30.3 ± 2.2**	**18.8 ± 1.8**	**23.2 ± 0.7**	**13.4 ± 0.3**
Polyunsaturated								
16:2ω6	0.0 ± 0.0	0.1 ± 0.1	0.1 ± 0.1	0.1 ± 0.0	0.0 ± 0.0	0.0 ± 0.0	0.1 ± 0.0	0.1 ± 0.0
16:2ω4	0.0 ± 0.0	0.4 ± 0.2	0.0 ± 0.0	0.5 ± 0.0	0.0 ± 0.0	0.1 ± 0.0	0.3 ± 0.1	0.4 ± 0.2
16:3ω6	0.0 ± 0.0	0.0 ± 0.0	0.0 ± 0.0	0.0 ± 0.0	0.0 ± 0.0	0.1 ± 0.0	0.1 ± 0.0	0.0 ± 0.0
16:3ω4	0.0 ± 0.0	0.7 ± 0.7	0.0 ± 0.0	0.2 ± 0.0	0.0 ± 0.0	0.0 ± 0.0	0.4 ± 0.2	0.4 ± 0.3
16:4ω3	0.0 ± 0.0	0.1 ± 0.1	0.1 ± 0.0	0.2 ± 0.1	0.0 ± 0.0	0.0 ± 0.0	0.1 ± 0.0	0.1 ± 0.0
18:2ω6	15.5 ± 2.6	4.3 ± 0.9	15.8 ± 2.4	3.0 ± 0.2	5.7 ± 1.0	3.6 ± 0.5	4.0 ± 0.3	0.7 ± 0.1
18:2ω3	0.2 ± 0.1	0.2 ± 0.0	0.1 ± 0.0	0.1 ± 0.0	0.1 ± 0.0	0.1 ± 0.0	0.2 ± 0.0	0.3 ± 0.0
18:3ω6	0.0 ± 0.0	0.4 ± 0.0	0.1 ± 0.0	0.8 ± 0.0	0.1 ± 0.0	0.1 ± 0.0	0.2 ± 0.0	0.2 ± 0.0
18:3ω3	6.8 ± 0.4	1.4 ± 1.1	0.9 ± 0.2	0.2 ± 0.1	2.3 ± 0.8	0.8 ± 0.2	1.2 ± 0.5	0.2 ± 0.1
18:4ω3	0.0 ± 0.0	0.4 ± 0.0	0.1 ± 0.0	0.4 ± 0.1	0.1 ± 0.0	0.1 ± 0.0	0.2 ± 0.1	0.2 ± 0.1
20:2ω6	1.1 ± 0.2	1.0 ± 0.2	1.4 ± 0.2	0.5 ± 0.1	0.4 ± 0.1	1.3 ± 0.3	0.9 ± 0.2	0.3 ± 0.1
20:3ω6,9,15 (NMI)	0.1 ± 0.0	0.1 ± 0.0	0.1 ± 0.0	0.1 ± 0.0	0.1 ± 0.0	0.4 ± 0.1	0.1 ± 0.1	0.1 ± 0.0
20:3ω6	0.1 ± 0.0	0.2 ± 0.0	0.1 ± 0.0	0.5 ± 0.1	0.1 ± 0.0	0.6 ± 0.1	0.2 ± 0.1	0.3 ± 0.0
20:3ω3	0.5 ± 0.1	0.3 ± 0.1	0.1 ± 0.1	0.2 ± 0.1	0.0 ± 0.0	0.0 ± 0.0	0.1 ± 0.0	0.0 ± 0.0
20:4ω6	5.5 ± 0.3	7.2 ± 0.5	9.1 ± 1.6	11.5 ± 0.9	8.0 ± 0.5	15.9 ± 1.0	6.7 ± 0.7	10.6 ± 0.6
20:4ω3	0.1 ± 0.0	0.1 ± 0.0	0.1 ± 0.0	0.2 ± 0.0	0.0 ± 0.0	0.1 ± 0.0	0.1 ± 0.0	0.2 ± 0.0
20:5ω3	8.5 ± 0.9	18.0 ± 2.4	17.7 ± 2.4	13.2 ± 1.0	7.5 ± 0.4	8.2 ± 1.4	7.3 ± 0.5	12.7 ± 0.8
22:2ω9 (NMI)	0.0 ± 0.0	0.0 ± 0.0	0.0 ± 0.0	0.0 ± 0.0	0.0 ± 0.0	0.1 ± 0.0	0.3 ± 0.3	0.1 ± 0.0
22:3ω6	0.1 ± 0.0	0.7 ± 0.2	0.2 ± 0.0	0.5 ± 0.1	0.1 ± 0.0	0.2 ± 0.0	0.3 ± 0.1	0.3 ± 0.0
22:4ω6	0.1 ± 0.0	0.2 ± 0.0	0.4 ± 0.2	0.1 ± 0.1	0.6 ± 0.1	1.8 ± 0.3	0.9 ± 0.3	1.2 ± 0.2
22:5ω6	0.6 ± 0.1	0.8 ± 0.1	0.4 ± 0.1	0.6 ± 0.1	0.6 ± 0.1	1.9 ± 0.2	0.6 ± 0.1	2.0 ± 0.2
22:5ω3	0.3 ± 0.0	0.5 ± 0.1	0.5 ± 0.1	0.4 ± 0.0	0.4 ± 0.0	1.1 ± 0.2	0.7 ± 0.1	3.7 ± 0.3
22:6ω3	6.5 ± 0.9	10.1 ± 1.6	8.1 ± 0.8	8.4 ± 0.9	3.6 ± 0.1	5.3 ± 0.5	4.5 ± 1.1	10.3 ± 1.0
∑PUFA	**46.0 ± 2.7**	**47.4 ± 1.7**	**55.2 ± 0.8**	**41.5 ± 2.2**	**29.9 ± 1.3**	**41.8 ± 1.6**	**29.5 ± 1.6**	**44.6 ± 1.2**
Branched								
15:0iso	0.1 ± 0.0	0.2 ± 0.1	0.1 ± 0.0	0.1 ± 0.0	0.3 ± 0.0	0.4 ± 0.0	0.4 ± 0.0	0.1 ± 0.0
15:0anteiso	0.0 ± 0.0	0.1 ± 0.0	0.0 ± 0.0	0.1 ± 0.0	0.1 ± 0.0	0.1 ± 0.0	0.2 ± 0.0	0.0 ± 0.0
16:0iso	0.1 ± 0.0	0.1 ± 0.0	0.1 ± 0.0	0.2 ± 0.2	0.2 ± 0.1	0.5 ± 0.1	0.2 ± 0.0	0.1 ± 0.0
10-methyl 16	0.0 ± 0.0	0.2 ± 0.1	0.1 ± 0.0	0.2 ± 0.1	0.1 ± 0.0	0.2 ± 0.1	0.1 ± 0.0	0.2 ± 0.0
17:0iso	0.3 ± 0.1	0.4 ± 0.1	0.3 ± 0.0	0.2 ± 0.1	0.4 ± 0.1	1.3 ± 0.3	0.6 ± 0.1	0.3 ± 0.0
17:0anteiso	0.1 ± 0.0	0.1 ± 0.1	0.1 ± 0.1	0.1 ± 0.0	0.2 ± 0.0	0.7 ± 0.1	0.2 ± 0.1	0.1 ± 0.0
18:0iso	0.1 ± 0.0	0.2 ± 0.1	0.1 ± 0.0	0.1 ± 0.0	0.1 ± 0.0	0.3 ± 0.2	0.1 ± 0.0	0.0 ± 0.0
∑BrFA	**0.7 ± 0.2**	**1.3 ± 0.3**	**0.7 ± 0.1**	**1.1 ± 0.4**	**1.5 ± 0.2**	**3.6 ± 0.7**	**1.9 ± 0.3**	**0.9 ± 0.1**
∑FA (mg g^{-1})	**19.8 ± 3.7**	**26.6 ± 21.4**	**18.2 ± 3.6**	**17.0 ± 2.8**	**49.1 ± 5.4**	**29.7 ± 3.0**	**73.0 ± 10.7**	**29.7 ± 1.5**

Appendix 7-1: Complete fatty acid compositions (% ± SD) of bordering fringe sediment samples in the Can Gio mangrove during both seasons

Fatty acids (%)	Dry Season			Wet Season			
	Site 1 (n = 4)	Site 2 (n = 4)	Site 3 (n = 4)	Site 1 (n = 4)	Site 2 (n = 4)	Site 3 (n = 4)	Site R (n = 4)
Saturated							
12:0	2.4 ± 1.2	1.8 ± 0.7	3.6 ± 1.6	1.1 ± 0.3	1.1 ± 0.5	2.0 ± 0.8	1.3 ± 0.4
13:0	0.2 ± 0.1	0.2 ± 0.1	0.2 ± 0.1	0.2 ± 0.0	0.2 ± 0.0	0.2 ± 0.0	0.3 ± 0.0
14:0	7.8 ± 1.1	7.1 ± 0.4	8.3 ± 1.2	5.9 ± 1.1	6.4 ± 0.6	6.9 ± 1.0	5.3 ± 0.2
15:0	1.8 ± 0.4	1.5 ± 0.0	1.5 ± 0.3	1.3 ± 0.3	2.1 ± 1.3	1.1 ± 0.1	2.0 ± 0.1
16:0	26.7 ± 4.3	20.4 ± 1.8	19.5 ± 2.3	21.7 ± 4.0	22.0 ± 2.8	24.3 ± 3.6	21.5 ± 0.6
17:0	0.6 ± 0.1	1.1 ± 0.2	2.4 ± 1.0	0.7 ± 0.2	1.1 ± 0.4	0.9 ± 0.5	1.1 ± 0.1
18:0	3.1 ± 0.3	5.2 ± 1.0	3.9 ± 1.5	5.4 ± 1.5	4.4 ± 1.6	3.0 ± 0.1	4.7 ± 0.2
19:0	0.2 ± 0.0	0.3 ± 0.0	0.3 ± 0.0	0.3 ± 0.1	0.2 ± 0.1	0.2 ± 0.0	0.4 ± 0.1
20:0	1.3 ± 0.4	1.2 ± 0.2	2.3 ± 1.6	1.9 ± 1.0	1.0 ± 0.3	1.2 ± 0.3	1.2 ± 0.1
21:0	0.2 ± 0.0	0.2 ± 0.0	0.2 ± 0.0	0.2 ± 0.1	0.2 ± 0.1	0.2 ± 0.1	0.3 ± 0.0
22:0	1.3 ± 0.4	1.6 ± 0.2	1.5 ± 0.4	1.6 ± 0.4	1.5 ± 0.4	1.3 ± 0.2	1.2 ± 0.1
24:0	2.0 ± 0.6	3.6 ± 0.4	3.8 ± 0.9	4.5 ± 1.2	3.9 ± 1.2	4.2 ± 1.2	2.0 ± 0.1
25:0	0.3 ± 0.1	0.5 ± 0.0	0.7 ± 0.2	0.6 ± 0.2	0.5 ± 0.1	0.5 ± 0.1	0.3 ± 0.0
26:0	2.0 ± 0.9	4.2 ± 0.2	7.2 ± 2.9	6.9 ± 2.9	5.0 ± 1.9	6.6 ± 2.4	1.6 ± 0.1
27:0	0.2 ± 0.1	0.2 ± 0.0	0.4 ± 0.2	0.4 ± 0.2	0.3 ± 0.1	0.3 ± 0.1	0.2 ± 0.0
28:0	1.4 ± 0.9	2.4 ± 0.9	5.1 ± 1.3	6.6 ± 3.1	4.3 ± 1.5	4.8 ± 1.7	1.4 ± 0.1
29:0	0.1 ± 0.1	0.1 ± 0.1	0.1 ± 0.1	0.3 ± 0.2	0.2 ± 0.1	0.2 ± 0.1	0.1 ± 0.0
30:0	0.4 ± 0.3	0.9 ± 0.7	0.6 ± 0.4	1.9 ± 1.3	1.0 ± 0.5	1.1 ± 0.6	0.8 ± 0.3
∑SFA	**52.0 ± 3.6**	**52.4 ± 1.6**	**61.6 ± 4.8**	**61.6 ± 6.8**	**55.4 ± 3.3**	**59.2 ± 3.8**	**45.6 ± 1.4**
Monounsaturated							
16:1ω7	14.0 ± 1.2	6.7 ± 1.4	4.2 ± 0.8	6.0 ± 2.1	9.8 ± 3.1	8.7 ± 2.8	7.2 ± 0.5
16:1ω5	0.7 ± 0.1	0.8 ± 0.4	0.3 ± 0.1	1.1 ± 1.6	0.8 ± 0.2	0.5 ± 0.3	1.3 ± 0.1
17:1ω9	0.2 ± 0.1	0.3 ± 0.0	0.3 ± 0.2	0.2 ± 0.1	0.5 ± 0.3	0.2 ± 0.0	0.5 ± 0.1
17:1ω7	0.3 ± 0.1	0.4 ± 0.1	0.4 ± 0.2	0.7 ± 0.7	0.1 ± 0.1	0.8 ± 0.7	0.9 ± 0.0
18:1ω9	5.3 ± 0.8	8.2 ± 1.2	3.9 ± 1.0	2.6 ± 0.6	3.4 ± 0.3	2.6 ± 0.4	4.6 ± 0.7
18:1ω7	3.3 ± 0.7	2.3 ± 0.4	2.0 ± 0.4	2.4 ± 0.8	2.6 ± 0.6	2.4 ± 0.9	7.4 ± 0.4
19:1ω9	0.2 ± 0.1	0.6 ± 0.2	0.6 ± 0.3	1.2 ± 0.6	0.4 ± 0.3	1.5 ± 1.2	1.7 ± 0.1
20:1ω9	0.2 ± 0.0	0.3 ± 0.0	1.1 ± 0.8	0.1 ± 0.0	0.2 ± 0.1	0.2 ± 0.1	0.3 ± 0.1
22:1ω9	3.5 ± 1.7	2.5 ± 0.9	2.9 ± 1.2	3.0 ± 0.5	1.8 ± 0.4	2.0 ± 0.6	3.2 ± 1.2
∑MUFA	**27.8 ± 3.1**	**22.0 ± 2.0**	**15.6 ± 2.3**	**17.4 ± 4.5**	**19.6 ± 2.8**	**18.9 ± 2.1**	**27.1 ± 2.3**
Polyunsaturated							
16:2ω6	0.1 ± 0.1	0.1 ± 0.0	0.2 ± 0.2	0.1 ± 0.1	0.3 ± 0.0	0.2 ± 0.1	0.2 ± 0.0
16:2ω4	1.2 ± 0.3	0.7 ± 0.2	0.5 ± 0.1	0.5 ± 0.2	1.5 ± 0.5	0.6 ± 0.2	0.4 ± 0.0
16:3ω4	2.0 ± 0.5	1.1 ± 0.3	1.0 ± 0.3	0.7 ± 0.3	2.3 ± 0.8	0.9 ± 0.4	0.2 ± 0.0
18:2ω6	0.7 ± 0.0	1.3 ± 0.7	0.8 ± 0.2	1.5 ± 0.5	1.4 ± 0.5	1.1 ± 0.1	1.6 ± 0.5
18:3ω6	0.3 ± 0.0	1.0 ± 0.6	0.3 ± 0.1	0.3 ± 0.1	0.3 ± 0.1	0.2 ± 0.0	0.2 ± 0.1
18:3ω3	0.2 ± 0.0	0.5 ± 0.3	0.3 ± 0.1	0.3 ± 0.2	0.7 ± 0.8	1.0 ± 0.7	0.4 ± 0.2
20:4ω6	0.7 ± 0.1	0.5 ± 0.1	0.7 ± 0.2	0.6 ± 0.5	1.4 ± 0.5	0.9 ± 0.4	0.9 ± 0.1
20:5ω3	2.1 ± 0.5	1.3 ± 0.4	1.6 ± 0.6	1.5 ± 1.4	3.5 ± 1.6	1.9 ± 0.6	0.9 ± 0.3
∑PUFA	**7.4 ± 1.4**	**6.6 ± 1.7**	**5.4 ± 0.7**	**5.5 ± 2.8**	**11.2 ± 3.3**	**6.8 ± 2.0**	**4.7 ± 0.6**
Branched							
13:0iso	0.2 ± 0.1	0.2 ± 0.1	0.2 ± 0.0	0.1 ± 0.0	0.1 ± 0.1	0.1 ± 0.0	0.3 ± 0.0
13:0anteiso	0.1 ± 0.0	0.1 ± 0.1	0.1 ± 0.0	0.1 ± 0.0	0.3 ± 0.5	0.1 ± 0.0	0.1 ± 0.0
14:0iso	2.6 ± 0.1	3.3 ± 0.4	3.9 ± 0.8	2.6 ± 0.6	2.2 ± 0.5	2.5 ± 0.3	1.7 ± 0.2
15:0iso	2.9 ± 0.4	4.2 ± 0.3	3.8 ± 0.6	3.2 ± 0.3	3.4 ± 0.7	3.6 ± 0.8	6.6 ± 0.5
15:0anteiso	1.7 ± 0.2	3.5 ± 0.5	2.8 ± 0.6	2.6 ± 0.2	2.4 ± 0.5	2.5 ± 0.7	3.9 ± 0.2
16:0iso	2.1 ± 0.0	3.2 ± 0.3	2.9 ± 0.5	2.5 ± 0.9	2.0 ± 0.5	2.3 ± 0.5	2.4 ± 0.2
10-methyl 16:0	1.8 ± 0.6	2.3 ± 0.4	2.2 ± 0.5	2.6 ± 0.4	1.7 ± 0.4	2.3 ± 1.2	4.6 ± 0.3
17:0iso	0.7 ± 0.0	1.1 ± 0.1	0.8 ± 0.1	0.9 ± 0.1	0.9 ± 0.1	0.9 ± 0.3	1.7 ± 0.1
17:0anteiso	0.5 ± 0.0	1.0 ± 0.1	0.6 ± 0.1	0.6 ± 0.1	0.6 ± 0.1	0.7 ± 0.2	1.3 ± 0.1
18:0iso	0.1 ± 0.0	0.1 ± 0.0	0.1 ± 0.1	0.2 ± 0.1	0.1 ± 0.0	0.1 ± 0.0	0.2 ± 0.0
∑BrFA	**12.8 ± 1.2**	**18.9 ± 1.5**	**17.4 ± 2.5**	**15.4 ± 2.3**	**13.8 ± 3.0**	**15.1 ± 3.7**	**22.6 ± 1.5**
∑FA (mg g^{-1})	**0.34 ± 0.19**	**0.28 ± 0.02**	**0.47 ± 0.19**	**0.20 ± 0.06**	**0.22 ± 0.08**	**0.34 ± 0.08**	**0.14 ± 0.02**

Appendix 7-2: Complete fatty acid compositions (% ± SD) of mangrove forest sediment samples in the Can Gio mangrove during both seasons

Fatty acids (%)	Dry Season		Wet Season		
	Site 2 (n = 4)	Site 3 (n = 4)	Site 2 (n = 4)	Site 3 (n = 4)	Site R (n = 4)
Saturated					
12:0	1.1 ± 0.3	1.5 ± 0.4	0.8 ± 0.1	0.9 ± 0.4	1.4 ± 0.4
13:0	0.2 ± 0.1	0.2 ± 0.0	0.2 ± 0.0	0.2 ± 0.1	0.3 ± 0.1
14:0	4.7 ± 1.1	5.6 ± 0.2	4.5 ± 0.2	4.9 ± 0.6	5.6 ± 0.2
15:0	1.5 ± 0.1	1.7 ± 0.2	1.6 ± 0.2	1.6 ± 0.2	2.5 ± 0.3
16:0	22.5 ± 3.5	19.9 ± 1.3	19.7 ± 1.2	18.8 ± 3.5	19.6 ± 0.7
17:0	1.0 ± 0.1	1.0 ± 0.1	1.2 ± 0.3	1.4 ± 0.5	1.2 ± 0.1
18:0	3.6 ± 0.2	3.0 ± 0.1	4.2 ± 0.3	3.6 ± 0.3	3.6 ± 0.1
19:0	0.2 ± 0.1	0.2 ± 0.0	0.3 ± 0.0	0.2 ± 0.0	0.3 ± 0.0
20:0	0.9 ± 0.2	1.1 ± 0.6	1.2 ± 0.3	2.8 ± 1.8	1.4 ± 0.2
21:0	0.2 ± 0.0	0.2 ± 0.0	0.7 ± 0.5	0.5 ± 0.2	1.0 ± 0.2
22:0	1.4 ± 0.3	1.4 ± 0.1	1.6 ± 0.4	1.4 ± 0.3	1.9 ± 0.1
24:0	1.7 ± 0.4	3.1 ± 0.5	3.4 ± 0.8	3.7 ± 0.7	3.3 ± 0.5
25:0	0.7 ± 0.9	0.5 ± 0.2	0.4 ± 0.1	0.5 ± 0.1	0.4 ± 0.0
26:0	1.4 ± 0.5	3.5 ± 1.5	3.7 ± 1.1	4.9 ± 1.3	3.2 ± 0.7
27:0	0.1 ± 0.0	0.2 ± 0.1	0.2 ± 0.1	0.3 ± 0.1	0.1 ± 0.0
28:0	0.8 ± 0.3	2.4 ± 1.4	2.5 ± 1.1	4.5 ± 2.2	1.7 ± 0.3
29:0	0.1 ± 0.0	0.1 ± 0.0	0.1 ± 0.1	0.2 ± 0.1	0.1 ± 0.0
30:0	0.2 ± 0.1	0.3 ± 0.2	0.5 ± 0.4	1.0 ± 0.6	0.5 ± 0.3
∑SFA	**42.2 ± 2.3**	**45.7 ± 2.7**	**47.1 ± 2.2**	**51.3 ± 3.3**	**48.0 ± 1.5**
Monounsaturated					
16:1ω7	5.1 ± 2.1	6.8 ± 0.7	4.6 ± 0.5	4.8 ± 1.9	6.0 ± 0.6
16:1ω5	3.4 ± 1.7	2.1 ± 0.4	2.6 ± 0.8	1.7 ± 0.3	1.2 ± 0.1
17:1ω9	0.5 ± 0.1	0.4 ± 0.1	0.3 ± 0.1	0.3 ± 0.0	0.6 ± 0.1
17:1ω7	1.2 ± 0.2	1.6 ± 0.2	1.3 ± 0.2	1.5 ± 0.4	1.2 ± 0.1
18:1ω9	7.4 ± 1.9	3.1 ± 0.7	3.6 ± 0.7	3.5 ± 1.1	2.9 ± 0.2
18:1ω7	4.2 ± 0.5	3.9 ± 0.8	4.1 ± 0.5	3.8 ± 0.6	6.1 ± 0.3
19:1ω9	3.4 ± 0.6	3.8 ± 0.3	3.8 ± 0.4	3.1 ± 0.6	1.1 ± 0.2
20:1ω9	0.3 ± 0.0	0.2 ± 0.0	0.3 ± 0.1	0.2 ± 0.1	0.1 ± 0.0
22:1ω9	2.6 ± 0.9	2.2 ± 0.6	2.0 ± 0.5	1.3 ± 0.6	3.1 ± 0.3
∑MUFA	**28.0 ± 2.6**	**24.0 ± 1.5**	**22.8 ± 1.6**	**20.3 ± 1.9**	**22.3 ± 1.1**
Polyunsaturated					
16:2ω6	0.1 ± 0.0	0.2 ± 0.0	0.2 ± 0.0	0.2 ± 0.0	0.1 ± 0.0
16:2ω4	0.8 ± 0.2	1.0 ± 0.2	0.6 ± 0.0	0.5 ± 0.2	0.3 ± 0.0
16:3ω4	0.5 ± 0.5	1.3 ± 0.3	0.3 ± 0.0	0.4 ± 0.4	0.1 ± 0.0
18:2ω6	1.6 ± 0.7	1.0 ± 0.3	1.3 ± 0.3	1.8 ± 0.9	1.1 ± 0.2
18:3ω6	0.5 ± 0.3	0.3 ± 0.1	0.1 ± 0.0	0.4 ± 0.2	0.2 ± 0.0
18:3ω3	0.4 ± 0.1	0.3 ± 0.1	0.5 ± 0.3	0.4 ± 0.2	0.5 ± 0.2
20:4ω6	1.8 ± 0.5	1.4 ± 0.3	1.1 ± 0.1	1.6 ± 0.7	0.6 ± 0.0
20:5ω3	0.9 ± 0.6	2.1 ± 0.6	1.1 ± 0.2	1.2 ± 1.1	0.7 ± 0.1
∑PUFA	**6.6 ± 1.4**	**7.4 ± 1.0**	**5.1 ± 0.8**	**6.4 ± 3.2**	**3.5 ± 0.3**
Branched					
13:0iso	0.2 ± 0.1	0.2 ± 0.0	0.2 ± 0.0	0.1 ± 0.0	0.2 ± 0.0
13:0anteiso	0.1 ± 0.1	0.1 ± 0.0	0.0 ± 0.0	0.1 ± 0.0	0.1 ± 0.0
14:0iso	1.5 ± 0.3	2.2 ± 0.2	1.7 ± 0.2	2.0 ± 0.3	2.2 ± 0.2
15:0iso	5.9 ± 0.6	6.1 ± 0.7	6.6 ± 0.3	5.7 ± 0.9	7.4 ± 0.5
15:0anteiso	3.4 ± 0.4	3.7 ± 0.4	4.4 ± 0.4	4.1 ± 0.7	6.2 ± 0.4
16:0iso	2.2 ± 0.3	2.3 ± 0.2	2.5 ± 0.0	2.4 ± 0.4	2.8 ± 0.4
10-methyl 16:0	6.6 ± 0.6	5.4 ± 1.0	6.3 ± 0.1	4.8 ± 1.2	4.1 ± 0.3
17:0iso	1.9 ± 0.2	1.8 ± 0.2	1.9 ± 0.1	1.5 ± 0.2	1.6 ± 0.1
17:0anteiso	1.2 ± 0.2	0.9 ± 0.1	1.3 ± 0.1	1.1 ± 0.2	1.5 ± 0.1
18:0iso	0.1 ± 0.0	0.1 ± 0.0	0.1 ± 0.0	0.3 ± 0.1	0.2 ± 0.0
∑BrFA	**23.1 ± 2.4**	**22.8 ± 2.4**	**25.1 ± 0.9**	**22.0 ± 3.1**	**26.2 ± 1.7**
∑FA (mg g^{-1})	**0.21 ± 0.08**	**0.37 ± 0.09**	**0.18 ± 0.04**	**0.31 ± 0.09**	**0.26 ± 0.02**

Appendix 7-3: Complete fatty acid compositions (% ± SD) of brown *Rhizophora apiculata* tree leaves in the Can Gio mangrove during both seasons

Fatty acids (%)	Dry Season			Wet Season			
	Site 1 (n = 4)	Site 2 (n = 4)	Site 3 (n = 4)	Site 1 (n = 4)	Site 2 (n = 4)	Site 3 (n = 4)	Site R (n = 4)
Saturated							
12:0	0.7 ± 0.5	0.7 ± 0.4	0.8 ± 0.6	1.4 ± 0.6	1.2 ± 0.4	1.1 ± 0.2	1.1 ± 0.3
14:0	1.8 ± 1.3	3.4 ± 0.5	2.6 ± 1.0	5.3 ± 1.2	4.3 ± 0.4	4.9 ± 0.6	5.3 ± 1.2
15:0	0.5 ± 0.1	0.5 ± 0.1	0.6 ± 0.1	0.6 ± 0.2	0.4 ± 0.1	0.5 ± 0.0	0.4 ± 0.0
16:0	29.4 ± 5.1	37.8 ± 0.9	35.3 ± 2.7	36.3 ± 2.3	37.0 ± 2.1	37.5 ± 2.1	35.1 ± 1.9
17:0	0.9 ± 0.1	1.4 ± 0.1	1.0 ± 0.1	1.4 ± 0.3	1.2 ± 0.3	1.2 ± 0.3	1.1 ± 0.1
18:0	4.3 ± 0.3	4.5 ± 0.3	3.6 ± 0.8	3.9 ± 0.2	4.1 ± 0.4	3.7 ± 0.2	3.7 ± 0.3
19:0	0.2 ± 0.1	0.1 ± 0.1	0.1 ± 0.1	0.1 ± 0.1	0.1 ± 0.0	0.1 ± 0.0	0.1 ± 0.0
20:0	1.4 ± 0.5	1.3 ± 0.3	1.2 ± 0.6	1.3 ± 0.5	1.5 ± 0.4	1.6 ± 1.0	1.1 ± 0.2
21:0	0.3 ± 0.1	0.3 ± 0.0	0.3 ± 0.1	0.2 ± 0.0	0.2 ± 0.0	0.2 ± 0.0	0.2 ± 0.1
22:0	1.5 ± 0.6	1.2 ± 0.4	1.1 ± 0.5	0.8 ± 0.2	1.0 ± 0.1	0.8 ± 0.1	0.7 ± 0.2
24:0	1.7 ± 0.6	1.1 ± 0.5	1.2 ± 0.5	1.0 ± 0.1	1.0 ± 0.1	0.8 ± 0.1	0.6 ± 0.2
25:0	0.2 ± 0.1	0.4 ± 0.2	0.3 ± 0.2	0.5 ± 0.3	0.4 ± 0.1	0.3 ± 0.0	0.2 ± 0.0
26:0	1.0 ± 0.4	0.2 ± 0.2	0.4 ± 0.5	0.6 ± 0.7	0.2 ± 0.0	0.2 ± 0.1	0.2 ± 0.1
∑SFA	**43.9 ± 7.3**	**52.7 ± 1.8**	**48.5 ± 3.6**	**53.6 ± 2.0**	**52.6 ± 2.2**	**53.1 ± 3.7**	**49.7 ± 2.6**
Monounsaturated							
15:1ω1	0.2 ± 0.1	0.3 ± 0.1	0.3 ± 0.2	0.3 ± 0.1	0.3 ± 0.0	0.3 ± 0.0	0.3 ± 0.0
16:1ω7	0.3 ± 0.1	0.2 ± 0.1	0.4 ± 0.1	0.3 ± 0.1	0.2 ± 0.0	0.2 ± 0.0	0.3 ± 0.0
17:1ω7	0.2 ± 0.0	0.2 ± 0.1	0.3 ± 0.2	0.3 ± 0.0	0.2 ± 0.0	0.2 ± 0.0	0.2 ± 0.1
18:1ω9	8.8 ± 4.7	9.0 ± 1.5	8.9 ± 3.7	7.3 ± 1.7	5.1 ± 1.5	5.5 ± 2.4	5.2 ± 0.8
18:1ω7	1.7 ± 1.2	0.9 ± 0.2	1.8 ± 0.9	0.9 ± 0.3	0.7 ± 0.1	0.9 ± 0.1	1.0 ± 0.1
20:1ω9	0.1 ± 0.0	0.1 ± 0.1	0.1 ± 0.1	0.1 ± 0.0	0.1 ± 0.0	0.0 ± 0.0	0.0 ± 0.0
22:1ω9	0.7 ± 1.0	0.5 ± 0.5	0.7 ± 0.4	0.1 ± 0.0	0.1 ± 0.1	0.1 ± 0.0	0.0 ± 0.0
∑MUFA	**12.0 ± 4.3**	**11.4 ± 2.0**	**12.5 ± 4.6**	**9.2 ± 1.7**	**6.5 ± 1.6**	**7.2 ± 2.4**	**7.0 ± 0.9**
Polyunsaturated							
16:2ω6	2.1 ± 2.3	0.5 ± 0.2	0.3 ± 0.2	0.4 ± 0.3	0.1 ± 0.0	0.3 ± 0.2	0.1 ± 0.0
18:2ω6	14.3 ± 0.9	12.7 ± 2.0	14.8 ± 5.0	13.3 ± 3.8	12.4 ± 1.1	12.9 ± 1.0	14.5 ± 3.1
18:3ω3	27.8 ± 6.4	22.7 ± 2.3	23.9 ± 2.9	23.5 ± 3.7	28.3 ± 4.3	26.5 ± 2.3	28.7 ± 2.2
∑PUFA	**44.1 ± 5.6**	**35.9 ± 3.0**	**39.0 ± 5.7**	**37.2 ± 2.9**	**40.8 ± 3.5**	**39.7 ± 2.6**	**43.3 ± 2.3**
∑FA (mg g^{-1})	**2.3 ± 1.3**	**2.0 ± 0.7**	**1.2 ± 0.4**	**3.7 ± 0.6**	**4.5 ± 0.6**	**3.9 ± 0.9**	**8.4 ± 2.1**

Appendix 7-4: Complete fatty acid compositions (% ± SD) of the mangrove murex snail *Chicoreus capucinus* in the Can Gio mangrove during both seasons

Fatty acids (%)	Dry Season		Wet Season		
	Site 2 (n = 4)	Site 3 (n = 4)	Site 2 (n = 4)	Site 3 (n = 4)	Site R (n = 4)
Saturated					
12:0	0.1 ± 0.0	0.1 ± 0.1	0.0 ± 0.0	0.1 ± 0.0	0.5 ± 0.5
13:0	0.1 ± 0.0	0.1 ± 0.0	0.0 ± 0.0	0.0 ± 0.0	0.1 ± 0.0
14:0	3.9 ± 1.1	3.4 ± 0.2	3.9 ± 1.2	3.8 ± 0.6	3.8 ± 0.7
15:0	0.8 ± 0.4	0.7 ± 0.1	0.6 ± 0.2	0.6 ± 0.2	1.1 ± 0.5
16:0	12.5 ± 3.9	11.0 ± 3.0	15.0 ± 4.5	14.0 ± 2.1	9.7 ± 1.6
17:0	2.3 ± 0.6	2.2 ± 0.3	2.5 ± 0.3	2.3 ± 0.5	1.8 ± 0.2
18:0	8.6 ± 1.0	9.3 ± 0.7	7.8 ± 0.3	7.8 ± 0.9	7.7 ± 0.5
19:0	0.2 ± 0.0	0.2 ± 0.0	0.2 ± 0.0	0.2 ± 0.0	0.2 ± 0.1
20:0	0.3 ± 0.1	0.3 ± 0.1	0.4 ± 0.1	0.5 ± 0.4	0.1 ± 0.0
22:0	0.7 ± 0.5	0.5 ± 0.2	0.6 ± 0.3	0.5 ± 0.2	0.4 ± 0.2
24:0	0.0 ± 0.0	0.0 ± 0.0	0.2 ± 0.1	0.1 ± 0.1	0.0 ± 0.0
∑SFA	**29.4 ± 4.3**	**27.7 ± 2.9**	**31.4 ± 5.6**	**30.0 ± 2.6**	**25.5 ± 1.6**
Monounsaturated					
16:1ω7	4.9 ± 2.7	3.8 ± 2.0	7.8 ± 2.7	5.5 ± 2.9	1.9 ± 1.5
16:1ω5	0.1 ± 0.1	0.1 ± 0.0	0.2 ± 0.1	0.2 ± 0.1	0.1 ± 0.1
17:1ω9	0.0 ± 0.0	0.0 ± 0.0	0.0 ± 0.0	0.0 ± 0.0	0.0 ± 0.1
18:1ω11	1.0 ± 0.4	0.9 ± 0.5	0.9 ± 0.2	1.7 ± 0.4	0.3 ± 0.2
18:1ω9	2.5 ± 0.5	2.6 ± 0.3	2.6 ± 0.6	2.5 ± 1.0	2.3 ± 0.6
18:1ω7	3.4 ± 1.6	2.4 ± 0.9	5.7 ± 2.1	5.1 ± 1.8	1.4 ± 0.6
18:1ω5	0.2 ± 0.1	0.2 ± 0.1	0.2 ± 0.0	0.3 ± 0.1	0.1 ± 0.1
19:1ω9	0.4 ± 0.1	0.3 ± 0.0	0.4 ± 0.1	0.6 ± 0.1	0.2 ± 0.0
20:1ω11	9.1 ± 0.4	9.6 ± 1.4	7.8 ± 1.8	11.1 ± 2.4	9.5 ± 0.4
20:1ω9	0.9 ± 0.6	0.6 ± 0.1	1.1 ± 0.4	1.1 ± 0.4	0.5 ± 0.1
20:1ω7	0.5 ± 0.3	0.4 ± 0.2	1.0 ± 0.5	1.6 ± 0.1	0.3 ± 0.1
22:1ω11	0.9 ± 0.1	0.7 ± 0.2	1.1 ± 0.4	1.6 ± 0.6	0.7 ± 0.2
∑MUFA	**24.0 ± 5.2**	**21.7 ± 2.2**	**29.0 ± 4.2**	**31.3 ± 3.6**	**17.4 ± 2.2**
Polyunsaturated					
16:2ω4	0.1 ± 0.0	0.1 ± 0.0	0.1 ± 0.0	0.1 ± 0.0	0.0 ± 0.0
16:3ω6	0.0 ± 0.0	0.0 ± 0.0	0.0 ± 0.0	0.0 ± 0.0	0.1 ± 0.1
16:4ω3	0.0 ± 0.0	0.0 ± 0.0	0.1 ± 0.1	0.0 ± 0.0	0.1 ± 0.1
18:2ω6	4.2 ± 1.1	4.5 ± 0.6	2.8 ± 0.7	2.6 ± 0.6	4.0 ± 0.4
18:2ω3	0.1 ± 0.1	0.1 ± 0.1	0.1 ± 0.0	0.1 ± 0.1	0.0 ± 0.0
18:3ω6	0.0 ± 0.0	0.0 ± 0.0	0.0 ± 0.0	0.0 ± 0.0	0.0 ± 0.0
18:3ω3	0.8 ± 0.2	0.9 ± 0.1	0.5 ± 0.1	0.7 ± 0.0	0.6 ± 0.2
18:4ω3	0.1 ± 0.0	0.1 ± 0.0	0.0 ± 0.0	0.0 ± 0.0	0.1 ± 0.0
20:2ω9 (NMI)	1.0 ± 0.4	0.9 ± 0.5	1.4 ± 0.4	2.4 ± 1.1	0.2 ± 0.1
20:2ω7 (NMI)	1.8 ± 0.4	1.5 ± 0.5	1.8 ± 0.2	3.0 ± 0.9	0.6 ± 0.4
20:2ω6	1.3 ± 0.6	1.8 ± 0.5	1.7 ± 1.0	0.9 ± 0.6	2.0 ± 0.3
20:3ω6,9,15 (NMI)	1.9 ± 0.8	2.3 ± 0.4	1.4 ± 0.6	2.2 ± 0.6	0.6 ± 0.2
20:3ω6	0.2 ± 0.1	0.4 ± 0.0	0.3 ± 0.1	0.3 ± 0.2	0.3 ± 0.1
20:4ω6	15.9 ± 5.5	17.2 ± 1.6	10.7 ± 3.9	8.5 ± 2.3	19.6 ± 0.8
20:4ω3	0.0 ± 0.0	0.0 ± 0.0	0.0 ± 0.0	0.0 ± 0.0	0.1 ± 0.0
20:5ω3	1.3 ± 0.5	1.6 ± 0.2	1.3 ± 0.2	1.1 ± 0.1	1.6 ± 0.1
22:2ω9 (NMI)	3.9 ± 0.3	4.4 ± 0.8	4.5 ± 1.6	5.0 ± 1.0	7.2 ± 0.7
22:2ω6	4.3 ± 0.5	4.3 ± 0.8	3.8 ± 1.0	4.1 ± 0.7	4.1 ± 1.2
22:3ω6	3.3 ± 0.3	3.3 ± 0.5	3.0 ± 0.8	3.3 ± 0.7	2.8 ± 0.7
22:4ω6	4.2 ± 1.5	4.4 ± 0.8	2.7 ± 1.0	2.0 ± 0.7	5.9 ± 0.6
22:5ω6	0.1 ± 0.1	0.1 ± 0.0	0.2 ± 0.1	0.4 ± 0.2	0.2 ± 0.1
22:5ω3	1.5 ± 0.8	2.0 ± 1.2	2.1 ± 1.5	1.1 ± 0.3	4.1 ± 0.9
22:6ω3	0.1 ± 0.0	0.1 ± 0.1	0.2 ± 0.2	0.2 ± 0.1	0.6 ± 0.2
∑PUFA	**46.1 ± 8.5**	**50.1 ± 5.0**	**38.6 ± 8.9**	**38.1 ± 5.3**	**54.8 ± 2.0**
Branched					
15:0iso	0.1 ± 0.0	0.1 ± 0.1	0.1 ± 0.0	0.1 ± 0.1	0.3 ± 0.3
15:0anteiso	0.0 ± 0.0	0.0 ± 0.0	0.0 ± 0.0	0.0 ± 0.0	0.1 ± 0.1
16:0iso	0.1 ± 0.0	0.1 ± 0.0	0.2 ± 0.1	0.1 ± 0.1	0.3 ± 0.2
17:0iso	0.2 ± 0.0	0.1 ± 0.0	0.3 ± 0.3	0.2 ± 0.2	0.8 ± 0.3
17:0anteiso	0.1 ± 0.0	0.2 ± 0.0	0.3 ± 0.2	0.2 ± 0.1	0.7 ± 0.5
18:0iso	0.0 ± 0.0	0.1 ± 0.0	0.1 ± 0.0	0.1 ± 0.0	0.2 ± 0.1
∑BrFA	**0.5 ± 0.1**	**0.5 ± 0.1**	**1.0 ± 0.5**	**0.7 ± 0.6**	**2.4 ± 1.3**
∑FA (mg g^{-1})	**24.3 ± 8.1**	**25.7 ± 9.1**	**27.3 ± 8.3**	**35.8 ± 10.0**	**14.3 ± 3.5**

Appendix 7-5: Complete fatty acid compositions (% ± SD) of the peneid shrimp *Metapenaeus ensis* in the Can Gio mangrove during both seasons

Fatty acids (%)	Dry Season	Wet Season			
	Site 1 (n = 4)	Site 1 (n = 4)	Site 2 (n = 4)	Site 3 (n = 4)	Site R (n = 4)
Saturated					
12:0	0.0 ± 0.0	0.1 ± 0.0	0.1 ± 0.0	0.1 ± 0.0	0.1 ± 0.1
13:0	0.0 ± 0.0	0.1 ± 0.0	0.0 ± 0.0	0.0 ± 0.0	0.1 ± 0.0
14:0	1.9 ± 0.8	1.6 ± 0.5	1.4 ± 0.8	1.3 ± 0.6	1.5 ± 0.3
15:0	1.9 ± 0.4	2.1 ± 0.4	1.8 ± 0.8	1.7 ± 0.4	2.1 ± 0.3
16:0	17.8 ± 1.7	15.8 ± 3.2	16.1 ± 1.8	15.3 ± 1.6	16.2 ± 0.7
17:0	3.3 ± 0.4	3.8 ± 0.8	4.0 ± 0.8	4.2 ± 0.6	3.6 ± 0.2
18:0	11.4 ± 0.5	11.7 ± 0.7	12.4 ± 1.3	10.9 ± 0.6	11.0 ± 0.7
19:0	0.4 ± 0.0	0.4 ± 0.1	0.4 ± 0.0	0.4 ± 0.0	0.4 ± 0.0
20:0	0.2 ± 0.1	0.3 ± 0.0	0.2 ± 0.1	0.2 ± 0.1	0.3 ± 0.0
22:0	0.2 ± 0.1	0.3 ± 0.1	0.1 ± 0.0	0.2 ± 0.0	0.5 ± 0.0
24:0	0.0 ± 0.0	0.1 ± 0.0	0.1 ± 0.0	0.1 ± 0.0	0.1 ± 0.0
∑SFA	**37.3 ± 2.0**	**36.3 ± 2.9**	**36.6 ± 4.1**	**34.4 ± 1.8**	**35.7 ± 0.9**
Monounsaturated					
16:1ω7	6.1 ± 2.2	4.2 ± 0.3	4.1 ± 0.2	4.4 ± 1.2	3.9 ± 0.7
16:1ω5	0.2 ± 0.0	0.3 ± 0.1	0.1 ± 0.0	0.3 ± 0.1	0.3 ± 0.2
17:1ω9	1.1 ± 0.3	1.3 ± 0.5	1.2 ± 0.4	1.2 ± 0.7	1.0 ± 0.2
17:1ω7	0.2 ± 0.1	0.2 ± 0.1	0.2 ± 0.1	0.2 ± 0.1	0.1 ± 0.0
18:1ω11	0.2 ± 0.0	0.2 ± 0.1	0.3 ± 0.2	0.2 ± 0.1	0.2 ± 0.0
18:1ω9	7.9 ± 2.2	6.2 ± 0.4	6.7 ± 1.7	6.4 ± 0.4	6.6 ± 0.9
18:1ω7	4.3 ± 0.8	4.6 ± 0.3	3.4 ± 0.5	4.6 ± 1.0	4.7 ± 0.2
18:1ω5	0.2 ± 0.1	0.3 ± 0.1	0.2 ± 0.0	0.3 ± 0.1	0.3 ± 0.1
19:1ω9	0.2 ± 0.0	0.2 ± 0.1	0.1 ± 0.0	0.2 ± 0.1	0.1 ± 0.0
20:1ω11	0.7 ± 0.2	0.7 ± 0.2	1.0 ± 0.5	1.1 ± 0.5	0.7 ± 0.1
20:1ω9	0.7 ± 0.6	0.5 ± 0.2	0.9 ± 0.5	1.0 ± 0.4	0.6 ± 0.2
20:1ω7	0.2 ± 0.1	0.2 ± 0.1	0.1 ± 0.0	0.1 ± 0.0	0.2 ± 0.1
22:1ω11	0.1 ± 0.0	0.1 ± 0.0	0.2 ± 0.1	0.2 ± 0.0	0.1 ± 0.0
24:1ω9	0.0 ± 0.0	0.1 ± 0.0	0.1 ± 0.1	0.1 ± 0.1	0.1 ± 0.0
∑MUFA	**22.2 ± 1.2**	**19.1 ± 1.6**	**18.7 ± 1.0**	**20.2 ± 2.3**	**18.9 ± 1.8**
Polyunsaturated					
16:2ω4	0.1 ± 0.1	0.1 ± 0.0	0.1 ± 0.0	0.1 ± 0.0	0.1 ± 0.0
16:3ω6	0.1 ± 0.0	0.1 ± 0.0	0.1 ± 0.0	0.1 ± 0.0	0.1 ± 0.0
18:2ω6	4.3 ± 1.8	3.8 ± 0.9	4.4 ± 2.5	5.8 ± 1.1	3.6 ± 0.5
18:2ω3	0.2 ± 0.0	0.1 ± 0.1	0.1 ± 0.0	0.1 ± 0.0	0.1 ± 0.0
18:3ω6	0.1 ± 0.1	0.1 ± 0.0	0.1 ± 0.0	0.1 ± 0.1	0.1 ± 0.0
18:3ω3	0.7 ± 0.3	0.6 ± 0.0	1.5 ± 0.5	1.3 ± 0.4	0.8 ± 0.2
18:4ω3	0.2 ± 0.0	0.1 ± 0.0	0.2 ± 0.1	0.2 ± 0.1	0.1 ± 0.0
20:2ω6	0.9 ± 0.3	1.1 ± 0.1	1.2 ± 0.5	1.3 ± 0.5	1.3 ± 0.3
20:3ω6,9,15 (NMI)	0.2 ± 0.1	0.3 ± 0.2	0.2 ± 0.1	0.2 ± 0.1	0.4 ± 0.1
20:3ω6	0.6 ± 0.2	0.6 ± 0.3	0.6 ± 0.4	0.8 ± 0.3	0.6 ± 0.1
20:4ω6	11.7 ± 2.9	14.6 ± 3.6	12.0 ± 4.0	14.7 ± 3.0	15.8 ± 1.0
20:4ω3	0.2 ± 0.1	0.1 ± 0.0	0.2 ± 0.1	0.2 ± 0.1	0.1 ± 0.0
20:5ω3	11.1 ± 1.3	9.2 ± 2.7	12.6 ± 3.1	10.0 ± 0.3	8.2 ± 1.4
22:3ω6	0.2 ± 0.0	0.2 ± 0.0	0.2 ± 0.1	0.2 ± 0.1	0.2 ± 0.0
22:4ω6	1.6 ± 0.5	1.5 ± 0.7	1.2 ± 0.4	1.1 ± 0.4	1.8 ± 0.3
22:5ω6	0.8 ± 0.1	1.6 ± 0.2	1.0 ± 0.2	1.1 ± 0.3	1.9 ± 0.2
22:5ω3	1.2 ± 0.2	1.1 ± 0.2	1.8 ± 1.0	1.2 ± 0.2	1.1 ± 0.2
22:6ω3	4.1 ± 1.1	5.7 ± 2.5	4.3 ± 1.6	3.3 ± 1.3	5.3 ± 0.5
∑PUFA	**38.2 ± 2.9**	**41.0 ± 0.7**	**41.8 ± 2.2**	**41.8 ± 3.0**	**41.8 ± 1.6**
Branched					
15:0iso	0.3 ± 0.1	0.4 ± 0.1	0.3 ± 0.1	0.4 ± 0.1	0.4 ± 0.0
15:0anteiso	0.1 ± 0.0	0.2 ± 0.1	0.1 ± 0.0	0.1 ± 0.0	0.1 ± 0.0
16:0iso	0.3 ± 0.1	0.5 ± 0.2	0.3 ± 0.1	0.4 ± 0.1	0.5 ± 0.1
10-methyl 16:0	0.0 ± 0.0	0.3 ± 0.1	0.1 ± 0.1	0.2 ± 0.1	0.2 ± 0.1
17:0iso	0.9 ± 0.2	1.2 ± 0.4	1.3 ± 0.9	1.4 ± 0.4	1.3 ± 0.3
17:0anteiso	0.4 ± 0.1	0.7 ± 0.3	0.5 ± 0.3	0.6 ± 0.1	0.7 ± 0.1
18:0iso	0.3 ± 0.0	0.3 ± 0.1	0.3 ± 0.2	0.4 ± 0.1	0.3 ± 0.2
∑BrFA	**2.3 ± 0.6**	**3.6 ± 1.2**	**2.9 ± 1.6**	**3.6 ± 0.6**	**3.6 ± 0.7**
∑FA (mg g^{-1})	**30.2 ± 8.3**	**29.9 ± 4.2**	**30.7 ± 8.6**	**35.7 ± 3.3**	**29.7 ± 3.0**

Appendix 7-6: Complete fatty acid compositions (% ± SD) of the claw muscles of the varunid crab *Metaplax elegans* in the Can Gio mangrove during both seasons

Fatty acids (%)	Dry Season		Wet Season		
	Site 1 (n = 4)	Site 2 (n = 4)	Site 1 (n = 4)	Site 3 (n = 4)	Site R (n = 4)
Saturated					
12:0	0.1 ± 0.0	0.1 ± 0.0	0.2 ± 0.1	0.1 ± 0.0	0.1 ± 0.1
13:0	0.0 ± 0.0	0.1 ± 0.0	0.0 ± 0.0	0.0 ± 0.0	0.0 ± 0.0
14:0	1.5 ± 0.3	1.0 ± 0.3	3.4 ± 1.2	1.1 ± 0.3	0.5 ± 0.4
15:0	0.8 ± 0.3	0.5 ± 0.1	0.7 ± 0.1	0.4 ± 0.1	1.6 ± 0.5
16:0	24.7 ± 2.5	20.8 ± 1.4	25.0 ± 1.5	22.9 ± 2.4	17.2 ± 2.0
17:0	0.8 ± 0.3	1.3 ± 0.2	0.5 ± 0.1	0.7 ± 0.1	1.6 ± 0.3
18:0	11.1 ± 1.1	11.3 ± 0.7	8.5 ± 1.4	11.0 ± 1.0	12.0 ± 1.4
19:0	0.2 ± 0.0	0.2 ± 0.0	0.2 ± 0.1	0.2 ± 0.0	0.3 ± 0.0
20:0	0.4 ± 0.1	0.3 ± 0.0	0.3 ± 0.1	0.3 ± 0.0	0.5 ± 0.1
22:0	0.3 ± 0.0	0.2 ± 0.1	0.0 ± 0.0	0.2 ± 0.0	0.5 ± 0.1
24:0	0.1 ± 0.0	0.1 ± 0.0	0.2 ± 0.1	0.1 ± 0.0	0.1 ± 0.0
∑SFA	**39.1 ± 3.3**	**34.7 ± 0.8**	**38.5 ± 1.6**	**36.3 ± 1.7**	**32.8 ± 0.7**
Monounsaturated					
14:1ω5	0.0 ± 0.0	0.0 ± 0.0	0.0 ± 0.0	0.0 ± 0.0	0.0 ± 0.0
14:1ω3	0.0 ± 0.0	0.0 ± 0.0	0.0 ± 0.0	0.0 ± 0.0	0.0 ± 0.0
16:1ω7	8.0 ± 1.4	4.3 ± 0.8	10.0 ± 2.5	6.4 ± 1.1	4.4 ± 0.5
16:1ω5	0.1 ± 0.0	0.2 ± 0.1	0.1 ± 0.0	0.1 ± 0.0	0.1 ± 0.1
17:1ω9	0.5 ± 0.3	0.1 ± 0.0	0.2 ± 0.2	0.2 ± 0.0	1.1 ± 0.4
17:1ω7	0.1 ± 0.0	0.1 ± 0.0	0.1 ± 0.0	0.0 ± 0.0	0.1 ± 0.1
18:1ω11	0.1 ± 0.0	0.1 ± 0.0	0.0 ± 0.0	0.0 ± 0.0	0.0 ± 0.0
18:1ω9	4.8 ± 0.5	5.6 ± 1.4	3.2 ± 1.3	5.2 ± 1.2	5.7 ± 0.6
18:1ω7	4.0 ± 0.5	4.1 ± 0.4	3.1 ± 0.5	3.3 ± 0.2	3.6 ± 0.3
18:1ω5	0.1 ± 0.0	0.2 ± 0.0	0.1 ± 0.0	0.1 ± 0.0	0.1 ± 0.0
19:1ω9	0.1 ± 0.0	0.0 ± 0.0	0.1 ± 0.0	0.1 ± 0.0	0.1 ± 0.0
20:1ω11	0.1 ± 0.0	0.1 ± 0.0	0.1 ± 0.0	0.1 ± 0.0	0.1 ± 0.0
20:1ω9	0.6 ± 0.1	0.4 ± 0.1	0.5 ± 0.2	0.4 ± 0.1	1.1 ± 0.2
20:1ω7	0.1 ± 0.0	0.1 ± 0.0	0.1 ± 0.0	0.1 ± 0.0	0.1 ± 0.0
22:1ω11	0.4 ± 0.1	0.4 ± 0.1	0.5 ± 0.0	0.4 ± 0.0	0.5 ± 0.0
24:1ω9	0.0 ± 0.0	0.0 ± 0.0	0.0 ± 0.0	0.0 ± 0.0	0.0 ± 0.0
∑MUFA	**19.0 ± 1.5**	**15.7 ± 0.3**	**18.2 ± 1.6**	**16.4 ± 1.3**	**16.9 ± 1.2**
Polyunsaturated					
16:2ω6	0.1 ± 0.0	0.1 ± 0.0	0.2 ± 0.1	0.1 ± 0.0	0.1 ± 0.1
16:2ω4	0.6 ± 0.2	0.2 ± 0.2	1.5 ± 0.6	0.3 ± 0.1	0.4 ± 0.2
16:3ω4	0.8 ± 0.5	0.7 ± 0.4	2.5 ± 0.8	0.4 ± 0.2	0.7 ± 0.7
16:4ω3	0.1 ± 0.0	0.1 ± 0.0	0.1 ± 0.0	0.1 ± 0.0	0.1 ± 0.1
18:2ω6	1.7 ± 0.1	2.8 ± 0.3	1.4 ± 0.1	2.0 ± 0.3	4.3 ± 0.9
18:2ω3	0.3 ± 0.1	0.1 ± 0.0	0.3 ± 0.0	0.1 ± 0.0	0.2 ± 0.0
18:3ω6	0.5 ± 0.1	0.6 ± 0.1	0.5 ± 0.1	0.4 ± 0.0	0.4 ± 0.0
18:3ω3	0.3 ± 0.0	0.4 ± 0.1	0.3 ± 0.0	0.7 ± 0.1	1.4 ± 1.0
18:4ω3	0.4 ± 0.1	0.4 ± 0.1	0.6 ± 0.1	0.5 ± 0.1	0.4 ± 0.0
20:2ω6	0.5 ± 0.1	0.8 ± 0.1	0.3 ± 0.0	0.7 ± 0.1	1.0 ± 0.2
20:3ω6,9,15 (NMI)	0.0 ± 0.0	0.1 ± 0.0	0.0 ± 0.0	0.0 ± 0.0	0.1 ± 0.0
20:3ω6	0.2 ± 0.0	0.3 ± 0.0	0.3 ± 0.1	0.2 ± 0.0	0.2 ± 0.0
20:3ω3	0.3 ± 0.0	0.1 ± 0.0	0.2 ± 0.0	0.3 ± 0.0	0.3 ± 0.1
20:4ω6	4.1 ± 0.5	9.5 ± 1.5	4.7 ± 0.3	5.4 ± 0.5	7.2 ± 0.5
20:4ω3	0.2 ± 0.0	0.1 ± 0.0	0.3 ± 0.0	0.2 ± 0.0	0.1 ± 0.0
20:5ω3	19.7 ± 2.8	20.7 ± 1.7	20.4 ± 1.3	22.0 ± 2.5	18.0 ± 2.4
22:3ω6	1.0 ± 0.2	0.6 ± 0.1	0.9 ± 0.1	0.9 ± 0.1	0.7 ± 0.2
22:4ω6	0.1 ± 0.0	0.2 ± 0.1	0.1 ± 0.0	0.1 ± 0.0	0.2 ± 0.0
22:5ω6	0.6 ± 0.1	0.8 ± 0.1	0.6 ± 0.1	0.7 ± 0.0	0.8 ± 0.1
22:5ω3	0.9 ± 0.1	0.7 ± 0.1	0.9 ± 0.1	0.7 ± 0.1	0.5 ± 0.1
22:6ω3	8.1 ± 1.2	7.4 ± 0.6	5.7 ± 1.7	10.1 ± 1.0	10.1 ± 1.6
∑PUFA	**40.3 ± 4.5**	**46.8 ± 0.8**	**41.9 ± 1.8**	**45.8 ± 3.2**	**47.3 ± 1.7**
Branched					
15:0iso	0.1 ± 0.0	0.2 ± 0.0	0.1 ± 0.0	0.1 ± 0.0	0.2 ± 0.1
15:0anteiso	0.0 ± 0.0	0.1 ± 0.0	0.0 ± 0.0	0.0 ± 0.0	0.1 ± 0.0
16:0iso	0.0 ± 0.0	0.1 ± 0.0	0.0 ± 0.0	0.1 ± 0.0	0.1 ± 0.0
10-methyl 16:0	0.2 ± 0.0	0.4 ± 0.1	0.2 ± 0.1	0.2 ± 0.1	0.2 ± 0.1
17:0iso	0.2 ± 0.0	0.4 ± 0.1	0.4 ± 0.1	0.2 ± 0.1	0.4 ± 0.1
17:0anteiso	0.1 ± 0.0	0.2 ± 0.0	0.0 ± 0.0	0.1 ± 0.1	0.1 ± 0.1
18:0iso	0.1 ± 0.0	0.1 ± 0.0	0.0 ± 0.0	0.1 ± 0.0	0.2 ± 0.1
∑BrFA	**0.5 ± 0.0**	**1.1 ± 0.2**	**0.6 ± 0.1**	**0.6 ± 0.2**	**1.1 ± 0.3**
∑FA (mg g^{-1})	**15.3 ± 4.7**	**18.0 ± 2.3**	**31.2 ± 6.7**	**18.4 ± 3.6**	**19.3 ± 6.9**

Appendix 7-7: Complete fatty acid compositions (% ± SD) of the hepatopancreas of the varunid crab *Metaplax elegans* in the Can Gio mangrove during both seasons.
Note that absolute concentrations were not calculated for these tissues

Fatty acids (%)	Dry Season		Wet Season		
	Site 1 (n = 4)	Site 2 (n = 4)	Site 1 (n = 4)	Site 3 (n = 4)	Site R (n = 4)
Saturated					
12:0	0.1 ± 0.0	0.5 ± 1.0	0.2 ± 0.2	0.1 ± 0.1	0.1 ± 0.0
13:0	0.1 ± 0.0	0.0 ± 0.0	0.0 ± 0.0	0.0 ± 0.0	0.1 ± 0.0
14:0	6.1 ± 0.2	4.0 ± 1.1	7.6 ± 0.4	4.7 ± 0.9	3.0 ± 1.3
15:0	1.7 ± 1.0	0.5 ± 0.1	1.1 ± 0.5	0.9 ± 0.2	3.6 ± 1.9
16:0	33.3 ± 1.8	26.0 ± 3.0	30.4 ± 0.8	32.8 ± 3.7	22.2 ± 1.5
18:0	2.8 ± 0.7	6.6 ± 3.5	2.9 ± 1.1	5.0 ± 1.0	7.2 ± 4.1
19:0	0.1 ± 0.0	0.2 ± 0.1	0.1 ± 0.1	0.1 ± 0.0	0.3 ± 0.1
20:0	0.1 ± 0.0	0.2 ± 0.1	0.1 ± 0.0	0.2 ± 0.0	0.6 ± 0.1
22:0	0.2 ± 0.1	0.4 ± 0.1	0.3 ± 0.1	0.4 ± 0.1	0.8 ± 0.1
24:0	0.0 ± 0.0	0.1 ± 0.2	0.4 ± 0.2	0.4 ± 0.1	0.5 ± 0.1
∑SFA	**44.4 ± 1.2**	**38.4 ± 2.2**	**43.2 ± 1.8**	**44.7 ± 3.7**	**38.4 ± 1.2**
Monounsaturated					
16:1ω7	18.3 ± 1.6	11.1 ± 3.0	17.5 ± 1.7	15.0 ± 1.9	8.2 ± 2.9
16:1ω5	0.3 ± 0.0	0.4 ± 0.2	0.2 ± 0.1	0.3 ± 0.1	0.5 ± 0.3
17:1ω9	0.4 ± 0.3	0.1 ± 0.0	0.2 ± 0.1	0.3 ± 0.1	1.2 ± 0.4
17:1ω7	0.1 ± 0.0	0.1 ± 0.0	0.1 ± 0.0	0.1 ± 0.0	0.2 ± 0.1
18:1ω11	0.0 ± 0.0	0.0 ± 0.0	0.0 ± 0.0	0.1 ± 0.0	0.1 ± 0.0
18:1ω9	2.0 ± 0.2	4.0 ± 1.9	1.6 ± 0.3	3.3 ± 0.2	4.6 ± 1.6
18:1ω7	1.6 ± 0.1	2.5 ± 0.6	1.4 ± 0.2	1.9 ± 0.3	3.8 ± 0.4
18:1ω5	0.1 ± 0.0	0.2 ± 0.0	0.1 ± 0.0	0.1 ± 0.0	0.1 ± 0.0
19:1ω9	0.1 ± 0.0	0.1 ± 0.0	0.1 ± 0.0	0.1 ± 0.0	0.1 ± 0.0
20:1ω11	0.1 ± 0.1	0.2 ± 0.1	0.1 ± 0.0	0.2 ± 0.1	0.2 ± 0.1
20:1ω9	0.3 ± 0.2	0.2 ± 0.1	0.2 ± 0.0	0.3 ± 0.1	1.5 ± 0.4
20:1ω7	0.1 ± 0.1	0.1 ± 0.0	0.1 ± 0.0	0.1 ± 0.0	0.1 ± 0.1
22:1ω11	0.2 ± 0.1	0.2 ± 0.1	0.4 ± 0.1	0.3 ± 0.1	0.5 ± 0.0
24:1ω9	0.0 ± 0.0	0.1 ± 0.1	0.0 ± 0.0	0.1 ± 0.1	0.1 ± 0.0
∑MUFA	**23.5 ± 1.0**	**19.3 ± 0.5**	**22.1 ± 1.2**	**22.0 ± 1.2**	**21.0 ± 2.1**
Polyunsaturated					
16:2ω6	0.5 ± 0.1	0.8 ± 0.2	0.4 ± 0.0	0.4 ± 0.1	0.5 ± 0.3
16:2ω4	2.7 ± 0.2	1.7 ± 0.8	3.5 ± 0.4	1.6 ± 0.2	1.6 ± 0.9
16:3ω4	5.5 ± 0.7	6.6 ± 3.5	5.8 ± 0.7	3.2 ± 0.3	4.2 ± 2.5
16:4ω3	0.0 ± 0.0	0.1 ± 0.0	0.0 ± 0.0	0.1 ± 0.0	0.1 ± 0.0
18:2ω6	1.1 ± 0.2	2.3 ± 0.7	1.1 ± 0.1	1.7 ± 0.3	3.9 ± 0.8
18:2ω3	0.1 ± 0.0	0.1 ± 0.0	0.2 ± 0.1	0.1 ± 0.0	0.3 ± 0.1
18:3ω6	0.8 ± 0.1	1.1 ± 0.4	0.7 ± 0.1	0.7 ± 0.0	0.6 ± 0.2
18:3ω3	0.3 ± 0.1	0.4 ± 0.2	0.3 ± 0.0	1.0 ± 0.2	2.1 ± 1.9
18:4ω3	1.2 ± 0.1	0.7 ± 0.2	0.9 ± 0.2	1.2 ± 0.2	0.6 ± 0.3
20:2ω6	0.1 ± 0.0	0.2 ± 0.2	0.1 ± 0.0	0.3 ± 0.0	0.6 ± 0.3
20:3ω6	0.3 ± 0.1	0.4 ± 0.0	0.4 ± 0.1	0.4 ± 0.0	0.4 ± 0.0
20:3ω3	0.2 ± 0.1	0.7 ± 0.6	0.0 ± 0.0	0.1 ± 0.0	0.1 ± 0.1
20:4ω6	2.8 ± 0.4	10.7 ± 1.2	3.4 ± 0.5	4.2 ± 1.1	5.8 ± 1.6
20:4ω3	0.3 ± 0.1	0.1 ± 0.1	0.4 ± 0.0	0.4 ± 0.0	0.2 ± 0.0
20:5ω3	12.5 ± 0.3	11.0 ± 2.2	13.7 ± 0.7	12.7 ± 2.6	10.9 ± 1.9
22:3ω6	0.2 ± 0.0	0.2 ± 0.1	0.3 ± 0.0	0.3 ± 0.1	0.3 ± 0.2
22:4ω6	0.3 ± 0.1	0.5 ± 0.4	0.1 ± 0.0	0.1 ± 0.0	0.4 ± 0.1
22:5ω6	0.3 ± 0.1	0.3 ± 0.2	0.3 ± 0.1	0.4 ± 0.1	0.7 ± 0.4
22:5ω3	0.4 ± 0.1	0.3 ± 0.2	0.5 ± 0.2	0.5 ± 0.1	0.5 ± 0.4
22:6ω3	1.2 ± 0.3	1.5 ± 0.8	1.4 ± 0.2	2.5 ± 0.8	3.9 ± 3.4
∑PUFA	**30.8 ± 1.3**	**39.9 ± 1.9**	**33.7 ± 0.9**	**31.8 ± 5.0**	**37.8 ± 3.0**
Branched					
14:0iso	0.0 ± 0.0	0.1 ± 0.0	0.0 ± 0.0	0.1 ± 0.0	0.1 ± 0.0
15:0iso	0.2 ± 0.0	0.5 ± 0.2	0.2 ± 0.0	0.4 ± 0.2	0.7 ± 0.2
15:0anteiso	0.1 ± 0.0	0.2 ± 0.1	0.0 ± 0.0	0.2 ± 0.1	0.3 ± 0.1
16:0iso	0.1 ± 0.0	0.3 ± 0.1	0.1 ± 0.0	0.2 ± 0.1	0.3 ± 0.1
17:0iso	0.7 ± 0.1	1.0 ± 0.2	0.7 ± 0.0	0.6 ± 0.2	1.0 ± 0.2
17:0anteiso	0.1 ± 0.0	0.2 ± 0.1	0.1 ± 0.0	0.1 ± 0.1	0.3 ± 0.0
18:0iso	0.0 ± 0.0	0.1 ± 0.0	0.0 ± 0.0	0.1 ± 0.0	0.1 ± 0.0
∑BrFA	**1.2 ± 0.2**	**2.3 ± 0.6**	**1.1 ± 0.1**	**1.5 ± 0.6**	**2.7 ± 0.7**

Frank DAVID

Né le 31/10/1989 à Albi (81)

frank.david@live.fr

N° ORCID :
orcid.org/0000-0002-6145-4618

Parcours universitaire

Doctorat - Ecologie Aquatique et Biogéochimie, Septembre 2017

Muséum National d'Histoire Naturelle – Paris

Dynamique du carbone et relations trophiques dans un estuaire à mangrove sous pression anthropique (Can Gio, Vietnam)

Ingénieur Agronome - Environnement et Gestion des Ressources, Septembre 2013

Ecole Nationale Supérieure Agronomique – Toulouse

Elevage larvaire d'un poisson chat amazonien en aquaculture multi-trophique (Iquitos, Pérou)

Master - Ecologie et Biogéosciences de l'Environnement, Juin 2013

Université Paul Sabatier – Toulouse

Colonisation des litières par les invertébrés benthiques en tête de bassin (Bangkok, Thaïlande)

DUT - Biologie, Juin 2009

Institut Universitaire de Technologie – Aurillac

Influence de la déforestation sur les ressources nutritives d'un poisson amphidrome (Dunedin, Nouvelle-Zélande)

ABSTRACT

Mangrove estuaries are highly dynamic environments importing carbon originating from both the watershed and the coastal ocean to the adjacent floodplain, and exporting to the ocean a fraction of that photosynthesised by the surrounding vegetation. Mangroves are very productive ecosystems. Thus, they serve as a nursery for a wide variety of coastal species entering the ecosystem during flood, and exporting during ebb the carbon they consumed. However, the quantities and the quality of carbon exchanged within the estuary, along with the transformations occurring during the water transit, are still not fully understood. This work aims to examine the carbon cycle in the main estuarine channel of the Can Gio mangrove, located in Southern Vietnam, along with macroscopic species connecting the mangrove ecosystem to the coastal ocean through their movements; this, in order to better understand the carbon budget of the Can Gio mangrove, and at a broader scale, of tropical mangroves. Results presented in this manuscript are originating from 3 sampling campaigns; the first performed during the dry season, along the main estuarine channel only; the second achieved during the wet season, along both the main estuarine channel and a mangrove tidal creek; and the last in order to simulate in controlled conditions the fate of shrimp pond effluents once released in the estuary. Water column parameters were surveyed at different sites located on the mangrove waterways, each during a complete tidal cycle (24 h), and various macroscopic species were sampled from both the intertidal zone and the water column. This study examines concomitantly mineral forms of carbon, particularly CO_2, which plays a major role in climate mitigation; its organic forms, especially fatty acids, used as biomarkers in trophic webs studies and implied in diverse metabolic functions; and specificities of the microbial compartment, contributing to the cycling of this carbon.

Keywords: Fatty acids, CO_2, trophic webs, anthropogenic influence, mangrove, Vietnam

RESUME

Les estuaires à mangroves sont des écosystèmes très dynamiques qui transportent du carbone provenant des eaux continentales et de la production côtière vers la plaine d'inondation, et exportent vers l'océan une partie de celui fixé par la végétation environnante. Les mangroves sont des milieux très productifs et servent ainsi de zones de nurserie et d'alimentation pour de nombreuses espèces côtières qui y pénètrent lors de la marée montante et exportent lors de la marée descendante la matière qu'ils y ont ingérée. Cependant, les quantités et la qualité du carbone qui est échangé dans l'estuaire, ainsi que les transformations qui s'y opèrent, sont encore mal connus. Ce travail de thèse a pour objectif d'étudier le cycle du carbone dans l'estuaire traversant la mangrove de Can Gio, au sud du Vietnam, ainsi que les organismes macroscopiques connectant la mangrove au compartiment océanique par leurs déplacements ; ceci, afin de mieux comprendre le bilan de carbone de la mangrove de Can Gio, et plus largement, celui des mangroves tropicales. Les résultats présentés sont issus de 3 campagnes d'échantillonnage ; la première en saison sèche, uniquement le long de l'estuaire traversant la mangrove ; la deuxième en saison humide, le long de l'estuaire et dans un chenal de vidange ; et la dernière afin de simuler en laboratoire le devenir d'effluents crevetticoles une fois rejetés dans l'estuaire. Des suivis des masses d'eau ont été effectués en différentes zones du réseau hydrographique de la mangrove, à chaque fois au cours d'un cycle tidal complet (24 h), et diverses espèces macroscopiques ont été capturées dans le lit mineur et la zone intertidale. Cette étude s'intéresse à la fois aux formes minérales du carbone, notamment le CO_2 qui joue un rôle clé dans la régulation du climat, à ses formes organiques, en particulier les acides gras qui sont utilisés comme traceurs de la matière organique dans les réseaux trophiques et qui possèdent de nombreuses fonctions métaboliques, et enfin à des spécificités du compartiment microbien, qui contribue au remaniement de ce carbone.

Mots clés : Acides gras, CO_2, réseaux trophiques, influence anthropique, mangrove, Vietnam